CWI Tracts

CWI
P.O. Box 4079, 1009 AB Amsterdam, The Netherlands
Telephone 31 - 20 592 9333, telex 12571 (mactr nl),
telefax 31 - 20 592 4199

CWI is the nationally funded Dutch institute for research in Mathematics and Computer Science.

Moment problems in Hilbert space with applications to magnetic resonance imaging

M. Zwaan

1991 Mathematics Subject Classification: 42B99, 46C99, 65D05, 94A12.
ISBN 90 6196 418 0
NUGI-code: 811

Introduction: Model Building

Practical and Mathematical Aspects

The analysis of images of two dimensional cross sections of human organs is one of the fields of interest in diagnostic medicine. The techniques of obtaining these images are referred to as tomography, which literally means 'writing in slices'. We only mention three such methods: Ultrasound Tomography, X-ray Computed Tomography (CT) and Magnetic Resonance Imaging (MRI). Any medical image, produced with the aid of ultrasonic waves, X-rays (CT) or electromagnetic waves (MRI), is the result of the interaction between the radiation employed and the tissue to be displayed. The reconstruction process consists of converting the information in the measured signals to images of cross sections of the human body. The reconstruction, processing and analysis of tomographic pictures constitutes an important area of research for mathematicians.

This tract is concerned with *mathematical and computational aspects* of reconstruction techniques by means of magnetic resonance imaging, in particular for the time-dependent case, referred to as dynamic MRI.
The main subjects of this tract are:

- a mathematical framework for dynamic MRI reconstruction;
- analytic solutions, numerical algorithms and development of reconstruction techniques;
- stability analysis of the reconstruction algorithms;
- comparison between these algorithms.

In the first section of this introduction we briefly present the physical aspects of magnetic resonance imaging. The second section discusses practical aspects and limitations of MRI. Some historical remarks are given in Section 3. An introduction to *dynamic* MRI is given in Section 4. In Section 5 we give the mathematical problem definition for dynamic MRI reconstruction and illustrate the solution method. The main results and conclusions of this dissertation are stated in the last section of this introduction.

1. Physical aspects of MRI

As we will see in this section the spatial Fourier coefficients of a *spin density* of the tissue in the cross section can be measured in MRI. It is the aim of MRI to reconstruct this density from the measured Fourier coefficients and to display its amplitude on a computer screen. In this section we explain how measurements are performed, how reconstructions are obtained and how they are displayed.

A spin density of tissue in a cross section of the human body is represented by a function $F : D \to \mathbb{C}$. The set D represents the cross section of the human body. For simplicity we assume that $D := [-\pi, \pi]^2 := [-\pi, \pi] \times [-\pi, \pi]$. The amplitude $|F(\mathbf{r})|$ is the proton density at position $\mathbf{r} \in D$, i.e. it is a measure for the 'number' of protons in the tissue per unit area. For example, for muscle and fat tissue the value of $|F(\mathbf{r})|$ is large and for bone or lung tissue smaller. This is because the density of hydrogen atoms, which are built up from elementary particles such as protons, is higher for muscle tissue than for lung or bone tissue.

The measurements are performed by means of magnetic fields and a radio frequency pulse, called *rf-pulse*, such that the spins of hydrogen protons in the human body are excited. This induces a signal in the detection coil of the MR-machine (see Chapter VI for more details),

$$S(t) \approx \int_D F(\mathbf{r}) e^{-j\gamma \mathbf{G}.\mathbf{r}t} d\mathbf{r}. \tag{0.1}$$

Here $j^2 = -1$, γ is the gyromagnetic ratio and $\mathbf{G} := (G_x, G_y)$ is the magnetic *gradient field*. In practice time dependent magnetic gradient fields are used, which are not taken into account in formula (0.1). We refer to Part II of this tract for a generalization of (0.1) to the case of time dependent gradient fields.

Now formula (0.1) will be derived in an intuitive manner. Since the human body consists mainly of water, there is an abundance of hydrogen atoms, which in their turn are built up from elementary particles like electrons and protons. A proton is a particle which posseses a spin, a magnetic dipole. The density of the spins of the protons in the tissue at position $\mathbf{r}$ and time t is called *the magnetization* $\mathbf{M}(\mathbf{r}, t)$. If the tissue is positioned in a homogeneous magnetic field with magnitude B and direction parallel to the z-axis, then the magnetization is also parallel to the z-axis. This magnetization can be forced to precess around the z-axis at the Larmor frequency γB, by applying an rf-pulse. This is a rotating magnetic field in the plane orthogonal to the z-direction (the xy-plane), which has frequency γB. Denote the magnetization vector $\mathbf{M}(\mathbf{r}, t)$ in three coordinates as

$$\mathbf{M}(\mathbf{r}, t) = (M_x(\mathbf{r}, t), M_y(\mathbf{r}, t), M_z(\mathbf{r}, t)).$$

Write the xy-component as a complex number,

$$M_\perp(\mathbf{r}, t) := M_x(\mathbf{r}, t) + jM_y(\mathbf{r}, t).$$

The precession around the z-axis of the magnetization vector can be described as

$$\mathbf{M}(\mathbf{r}, t) = \begin{pmatrix} M_\perp(\mathbf{r}) e^{-j\omega t} \\ M_z(\mathbf{r}) \end{pmatrix},$$

where ω is the Larmor frequency γB.

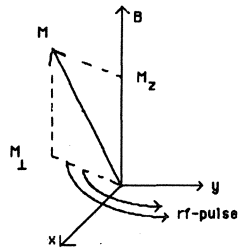

Figure 0.1. Precession of the magnetization vector around the direction of the homogeneous field.

A *changing* magnetic field induces a current in a coil. So, the xy-component of the magnetization induces a signal $S(t)$ in the receiver coil of the MR-machine, which is the sum of the contributions $M_\perp(\mathbf{r})e^{-j\omega t}d\mathbf{r}$ of all the volume elements $d\mathbf{r}$. This results in

$$S(t) \approx const \int M_\perp(\mathbf{r})\, e^{-j\omega t} d\mathbf{r}, \tag{0.2}$$

where $\omega = \gamma B$.

We now discuss the effect of the magnetic gradient field on the magnetization vector. Suppose that an object is positioned in a strong homogeneous magnetic field with magnitude B. Then apply a gradient field $\mathbf{G}$ which results in a position dependent magnetic field. That is, the magnetic gradient field has magnitude $\mathbf{G}.\mathbf{r}$ at position $\mathbf{r}$. The combination of these two fields yield the magnitude $(B + \mathbf{G}.\mathbf{r})$ at position $\mathbf{r}$. If an rf-pulse is applied to excite the magnetization, the precession frequency is $\gamma(B + \mathbf{G}.\mathbf{r})$. By putting $\omega = \gamma(B + \mathbf{G}.\mathbf{r})$ in formula (0.2) it follows that the induced signal is

$$S(t) \approx const \int M_\perp(\mathbf{r}) e^{-j\gamma(B+\mathbf{G}.\mathbf{r})t} d\mathbf{r}.$$

The contribution due to the homogeneous field can be discarded by modulation, which results in

$$S(t) \approx const \int M_\perp(\mathbf{r}) e^{-j\gamma\mathbf{G}.\mathbf{r}t} d\mathbf{r}.$$

Formula (0.1) follows by putting $F(\mathbf{r}) := M_\perp(\mathbf{r})$.

In the following we discuss how the information in the signal $S(t)$ from formula (0.1) is used in MRI reconstruction. By putting $k_x := \gamma G_x t$ and $k_y := \gamma G_y t$ in formula (0.1), for t fixed, it follows that $S(t)$ is the Fourier coefficient of F at the frequency pair (or *wave vector*) (k_x, k_y), denoted by $\widehat{F}(k_x, k_y)$. In practice one can only measure the Fourier transform at a finite number of frequencies, where k_x and k_y run from $-N$ up to $N-1$, say. The Fourier coefficients are obtained by measuring for each value of k_y, called the k_yth *phase encoding step*, the corresponding sequence

$$\{\widehat{F}(-N, k_y), \widehat{F}(-N+1, k_y), ..., \widehat{F}(N-2, k_y), \widehat{F}(N-1, k_y)\}.$$

Such a sequence is called a *profile*. Here k_y runs form $-N$ up to $N-1$. This scanning geometry is illustrated in Figure 0.2.

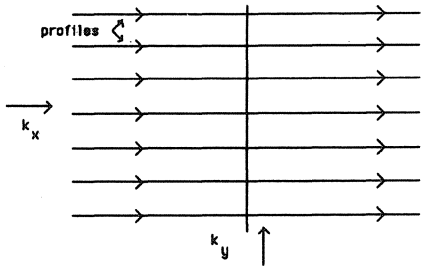

Figure 0.2. Scanning geometry for MRI along horizontal lines on a rectangular grid

For notational convenience we write the pair (k_x, k_y) as $\mathbf{k}$ and we define the index set

$$\mathbb{K} := \{\mathbf{k} = (k_x, k_y) \mid k_x, k_y = -N, ..., N-1\}.$$

In this manner one obtains the data

$$g_{\mathbf{k}} := \widehat{F}(\mathbf{k}), \quad \mathbf{k} \in \mathbb{K}.$$

The *reconstruction problem* of MRI is to recover the proton density F from the data $\{g_{\mathbf{k}}\}$. That is, we want to find a function $F : D \to \mathbb{C}$ which satisfies

$$\widehat{F}(\mathbf{k}) = g_{\mathbf{k}}, \quad \mathbf{k} \in \mathbb{K}. \tag{0.3}$$

Since there are a finite number of Fourier coefficients of the spin density F available, it is not possible to reconstruct F uniquely. In general a solution $f : D \to \mathbb{C}$ which is called *reconstruction*, will not be equal to the spin density F. One possible solution to problem (0.3) can be obtained by partial Fourier inversion:

$$f(\mathbf{r}) = \sum_{\mathbf{k} \in \mathbb{K}} g_{\mathbf{k}} e^{j\mathbf{k}.\mathbf{r}}.$$

The amplitude of the reconstruction is then displayed on a computer screen represented here as the square $[0, 2\pi]^2$. The screen is divided up into pixels (picture elements). Assume here that there are $2N$ pixels both in the horizontal and the vertical direction. Digital images are obtained by assigning grey values to pixels. An image of the function $|f|$ is then obtained by assigning the grey value $|f(i\pi/N, j\pi/N)|$ to the i, jth pixel, $i, j = 0, ..., 2N-1$.

2. Practical notes on MRI

In this section we discuss image resolution and signal to noise ratio.

In the previous section we saw that a digital image on a computer screen is built up from pixels. The *resolution* of an image is defined as the number of pixels per unit area. Since the image is assumed to be of a standard size, resolution will in the sequel be identified with the number of pixels. In the case of MRI the reconstructed image $|f|$, which has to

be displayed, is obtained from $2N \times 2N$ Fourier coefficients. From sampling theory it is known that in this case the resolution equals the number of Fourier coefficients: $4N^2$.

The spatial resolution cannot become arbitrarily high in the practice of MRI for physical reasons. If the signal $S(t)$ of formula (0.1) is sampled at time τ, then the Fourier coefficient of F at the wave vector $(\gamma G_x \tau, \gamma G_y \tau)$ is obtained (see Section 1). In practice this signal decays within a few milliseconds, so it can only be sampled within a certain time period $\Delta\tau$. Therefore, the highest frequency for which a Fourier coefficient can be measured is $(\gamma G_x \Delta\tau, \gamma G_y \Delta\tau)$. The resolution is then $\gamma^2 \Delta\tau^2 G_x \times G_y$. It follows that the amplitude (G_x, G_y) of the magnetic gradient field has to be increased, to obtain higher resolution images. On the other hand, in magnetic resonance imaging thermal noise plays an important role, which is explained in the next paragraph.

Divide each pixel into two smaller pixels. That is, the resolution is doubled and the magnetic gradient field is chosen correspondingly. Now, for the sake of argument, consider one large pixel containing the two smaller ones. The signal amplitude coming from each of these parts is half of the amplitude that would have come from the large pixel. But the amplitude of the thermal noise only depends on $\Delta\tau$ and is independent of the gradient field. This means that the *signal to noise ratio* is decreased by a factor two when doubling the resolution.

One important thermal noise source is the human body within the MRI-scanner. This means that the noise cannot completely be removed by improving the quality of the magnet coils. In practice the magnitude of the gradient field is chosen such that the signal to noise ratio is at least one, which determines the spatial resolution of the reconstructed images. In practice the resolution is often 128^2 or 256^2.

This yields the following behaviour of the relative error in the data. The amplitude of Fourier coefficients of any L^2-function decreases as the frequency increases. If a noise term which is independent from the frequency, is added to these coefficients, the relative error in the coefficients increases with the frequency. In the practice of MRI, the noise in the signal depends on $\Delta\tau$ which is fixed after the data collection strategy is chosen. So the noise is constant, while the amplitude of the Fourier coefficients is decreasing. Hence, the relative error in the data increases with the frequency.

3. Historical notes on MRI

The subject of magnetic resonance (MR) has grown rapidly from its beginning in 1946 into a very sophisticated technique with very wide applications in physics, organic chemistry and biological medicine. The principle of magnetic resonance was discovered by Purcell and Bloch, who received for their work the Nobel Prize for physics in 1952.

At first magnetic resonance was used for spectroscopy. An object or tissue was placed in a strong homogeneous magnetic field. By means of an rf-pulse a signal was induced in the receiver coil, cf. formula (0.2). From the spectrum of this signal, information about the chemical elements in the tissue or object can be obtained.

Later, around 1970, one became interested in imaging cross sections of human organs. In 1973 it was discovered (cf. [39] p. 5-6) by Lauterbur and independently by Mansfield and Granell that the MR principle could be used to provide spatially encoded signals, enabling the study of inhomogeneous objects, like cross sections of human organs. This gave rise to magnetic resonance imaging for diagnostic purposes. The choice of the magnetic gradient fields at this stage was such that the Fourier coefficients of F were obtained on a polar grid (see Figure 0.3). The reconstruction of the spin density could be done by first interpolating the data to a rectangular grid and then performing a Fourier inversion. Lauterbur called his

imaging technique *zeugmatography*, which comes from the Greek word 'zeugma', meaning yoke ('that which is used for joining'). That is, the information about the spin density along the lines through the origin (see Figure 0.3) has to be 'joined' to reconstruct an image.

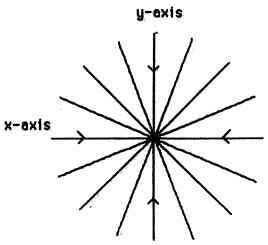

Figure 0.3. The polar grid proposed by Lauterbur

However, it turned out in 1975 that the Fourier coefficients can be obtained directly on a rectangular grid as in Figure 0.2, by means of an appropriate choice of magnetic gradient fields. This scanning geometry was proposed by Kumar, Welti and Ernst [31] and is used in current practice. By 1983, systems capable of obtaining images of cross sections of the human body had been developed as a result of continuing improvements in MRI techniques.

4. Model building and principles of dynamic MRI

In this section we explain the data collection strategy for MRI-reconstruction of a cross section of the beating human heart. We explain one of the reconstruction methods which is currently used in practice. Part Two, Chapter VI, considers this subject more extensively. Previously we described how the measurements are made in the case of an object which does not move. It turned out that the Fourier coefficients of a function $\mathbf{r} \rightarrow F(\mathbf{r})$ can be obtained in MRI. If MRI is used to measure and display cross sections of 'dynamic' organs, like the heart, then a function F depending on both the spatial parameter $\mathbf{r}$ and the temporal parameter τ has to be considered. In the following the spin density of the beating human heart is represented by the function $(\mathbf{r}, \tau) \rightarrow F(\mathbf{r}, \tau)$. MRI reconstruction in this time dependent case is referred to as *dynamic* MRI. This dynamic case is more complicated than the time independent case. In the practice of dynamic MRI the electrocardiogram is recorded, while the measurements are being obtained. The following terminology is commonly used in this context.

R-pulse: the electric pulse in the electrocardiogram that marks the beginning of a heart-beat. The ECG is recorded simultaneously with the measuremements.

RR-interval: the duration (in seconds) between two consecutive R-pulses.

Unit RR-interval: an RR-interval of unit length which will be used as a reference interval. This interval is called $J := [0, 1]$.

Heart phase: a phase in the (approximately) periodic motion of the heart.

The main idea of dynamic MRI schematically is as follows:

— a collection of Fourier coefficients at various time markers of the function F is obtained;

— information from the ECG signal is recorded;
— the measurements are related to a *model heartbeat*, by means of *rescaling* of the time markers, using the information from the ECG;
— the function to be reconstructed from these data is this model heartbeat.

In the remainder of this section the principles of dynamic MRI reconstruction are explained.

Acquisition method.

We explain the data-acquisition method *retrospective triggering* for dynamic MRI reconstruction, which was proposed by Bohning [8].

The profile which is measured in the k_yth phase encoding step at the time τ_i, is denoted by $\{\widehat{F}(k_x, k_y, \tau_i\}_{k_x=-N,\ldots,N-1}$. In order to reconstruct the function F at time τ_i with the partial Fourier inversion formula, $2N$ profiles (i.e. for $k_y = -N, \ldots, N-1$) at the time τ_i should be measured. In practice one cannot measure fast enough with MRI to obtain all these profiles at one time instant. Instead they are obtained during several RR-intervals as follows. Fix k_y and measure the profile at time τ_1,

$$\{\widehat{F}(\ k_x, k_y, \tau_1)\}_{k_x=-N,\ldots,N-1},$$

briefly denoted as $\{\widehat{F}(k_x, k_y, \tau_1)\}$. After some time, denoted by ΔT, (this may be from 10 up to 100 *msec*) the next profile is measured for this value of k_y, at time τ_2, etc; the time at which the measurements take place is recorded. After obtaining a fixed number N_{pr} of profiles (in practice this may be up to 200) the value of k_y is increased. If an R-pulse has occurred, it is registered, so that, afterwards, the measured profile can be assigned to the corresponding phase on the unit RR-interval. For an example of how the data are obtained, see Figure 0.4.

The total amount of data which is thus obtained is $4N^2 \times N_{pr}$, which implies that the data collection time depends on N, ΔT and N_{pr}. In the practice of MRI it is required that data collection can be done quickly. On the other hand, for diagnostic purposes, it is important to have high resolution images, i.e. the value of $2N$ is desired to be 128 or 256. So, the values of N_{pr} and ΔT have to be chosen small in order to reduce the data collection time. However, there is a lower bound for the parameter ΔT, due to physical reasons (see Mansfield and Morris [39]) and from the point of view of image quality, the value of N_{pr} cannot become too small. The value of N_{pr} is empirically determined. In practice one often takes $N_{pr} = 25$ or $N_{pr} = 50$.

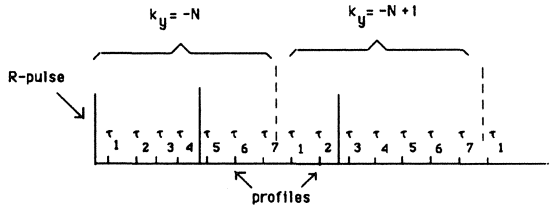

Figure 0.4. The data collection strategy for dynamic MRI

The data $\{\widehat{F}(\mathbf{k}, \tau_i)\}$ will be related to the model heartbeat by *model assumptions* as expained in the next paragraph.

Model assumptions.

We presuppose the existence of a density function g: $\mathbb{R}^2 \times J \to \mathbb{C}$, which is referred to as the *model heartbeat.* J is the unit RR-interval. The model heartbeat depends on the spatial parameter $\mathbf{r}$ and the temporal parameter $t \in J$, called *phase*, denoted as $(\mathbf{r}, t) \to g(\mathbf{r}, t)$. We emphasize that g is only an artificial construction and not a physical reality.

This model heartbeat is such that a copy of g which is rescaled in time to an arbitrary RR-interval is a realistic approximation of the the function F; this rescaling should be based on a biological model of the motion of the heart. In current practice the rescaling is assumed to be linear on each RR-interval. For example, suppose the k-th R-pulse is measured at the time r_k, for $k = 1, 2, \ldots$, then

$$g(\mathbf{r}, \frac{\tau - r_k}{r_{k+1} - r_k}) \approx F(\mathbf{r}, \tau),$$

where $\tau \in [r_k, r_{k+1})$.

We want to relate the data $\{\widehat{F}(\mathbf{k}, \tau_i)\}_{\mathbf{k},i}$ to the model heartbeat g, using the idea that scaled copies of g are approximately equal to F on each RR-interval. First, the relative positions of time markers $\{\tau_i\}$ on the RR-intervals are computed, i.e. the time markers $\{\tau_i\}$ are mapped onto the unit RR-interval J by the following rule. Let τ_i be lying in $[r_k, r_{k+1})$, then the corresponding time marker t_i on the unit heart interval is defined as

$$t_i := \frac{\tau_i - r_k}{r_{k+1} - r_k}, \quad \tau \in [r_k, r_{k+1}). \tag{0.4}$$

The conversion from τ_i to t_i is called rescaling. In this case the rescaling is linear on each heart interval, which is the first model assumption. The second assumption is that the Fourier coefficients of the model heartbeat at the time t_i are equal to the data:

$$\widehat{g}(\mathbf{k}, t_i) := \widehat{F}(\mathbf{k}, \tau_i), \quad \mathbf{k}, i. \tag{0.5}$$

The aim of dynamic MRI is to reconstruct the model heartbeat g from the data obtained by formula (0.5). After the reconstruction, images of the model heartbeat are displayed at consecutive phases in a movie loop. Denote the equidistant phases on the unit RR-interval as $\phi_l := l/L$, $l = 0, \ldots, L-1$. An image at the phase ϕ_l is then obtained taking $|g(i\pi/N, j\pi/N, \phi_l)|$ as grey value for the i,jth pixel, $i, j = 0, \ldots, 2N-1$. The 'movie' of the model heartbeat is obtained by displaying the images at the consecutive phases $\phi_0, \phi_1, \ldots, \phi_{L-1}$. This procedure is illustrated in Figure 0.5.

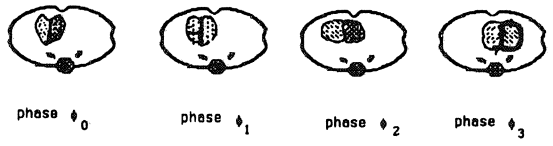

Figure 0.5. Illustration of a 'movie' of the model heartbeat at four phases.

We explicitly state the *model assumptions*:

— the scaling method is linear scaling on each RR-interval;

— there exists a model heartbeat such that its Fourier coefficients at the rescaled time markers are equal to the data.

How these assumptions are used in dynamic MRI reconstruction is explained in the next paragraph.

Used reconstruction method.

Here we explain how the reconstruction is currently done in practice. This method, proposed by Bohning [8], is called *retrospective triggering*. In order to do this we refer to Figures 0.4 and 0.6. In the example in Figure 0.4 the value of k_y is increased after seven profiles are measured. It is illustrated there that the profiles $\{\widehat{F}(k_x, k_y, \tau_i)\}$ for $k_y = -N, ..., N-1$, are measured during different RR-intervals. The rescaling is done as follows.

— The length of the heartbeat (i.e. the RR-interval) is determined from the ECG-signal, in which the measurement under consideration occurred. The time of a measurement, relative to the unit RR-interval is computed, e.g. in the case of linear rescaling by formula (0.4). For example, (cf. Figure 0.4) for $k_y = -N$ we have measured the consecutive profiles $\{\widehat{F}(k_x, k_y, \tau_1)\}$, $\{\widehat{F}(k_x, k_y, \tau_2)\}$, $\{\widehat{F}(k_x, k_y, \tau_3)\}$, $\{\widehat{F}(k_x, k_y, \tau_4)\}$, $\{\widehat{F}(k_x, k_y, \tau_5)\}$, $\{\widehat{F}(k_x, k_y, \tau_6)\}$ and $\{\widehat{F}(k_x, k_y, \tau_7)\}$. After rescaling the time markers τ_i to the unit RR-interval (Figure 0.6), these profiles become reordered by formulas (0.4) and (0.5) as $\{\widehat{g}(k_x, k_y, t_5)\}$, $\{\widehat{g}(k_x, k_y, t_1)\}$, $\{\widehat{g}(k_x, k_y, t_2)\}$, $\{\widehat{g}(k_x, k_y, t_6)\}$, $\{\widehat{g}(k_x, k_y, t_3)\}$, $\{\widehat{g}(k_x, k_y, t_7)\}$, $\{\widehat{g}(k_x, k_y, t_4)\}$, respectively. Note that the t_i's depend on the value of k_y, in the sense that other values for k_y will give rise to another arrangement on the unit RR-interval. To express this dependence this time marker is denoted as $t_i(k_y)$; in the above case this should be $t_i(-N)$, for $i = 1, \ldots, 7$.

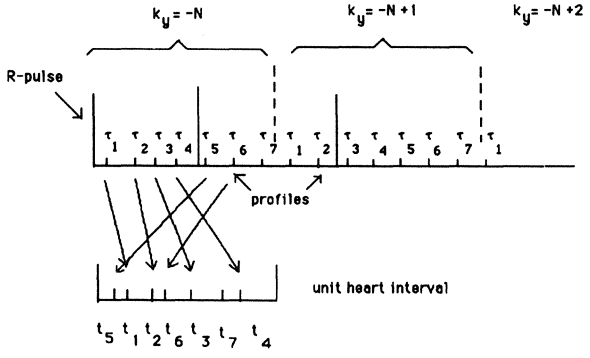

Figure 0.6. The measurements are rescaled to the unit heart interval.

— To display the model heartbeat at various phases, the unit RR-interval is divided into several parts (see Figure 0.7, for the case that the model heartbeat is displayed at four phases). All profiles on the unit RR-interval between phase ϕ_1 and phase ϕ_2 are, in practice, considered to be measured at phase ϕ_1. All measurements between phase ϕ_2 and phase ϕ_3 are considered to be measured at phase ϕ_2, etc. If several measurements belong to phase ϕ_n, then the average of these is assigned to phase ϕ_n.

In order to reconstruct the image of the model heartbeat at e.g. phase ϕ_1, the profiles belonging to $k_y = 0, .., 255$ are collected, as far as they were measured. It may happen that there are no data at all at some phases (see Figure 0.7), because the position of the rescaled time markers in the unit heart interval cannot be controlled. In the case of Figure 0.7 the profiles for the phases ϕ_0 and ϕ_4 are missing, for $k_y = -N$.

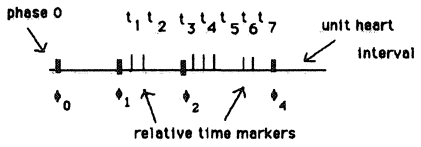

Figure 0.7. Missing data at phase ϕ_0 and phase ϕ_4

In practice it may be the case that there are missing profiles for several values of k_y. In the reconstruction method proposed by Bohning [8] the missing values are then set to zero whereafter the Fourier inversion formula is applied to obtain images at the desired phase.

In this section we described how in current practice the time markers are rescaled to the unit RR-interval and how measurements between phase ϕ_n and phase ϕ_{n+1} are assigned to phase ϕ_n. This last operation will cause a time jitter error in the image. To reduce this error the use of interpolation techniques is proposed in this tract to obtain more accurate data at the desired phases.
The next section presents the mathematical problem definition.

5. Mathematical problem definition

The central theme of this tract is to formulate the reconstruction problem for dynamic MRI in the mathematical setting of Hilbert spaces. Solution methods will be given and proved to be optimal in terms of a sensible criterion.
First we introduce some notation. Let $D \subset \mathbb{R}^2$ be the square $D = [-\pi, \pi]^2$. J is the unit RR-interval. Suppose the object to be measured has support in this interval D. The function $g : D \times J \ni (\mathbf{r}, t) \rightarrow \mathbb{R}$ is the model heartbeat. The Fourier transform of g, taken with respect to the variable $\mathbf{r}$, is defined by

$$\widehat{g}(\mathbf{k}, t) := \frac{1}{2\pi} \int_D g(\mathbf{r}, t) e^{-j\mathbf{k}.\mathbf{r}} d\mathbf{r}.$$

The profile $\{\widehat{g}(k_x, k_y, t_i(k_y))\}_{k_x=-N,\ldots,N-1}$ is obtained, for fixed k_y, at the rescaled time markers $t_i(k_y)$, for $i = 1, \ldots, N_{pr}$. The rescaled time markers only depend on the variable

k_y. This assertion holds because the time needed to measure a profile was, until now, not taken into account. For later purposes we want to distinguish the measurement times of samples within a profile. Therefore we want to express the dependence of the time markers on both variables k_x and k_y. Denoting the pair (k_x, k_y) as $\mathbf{k}$, the notation $\{t_{\mathbf{k},i}\}$ is used for the rescaled time markers. Define the index set $\mathbb{I}$ by $\mathbb{I} := \{1, 2, ..., N_{pr}\}$.

The problem formulation for dynamic MRI is as follows. Define the sequence $\{g_{\mathbf{k},i}\}$ by

$$g_{\mathbf{k},i} := \hat{g}(\mathbf{k}, t_{\mathbf{k},i}), \quad \mathbf{k} \in \mathbb{K}, i \in \mathbb{I}. \tag{0.6}$$

Determine a function $f : D \times J \rightarrow \mathbb{R}$ such that

$$\hat{f}(\mathbf{k}, t_{\mathbf{k},i}) = g_{\mathbf{k},i}, \quad \mathbf{k} \in \mathbb{K}, i \in \mathbb{I}. \tag{0.7}$$

The sequence $\{g_{\mathbf{k},i}\}$ is called *data*. In general, a solution f to problem (0.7) is not unique and will not be equal to the function g from which the data have been derived, because g is not uniquely determined by a finite number of Fourier coefficients sampled at rescaled time markers. A solution f to (0.7) is called a *reconstruction*. The inversion problem (0.7) is called *mixed Fourier interpolation problem*.

In the remainder of this section we give the intuitive idea how problem (0.7) can be solved. It is important to note that in general the rescaled time markers do not coincide with the phases at which the reconstructed images of the model heartbeat are desired. These phases are $\phi_l := l/L$ for $l = 0, ..., L-1$. The following picture illustrates the distribution of the relative time markers in the unit heart interval J and the corresponding profiles for two different values of k_y. The positions of the relative time markers are indicated by tick marks, the phases by bold tick marks and the data by '•'-marks. Note that one '•' in the picture denotes a profile.

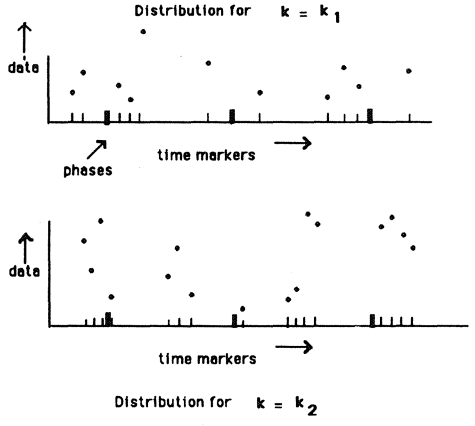

Figure 0.8. Distribution of relative time markers and data for two distinct values of k_y.

For a fixed value of k_y a sequence of profiles at relative time markers is available. By means of interpolation techniques the profile at the desired phase ϕ_l can be approximated, Figure (0.9). This procedure is repeated for k_y from $-N$ up to $N-1$. In this manner an

array of $N \times N$ Fourier coefficients is filled at each phase ϕ_l in the unit RR-interval. The images at the phases to be displayed are obtained by Fourier inversion.

In this tract we will use interpolation by spline functions of order 1, order 3 and bandlimited functions and we prove that these methods are optimal. The use of bandlimited functions is motivated by the assumption that the motion of the heart does not contain arbitrarily high frequencies. The practical importance of splines is the motivation for their use.

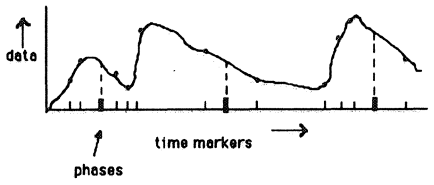

Figure 0.9. Evaluation of interpolation curve at the phases ϕ_l

Note that the algorithm to solve problem (0.7) is in this form well-suited for implementation on a parallel computer. For each value of k_y one has to evaluate the corresponding interpolation curve, which can be done separately by the different processors.

6. Guide for the reader

This tract consists of two parts. The first part covers the mathematics of dynamic MRI, giving a Hilbert space setting for the reconstruction problem, finding solutions reconstruction techniques, and proving stability of the solutions under perturbation of the data and time markers. The second part can be read independently of the first part. It covers the physical aspects of MRI, presents simulations for reconstruction from test-data and MR-data, and states conclusions about the performance of the different reconstruction methods.
Since the mathematical problem under consideration is a model for dynamic MRI- reconstruction, the relevant mathematical questions arise from criteria which are important in practice. Section 5 in this introduction discusses the choice of the values of the parameters N and N_{pr}. The performance between the several reconstruction algorithms is compared for fixed values of N and N_{pr}.

About Part One

The intuitive idea for solving the mixed Fourier interpolation problem is given in the previous section, but there are still many unsolved questions.

- Does a solution always exist?
- Is this solution unique?
- If not, is it possible to select an optimal solution?
- Does it make sense to use interpolation in the Fourier domain?

It is clear that these questions can only be answered after an appropriate mathematical setting has been chosen.

The mixed Fourier interpolation problem (0.7) is studied within the theoretical framework of Hilbert spaces in Part One of this tract. One of the most important examples of a Hilbert space is the space of L^2-functions. For purposes of image analysis this may be a suitable space, because the difference of two digital images on a computer display can be expressed as the sum over all pixels of the squares of the grey value-differences. The motivation for choosing Hilbert spaces is that on one hand it allows a theoretical framework to answer the questions above, whereas on the other hand the results of this setting are still concrete enough for practical purposes.

The mixed Fourier interpolation problem (0.7) is considered in the setting of the L^2-space of *vector valued functions*: $L^2(D,\mathcal{H})$. Here (D,μ) is a finite measure space and $\mathcal{H}$ is a Hilbert space with inner product $\langle\ ,\ \rangle$. A vector valued function is a function that maps elements x of D into the space $\mathcal{H}$, i.e. $f(x) \in \mathcal{H}$. For our purposes it is assumed that $\mathcal{H}$ consists of time dependent functions. So, $f(x)$ is a function of time denoted as $t \rightarrow f(x,t)$. The inner product of the Hilbert space $L^2(D,\mathcal{H})$ is denoted by $\langle\langle\ ,\ \rangle\rangle$.
The main theme is to find a solution $f \in L^2(D,\mathcal{H})$ of the mixed Fourier interpolation problem (0.7) and to analyze stability of this solution. In this dissertation we solve the mixed Fourier interpolation problem in the case of both finite and infinite index sets $\mathbb{K}$ and $\mathbb{I}$. For $\mathcal{H}$ we either take the space of bandlimited functions $\mathbb{P}_r$ or the space of odd order polynomial splines $\mathcal{K}^{2n-1}$. In this manner the model heartbeat is mathematically represented as a vector valued function.

The organization of this part is as follows. Chapter I defines the notions of Riesz-Fischer system, Riesz basis and Bessel system in terms of an orthonormal basis $\{h_i\}$ for a Hilbert space $\mathcal{H}$. Furthermore, it gives relevant subjects from Hilbert space theory, such as linear operators, the inverse of an operator, direct sums of Hilbert spaces and Tychonov-Phillips regularization.

Chapter II introduces the L^2-space of $\mathcal{H}$ valued functions $L^2(D,\mathcal{H})$. It provides criteria such that a system of the form $\{e_{\mathbf{k}}\varphi_{\mathbf{k},i}\}$ is a Riesz-Fischer system, a Riesz basis or a Bessel system in $L^2(D,\mathcal{H})$. Here $\{e_{\mathbf{k}}\}$ is an orthonormal basis for $L^2(D)$ and $\{\varphi_{\mathbf{k},i}\}$ is a sequence of elements of $\mathcal{H}$. By the notation $e_{\mathbf{k}}\varphi_{\mathbf{k},i}$ we denote the $\mathcal{H}$-valued function $x \rightarrow e_{\mathbf{k}}(x)\ \varphi_{\mathbf{k},i} \in \mathcal{H}$, for $x \in D$. In this chapter an $\mathcal{H}$-valued integral, called *Pettis integral*, is introduced.

Chapter III deals with conditions for existence, unicity or minimum norm property of solutions of moment problems in Hilbert space. Given are the *data* $\{g_i\}$ and a system of vectors $\{\varphi_i\} \subset \mathcal{H}$. A moment problem consists in finding an element f of a Hilbert space $\mathcal{H}$ such that

$$\langle f, \varphi_i \rangle_{\mathcal{H}} = g_i, \quad i \in \mathbb{I}.$$

We give necessary and sufficient conditions for the existence and unicity of a solution of the moment problem.

In Chapter IV it is shown that the mixed Fourier interpolation problem (0.7) is a special type of moment problem in $L^2(D,\mathcal{H})$, called *mixed Fourier moment problem*. This problem consists of finding an element $f \in L^2(D,\mathcal{H})$ such that

$$\langle \widehat{f}(\mathbf{k}), \varphi_{\mathbf{k},i} \rangle = g_{\mathbf{k},i}, \quad \mathbf{k} \in \mathbb{K}, i \in \mathbb{I}, \tag{0.8}$$

where the system of *point evaluation functionals* $\{\varphi_{\mathbf{k},i}\} \subset \mathcal{H}$ is such that

$$\widehat{f}(\mathbf{k}, t_{\mathbf{k},i}) = \langle \widehat{f}(\mathbf{k}), \varphi_{\mathbf{k},i} \rangle. \tag{0.9}$$

By this relation it follows that a solution of problem (0.8) is also a solution of the mixed Fourier interpolation problem (0.7).

The notion of Fourier coefficient of f is more general here than in Section 5. Here it is defined as

$$\hat{f}(\mathbf{k}) := \int_D f(x)\overline{e_{\mathbf{k}}(x)}d\mu(x), \tag{0.10}$$

where $\{e_{\mathbf{k}}(x)\}$ is an orthonormal basis for $L^2(D)$. The integral in (0.10) is the *Pettis integral* which is defined in Chapter II.

It is shown that problem (0.8) is equivalent to the following moment problem: find a function $f \in L^2(D,\mathcal{H})$ such that

$$\langle\langle f, e_{\mathbf{k}}\varphi_{\mathbf{k},i}\rangle\rangle = g_{\mathbf{k},i}, \quad \mathbf{k} \in \mathbb{K}, i \in \mathbb{I}. \tag{0.11}$$

The theory of moment problems from Chapter III can then be used to solve the mixed Fourier interpolation problem.

Chapter V considers various errors encountered in practice, e.g. the aliasing error, the time jitter error and the amplitude error. In practice, a reconstruction method is only useful if small errors in the data or in the time markers yield small errors in the solution. It turns out in Chapter V that the the mixed problem is stable for perturbation of the data and the time markers in this sense.

The *truncation error* is not considered in this tract. The truncation error is caused by reconstructing a function from a finite data set instead of a required countable data set. Theorem III.2.2 shows that under certain conditions the minimum norm solution corresponding to a finite data set of any moment problem in a Hilbert space converges to the unique solution corresponding to a countable data set. In practice however, physical and not mathematical arguments determine the optimal choice of the parameters N_{pr} and N. So, the value of these parameters cannot be chosen arbitrarily high.

About Part Two

The organization of Part Two is as follows. Chapter VI explains the principles and acquisition methods of dynamic MRI. Examples showing how to compute a solution of the mixed Fourier interpolation problem (0.7) by various reconstruction algorithms are followed by a comparison between these methods. In order to test the performance of different algorithms, the structure and motion of the beating human heart are simulated by a sequence of test images at consecutive phases. These images consist of several solid ellipses, displayed on a computer screen. In this manner the bone structures of the chest and spine are imitated. Ellipses varying in time are taken to imitate a heart-like structure. Then the MRI-data collection strategy is simulated for these test images, followed by application of the several reconstruction methods. Finally the reconstructed images are compared with the original test image at the corresponding phases. We also compute the L^2-difference of the reconstructions with the original. The conclusion is that reconstruction by means of first order and third order splines compared to the other methods perform best in this test situation.

The performance of these methods in practice is shown by reconstruction of MR-data obtained by the Gyroscan S-15, an MR-scanner of Philips Medical Systems. Conclusions about the image quality of the reconstructions of the beating human heart are given at the end of Chapter VI. It turns out that no reconstruction method prevails over the other methods in practice.

In the practice of MRI many error sources exist perturbing the measurements. In Section 2 we mentioned the most important sources. For example, the measured Fourier coefficients

are perturbed by thermal noise (see Section 2). Another error is due to the assumption that the rescaling is linear on each RR-interval. Since the time-stretching algorithm is in general only an approximation of the real situation, the positions of the rescaled time markers are likely to be incorrect. The performance of the reconstruction algorithms when applied to perturbed Fourier coefficients and incorrectly rescaled time markers is the subject of Chapter VII.

These effects are simulated by perturbation of the data and rescaled time markers of the test images followed by application of the several reconstruction techniques. The theoretical conclusions of the error estimates of Chapter V are in this manner illustrated by reconstructions of test images in the case of perturbed Fourier coefficients and perturbed rescaled time markers. The effect of the different kinds of perturbations on the images is discussed. One of the conclusions of Chapter VII is that the reconstruction by means of order 3 reconstruction is ill-conditioned for perturbation of the relative time markers.

A final, short Section, puts the conclusions presented in Chapters VI and VII together and contains some suggestions for possible future directions for improving the quality of the reconstructions.

Part One

Moment Problems in Hilbert Space

This part consists of five chapters and deals with solvability conditions and stability of several moment problems in a Hilbert space.

Chapters one and two are of a preliminary nature introducing basic theory, notation and terminology.
The subject of chapter one is Hilbert spaces, linear operators, systems of vectors and Tychonov-Phillips regularization. References for Hilbert spaces and linear operators are Conway [15], Gohberg and Krein [19], Gohberg and Goldberg [18], Goldberg [20] and Rudin [45] [46]. For a treatment of regularization see Groetsch [22], Morozov [41] and Louis [38]. Riesz bases, Bessel systems and Riesz-Fischer systems are introduced in Young [55], Higgins [23] and Gohberg and Krein [19].

The second chapter deals with the L^2 space of vector-valued functions $L^2(D,\mathcal{H})$, see Hille and Phillips [24], Balakrishnan [3] and Sz-Nagy and Foias [53]. The results in the section II.2 about Bessel systems, Riesz-Fischer systems and Riesz bases in the space $L^2(D,\mathcal{H})$ appear to be new.

Existence and uniqueness of a solution of the moment problem is the subject of Chapter three. If the moment problem lacks a solution, then a generalized notion of solution is introduced, which may be stabilized by a regularization technique, where we use Tychonov-Phillips regularization.
The theory of moment problems is dealt with in the following books. Akhiezer [2] gives an overview of several types of moment problems. The theory of the generalized (minimum norm) solution corresponding to the moment problem in a Hilbert space is applied by Bertero, de Mol and Pike [5] [6]. Young [55] applies the theory of Riesz bases and Riesz-Fischer systems to the moment problem in a Hilbert space. The moment problem in Hilbert spaces with reproducing kernel is considered by Shapiro [48] and Landau [32] gives an overview of applications and of the theory of moment problems.

The results from section III.1 can mainly be found in Young [55], except for regularization of the moment problem in the case of Bessel systems, Formula's (III.1.5) and (III.1.6) and Theorem III.1.5. The results of section III.2 appear to be new. However, the technique

applied there has been used earlier by Natterer in [43] to approximate a solution of an operator equation. The mixed type of moment problem in section III.3 has not been considered before. The results obtained there are derived by means of the theory of section III.1 and of Chapter II.

It turns out that a moment problem of mixed type, called the mixed Fourier moment problem, is important for practical applications (as is explained in Part two). Chapters four and five deal with existence, uniqueness and stability of solutions of the mixed Fourier interpolation problem, after restating it as mixed Fourier moment problem. The results developed in these chapters are used in Part two.

The material of sections IV.1 and IV.2 can be found in Young [55], except for the estimates of the norms of the operators R and T in Theorems IV.2.4 and IV.2.6. The result of Theorem IV.2.2 follows directly from Lemma IV.2.1, but it seems to be new. The main idea of section IV.3 is to be found in Bertero, de Mol and Pike [5], but here slightly different definitions are used. The estimates (IV.3.2) and (IV.3.3) appear to be new. Section IV.5 is an application of Chapter III.

As far as I know error estimates (Chapter V) for the moment problem and the mixed Fourier interpolation problem have never been considered upto this extent. The proofs of Lemma's V.2.2 and V.2.6 are standard.

Chapter I

Basic Properties of Hilbert Spaces

This chapter gives a survey of that part of the theory of Hilbert spaces which is relevant for our purposes.

The first section deals with linear operators between Hilbert spaces. The inverse and Moore-Penrose inverse are introduced in the second section. In section three we consider direct sums of Hilbert spaces and in the fourth section we study systems of vectors. The last section pays attention to Bessel systems, Riesz-Fischer systems and Riesz bases.

I.1. Linear Operators

Let $\mathcal{G}$ and $\mathcal{H}$ be Hilbert spaces over the complex numbers $\mathbb{C}$ with corresponding inner products $\langle\ ,\ \rangle_{\mathcal{G}}$ and $\langle\ ,\ \rangle_{\mathcal{H}}$. We will drop the subscripts if this does not cause confusion. The *domain* of definition of an operator T from $\mathcal{G}$ into $\mathcal{H}$ is denoted by $\mathrm{D}(T)$. Note that $\mathrm{D}(T) \subset \mathcal{G}$. Most of the time, however, we will consider bounded linear operators. In that case we can extend the operator T to the closure of its domain, which is itself a Hilbert space. Without loss of generality we then assume that $\mathrm{D}(T) = \mathcal{G}$.

The *null space* of T is

$$\mathcal{N}(T) := \{g \in \mathrm{D}(T) \mid Tg = 0\},$$

and its *range* is

$$\mathcal{R}(T) := \{Tg \mid g \in \mathrm{D}(T)\}.$$

The *norm* of a bounded linear operator T is defined by

$$\|T\| := \sup\{\ \|Tg\|_{\mathcal{H}} \mid\ g \in \mathrm{D}(T), \|g\|_{\mathcal{G}} = 1\}.$$

Let $T : \mathrm{D}(T) \to \mathcal{H}$ be a one-to-one linear operator. The *inverse* of T, written as T^{-1}, is the mapping from the subspace $\mathcal{R}(T)$ into $\mathcal{G}$ given by $T^{-1}(Tg) = g$, for $g \in \mathrm{D}(T)$. A bounded linear operator $T : \mathcal{G} \to \mathcal{H}$ is called *invertible* if the inverse $T^{-1} : \mathcal{H} \to \mathcal{G}$ exists and is a bounded linear operator.

The *adjoint* of a bounded linear operator $T : \mathcal{G} \to \mathcal{H}$ is a bounded linear operator $T^* : \mathcal{H} \to \mathcal{G}$ which satisfies

$$\langle Tg, h\rangle_{\mathcal{H}} = \langle g, T^*h\rangle_{\mathcal{G}}, \quad g \in \mathcal{G}, h \in \mathcal{H}.$$

Moreover $(T^*)^* = T$ and $\|T\| = \|T^*\|$. If T is a bounded linear invertible operator, then T^* is invertible and

$$(T^*)^{-1} = (T^{-1})^*.$$

The operator $T^*\ T$ has norm $\|T^*\ T\| = \|T\|^2$. For,

$$\|Tg\|^2_{\mathcal{H}} = \langle Tg, Tg\rangle_{\mathcal{H}} = \langle T^*\ Tg, g\rangle_{\mathcal{G}} \leq$$

$$\leq \|T^*\ T\|\|g\|^2_{\mathcal{G}} \leq \|T^*\|\ \|T\|\|g\|^2_{\mathcal{G}} = \|T\|^2\|g\|^2_{\mathcal{G}}.$$

The result follows by taking the supremum over $g \in \mathcal{G}$ such that $\|g\|_{\mathcal{G}} = 1$.

We have the following relations,

$$\mathcal{N}(T^*) = \mathcal{R}(T)^{\perp}$$

$$\mathcal{N}(T^*)^{\perp} = \overline{\mathcal{R}(T)}$$

Here $\overline{M}$ denotes the norm closure of a subspace M of a Hilbert space $\mathcal{H}$ and $M^{\perp}$ denotes the annihilator,

$$M^{\perp} := \{h \in \mathcal{H} \mid \langle m, h\rangle_{\mathcal{H}} = 0, \quad m \in M\ \}.$$

A useful property is closedness of an operator.

Definition 1.1 . A linear operator $T : \mathrm{D}(T) \to \mathcal{H}$ is called *closed* if for all sequences $\{g_n\} \in \mathrm{D}(T)$ such that $\lim_{n\to\infty} g_n = g$ and $\lim_{n\to\infty} Tg_n = h$ it follows that $g \in \mathrm{D}(T)$ and $Tg = h$.

Theorem 1.2 *Closed graph theorem .*
If $T : \mathcal{G} \to \mathcal{H}$ is closed, then T is bounded.

For any fixed $g \in \mathcal{H}$, the operator $T : \mathcal{H} \to \mathbb{C}$ given by

$$Th := \langle h, g \rangle_{\mathcal{H}}, \quad h \in \mathcal{H}$$

defines a bounded linear functional, with $\|T\| = \|g\|_{\mathcal{H}}$. The converse is also true (cf. Goldberg [20]. Theorem 1.7.18, p. 38):

Theorem 1.3 *Riesz representation theorem .*
If T is a bounded linear functional on a Hilbert space $\mathcal{H}$, then there exists a unique element $g \in \mathcal{H}$ such that

$$Th = \langle h, g \rangle_{\mathcal{H}}, \quad h \in \mathcal{H}.$$

Moreover $\|T\| = \|g\|_{\mathcal{H}}$.

An application of the Riesz representation theorem is found in Hilbert spaces with reproducing kernel. A Hilbert space $\mathcal{H}$ of functions $f : \mathbb{R} \to \mathbb{C}$ is a *Hilbert space with reproducing kernel* (also called reproducing kernel Hilbert space), if there exists a function $k : \mathbb{R}^2 \to \mathbb{C}$ such that

(i) $k(t, .) \in \mathcal{H}$, for all $t \in \mathbb{R}$.
(ii) $f(t) = \langle f(.), k(t, .) \rangle_{\mathcal{H}}$, for all $f \in \mathcal{H}$.

It follows from the definition that the reproducing kernel k is unique. Namely, if k and h are two reproducing kernels, then

$$h(t, s) = \langle h(t, \cdot), k(s, \cdot) \rangle = \overline{\langle k(s, \cdot), h(t, \cdot) \rangle} = \overline{k(s, t)} =$$

$$\overline{\langle k(s, \cdot), k(t, \cdot) \rangle} = \langle k(t, \cdot), k(s, \cdot) \rangle = k(t, s).$$

If $\mathcal{H}$ has the property that for each $t \in \mathbb{R}$ there exists a $C_t \in \mathbb{R}^+$ such that for all $f \in \mathcal{H}$,

$$|f(t)| \leq C_t \|f\|_{\mathcal{H}}, \tag{1.1}$$

then $\mathcal{H}$ is a Hilbert space with reproducing kernel. For, the point evaluation functional $\mathcal{E}_t f := f(t)$ is bounded by estimate (1.1). By the Riesz representation theorem it follows that (for fixed $t \in \mathbb{R}$) there exists a unique $g_t \in \mathcal{H}$ such that

$$\mathcal{E}_t f = \langle f, g_t \rangle_{\mathcal{H}}.$$

The reproducing kernel is

$$k(t, s) := \langle g_t, g_s \rangle_{\mathcal{H}}.$$

The converse statement is also true: if $\mathcal{H}$ has a reproducing kernel, then by the Cauchy-Schwarz inequality (1.1) is satisfied.

I.2. Invertibility of linear operators and regularization

Let $T : \mathcal{H} \to \mathcal{H}$ be a linear operator. The following theorem provides a condition for T to be invertible. I is the identity operator on $\mathcal{H}$.

Theorem 2.1 . *T is invertible if $\|I - T\| < 1$. Moreover,*

$$\|T^{-1}\| \leq \frac{1}{1 - \|I - T\|}.$$

An operator T on $\mathcal{H}$ is called *positive* (*strictly positive*) if $\langle Th, h\rangle_{\mathcal{H}} \geq 0$ (> 0), for all $h \in \mathcal{H}$, $h \neq 0$. Note that a strictly positive operator always is invertible.

Before introducing the generalized inverse, we define the direct sum of two (not necessarily closed) linear subspaces $M, N \subset \mathcal{H}$ with $M \cap N = \{0\}$ as

$$M \oplus N := \{m + n \mid m \in M, n \in N\}.$$

The following result gives a direct-sum decomposition of a Hilbert space.

Theorem 2.2 . *If M is a closed linear subspace of a Hilbert space $\mathcal{H}$, then*

$$\mathcal{H} = M \oplus M^{\perp}.$$

Let $T : \mathcal{G} \to \mathcal{H}$ be a bounded linear operator. Suppose we want to find $g \in \mathcal{G}$ satisfying

$$Tg = h,$$

where $h \in \mathcal{H}$ is given. If T is invertible, then this problem is solvable, and the solution depends continuously on the data h. In this case the problem is called *well-posed* (in the sense of Hadamard). Otherwise it is called *ill-posed*, i.e. if the inverse of T either is not defined on the whole space, or is not continuous. We circumvent the difficulties of an ill posed problem as follows. First we define a substitute for a solution (if there is none) by taking the minimizer of $\|Tg - h\|$. This makes sense if $h \in \Re(T) \oplus (\Re(T))^{\perp}$. Then we dispose of a possible non-uniqueness by choosing among all minimizers the one with the smallest norm (i.e. we choose the solution lying in $\mathcal{N}(T)^{\perp}$). This well-defined element of $\mathcal{H}$ is called the *Moore Penrose solution* of the problem, denoted by T^+h. The linear operator $T^+ : \mathrm{D}(T^+) \to \mathcal{G}$ is called the *Moore-Penrose inverse*, where $\mathrm{D}(T^+) := \Re(T) \oplus \Re(T)^{\perp} \subset \mathcal{H}$. It follows by Theorem 2.2 that $\mathrm{D}(T^+)$ lies dense in $\mathcal{H}$, i.e. T^+ is called a *densely defined operator.*

We summarize some results on the generalized inverse (cf. Groetsch [22]).

Proposition 2.3 . *Let $T : \mathcal{G} \to \mathcal{H}$ be a bounded linear operator. Then the following holds.*

(i) For $h \in \mathrm{D}(T^+)$, $f^+ := T^+h$ is the unique element in $\mathcal{N}(T)^{\perp}$ which satisfies the normal equations:

$$T^*Tf = T^*h.$$

(ii) T^+ is a closed linear operator.
(iii) T^+ is a bounded linear operator, if and only if $\Re(T)$ is closed.
(iv) $\Re(T^+) = \mathcal{N}(T)^{\perp}$.
(v) $\mathcal{N}(T^+) = \Re(T)^{\perp}$.

In general T^+ is not a bounded linear operator. To restore the boundedness, we introduce the notion of regularization of T^+.

Definition 2.4 . A family $\{T^\gamma\}_{\gamma>0}$ of bounded linear operators from $\mathcal{H}$ to $\mathcal{G}$ is called a *regularization* of T^+ if

$$\lim_{\gamma \downarrow 0} T^\gamma h = T^+ h, \quad h \in \mathrm{D}(T^+).$$

In the sequel we use Tychonov-Phillips regularization:

$$T^\gamma := (T^*T + \gamma I)^{-1} T^* = T^*(TT^* + \gamma I)^{-1}. \tag{2.1}$$

Note that for $\gamma > 0$, the operator $T^*T + \gamma I$ is invertible, since it is strictly positive.

Proposition 2.5 . *$f^\gamma := T^\gamma h$ is the unique minimizer of the expression*

$$\|Tf - h\|^2_{\mathcal{H}} + \gamma \|f\|^2_{\mathcal{G}}, \quad \text{for } f \in \mathcal{G}. \tag{2.2}$$

Proof:

Fix $\gamma > 0$ and define $C := T^*T + \gamma I$. C is a strictly positive operator, so $C^* = C$ and C is invertible. From the definition it follows that $Cf^\gamma = T^*h$. Hence

$$\|Tf - h\|^2_{\mathcal{H}} + \gamma \|f\|^2_{\mathcal{G}} = \langle T^*Tf, f\rangle_{\mathcal{G}} - \langle T^*h, f\rangle_{\mathcal{G}} - \langle f, T^*h\rangle_{\mathcal{G}} - \|h\|^2_{\mathcal{H}} - \gamma\|f\|^2_{\mathcal{G}} =$$

$$= \langle Cf, f\rangle_{\mathcal{G}} - \langle Cf^\gamma, f\rangle_{\mathcal{G}} - \langle f, T^*h\rangle_{\mathcal{G}} + \|h\|^2_{\mathcal{H}} =$$

$$= \langle C(f - f^\gamma), f\rangle_{\mathcal{G}} - \langle (C^{-1})^* Cf, T^*h\rangle_{\mathcal{G}} + \|h\|^2_{\mathcal{H}} =$$

$$= \langle C(f - f^\gamma), f - f^\gamma\rangle_{\mathcal{G}} - \langle Cf^\gamma, f^\gamma\rangle_{\mathcal{G}} + \|h\|^2_{\mathcal{H}}.$$

Since C is a positive operator (2.2) attains its unique minimum for $f = f^\gamma$. □

That $\{T^\gamma\}$ as given by (2.1) is indeed a regularization is proved in Natterer [42] pp. 88-89:

Proposition 2.6 . $\lim_{\gamma \downarrow 0} \|T^\gamma h - T^+ h\|_{\mathcal{G}} = 0$, *for* $h \in \mathrm{D}(T^+)$.

I.3. Direct products

Let $\mathbb{K}$ be a countable index set. Let $\mathcal{H}_\kappa$ be a collection of Hilbert spaces and let for each $k \in \mathbb{K}$, M_κ be a (not necessarily closed) linear subspace of $\mathcal{H}_\kappa$.

Definition 3.1 . The *direct product* $\otimes_{\kappa\in K} M_\kappa$ is the collection of sequences $h := \{h_\kappa\}_{\kappa\in K}$, where $h_\kappa \in M_\kappa$, satisfying $\|h\|^2_\otimes := \sum_{\kappa\in K} \|h_\kappa\|^2_{\mathcal{H}_\kappa} < \infty$.

Vector addition and scalar multiplication on $\otimes M_\kappa$ are defined componentwise. The direct product $\otimes_{\kappa\in K}\mathcal{H}_\kappa$ is a Hilbert space with inner product,

$$\langle f, h\rangle_\otimes := \sum_{\kappa\in K} \langle f_\kappa, h_\kappa\rangle_{\mathcal{H}_\kappa}$$

for $f, h \in \otimes_{\kappa\in K}\mathcal{H}_\kappa$.
If all the spaces $\mathcal{H}_\kappa$ are the same, we define the following.

Definition 3.2 . $\ell^2(\mathbb{K}, \mathcal{H}) := \otimes_{\kappa\in K}\mathcal{H}$.

Note that the direct product of two spaces $\mathcal{H}_1$ and $\mathcal{H}_2$ can be identified with the direct sum (cf. Section 2). For, define $M := \{\{h,0\} \mid h \in \mathcal{H}_1\}$ and $N := \{\{0,h\} \mid h \in \mathcal{H}_2\}$. Then $\mathcal{H}_1 \otimes \mathcal{H}_2 = M \oplus N$.

Suppose $\{\mathcal{G}_\kappa\}_{\kappa\in K}$ and $\{\mathcal{H}_\kappa\}_{\kappa\in K}$ are families of Hilbert spaces. Introduce $\mathcal{G} := \otimes_{\kappa\in K}\mathcal{G}_\kappa$ and $\mathcal{H} := \otimes_{\kappa\in K}\mathcal{H}_\kappa$. We want to consider linear operators between $\mathcal{G}$ and $\mathcal{H}$. Suppose $\{T_\kappa\}_{\kappa\in K}$ is a family of bounded linear operators, where $T_\kappa : \mathcal{G}_\kappa \to \mathcal{H}_\kappa$. Assume that $\{T_\kappa\}$ is a ***uniformly bounded family***, i.e.

$$\sup_{\kappa\in K}\|T_\kappa\| < \infty. \tag{3.1}$$

Define $\mathcal{T} : \mathcal{G} \to \mathcal{H}$ by

$$\mathcal{T}g := \{T_\kappa g_\kappa\}_{\kappa\in K}, \quad g \in \mathcal{G}. \tag{3.2}$$

We denote (3.2) symbolically by

$$\mathcal{T} = \{T_\kappa\}_{\kappa\in K}. \tag{3.3}$$

The adjoint of such an operator $\mathcal{T}$ is

$$\mathcal{T}^* = \{T_\kappa^*\}_{\kappa\in K}.$$

There exists a criterion to check the boundedness of a linear operator $\mathcal{T} : \mathcal{G} \to \mathcal{H}$ of the form (3.3), see Conway [15] p. 30 Exercise 12.

Theorem 3.3 . *Let $\{T_\kappa\}_{\kappa\in K}$ be a family of bounded linear operators, where for each $\kappa \in K$, T_κ acts from $\mathcal{G}_\kappa$ to $\mathcal{H}_\kappa$. Let $\mathcal{G} := \otimes\mathcal{G}_\kappa$ and $\mathcal{H} := \otimes\mathcal{H}_\kappa$. The linear operator $\mathcal{T} : \mathcal{G} \to \mathcal{H}$ given by (3.3) is bounded if and only if $\{T_\kappa\}$ is uniformly bounded. In this case*

$$\|\mathcal{T}\| = \sup_{\kappa\in K}\|T_\kappa\|.$$

We want to express the null space and the range of an operator $\mathcal{T}$ of the form (3.3) in terms of the null spaces and ranges of the operators T_κ. If $\mathcal{T}$ is of the form (3.3) and satisfies the conditions of Theorem 3.3, then

$$\mathcal{N}(\mathcal{T}) = \otimes_{\kappa\in K}\mathcal{N}(T_\kappa).$$

Namely, $g \in \mathcal{N}(\mathcal{T})$ if and only if $\sum_{\kappa\in K}\|g_\kappa\|^2_{\mathcal{G}_\kappa} < \infty$ and $T_\kappa g_\kappa = 0$ for arbitrary $\kappa \in K$. This is the case if and only if $g \in \otimes_{\kappa\in K}\mathcal{N}(T_\kappa)$.
For the range of $\mathcal{T}$ such a statement is not true. If $\mathcal{T}$ satisfies the conditions of Theorem 3.3 we have the strict inclustion $\mathcal{R}(\mathcal{T}) \subset \otimes_{\kappa\in K}\mathcal{R}(T_\kappa)$.

Example 3.4 .

We give an example of a linear operator $\mathcal{T}$ of the form (3.3) such that the inclusion $\mathcal{R}(\mathcal{T}) \subset \otimes_{\kappa\in K}\mathcal{R}(T_\kappa)$ is strict. Let the index set $K = \mathbb{N}$. The operator T_κ on a Hilbert space $\mathcal{H}$ is given by

$$T_\kappa h := (1/\kappa)\, h, \quad \text{for } h \in \mathcal{H},$$

where $\kappa \in K$. Then the linear operator $\mathcal{T} := \{T_\kappa\}_{\kappa\in K}$ on $\ell^2(K,\mathcal{H})$ satisfies the conditions of Theorem 3.3. We have that

$$\mathcal{R}(\mathcal{T}) = \{g \in \ell^2(K,\mathcal{H}) \mid \sum_{\kappa\in K} \kappa^2\, \|g_\kappa\|^2 < \infty\}.$$

$\mathcal{R}(\mathcal{T}) \neq \ell^2(K,\mathcal{H})$, because if we fix $h \in \mathcal{H}$ with $\|h\| = 1$, then the sequence $\{(1/\kappa)h\}_{\kappa\in K}$ lies in $\ell^2(K,\mathcal{H})$ but does not lie in $\mathcal{R}(\mathcal{T})$. It is clear that $\mathcal{R}(T_\kappa) = \mathcal{H}$ and by definition $\otimes_{\kappa\in K}\mathcal{R}(T_\kappa) = \ell^2(K,\mathcal{H})$. Now we have shown that the inclusion is strict.

If T satisfies the conditions of Theorem 3.3, then we have

$$\Re(T)^{\perp} = \otimes_{\kappa\in K}(\Re(T_\kappa)^{\perp}).$$

For, by Section 1,

$$\Re(T)^{\perp} = \mathcal{N}(T^*) = \otimes_{\kappa\in K}\mathcal{N}(T_\kappa^*) = \otimes_{\kappa\in K}(\Re(T_\kappa)^{\perp}).$$

To characterize $\mathcal{N}(T)^{\perp}$ we prove the following lemma.

Lemma 3.5 . *Let M_κ be a collection of linear subspaces of Hilbert spaces $\mathcal{H}_\kappa$, i.e. for $\kappa \in \mathbb{K}$, $M_\kappa \subset \mathcal{H}_\kappa$. Then*

$$(\otimes_{\kappa\in K}M_\kappa)^{\perp} = \otimes_{\kappa\in K}(M_\kappa^{\perp}).$$

Proof:

$\subset$ Take $h \in (\otimes_{\kappa\in K}M_\kappa)^{\perp}$. So $\sum \|h_\kappa\|^2 < \infty$ and $0 = \langle h, m'\rangle_{\otimes}$ for all $m' \in \otimes M_\kappa$. Fix $\kappa \in \mathbb{K}$. Take $m \in M_\kappa$ arbitrarily and define $m' := \{m\delta_{\kappa\lambda}\}_{\lambda\in K}$. m' is the sequence with zero's everywhere, except at the κth coordinate which is m. Then

$$0 = \langle h, m'\rangle_{\otimes} = \sum_{\lambda\in K}\langle h_\lambda, m'_\lambda\rangle_{\mathcal{H}_\lambda} = \langle h_\kappa, m\rangle_{\mathcal{H}_\kappa}.$$

Hence $h_\kappa \in M_\kappa^{\perp}$, for all $\kappa \in \mathbb{K}$, so $h \in \otimes_{\kappa\in K}(M_\kappa^{\perp})$.

$\supset$ Suppose $h \in \otimes_{\kappa\in K}(M_\kappa^{\perp})$. So, $\sum_{\kappa\in K}\|h_\kappa\|^2_{\mathcal{H}_\kappa} < \infty$ and $h_\kappa \in M_\kappa^{\perp}$ for all $\kappa \in \mathbb{K}$. Hence for $g \in \otimes_{\kappa\in K}M_\kappa$ we obtain

$$\langle g, h\rangle_{\otimes} = \sum_{\kappa\in K}\langle g_\kappa, h_\kappa\rangle_{\mathcal{H}_\kappa} = 0.$$

It follows that $h \in (\otimes_{\kappa\in K}M_\kappa)^{\perp}$. □

It is now clear that

$$\mathcal{N}(T)^{\perp} = \otimes_{\kappa\in K}(\mathcal{N}(T_\kappa)^{\perp}).$$

We summarize the results:

Proposition 3.6 . *Let T be of the form $T = \{T_\kappa\}$, where $\{T_\kappa\}$ is a uniformly bounded family. For $\kappa \in \mathbb{K}$ fixed $T_\kappa : \mathcal{G}_\kappa \to \mathcal{H}_\kappa$. Then*

(i) $\Re(T) \subset \otimes_{\kappa\in K}\Re(T_\kappa)$.
(ii) $\Re(T)^{\perp} = \otimes_{\kappa\in K}(\Re(T_\kappa)^{\perp})$.
(iii) $\mathcal{N}(T) = \otimes_{\kappa\in K}\mathcal{N}(T_\kappa)$.
(iv) $\mathcal{N}(T)^{\perp} = \otimes_{\kappa\in K}(\mathcal{N}(T_\kappa)^{\perp})$.

We now want to consider the invertibility of operators T of the form (3.3). It is clear by Theorem 3.3 that a bounded linear operator T of the form (3.3) is invertible if all the operators T_κ are invertible and if $\{T_\kappa^{-1}\}$ is a uniformly bounded family. Moreover $T^{-1} : \mathcal{H} \to \mathcal{G}$ is

$$T^{-1} = \{T_\kappa^{-1}\}_{\kappa\in K}.$$

So, if T is of the form (3.3), its inverse T^{-1} can be found by computing for each $\kappa \in \mathbb{K}$ the inverse of T_κ. This decomposition for the inverse of T is important for practical purposes, since it implies that we only need the κth component T_κ^{-1} and h_κ of the operator T

and of the data h to compute the κth component of $T^{-1}h$. For the same reason we are interested in the decomposition of the Moore-Penrose inverse and of the Tychonov-Phillips regularization, which will be applied in Sections III.3 and IV.5.

Theorem 3.7 *Let $\{T_\kappa\}$ be a uniformly bounded family, where $T_\kappa : \mathcal{G}_\kappa \to \mathcal{H}_\kappa$. Let $\mathcal{G} := \otimes\mathcal{G}_\kappa$ and $\mathcal{H} := \otimes\mathcal{H}_\kappa$. If $T : \mathcal{G} \to \mathcal{H}$ is a bounded linear operator of the form (3.3) then $\mathrm{D}(T^+) \subset \otimes_{\kappa\in K}\mathrm{D}(T_\kappa^+)$. If in addition,*

$$\sum_{\kappa\in K} \|T_\kappa^+ h_\kappa\|^2 < \infty, \quad h \in \mathrm{D}(T^+), \tag{3.4}$$

then $T^+ : \mathrm{D}(T^+) \to \mathcal{G}$, is of the form

$$T^+ = \{T_\kappa^+\}_{\kappa\in K}.$$

Proof:

First we prove that $\mathrm{D}(T)^+)$ is a subset of $\otimes_{\kappa\in K}\mathrm{D}(T_\kappa^+)$. $\mathrm{D}(T^+) := \Re(T) \oplus \Re(T)^\perp$ and for $\kappa \in I\!K$ fixed, $\mathrm{D}(T_\kappa^+) = \Re(T_\kappa) \oplus \Re(T_\kappa)^\perp$. By Proposition 3.6 and by the distributivity of $\otimes$ and $\oplus$ it follows that

$$\mathrm{D}(T^+) \subset (\otimes\Re(T_\kappa)) \oplus (\otimes(\Re(T_\kappa)^\perp)) = \otimes(\Re(T_\kappa) \oplus \Re(T_\kappa)^\perp) = \otimes\mathrm{D}(T_\kappa).$$

Note that the operator $U := \{T_\kappa^+\}$ is well defined on $\mathrm{D}(T^+)$. Namely, let $h \in \mathrm{D}(T^+)$ be arbitrary, then by (3.4)

$$\|Uh\|_{\mathcal{H}}^2 = \sum_{\kappa\in K} \|T_\kappa^+ h_\kappa\|_{\mathcal{H}_\kappa}^2 < \infty.$$

Next we prove that T^+ is of the desired form. Let $h \in \mathrm{D}(T^+)$. For all $\kappa \in I\!K$, the term $T_\kappa^+ h_\kappa$ is the unique element of $\mathcal{N}(T_\kappa)^\perp \subset \mathcal{G}_\kappa$ that minimizes

$$\|T_\kappa f - h_\kappa\|_{\mathcal{H}_\kappa}^2, \quad \text{for } f \in \mathcal{G}_\kappa.$$

Since T is of the form (3.3), we have

$$\|Tg - h\|_{\mathcal{H}}^2 = \sum_{\kappa\in K} \|T_\kappa g_\kappa - h_\kappa\|_{\mathcal{H}_\kappa}^2, \quad g \in \mathcal{G}.$$

It follows that $\{T_\kappa^+ h_\kappa\}_{\kappa\in K}$ minimizes $\|Tg - h\|_{\mathcal{H}}$. Furthermore, by Proposition 3.6, $\{T_\kappa^+ h_\kappa\}_{\kappa\in K}$ lies in $\otimes_{\kappa\in K}(\mathcal{N}(T_\kappa)^\perp) = \mathcal{N}(T)^\perp$. But, by definition, T^+h is the unique minimizer of $\|Tg - h\|_{\mathcal{H}}$ which lies in $\mathcal{N}(T)^\perp$, whence $T^+ = \{T_\kappa^+\}$. □

We now give an example of a Moore-Penrose inverse which is of the form $T^+ = \{T_\kappa^+\}$.

Example 3.8 .

Let T be defined as in Example 3.4:

$$T := \{T_\kappa\},$$

where $T_\kappa := (1/\kappa)h$ for $h \in \mathcal{H}$. In Example 3.4 we showed that

$$\Re(T) = \{h \in \ell^2(I\!K, \mathcal{H}) \mid \sum_{\kappa\in K} \kappa^2\|h_\kappa\|^2 < \infty\}.$$

$\Re(T)^\perp = \{0\}$, because by the results of Section 1, $\Re(T)^\perp = \mathcal{N}(T^*) = \{0\}$. So, $\mathrm{D}(T^+) = \Re(T)$. It then follows from Example 3.4 that $\mathrm{D}(T^+)$ is strictly included in $\otimes_{\kappa\in K}\mathrm{D}(T_\kappa^+)$. It is clear that for $f \in \mathcal{H}_\kappa$, $T_\kappa^{-1}f = \kappa f = T_\kappa^+ f$, so

$$T^{-1}h = \{T_\kappa^{-1}h_\kappa\}_{\kappa\in K}, \quad \text{for } h \in \Re(T).$$

Note that the linear operator T^{-1} is not bounded on its domain, i.e. T is not invertible. We now have that T^+ is equal to T^{-1} on $\mathrm{D}(T^+)$, whence T^+ is of the desired form.

The following theorem gives a decomposition of the Tychonov-Phillips regularization. Its proof is analogous to that of Theorem 3.7.

Theorem 3.9 . *Let $\mathcal{G} := \otimes_{\kappa\in K}\mathcal{G}_\kappa$ and $\mathcal{H} := \otimes_{\kappa\in K}\mathcal{H}_\kappa$. Assume that $\{T_\kappa\}$ is a uniformly bounded family of operators and suppose $T : \mathcal{G} \to \mathcal{H}$ is of the form*

$$T = \{T_\kappa\}.$$

$\{T_\kappa^\gamma\}_{\gamma>0}$ denotes a family of Tychonov-Phillips regularizations, where (for each $\gamma > 0$ and for each $\kappa \in K$) $T_\kappa^\gamma : \mathcal{H}_\kappa \to \mathcal{G}_\kappa$ is the Tychonov-Phillips regularizer of T_κ^+. If for each $\gamma > 0$

$$\sum_{\kappa\in K} \|T_\kappa^\gamma h_\kappa\|^2 < \infty, \quad h \in \mathcal{H},$$

then the Tychonov-Phillips regularization $T^\gamma : \mathcal{H} \to \mathcal{G}$ of T^+ is of the form

$$T^\gamma = \{T_\kappa^\gamma\}_{\kappa\in K}, \quad \gamma > 0.$$

Proof:

Without loss of generality, we assume that $K = \mathbb{N}$. Denote the Tychonov-Phillips regularization of T^+ and T_κ^+ by $\{T^\gamma\}_{\gamma>0}$ and $\{T_\kappa^\gamma\}_{\gamma>0}$, respectively. Then by Proposition 2.5, $T^\gamma h$ with $h \in \mathcal{H}$ minimizes

$$\|Tf - h\|_{\mathcal{H}}^2 + \gamma\|f\|_{\mathcal{G}}^2, \quad \text{for } f \in \mathcal{G}$$

and for $\kappa \in K$ fixed, $T_\kappa^\gamma h$ with $h \in \mathcal{H}_\kappa$ minimizes

$$\|T_\kappa f - h\|_{\mathcal{H}_\kappa}^2 + \gamma\|f\|_{\mathcal{G}_\kappa}^2, \quad \text{for } f \in \mathcal{G}_\kappa.$$

The result follows by the relation

$$\|Tf - h\|_{\mathcal{H}}^2 + \gamma\|f\|_{\mathcal{G}}^2 = \sum_{\kappa\in K} \|T_\kappa f_\kappa - h_\kappa\|_{\mathcal{H}_\kappa}^2 + \gamma\|f_\kappa\|_{\mathcal{G}_\kappa}^2.$$

□

The following result summarizes Theorems 3.7, 3.8 and Proposition 2.6:

Theorem 3.10 . *Let $\{T_\kappa\}$ be a uniformly bounded family of linear operators with $T_\kappa : \mathcal{G}_\kappa \to \mathcal{H}_\kappa$. Denote $\mathcal{G} := \otimes_{\kappa\in K}\mathcal{G}_\kappa$ and $\mathcal{H} := \otimes_{\kappa\in K}\mathcal{H}_\kappa$ and suppose that $T : \mathcal{G} \to \mathcal{H}$ is of the form*

$$T = \{T_\kappa\}.$$

If for all $h \in \mathrm{D}(T^+)$

$$\sum_{\kappa\in K} \|T_\kappa^+ h_\kappa\|_{\mathcal{H}_\kappa}^2 < \infty,$$

then

$$\lim_{\gamma\downarrow 0} \|\{T_\kappa^\gamma h_\kappa\}_{\kappa\in K} - \{T_\kappa^+ h_\kappa\}_{\kappa\in K}\|_{\mathcal{G}} = 0.$$

I.4. Bases and biorthogonal systems

In this section we examine properties of systems of vectors in a Hilbert space.

Let $\{\varphi_i\}_{i\in I}$ be a system of vectors lying in a Hilbert space $\mathcal{H}$, where $I = \mathbb{N}$.

Definition 4.1 . The *span* of a system $\{\varphi_i\}_{i\in I}$ denoted by $\operatorname{span}\{\varphi_i\}_{i\in I}$ is the set of finite linear combinations of the φ_i.
A system $\{\varphi_i\}_{i\in I}$ is called *complete* if $\overline{\operatorname{span}}\{\varphi_i\}_{i\in I} = \mathcal{H}$. Here the bar denotes the norm closure.

Complete systems are characterized by the following result:

Proposition 4.2 . *The following statements are equivalent.*
(i) $\{\varphi_i\}_{i\in I}$ *is complete*
(ii) If $\langle h, \varphi_i\rangle_{\mathcal{H}} = 0$ *for all* $i \in I$, *then* $h = 0$.

Definition 4.3 . $\{\varphi_i\}_{i\in I}$ is a basis for $\mathcal{H}$ if any element $h \in \mathcal{H}$ can uniquely be written as

$$h = \sum_{i\in I} c_i\varphi_i, \tag{4.1}$$

for certain complex numbers c_i, $i \in I$. Here (4.1) converges in norm.

If in addition $\langle \varphi_j, \varphi_i\rangle_{\mathcal{H}} = \delta_{ij}$ for all $i, j \in I$, where δ is the Kronecker delta, then $\{\varphi_i\}$ is an *orthonormal basis.*

Theorem 4.4 . *If* $\{\varphi_i\}_{i\in I}$ *is an orthonormal basis for* $\mathcal{H}$, *then any* $h \in \mathcal{H}$ *can be represented as*

$$h = \sum_{i\in I}\langle h, \varphi_i\rangle\varphi_i.$$

Moreover

$$\|h\|^2 = \sum_{i\in I}|\langle h, \varphi_i\rangle|^2.$$

From the last equality it follows that for any $h \in \mathcal{H}$

$$\lim_{i\to\infty}\langle h, \varphi_i\rangle = 0. \tag{4.2}$$

A system $\{\varphi_i\}$ is called *independent* if for each $i \in I$ the vector φ_i is not contained in the closed linear span of the others.
If a system $\{\varphi_i\}_{i\in I}$ is a basis, then it is complete and independent. The converse is not true.

Example 4.5 .

Here we give an example of a system $\{\varphi_i\}_{i\in I}$ which is complete and independent, but which is not a basis. Let $\{h_i\}_{i\in I}$ be an orthonormal basis for $\mathcal{H}$. Define

$$\varphi_i := h_1 + h_{i+1}, \quad i = 1, 2, 3, \ldots.$$

We show that $\{\varphi_i\}$ is complete. Suppose that for $g \in \mathcal{H}$ holds that $\langle g, \varphi_i\rangle = 0$ for all $i \in I$. So, $\langle g, h_1\rangle = -\langle g, h_{i+1}\rangle$, for all $i \in I$. Since, by (4.2),

$$\lim_{i\to\infty}\langle g, h_i\rangle = 0,$$

it follows that $\langle g, h_i\rangle = 0$ for all $i \in I$. Hence $g = 0$. Next we prove that $\{\varphi_i\}$ is independent. Suppose $\{\varphi_i\}$ were not independent, say φ_1 lies in $\mathcal{H}_1 := \overline{\operatorname{span}}\{\varphi_2, \varphi_3, \ldots\}$.

Now define the bounded linear functional T on $\mathcal{H}$ by $Tg := \langle g, h_2 \rangle$ for $g \in \mathcal{H}$. By definition we have $T\varphi_1 = 1$ and $T_{|\mathcal{H}_1} \equiv 0$, which contradicts the boundedness of T. So, $\{\varphi_i\}$ must be independent. Finally we show that $\{\varphi_i\}$ cannot be a basis. Suppose it were a basis, then we could represent any element of $\mathcal{H}$ in the form (4.1), in particular

$$h_1 = \sum_{j \in I} c_j \varphi_j.$$

Compute, for $i > 1$, the inner products $\langle h_1, h_i \rangle$.

$$0 = \langle h_1, h_i \rangle = \sum_{j \in I} c_j \langle \varphi_j, h_i \rangle =$$

$$= \sum_{j \in I} c_j \langle h_1 + h_{j+1}, h_i \rangle = c_{i-1}.$$

Hence $c_i = 0$ for all $i \in \mathbb{I}$, so $h_1 = 0$. This is impossible, because $\{h_i\}_{i \in I}$ is a basis.

(Another example is found in Singer [49] Example 11.3, p. 359)

For orthonormal bases, however, such a counterexample cannot be found (cf. Gohberg [18] Theorem 11.3, p. 27):

Theorem 4.6 . *Let $\{\varphi_i\}_{i \in I}$ be an orthonormal system. $\{\varphi_i\}_{i \in I}$ is a basis if and only if $\{\varphi_i\}_{i \in I}$ is complete.*

Hilbert spaces with orthonormal bases are called *separable Hilbert spaces.* Important examples of such spaces are the following.

Example 4.7 .

Let $\mathbb{M}$ be a finite or countable index set. $\ell^2(\mathbb{M})$ consists of sequences of complex numbers $g := \{g_m\}_{m \in \mathbb{M}}$ such that

$$\|g\|^2_{\ell^2(\mathbb{M})} := \sum_{m \in \mathbb{M}} |g_m|^2 < \infty.$$

Note that $\ell^2(\mathbb{M})$ is equal to $\ell^2(\mathbb{M}, \mathcal{H})$ if $\mathcal{H} = \mathbb{C}$. It is a Hilbert space with inner product

$$\langle f, g \rangle_{\ell^2(\mathbb{M})} := \sum_{m \in \mathbb{M}} f_m \overline{g}_m,$$

where the bar denotes complex conjugation. The canonical orthonormal basis for $\ell^2(\mathbb{M})$ is $\{e_i\}_{i \in \mathbb{M}}$, with (for $m \in \mathbb{M}$)

$$(e_i)_m := \begin{cases} 0 \text{ if } m \neq i \\ 1 \text{ if } m = i \end{cases}.$$

Example 4.8 .

$L^2([-\pi, \pi]^n)$ consists of square integrable functions on the set $[-\pi, \pi]^n$ in $\mathbb{R}^n$. We sometimes write it as $L^2([-\pi, \pi]^n, \mathbb{C})$. It is a Hilbert space with inner product

$$\langle f, g \rangle_{L^2} := \int_{[-\pi, \pi]^n} f(x) \overline{g(x)} d\mu(x).$$

μ is the Lebesgue measure on $[-\pi,\pi]^n$. Define (for $\kappa \in \mathbb{Z}^n$) $e_\kappa \in L^2([-\pi,\pi]^n)$ by

$$e_\kappa(x) := (1/2\pi)^{n/2}\, e^{i\kappa x},$$

then $\{e_\kappa\}_{\kappa \in \mathbb{Z}^n}$ is the canonical orthonormal basis for $L^2([-\pi,\pi]^n)$. The κth Fourier coefficient of a function $f \in L^2([-\pi,\pi]^n)$ is defined as

$$\hat{f}(\kappa) := \langle f, e_\kappa \rangle_{L^2} = \int_{[-\pi,\pi]^n} f(x)\overline{e_\kappa(x)}d\mu(x).$$

By Theorem 4.4 we obtain the Fourier inversion formula

$$f = \sum_{\kappa \in \mathbb{Z}^n} \hat{f}(\kappa) e_\kappa,$$

and Parseval's relation

$$\|f\|^2_{L^2} = \sum_{\kappa \in \mathbb{Z}^n} |\hat{f}(\kappa)|^2.$$

In the preceding paragraphs we represented elements of Hilbert spaces in terms of orthonormal bases. Next we consider bases that are not (necessarily) orthonormal. For our purpose biorthogonal systems are important.

Definition 4.9 . Two systems $\{\varphi_i\}_{i\in I}$ and $\{\psi_i\}_{i\in I}$ are called *biorthogonal* if

$$\langle \varphi_i, \psi_j \rangle_{\mathcal{H}} = \delta_{ij}, \quad i,j \in I\!I.$$

We often say that $\{\psi_i\}$ is a biorthogonal system of $\{\varphi_i\}$. If $\{\varphi_i\}_{i\in I}$ is a basis, with biorthogonal system $\{\psi_i\}_{i\in I}$, then any $f \in \mathcal{H}$ can be written in the form

$$f = \sum_{i\in I} \langle f, \psi_i \rangle_{\mathcal{H}} \varphi_i. \tag{4.3}$$

The following theorem shows that in this case $\{\psi_i\}_{i\in I}$ is a basis too.

Theorem 4.10 . *If $\{\varphi_i\}_{i\in I}$ is a basis, with biorthogonal system $\{\psi_i\}_{i\in I}$, then $\{\psi_i\}$ is a basis and for any $f \in \mathcal{H}$,*

$$f = \sum_{i\in I} \langle f, \varphi_i \rangle \psi_i. \tag{4.4}$$

Proof:

We first show that any $f \in \overline{\text{span}}\{\psi_i\}$ can be written as (4.4). Introduce the linear operator

$$T_n f := \sum_{i=1}^{n} \langle f, \varphi_i \rangle \psi_i.$$

Then

$$T_n^* f := \sum_{i=1}^{n} \langle f, \psi_i \rangle \varphi_i.$$

Since $\{\varphi_i\}_{i\in I}$ is a basis, we have

$$\lim_{n\to\infty} T_n^* f = f.$$

By the uniform boundedness principle (cf. Gohberg [18] Theorem 4.4, p. 223) it follows that

$$\sup_{n\in I}\|T_n\| = \sup_{n\in I}\|T_n^*\| < \infty.$$

Take $f \in \overline{\text{span}}\{\varphi_i\}$ arbitrarily. We must show that $\lim_{n\to\infty}\|T_n f - f\| = 0$. For arbitrary $\epsilon > 0$, there exist an $m \in \mathbb{I}$ and a sequence $\{c_i\}_{i=1,\ldots,m}$ such that for $g := \sum_{i=1}^m c_i\psi_i$,

$$\|f - g\| < \frac{\epsilon}{\sup_{n\in I}\|T_n\| + 1}.$$

For $n \geq m$, we have $T_n g = g$. So,

$$\|T_n f - f\| \leq \|T_n f - g\| + \|g - f\| \leq (\sup_{n\in\mathbb{N}}\|T_n\| + 1)\|f - g\| < \epsilon.$$

Next we show that $\{\psi_i\}_{i\in I}$ is complete. Take $f \in \mathcal{H}$ and suppose $\langle f, \psi_i\rangle = 0$ for all $i \in \mathbb{I}$. By (4.3) we then have that $f = 0$. So $\{\psi_i\}_{i\in I}$ is complete. □

If $\{\varphi_i\}_{i\in I}$ is not a basis, this result need not holds, i.e. if $\{\varphi_i\}$ is not a basis but if it is complete, then its biorthogonal system $\{\psi_i\}$ need not even be complete.

Example 4.11 .

Let $\{h_i\}_{i\in I}$ be an orthonormal basis for $\mathcal{H}$. Define $\varphi_i := h_1 + h_{i+1}$ for $i \in \mathbb{I}$, as in Example 4.5. We have already shown that this is a complete independent system which is not a basis. Its biorthogonal system $\{\psi_i\}$ is given by

$$\psi_i = h_{i+1}, \quad i \in \mathbb{I},$$

which is obviously not complete.

I.5. Bessel systems, Riesz-Fischer systems and Riesz bases

We assume that $\mathcal{H}$ is a separable Hilbert space with orthonormal basis $\{h_i\}_{i\in I}$, where the index set $\mathbb{I} = \mathbb{N}$.

Definition 5.1 .

(i) $\{\varphi_i\}_{i\in I}$ is a *Bessel system* if there exists a bounded linear operator R on $\mathcal{H}$ such that

$$Rh_i = \varphi_i, \quad i \in \mathbb{I}.$$

(ii) $\{\varphi_i\}_{i\in I}$ is a *Riesz-Fischer system* if there exists a bounded linear operator T on $\mathcal{H}$ such that

$$T\varphi_i = h_i, \quad i \in \mathbb{I}.$$

(iii) $\{\varphi_i\}_{i\in I}$ is a *Riesz basis* if there exists a bounded linear invertible operator T on $\mathcal{H}$ such that

$$T\varphi_i = h_i, \quad i \in \mathbb{I}.$$

That $\{\varphi_i\}$ of Definition 5.1 (*iii*) is indeed a basis is proved as follows. For any $f \in \mathcal{H}$ we have

$$Tf = \sum_{i \in I} c_i h_i$$

because $\{h_i\}$ is a basis. By the boundedness of T^{-1} and by Definition 5.1 (*iii*) it follows that

$$f = \sum_{i \in I} c_i \varphi_i.$$

The following result summarizes Young [55] pp. 154-157 and Young [55] Theorem 9, p.32. First introduce the *Gram matrix* G of a system $\{\varphi_i\}_{i \in I}$ by

$$G_{ij} := \langle \varphi_j, \varphi_i \rangle_{\mathcal{H}}, \quad i, j \in I\!I.$$

The matrix G generates a linear operator, which we also denote by G, on $\ell^2(I\!I)$ as follows. Define

$$Gg := \{\sum_{j \in I} G_{ij}\ g_j\}_{i \in I}$$

for all $\{g_i\} \in \ell^2(I\!I)$ such that

$$\sum_{i \in I} |\sum_{j \in I} G_{ij}\ g_j|^2 < \infty. \tag{5.1}$$

Proposition 5.2

(i) The following statements are equivalent.

(a) $\{\varphi\}_{i \in I}$ *is a Bessel system.*

(b)

$$\sum_{i \in I} |\langle f, \varphi_i \rangle|^2 < \infty, \quad f \in \mathcal{H}.$$

(c) There exists a positive constant M *such that*

$$\sum_{i \in I} |\langle f, \varphi_i \rangle|^2 \leq M \|f\|^2, \quad f \in \mathcal{H}.$$

(ii) The following statements are equivalent.

(a) $\{\varphi\}_{i \in I}$ *is a Riesz-Fischer system.*

(b) There is a positive constant m *such that for all* $n \in I\!I$ *and* $\{c_i\}_{i=1,\ldots,n}$

$$m \sum_{i=1}^{n} |c_i|^2 \leq \| \sum_{i=1}^{n} c_i \varphi_i \|^2.$$

(c) For each $g \in \ell^2(I\!I)$ *there exists an* $f \in \mathcal{H}$ *(which is not necessarily unique) such that*

$$\langle f, \varphi_i \rangle = g_i, \quad i \in I\!I.$$

(iii) The following statements are equivalent.

(a) $\{\varphi\}_{i \in I}$ *is a Riesz basis.*

(b) $\{\varphi_i\}_{i \in I}$ *is complete and its Gram matrix* G *generates a bounded linear invertible operator on* $\ell^2(I\!I)$.

It follows that the notions of Bessel system, Riesz-Fischer system and Riesz basis are independent of the choice of the orthonormal basis.

If $\{\varphi_i\}$ is a Bessel system, its Gram matrix G is the matrix representation of the operator R^*R in terms of the basis $\{h_i\}$. Here R is given by Definition 5.1 (i). For,

$$G_{ij} = \langle \varphi_j, \varphi_i \rangle = \langle Rh_j, Rh_i \rangle_{\mathcal{H}} = \langle R^*Rh_j, h_i \rangle_{\mathcal{H}}.$$

Hence G generates a positive operator on $\ell^2(\mathbb{I})$. Similarly, if $\{\varphi_i\}$ is a Riesz basis, its Gram matrix G is the matrix representation of $(TT^*)^{-1}$, where T is given by Definiton 5.1 (iii). Hence, by Section 1,

$$\|G\|^{1/2} = \|T^{-1}\| \quad \text{and} \quad \|G^{-1}\|^{1/2} = \|T\|. \tag{5.2}$$

In the case that $\{\varphi_i\}$ is a Riesz basis, its biorthogonal system $\{\psi_i\}$ is also a Riesz basis, and

$$\psi_i = T^*h_i, \quad i \in \mathbb{I}. \tag{5.3}$$

The Gram matrix F of this system is

$$F_{ij} := \langle \psi_j, \psi_i \rangle, \quad i, j \in \mathbb{I}.$$

F is the matrix representation of the operator TT^*. So, $F = G^{-1}$. By (4.3) we can express ψ_i in terms of the basis $\{\varphi_i\}$,

$$\psi_i = \sum_{j \in I} \langle \psi_i, \psi_j \rangle_{\mathcal{H}} \varphi_j, \quad i \in \mathbb{I}.$$

Hence,

$$\psi_i = \sum_{j \in I} \overline{(G^{-1})}_{ij} \varphi_j, \quad i \in \mathbb{I}. \tag{5.4}$$

It may be hard to check whether a system is a Riesz basis. The next result provides a criterion.

Theorem 5.3. *Paley-Wiener theorem .*
Suppose $\{\varphi_i\}_{i \in I}$ is a system in $\mathcal{H}$ for which there exists a positive number $\lambda < 1$ such that for all $n \in \mathbb{N}$ and complex numbers c_i, $i = 1, \ldots, n$,

$$\|\sum_{i=1}^{n} c_i(h_i - \varphi_i)\|_{\mathcal{H}} \leq \lambda \, (\sum_{i=1}^{n} |c_i|^2)^{1/2}.$$

Then there exists a bounded linear invertible operator T on $\mathcal{H}$ such that

$$T\varphi_i = h_i, \quad i \in \mathbb{I}.$$

Moreover,

$$\|T\| \leq \frac{1}{1-\lambda} \quad \text{and} \quad \|T^{-1}\| \leq 1 + \lambda.$$

Proof:

Let $\{h_i\}_{i \in I}$ be an orthonormal basis for $\mathcal{H}$. Define the linear operator U on $\mathcal{H}$ by

$$U(\sum_{i \in I} c_i h_i) := \sum_{i \in I} c_i(h_i - \varphi_i).$$

By assumption, we have $\|U\| \leq \lambda < 1$. Hence, by Theorem 2.1, $(I - U)$ is an invertible operator and

$$(I - U)h_i = \varphi_i, \quad i \in \mathbb{I}.$$

The result follows by taking $T := (I - U)^{-1}$. □

Chapter II

L^2-Spaces of Vector Valued Functions

Let (D, μ) be a finite measure space and X an arbitrary Banach space. In this chapter we consider the space $L^2(D, X)$ of vector-valued functions $f : D \to X$. Most of the time, however, we will assume that X is a Hilbert space, which is then denoted by $\mathcal{H}$.

In section one we consider the Pettis integral and the Fourier transform. Bessel systems, Riesz-Fischer systems and Riesz bases are the subject of the second section. These notions are used in Section III.3 and in Chapter IV to solve the mixed Fourier moment problem in the space $L^2(D, \mathcal{H})$.

The notational convention throughout this chapter is as follows. X is a Banach space with norm $\| \ \|$ and $\mathcal{H}$ is a Hilbert space with inner product $\langle \ , \ \rangle$. If $\mathcal{H}$ is separable, then $\{h_i\}_{i \in I}$ denotes an orthonormal basis. $I\!I$ and $I\!K$ are countable index sets. We assume that $L^2(D, \mathbb{C})$ has orthonormal basis $\{e_\kappa\}_{\kappa \in K}$.

II.1. Definition of $L^2(D,X)$

In this section we consider the L^2-space $L^2(D,X)$ of vector-valued functions, mainly following Balakrishnan [3], and Hille and Phillips [24].

A function that maps D into X is called a *vector-valued function.*

Definition 1.1 . A function $f : D \to X$ is called *simple*, if it is of the form $f = \sum_{j=1}^{n} c_j \chi_{E_j}$, where the E_j are disjoint measurable subsets of D and $c_j \in X$, for $j = 1, ..., n$.

Definition 1.2 . A vector-valued function $f : D \to X$ is called *strongly measurable* if it is the limit almost everywhere of a sequence of simple functions.

If f is strongly measurable, then $D \ni x \to \|f(x)\|$ is a measurable function. In this case the integral

$$\int_D \|f(x)\|^2 d\mu(x), \tag{1.1}$$

is well-defined in $\mathbb{R}^+ \cup \{\infty\}$.

Definition 1.3 . $L^2(D,X)$ is the space of strongly measurable functions for which (1.1) is finite (identifying functions that are equal up to a set of measure zero).

$L^2(D,X)$ is a Banach space. The norm of $f \in L^2(D,X)$ is defined by

$$|||f|||^2 := \int_D \|f(x)\|^2 d\mu(x).$$

Definition 1.4 . A vector-valued function $f : D \to X$, is called *almost separably valued*, if there is a set $E \subset D$ of measure zero, such that the set $f(D \setminus E)$ is separable in X.

A function $f : D \to X$, is called *weakly measurable*, if for each bounded linear functional h^* on X, the scalar-valued function $x \to \langle f(x), h^* \rangle$ is measurable. (Here the brackets denote the action of the functional h^* on $f(x) \in X$.)
The following result relates the notions of strong and weak measurability, cf. Hille and Phillips [24] Theorem 3.5.3.

Theorem 1.5 . *A vector-valued function is strongly measurable if and only if it is weakly measurable and almost separably valued.*

From this it follows that for separable spaces X weak and strong measurability are equivalent notions (Hille and Phillips [24] Corollary 2, p.73).

For the remainder of this section we take for X the Hilbert space $\mathcal{H}$. In that case $L^2(D,\mathcal{H})$ is a Hilbert space with the inner product $\langle\langle\ ,\ \rangle\rangle$, defined by

$$\langle\langle f, g \rangle\rangle := \int_D \langle f(x), g(x) \rangle d\mu(x).$$

If $\mathcal{H}$ is separable, then $L^2(D,\mathcal{H})$ is separable with orthonormal basis $\{e_\kappa h_i\}_{\kappa \in K, i \in I}$, where $e_\kappa\ h_i$ denotes the $\mathcal{H}$-valued function $x \to e_\kappa(x) h_i \in \mathcal{H}$. The orthonormality is established as follows.

$$\langle\langle e_\kappa h_i, e_\lambda h_j \rangle\rangle = \int_D \langle e_\kappa(x) h_i, e_\lambda(x) h_j \rangle d\mu(x) =$$

$$= \int_D \langle h_i, h_j \rangle e_\kappa(x) \overline{e_\lambda(x)} d\mu(x) = \delta_{ij} \delta_{\kappa\lambda}.$$

For functions $f \in L^2(D,\mathcal{H})$ the $\mathcal{H}$-valued integral, denoted by

$$(\mathcal{P})\int_D f(x)d\mu(x),$$

can be defined by its action on $h \in \mathcal{H}$

$$\langle (\mathcal{P})\int_D f(x)d\mu(x), h\rangle := \int_D \langle f(x), h\rangle d\mu(x).$$

It is called the *Pettis integral.* The *generalized Fourier coefficient* of f at $\kappa \in \mathbb{K}$ can then be defined by

$$\hat{f}(\kappa) := (\mathcal{P})\int_D f(x)\overline{e_\kappa(x)}d\mu(x).$$

By definition of the Pettis integral we have for arbitrary $h \in \mathcal{H}$,

$$\langle \hat{f}(\kappa), h\rangle = \langle (\mathcal{P})\int_D f(x)\overline{e_\kappa(x)}d\mu(x), h\rangle = \int_D \langle f(x), h\rangle \overline{e_\kappa(x)}d\mu(x).$$

Or, equivalently,

$$\langle \hat{f}(\kappa), h\rangle = \langle\langle f, e_\kappa h\rangle\rangle. \tag{1.2}$$

Parseval's relation and the inversion formula for the generalized Fourier transform are the contents of the following theorem.

Theorem 1.6 . *Let $\mathcal{H}$ be a separable Hilbert space. For any $f \in L^2(D,\mathcal{H})$ the following identities hold:*

$$|||f|||^2 = \sum_{\kappa\in K} \|\hat{f}(\kappa)\|^2, \tag{1.3}$$

$$f = \sum_{\kappa\in K} \hat{f}(\kappa)e_\kappa. \tag{1.4}$$

Here (1.4) converges in the norm topology of $L^2(D,\mathcal{H})$.

Proof:

Let $f \in L^2(D,\mathcal{H})$ be arbitrary. Then

$$|||f|||^2 = \sum_{\kappa,i} |\langle\langle f, e_\kappa h_i\rangle\rangle|^2 = \sum_\kappa \Big(\sum_i |\langle \hat{f}(\kappa), h_i\rangle|^2\Big) = \sum_\kappa \|\hat{f}(\kappa)\|^2,$$

which proves (1.3). Furthermore

$$f = \sum_\kappa \Big(\sum_i \langle\langle f, e_\kappa h_i\rangle\rangle e_\kappa h_i\Big) = \sum_\kappa \Big(\sum_i \langle \hat{f}(\kappa), h_i\rangle h_i\Big) e_\kappa = \sum_\kappa \hat{f}(\kappa)e_\kappa.$$

□

Another proof of this theorem can be found in Sz-Nagy and Foias [53] pp.183-184.

Theorem 1.6 shows that $\jmath : L^2(D,\mathcal{H}) \to \ell^2(\mathbb{K},\mathcal{H})$,

$$\jmath(f) := \{\hat{f}(\kappa)\}_{\kappa\in K},$$

is an isometric isomorphism. So, $L^2(D,\mathcal{H})$ and $\ell^2(\mathbb{K},\mathcal{H})$ are isometrically isomorphic, denoted by,

$$L^2(D,\mathcal{H}) \simeq \ell^2(\mathbb{K},\mathcal{H}).$$

Let $\{T_\kappa\}$ be a uniformly bounded family of linear operators on $\mathcal{H}$. The operator $\mathcal{U}$ on $\ell^2(\mathbb{K},\mathcal{H})$, which is of the form $\mathcal{U} = \{T_\kappa\}$ corresponds to an operator T on $L^2(D,\mathcal{H})$ as follows:

$$Tf = \sum_{\kappa\in\mathbb{K}} T_\kappa[\widehat{f}(\kappa)]\, e_\kappa, \quad \text{for } f \in L^2(D,\mathcal{H}). \tag{1.5}$$

II.2. Bessel systems, Riesz-Fischer systems and Riesz bases in $L^2(D,\mathcal{H})$

In this section we present necessary and sufficient conditions for

$$\{e_\kappa\varphi_{\kappa,i}\}_{\kappa\in\mathbb{K},i\in\mathbb{I}} \tag{2.1}$$

to be a Bessel system, Riesz-Fischer system, or Riesz basis in $L^2(D,\mathcal{H})$, where $\varphi_{\kappa,i} \in \mathcal{H}$ for $\kappa \in \mathbb{K}, i \in \mathbb{I}$. The results from this section will be used in Sections III.3 and IV.5 to give solvability conditions for the mixed Fourier moment problem of mixed type, which also occurs in Part two.

Let $\kappa \in \mathbb{K}$ be fixed. Assume that the sequence $\{\varphi_{\kappa,i}\}_{i\in\mathbb{I}}$ is a Bessel system in $\mathcal{H}$. Then, by Definition I.5.1 (i) there exists a bounded linear operator R_κ on $\mathcal{H}$ such that

$$R_\kappa h_i = \varphi_{\kappa,i}, \quad i \in \mathbb{I}. \tag{2.2}$$

If we want to prove that (2.1) is a Bessel system, we have to find a bounded linear operator $\mathcal{R}$ on $L^2(D,\mathcal{H})$ such that

$$\mathcal{R}(e_\kappa h_i) = e_\kappa\varphi_{\kappa,i}, \quad \kappa \in \mathbb{K}, i \in \mathbb{I}. \tag{2.3}$$

The following theorem provides a useful criterion.

Theorem 2.1 . *A bounded linear operator $\mathcal{R}$ on $L^2(D,\mathcal{H})$ satisfies (2.3) if and only if there is a uniformly bounded family of linear operators $\{R_\kappa\}_{\kappa\in\mathbb{K}}$ on $\mathcal{H}$ satisfying (2.2). Moreover,*

$$\|\mathcal{R}\| = \sup_{\kappa\in\mathbb{K}}\|R_\kappa\|.$$

Proof:

We prove the result in the space $\ell^2(\mathbb{K},\mathcal{H})$ instead of $L^2(D,\mathcal{H})$. If $\{R_\kappa\}$ is a uniformly bounded family, we have by Theorem I.3.5 that

$$\mathcal{U} = \{R_\lambda\}_{\lambda\in\mathbb{K}}$$

is bounded. By (1.5) we associate with $\mathcal{U}$ a bounded linear operator $\mathcal{R}$ on $L^2(D,\mathcal{H})$. We show that $\mathcal{R}$ satisfies (2.3), if R_κ satisfies (2.2). Fix $\kappa \in \mathbb{K}$ and $i \in \mathbb{I}$. Note that the λth Fourier coefficient of the function $e_\kappa h_i$ is $h_i\delta_{\kappa\lambda}$. Hence by (1.5) and (2.2)

$$\mathcal{R}(e_\kappa h_i) = \sum_{\lambda\in\mathbb{K}} R_\lambda(h_i\delta_{\kappa\lambda})e_\lambda = \varphi_{\kappa,i}e_\kappa.$$

By Theorem I.3.5 it follows that $\mathcal{R}$ is bounded and that $\|\mathcal{R}\| = \sup_{\kappa\in\mathbb{K}}\|R_\kappa\|$.
On the other hand, assume that there exists a bounded linear operator $\mathcal{R}$ on $L^2(D,\mathcal{H})$ satisfying (2.3). Fix $\kappa \in \mathbb{K}$ and define R_κ on $\mathcal{H}$ by

$$R_\kappa h := (\mathcal{R}(he_\kappa))\widehat{}(\kappa).$$

$(\mathcal{R}f)\widehat{\ }(\kappa)$ denotes the κth Fourier coefficient of $\mathcal{R}f$, where $f \in L^2(D,\mathcal{H})$. We show that R_κ satisfies (2.2). By definition

$$R_\kappa h_i := (\mathcal{R}(h_i e_\kappa))\widehat{\ }(\kappa) = (\varphi_{\kappa,i} e_\kappa)\widehat{\ }(\kappa) = \varphi_{\kappa,i}.$$

Next we prove that $\{R_\kappa\}$ is uniformly bounded. Choose $h \in \mathcal{H}$ and $\kappa \in I\!K$ arbitrarily. Then by Theorem 1.6

$$\|R_\kappa h\| = \|(\mathcal{R}(he_\kappa))\widehat{\ }(\kappa)\| \le |||\mathcal{R}(he_\kappa)||| \le |||\mathcal{R}|||||he_\kappa||| = |||\mathcal{R}|||||h||.$$

Hence

$$\sup_{\kappa\in K}\|R_\kappa\| \le |||\mathcal{R}|||.$$

Finally we prove that

$$|||\mathcal{R}||| \le \sup_{k\in K}\|R_\kappa\|.$$

Take $f \in L^2(D,\mathcal{H})$. Since $\{h_i e_\kappa\}$ is an orthonormal basis, there exists a sequence $\{s_n\} \subset L^2(D,\mathcal{H})$ such that

$$\lim_{n\to\infty} |||s_n - f||| = 0$$

where for each n, s_n is a finite series of the form

$$s_n := \sum_{\kappa,i} c_{\kappa,i} h_i e_\kappa.$$

We prove that for each n

$$|||\mathcal{R}s_n||| \le (\sup_{\kappa\in K}\|R_\kappa\|)|||s_n|||.$$

The desired result then follows by the continuity of $\mathcal{R}$. By (2.3) and by the definition of R_κ,

$$\mathcal{R}s_n = \sum_{\kappa,i} c_{\kappa,i}\varphi_{\kappa,i}e_\kappa = \sum_{\kappa,i} c_{\kappa,i}(\mathcal{R}(h_i e_\kappa))\widehat{\ }(\kappa)e_\kappa = \sum_{\kappa,i} c_{\kappa,i}R_\kappa(h_i)e_\kappa,$$

whence

$$|||\mathcal{R}s_n|||^2 = \sum_{\lambda\in K}\|(\mathcal{R}s_n)\widehat{\ }(\lambda)\|^2 = \sum_\lambda \|\sum_i c_{\lambda,i}R_\lambda(h_i)\|^2 \le$$

$$\le (\sup_{\kappa\in K}\|R_\kappa\|)^2 \sum_{\lambda,i}|c_{\lambda,i}|^2 = (\sup_{\kappa\in K}\|R_\kappa\|)^2|||s_n|||^2.$$

□

Analogous results hold if for each $\kappa \in I\!K$ the sequence $\{\varphi_{\kappa,i}\}_{i\in I}$ is a Riesz-Fischer system or a Riesz basis. If $\{\varphi_{\kappa,i}\}_{i\in I}$ is a Riesz-Fischer system (Riesz basis) for each $\kappa \in I\!K$, then there exists a family of bounded linear (invertible) operators $\{T_\kappa\}_{\kappa\in K}$, such that

$$T_\kappa\varphi_{\kappa,i} = h_i, \quad i \in I\!I. \tag{2.4}$$

In the case of Riesz-Fischer systems, the following result holds.

Theorem 2.2 . *Let $\varphi_{\kappa,i} \in \mathcal{H}$, for $\kappa \in \mathbb{K}, i \in \mathbb{I}$. The collection $\{\varphi_{\kappa,i}e_\kappa\}_{\kappa\in K,i\in I}$ is a Riesz-Fisher system in $L^2(D,\mathcal{H})$ if and only if there exists a uniformly bounded family $\{T_\kappa\}$ of linear operators on $\mathcal{H}$, such that*

$$T_\kappa\varphi_{\kappa,i} = h_i, \quad i \in \mathbb{I}. \tag{2.5}$$

There exists a bounded linear operator $\mathcal{T}$ such that

$$\mathcal{T}(\varphi_{\kappa,i}e_\kappa) = h_i e_\kappa, \quad \kappa \in \mathbb{K}, i \in \mathbb{I} \tag{2.6}$$

and

$$\|\mathcal{T}\| = \sup_{\kappa\in K}\|T_\kappa\|.$$

Proof:

Assume that the family $\{T_\kappa\}$ satisfies (2.5) and is uniformly bounded. That there exists a bounded linear operator $\mathcal{T}$ on $L^2(D,\mathcal{H})$ which satisfies (2.6) is proved similarly as in Theorem 2.1. Now we prove the if-part. Suppose $\{\varphi_{\kappa,i}e_\kappa\}$ is a Riesz-Fischer system in $L^2(D,\mathcal{H})$. Then, by Definition I.5.1 (ii) there exists a bounded linear operator $\mathcal{U}$ on $L^2(D,\mathcal{H})$ such that

$$\mathcal{U}(\varphi_{\kappa,i}e_\kappa) = h_i e_\kappa.$$

Now define an associated bounded linear operator $\mathcal{T}$ on $L^2(D,\mathcal{H})$ by

$$\mathcal{T}f := \begin{cases} \mathcal{U}f, & \text{on } \overline{\text{span}}\{\varphi_{\kappa,i}e_\kappa\}_{\kappa\in K,i\in I} \\ 0, & \text{on } (\overline{\text{span}}\{\varphi_{\kappa,i}e_\kappa\}_{\kappa\in K,i\in I})^\perp \end{cases}.$$

It is clear by definition that $\mathcal{T}$ satisfies (2.6). Fix $\kappa \in \mathbb{K}$ and choose $h \in \mathcal{H}$. Define the linear operator T_κ on $\mathcal{H}$ by

$$T_\kappa h := (\mathcal{T}(he_\kappa))\widehat{\ }(\kappa).$$

In the same manner as in the proof of Theorem 2.1, we show that T_κ satisfies (2.5) and

$$\sup_{\kappa\in K}\|T_\kappa\| \le \|\mathcal{T}\|.$$

To prove $\|\mathcal{T}\| \le \sup\|T_\kappa\|$, choose $f \in \overline{\text{span}}\{\varphi_{\kappa,i}e_\kappa\}$. (Since $\mathcal{T}$ is the zero operator on $(\overline{\text{span}}\{\varphi_{\kappa,i}e_\kappa\})^\perp$ the inequality trivially holds on this subspace.) The system $\{\varphi_{\kappa,i}\}$ need not be a basis, but by definition of closed linear span, we can find a sequence $\{s_n\} \subset \text{span}\{\varphi_{\kappa,i}e_\kappa\}$ such that

$$\lim_{n\to\infty}|||s_n - f||| = 0,$$

where for each n, s_n is a finite series of the form $\sum_{\kappa,i} c_{\kappa,i}\varphi_{\kappa,i}e_\kappa$. We prove that for each n

$$|||\mathcal{T}s_n||| \le (\sup_{\kappa\in K}\|T_\kappa\|)|||s_n|||.$$

The desired result then follows by the continuity of $\mathcal{T}$. By (2.5) and by the definition of T_κ,

$$\mathcal{T}s_n = \sum_{\kappa,i} c_{\kappa,i}h_i e_\kappa = \sum_{\kappa,i} c_{\kappa,i}(\mathcal{T}(\varphi_{\kappa,i}e_\kappa))\widehat{\ }(\kappa)e_\kappa = \sum_{\kappa,i} c_{\kappa,i}T_\kappa(\varphi_{\kappa,i})e_\kappa,$$

whence

$$|||\mathcal{T}s_n|||^2 = \sum_{\lambda\in K}\|(\mathcal{T}s_n)\widehat{\ }(\lambda)\|^2 = \sum_\lambda\|\sum_i c_{\lambda,i}T_\lambda(\varphi_{\lambda,i})\|^2 \le$$

$$\le (\sup_{\kappa\in K}\|T_\kappa\|)^2\sum_\lambda\|\sum_i c_{\lambda,i}\varphi_{\lambda,i}\|^2 = (\sup_{\kappa\in K}\|T_\kappa\|)^2|||s_n|||^2.$$

□

In the case of Riesz bases, we have the following result.

Theorem 2.3 . *Let $\varphi_{\kappa,i} \in \mathcal{H}$, for $\kappa \in \mathbb{K}$ and $i \in \mathbb{I}$. The collection $\{\varphi_{\kappa,i}e_\kappa\}_{\kappa\in K, i\in I}$ is a Riesz basis for $L^2(D,\mathcal{H})$ if and only if there exists a family $\{T_\kappa\}$ of linear operators such that*

$$T_\kappa \varphi_{\kappa,i} = h_i, \quad i \in \mathbb{I},$$

and $\{T_\kappa\}$ and $\{T_\kappa^{-1}\}$ are uniformly bounded. The bounded linear invertible operator T given by

$$T(\varphi_{\kappa,i}e_\kappa) = h_i e_\kappa, \quad \kappa \in \mathbb{K}, i \in \mathbb{I}$$

satisfies

$$\|T\| = \sup_{\kappa\in K}\|T_\kappa\| \quad \text{and} \quad \|T^{-1}\| = \sup_{\kappa\in K}\|T_\kappa^{-1}\|.$$

The above theorems completely characterize Bessel systems, Riesz-Fischer systems and Riesz bases of the form $\{e_\kappa\varphi_{\kappa,i}\}$ in the space $L^2(D,\mathcal{H})$.

We want to compute the biorthogonal system of $\{e_\kappa\varphi_{\kappa,i}\}$ in $L^2(D,\mathcal{H})$. If for each $\kappa \in \mathbb{K}$ $\{\varphi_{\kappa,i}\}_{i\in I}$ and $\{\psi_{\kappa,i}\}_{i\in I}$ are biorthogonal systems in $\mathcal{H}$, then $\{e_\kappa\varphi_{\kappa,i}\}$ and $\{e_\kappa\psi_{\kappa,i}\}$ are biorthogonal systems in $L^2(D,\mathcal{H})$. For,

$$\langle\langle e_\kappa\varphi_{\kappa,i}, e_\lambda\psi_{\lambda,j}\rangle\rangle = \int_D \langle e_\kappa(x)\varphi_{\kappa,i}, e_\lambda(x)\psi_{\lambda,j}\rangle d\mu(x) =$$

$$= (\langle\varphi_{\kappa,i}, \psi_{\lambda,j}\rangle) \int_D e_\kappa(x)\overline{e_\lambda(x)}d\mu(x) = \delta_{\kappa\lambda}\delta_{ij}.$$

If $\{\varphi_{\kappa,i}\}$ satisfies the conditions of Theorem 2.3, then we can compute this system in terms of the Gram matrix, (for $\kappa \in \mathbb{K}$)

$$(G(\kappa))_{ij} := \langle\varphi_{\kappa,j}, \varphi_{\kappa,i}\rangle, \quad i,j \in \mathbb{I}. \tag{2.7}$$

By Section I.5 we obtain for fixed $\kappa \in \mathbb{K}$,

$$\psi_{\kappa,i} := \sum_{j\in I} \overline{(G(\kappa)^{-1})}_{ij}\varphi_{\kappa,j}, \quad i \in \mathbb{I}. \tag{2.8}$$

Chapter III

Moment Problems in Hilbert Space

In this chapter we consider a moment problem in a Hilbert space, which consists in finding an element $f \in \mathcal{H}$ such that

$$\langle f, \varphi_i \rangle_{\mathcal{H}} = g_i, \quad i \in I\!I. \tag{0.1}$$

Here $\{g_i\} \in \ell^2(I\!I)$ and $\{\varphi_i\}_{i \in I} \subset \mathcal{H}$ is a given system. The index set $I\!I$ is equal to $I\!N$ in this chapter.

In Section one we discuss conditions on the system $\{\varphi_i\}$ in order that the moment problem has a solution. At the end of this section the Tychonov-Phillips regularization corresponding to the moment problem is considered. An approximation scheme for computing the solution is found in the second section and in the last section we give solvability conditions for a mixed Fourier moment problem in $L^2(D, \mathcal{H})$.

III.1. Solutions of the moment problem

Without conditions on $\{\varphi_i\}$, problem (0.1) need not have a solution; even if $\{\varphi_i\}_{i\in I}$ is a Bessel system and a basis.

Example 1.1 .

Let $\mathcal{H}$ be a Hilbert space with orthonormal basis $\{h_i\}_{i\in I}$. $\{\varphi_i\}$ defined by $\varphi_i := (1/i)h_i$ for $i \in \mathbb{I}$, is a Bessel system and a basis for $\mathcal{H}$. Take $g_i = 1/i$, for $i \in \mathbb{I}$. Suppose f is a solution of the moment problem

$$\langle f, \varphi_i\rangle_{\mathcal{H}} = g_i, \quad i \in \mathbb{I}. \tag{1.1}$$

f can be represented in terms of the φ_i,

$$f = \sum_{i\in I} c_i\varphi_i.$$

Since $\langle f, \varphi_i\rangle_{\mathcal{H}} = c_i/(i^2)$, we obtain $c_i = (i^2)g_i$. Hence

$$f = \sum_{i\in I} ig_ih_i = \sum_{i\in I} h_i,$$

which does not converge in $\mathcal{H}$. This is a contradiciton, so there does not exist a solution of the moment problem (1.1) in $\mathcal{H}$.

A necessary and sufficient condition for (0.1) to have a solution is that $\{\varphi_i\}_{i\in I}$ is a Riesz-Fischer system (Proposition I.5.2 (*ii*)). The solution f of problem (0.1) is unique if and only if $\{\varphi_i\}$ is complete. If this is not the case, then other solutions of (0.1) are obtained by adding elements lying in $(\text{span}\{\varphi_i\})^{\perp}$ to f. The solution which has smallest norm among all solutions is called *minimum norm solution.*

Proposition 1.2 . *If the moment problem admits a solution, then there exists a unique minimum norm solution, which lies in the subspace* $\overline{\text{span}}\{\varphi_i\}$.

Proof:

First we prove uniqueness of the solution in the subspace $\mathcal{G} := \overline{\text{span}}\{\varphi_i\}$. Let f and g be solutions of the moment problem (0.1), both lying in $\mathcal{G}$. Then also $f - g \in \mathcal{G}$, because both f and g are solutions of problem (0.1),

$$\langle f - g, \varphi_i\rangle_{\mathcal{H}} = 0, \quad i \in \mathbb{I}.$$

So, $f - g \in \mathcal{G}^{\perp}$. This can only be the case if $f - g = 0$.
Next we prove that the minimum norm solution lies in $\mathcal{G}$. Suppose h is an arbitrary solution of problem (0.1). By Theorem I.2.2 we write h as $h = h_1 + h_2$ with $h_1 \in \mathcal{G}$ and $h_2 \in \mathcal{G}^{\perp}$. It is clear that h_1 is a solution of the moment problem. Furthermore,

$$\|h_1\|^2_{\mathcal{H}} = \|h\|^2_{\mathcal{H}} - \|h_2\|^2_{\mathcal{H}} \leq \|h\|^2_{\mathcal{H}}.$$

So, $h_1 \in \mathcal{G}$ is minimum norm solution. □

By Proposition I.5.2 (*ii*) and Proposition 1.2 we obtain the following result.

Theorem 1.3 . *If* $\{\varphi_i\}$ *is a Riesz-Fischer system, then the moment problem has a unique minimum norm solution which lies in the subspace* $\overline{\text{span}}\{\varphi_i\}$.

If $\{\varphi_i\}$ is a Riesz basis, then we obtain a stronger result, by the representation (I.4.4).

Theorem 1.4 . *If $\{\varphi_i\}$ is a Riesz basis, then*

$$f = \sum_{i \in I} g_i \psi_i \tag{1.2}$$

is the unique solution of the moment problem.

Here $\{\psi_i\}_{i \in I}$ is the biorthogonal system of $\{\varphi_i\}_{i \in I}$, which can be computed by (I.5.4). Formula (1.2) can then be rewritten as

$$f = \sum_{j \in I} \sum_{i \in I} (G^{-1})_{ji}\, g_i\, \varphi_j, \tag{1.3}$$

where G is the Gram matrix of the system $\{\varphi_i\}$.

We rewrite the moment problem as an equation:

$$Af = g, \tag{1.4}$$

where $A : \mathcal{H} \to \ell^2(I\!I)$ is given by

$$Af := \{\langle f, \varphi_i \rangle_{\mathcal{H}}\}_{i \in I}.$$

Note that the inverse A^{-1} is given by (1.3) if $\{\varphi_i\}$ is a Riesz basis.

Assume for the remainder of the section that $\{\varphi_i\}_{i \in I}$ is a Bessel system. In this case A need not have an inverse (cf. Example 1.1). We give a formula for the Tychonov-Phillips regularization in terms of the Bessel system (cf. Section I.2)). The regularization $\{T^\gamma\}_{\gamma > 0}$ of the Moore-Penrose inverse A^+ (see section I.2) is of the form

$$T^\gamma g := A^*(AA^* + \gamma I)^{-1} g. \tag{1.5}$$

Obviously, $A^* g = \sum_{i \in I} g_i \varphi_i$, for $g \in \ell^2(I\!I)$. So, $AA^* g = \{\sum_{i \in I} G_{ji} g_i\}_{j \in I}$, and by straightforward computation one finds that

$$T^\gamma g = \sum_{j \in I} \sum_{i \in I} ((G + \gamma I)^{-1})_{ji}\, g_i\, \varphi_j, \tag{1.6}$$

which is the generalization of formula (1.3) in the case of Bessel systems. We have obtained the following result.

Theorem 1.5 . *Let $\{\varphi_i\}$ is a Bessel system for $\mathcal{H}$ and define its Gram matrix G by*

$$G_{ij} := \langle \varphi_j, \varphi_i \rangle, \quad i, j \in I\!I.$$

Denote the identity operator on $\ell^2(I\!I)$ as I. Then (for $g \in \ell^2(I\!I)$)

$$T^\gamma g = \sum_{j \in I} \sum_{i \in I} ((G + \gamma I)^{-1})_{ji}\, g_i\, \varphi_j,$$

is the Tychonov-Phillips regularization corresponding to the moment problem.

III.2. Approximation of the solution of the moment problem

The results of Section 1 are still not in a practical form, as formulae (1.2) and (1.3) deal with an infinite sum and the inverse of an infinite matrix. Therefore we look for solutions of the truncated moment problem

$$\langle f_n, \varphi_i \rangle_{\mathcal{H}} = g_i, \quad i = 1, ..., n, \tag{2.1}$$

where $n \in \mathbb{I}$ is fixed. It is clear from the previous section that

$$f_n := \sum_{i=1}^{n} g_i \psi_i^n \tag{2.2}$$

is a solution of problem (2.1). Here $\{\psi_i^n\}_{i\in\{1,...,n\}}$ is the biorthogonal system of $\{\varphi_i\}_{i\in\{1,...,n\}}$ in the subspace

$$\mathcal{H}_n := \text{span}\{\varphi_i\}_{i\in\{1,...,n\}}.$$

By Propositon 1.2 it follows that f_n (which lies in $\mathcal{H}_n$) is the unique minimum norm solution of the truncated problem. By repeating this procedure for all $n \in \mathbb{I}$, we obtain a sequence $\{f_n\}_{n\in I}$. The aim of this section is to prove that $\|f - f_n\| \to 0$, (for $n \to \infty$) where $f \in \mathcal{H}$ is the unique solution of problem (0.1).

First we construct an orthonormal basis $\{h_i\}_{i\in I}$ for $\mathcal{H}$, e.g. by Gram-Schmidt orthogonalization, such that (for $n \in \mathbb{I}$) $\{h_i\}_{i\in\{1,...,n\}}$ is an orthonormal basis for $\mathcal{H}_n$. In this case the operator T from Definition I.5.1 (*iii*) which satisfies

$$T\varphi_i = h_i, \quad i \in \mathbb{I}$$

leaves all the subspaces $\mathcal{H}_n$ invariant. However, the adjoint of T need not to leave the subspaces $\mathcal{H}_n$ invariant. Denoting the restriction of T to $\mathcal{H}_n$ by T_n and its adjoint in $\mathcal{H}_n$ by T_n^*, the system $\{\psi_i^n\}_{1,...,n} \subset \mathcal{H}_n$ is given by formula (I.5.3)

$$\psi_i^n := T_n^* h_i, \quad i = 1, ..., n, \tag{2.3}$$

which is the unique biorthogonal system of $\{\varphi_i\}_{1,...,n}$ in $\mathcal{H}_n$. An alternative formula for ψ_i^n is (cf. formula (I.5.4))

$$\psi_i^n = \sum_{j=1}^{n} \overline{(G_n^{-1})}_{ij} \varphi_j,$$

where G_n is the truncated Gram matrix,

$$(G_n)_{ij} := G_{ij}, \quad i, j \in \{1, ..., n\}.$$

We define the projection operator $P_n : \mathcal{H} \to \mathcal{H}_n$, as

$$P_n f = \sum_{i=1}^{n} \langle f, \varphi_i \rangle_{\mathcal{H}} \psi_i^n. \tag{2.4}$$

P_n is a normal operator ($P_n^* P_n = P_n P_n^*$) from $\mathcal{H}$ onto $\mathcal{H}_n$ and it reduces to the identity operator on $\mathcal{H}_n$, i.e. $P_n g = g$ for $g \in \mathcal{H}_n$. If $f \in \mathcal{H}$ is the solution of problem (0.1), then

it follows by substitution that the minimum norm solution of problem (2.1) is $f_n = P_n f$. For any $g \in \mathcal{H}_n$ we have

$$f - f_n = (I - P_n)f = (I - P_n)(f - g).$$

Hence

$$\|(I - P_n)f\| \leq \|I - P_n\| \operatorname{dist}(f, \mathcal{H}_n). \tag{2.5}$$

Here the distance between an element f lying in $\mathcal{H}$ and a subspace $M \subset \mathcal{H}$ is

$$\operatorname{dist}(f, M) := \inf \{\|f - m\| \mid m \in M\}.$$

We know that for all $f \in \mathcal{H}$

$$\lim_{n \to \infty} \operatorname{dist}(f, \mathcal{H}_n) = 0. \tag{2.6}$$

The next lemma proves that $\|I - P_n\| \leq c$, where c is a constant independent of n.

Lemma 2.1 . *Let $\{\varphi_i\}_{i \in I}$ be a Riesz basis for $\mathcal{H}$, and let P_n be given by (2.4). Then*

$$\|I - P_n\| \leq 1 + (\|G^{-1}\| \, \|G\|)^{1/2}, \quad n \in \mathbb{N}. \tag{2.7}$$

Proof:

Using $\psi_i = T^* h_i$, and (2.3), we obtain

$$\|P_n f\| = \|\sum_{i=1}^{n} \langle f, \varphi_i \rangle \psi_i^n\| = \|\sum_{i=1}^{n} \langle f, \varphi_i \rangle_{\mathcal{H}} T_n^* h_i\| \leq$$

$$\leq \|T_n\| \|\sum_{i=1}^{n} \langle f, \varphi_i \rangle_{\mathcal{H}} h_i\| \leq \|T\| \|\sum_{i \in \mathbb{Z}} \langle f, \varphi_i \rangle_{\mathcal{H}} T^{*^{-1}} \psi_i\| \leq \|T\| \|T^{-1}\| \|f\|.$$

Hence, by (I.5.2),

$$\|I - P_n\| \leq 1 + (\|G\| \|G^{-1}\|)^{1/2} < \infty, \quad n \in \mathbb{N}.$$

This proves the estimate. □

By (2.5) and (2.7) it follows that

$$\|(I - P_n)f\| \leq (1 + (\|G^{-1}\| \, \|G\|)^{1/2}) \operatorname{dist}(f, \mathcal{H}_n). \tag{2.8}$$

Hence, by (2.6), for all $f \in \mathcal{H}$,

$$\lim_{n \to \infty} \|(I - P_n)f\| = 0. \tag{2.9}$$

We have proved the following result.

Theorem 2.2 . *If $\{\varphi_i\}_{i \in I}$ is a Riesz basis and if f_n (formula (2.4)) is the minimum norm solution of the truncated problem (2.1), then $\{f_n\}_{n \in \mathbb{N}}$ converges to the solution of problem (0.1).*

Equation (2.9) applies in particular to biorthogonal sequences $\{\psi_i\}_{i\in I}$ of a Riesz basis. It follows by definition of P_n that $\psi_i^n = P_n\psi_i$, for $i \in \{1,...,n\}$. Hence by (2.9)

$$\lim_{n\to\infty} \|\psi_i^n - \psi_i\| = 0, \tag{2.10}$$

for $i \in \mathbb{I}$.

III.3. Mixed Fourier moment problems in $L^2(D,\mathcal{H})$

In this section we consider the mixed Fourier moment problem, which consists in finding a function $f \in L^2(D,\mathcal{H})$ such that

$$\langle \widehat{f}(\kappa), \varphi_{\kappa,i}\rangle_{\mathcal{H}} = g_{\kappa,i}, \quad \kappa \in \mathbb{K}, i \in \mathbb{I}. \tag{3.1}$$

Here $\mathbb{K}$ and $\mathbb{I}$ are countable index sets, $\{g_{\kappa,i}\}$ lies in $\ell^2(\mathbb{K}\times\mathbb{I})$ and $\{\varphi_{\kappa,i}\}$ is a sequence of vectors lying in $\mathcal{H}$. The Fourier transform $\widehat{f}(\kappa)$ of f is defined in Section II.1.

In Chapter IV we shall see that the mixed Fourier moment problem is related to the mixed Fourier interpolation problem, which is a mathematical model for reconstructing magnetic resonance images. Magnetic resonance imaging (MRI) is a diagnostic method to measure and display cross sections of human organs (cf. Part two). The theory of this chapter forms the basis for Chapter IV and for Part two, where we explain how to solve the mixed Fourier interpolation problem.

The idea for solving (3.1) is as follows. First, find for $\kappa \in \mathbb{K}$ fixed, a solution c_κ of the moment problem in $\mathcal{H}$

$$\langle c_\kappa, \varphi_{\kappa,i}\rangle_{\mathcal{H}} = g_{\kappa,i}, \quad i \in \mathbb{I}. \tag{3.2}$$

Next, putting $\widehat{f}(\kappa) := c_\kappa$, we obtain

$$f = \sum_{\kappa\in K} c_\kappa e_\kappa. \tag{3.3}$$

Problem (3.1) can also be solved directly. Using identity (II.1.2), we see that the mixed Fourier moment problem amounts to finding an element $f \in L^2(D,\mathcal{H})$ such that

$$\langle\!\langle f, e_\kappa\varphi_{\kappa,i}\rangle\!\rangle = g_{\kappa,i}, \quad \kappa \in \mathbb{K}, i \in \mathbb{I}. \tag{3.4}$$

So, if $\{e_\kappa\varphi_{\kappa,i}\}$ is a Riesz-Fischer system then (3.4) has a unique minimum norm solution.

Theorem 3.1 . *If $\{e_\kappa\varphi_{\kappa,i}\}$ is a Riesz-Fischer system, then the unique minimum norm solution f of problem (3.4) is of the form*

$$f = \sum_{\kappa\in K} c_\kappa e_\kappa,$$

where for each $\kappa \in \mathbb{K}$, c_κ is the unique minimum norm solution of (3.2)

Proof:

The existence of a solution f is guaranteed by Theorem 1.3. If f is a solution of problem (3.4), then for each $\kappa \in \mathbb{K}$ its Fourier coefficient c_κ is a solution of

$$\langle c_\kappa, \varphi_{\kappa,i}\rangle = g_{\kappa,i}, \quad i \in \mathbb{I}.$$

By Theorem II.1.6 we have that

$$|||f|||^2 = \sum_{\kappa\in K} \|c_\kappa\|^2.$$

So, f is the minimum norm solution of problem (3.4) in $L^2(D,\mathcal{H})$ if and only if all the c_κ's are minimum norm solutions of (3.2) in $\mathcal{H}$. □

If $\{e_\kappa \varphi_{\kappa,i}\}$ is a Riesz basis then we have the following stronger result.

Theorem 3.2 . *If $\{e_\kappa \varphi_{\kappa,i}\}$ is a Riesz basis, then (3.4) has the unique solution*

$$f = \sum_{\kappa \in K} c_\kappa e_\kappa,$$

where

$$c_\kappa = \sum_{i \in I} g_{\kappa,i} \psi_{\kappa,i}$$

and

$$\psi_{\kappa,i} = \sum_{j \in I} \overline{(G(\kappa)^{-1})}_{ij} \varphi_{\kappa,j}.$$

The Gram matrix is given by

$$(G(\kappa))_{ij} := \langle \varphi_{\kappa,j}, \varphi_{\kappa,i} \rangle.$$

For the remainder of this section we assume that $\{e_\kappa \varphi_{\kappa,i}\}$ is a Bessel system (cf. Section 1). Then (3.4) need not have a solution (cf. Example 1.1). We give an explicit formula of the Tychonov-Phillips regularization corresponding to the mixed Fourier moment problem. We rewrite (3.4) as an operator equation:

$$\mathcal{A} f = g.$$

First define for $\kappa \in \mathbb{K}$ the family of operators $\{A_\kappa\}_{\kappa \in K}$ from $\mathcal{H}$ to $\ell^2(\mathbb{I})$,

$$A_\kappa h := \{\langle h, \varphi_{\kappa,i} \rangle_{\mathcal{H}}\}_{i \in I}.$$

Finally, identifying $\ell^2(\mathbb{K}, \ell^2(\mathbb{I}))$ with $\ell^2(\mathbb{K} \times \mathbb{I})$, let the operator $\mathcal{A} : \ell^2(\mathbb{K}, \mathcal{H}) \to \ell^2(\mathbb{K} \times \mathbb{I})$ be given by

$$\mathcal{A} := \{A_\kappa\}_{\kappa \in K}.$$

Suppose $\{T_\kappa^\gamma\}_{\gamma > 0}$ and $\{T^\gamma\}_{\gamma > 0}$ are the Tychonov-Phillips regularizations of A_κ^+ and $\mathcal{A}^+$ respectively. By Theorem I.3.9 we have the following result.

Theorem 3.3 . *Let $\{e_\kappa \varphi_{\kappa,i}\}$ be a Bessel system. If*

$$\sum_{\kappa \in K} \|T_\kappa^\gamma g_\kappa\|^2 < \infty, \quad g \in \ell^2(\mathbb{K} \times \mathbb{I}),$$

then the Tychonov-Phillips regularization corresponding to the mixed Fourier moment problem is

$$T^\gamma = \{T_\kappa^\gamma\}_{\kappa \in K}.$$

Here for $\kappa \in \mathbb{K}$ fixed,

$$T_\kappa^\gamma g = \sum_{j \in I} \sum_{i \in I} ((G(\kappa) + \gamma I)^{-1})_{ij} \; g_i \; \varphi_{\kappa,j}, \quad g \in \ell^2(\mathbb{I})$$

Chapter IV

Mixed Fourier Interpolation Problem

Let (D,μ) be a finite measure space and assume that $\{e_\kappa\}_{\kappa\in K}$ is an orthonormal basis for $L^2(D,\mathbb{C})$, where K is a countable index set. $\mathcal{H}$ is assumed to be a Hilbert space of functions which has a reproducing kernel. Then $L^2(D,\mathcal{H})$ consists of functions f such that $f(x)$ lies in $\mathcal{H}$, for almost all $x \in D$. In our application the functions in $\mathcal{H}$ depend on the time-parameter t. So, $f(x)$ is a time-dependent function, which we denote as $t \to f(x,t)$. The Fourier coefficient with respect to the parameter x is defined by

$$\hat{f}(\kappa,t) := \int_D f(x,t)\overline{e_\kappa(x)}d\mu(x), \quad \kappa \in K.$$

In this chapter we consider a mixed Fourier interpolation problem which consists in finding a function f lying in $L^2(D,\mathcal{H})$ such that

$$(\sqrt{\pi/r})\ \hat{f}(\kappa,t_{\kappa,i}\pi/r) = g_{\kappa,i}, \quad \kappa \in K, i \in I. \tag{0.1}$$

Here $\{g_{\kappa,i}\} \in \ell^2(K \times I)$ and $\{t_{\kappa,i}\}_{\kappa\in K,i\in I}$ is a sequence of real numbers.

The mixed Fourier interpolation problem is a mathematical model for a reconstruction problem in magnetic resonance imaging (MRI), a diagnostic method to measure and display cross sections of human organs. In Part two we are particularly interested in reconstructing cross sections of the beating human heart at consecutive time instants. The function f serves as a model for such a cross section, where the temporal parameter takes account of the motion of the heart.

The idea for solving (0.1) is as follows. For fixed $\kappa \in K$ problem (0.1) is an interpolation problem with respect to the temporal parameter, i.e. we have to find a Fourier coefficient c_κ which lies in $\mathcal{H}$ such that

$$(\sqrt{\pi/r})c_\kappa(t_{\kappa,i}\pi/r) = g_{\kappa,i}, \quad i \in I.$$

In a Hilbert space $\mathcal{H}$ with reproducing kernel, we can always write this interpolation problem as a moment problem, because then there exists a system of vectors $\{\varphi_{\kappa,i}\}$ such that

$$\langle h,\varphi_{\kappa,i}\rangle = (\sqrt{\pi/r})\ h(t_{\kappa,i}\pi/r), \quad \text{for } h \in \mathcal{H}.$$

We consider two such Hilbert spaces with reproducing kernel: the space of bandlimited functions $\mathcal{P}_r$ and the space of odd degree splines $\mathcal{K}^{2n-1}$.
The solution of problem (0.1) is then obtained by the Fourier inversion formula: $f = \sum_{\kappa\in K} c_\kappa e_\kappa$.

It is shown in this chapter that an equivalent manner to obtain a solution of problem (0.1) is to reformulate it as the mixed Fourier moment problem in the space $L^2(D,\mathcal{H})$:

$$(\widehat{f}(\kappa),\varphi_{\kappa,i}) = g_{\kappa,i}, \quad \kappa \in \mathbb{K}, i \in \mathbb{I},$$

which was solved in Section III.3.

In the first section we introduce the Hilbert space $\mathbb{P}_r$, which is also called Paley-Wiener space. Section 2 gives examples of Bessel systems, Riesz-Fischer systems and Riesz bases in $\mathbb{P}_r$. The Hilbert space $\mathcal{K}^{2n-1}$ is introduced in section 3. In section 4 we illustrate interpolation by bandlimited functions and odd degree splines and give a motivation for using Tychonov-Phillips regularization. The mixed Fourier interpolation problem is solved in section 5. Section 6 gives examples of solutions of the mixed problem in the space $L^2(D,\mathbb{P}_r)$. Some historical remarks about Riesz bases are given in the last section.
The notational convention during this chapter is that the index set $\mathbb{I}$ is the finite set $\{1,...,I\}$ in the case of spline functions and $\mathbb{Z}$ in the case of bandlimited functions.

IV.1. Interpolation in the Paley-Wiener Space

We denote the support of a function f by $supp(f)$. The Fourier transform of a function $f \in L^1(\mathbb{R}) \cap L^2(\mathbb{R})$ is defined by

$$\hat{f}(\xi) := (\frac{1}{\sqrt{2\pi}}) \int_R f(x) e^{-ix\xi} dx.$$

Since $L^1(\mathbb{R}) \cap L^2(\mathbb{R})$ lies dense in $L^2(\mathbb{R})$ it follows by Rudin [45] Theorem 9.13 that the Fourier transform can be extended to L^2-functions; which is then also denoted by $\hat{f}$.

Definition 1.1. The *Paley-Wiener space* is defined as

$$\mathbb{P}_r := \{ f \in L^2(\mathbb{R}) \mid \text{supp } (\hat{f}) \subset [-r, r] \}.$$

$\mathbb{P}_r$ is a Hilbert space with inner product

$$\langle f, g \rangle_{\mathbb{P}_r} := \int_R f(x) \overline{g(x)} dx$$

and with orthonormal basis, $\{h_i\}_{i \in I}$, given by

$$h_i(t) := \sqrt{r/\pi}\, \text{sinc}_r(t - i\,\pi/r), \quad i \in I. \tag{1.1}$$

Here the *sinc*-function is defined by

$$\text{sinc}_r(t) := \begin{cases} \dfrac{\sin(rt)}{rt}, & t \neq 0 \\ 1, & t = 0 \end{cases}.$$

By the Theorem of Paley-Wiener (see Young [55] Theorem 18, p. 101) any element $f \in \mathbb{P}_r$ can be extended to an entire function $f : \mathbb{C} \to \mathbb{C}$ which satisfies

$$|f(z)| \leq \|f\|_{\mathbb{P}_r} e^{r|\text{ Im } z|}$$

for all $z \in \mathbb{C}$.

Define for fixed $t \in \mathbb{R}$,

$$\varphi(s) := \sqrt{r/\pi}\, \text{sinc}_r(s - t\,\pi/r), \quad s \in \mathbb{R}.$$

Then for any $f \in \mathbb{P}_r$

$$(\sqrt{\pi/r})\, f(t\pi/r) = \langle f, \varphi \rangle_{\mathbb{P}_r}. \tag{1.2}$$

Hence $\mathbb{P}_r$ is a Hilbert space with reproducing kernel

$$k(s,t) = (r/\pi)\, \text{sinc}_r(t - s).$$

Representing $f \in \mathbb{P}_r$ in terms of the orthonormal basis $\{h_i\}$ we obtain by (1.2)

$$f = \sum_{i \in I} f(i\pi/r)\, \text{sinc}_r(\cdot - i\pi/r).$$

This expansion is called the *Shannon sampling series*, which shows that any function $f \in \mathbb{P}_r$ can be reconstructed from its values at the equidistant points $i\pi/r$, for $i \in \mathbb{I}$. In the following we are concerned with the problem of reconstructing $f \in \mathbb{P}_r$, given its values at non-equidistant points $\{t_i\}$. Corresponding to a given sequence of increasing real numbers $\{t_i\}_{i\in I}$ we define the vector system $\{\varphi_i\}$ in $\mathbb{P}_r$ by

$$\varphi_i := \sqrt{r/\pi}\ \mathrm{sinc}_r(\cdot - t_i\ \pi/r), \quad i \in \mathbb{I}.$$

We obtain by (1.2) the formula for the Gram matrix G corresponding to the system $\{\varphi_i\}$,

$$G_{ij} = \mathrm{sinc}_\pi(t_i - t_j), \quad i,j \in \mathbb{I}. \tag{1.3}$$

Now consider the interpolation problem in $\mathbb{P}_r$ which consists in finding an element f lying in $\mathbb{P}_r$ such that

$$(\sqrt{\pi/r})\ f(t_i\pi/r) = g_i, \quad i \in \mathbb{I}, \tag{1.4}$$

where $\{g_i\} \in \ell^2(\mathbb{I})$ is given. It follows from (1.2) that the interpolation problem (1.4) is a special type of moment problem in $\mathbb{P}_r$. That is, we want to find a function f which lies in $\mathbb{P}_r$ such that

$$\langle f, \varphi_i\rangle_{P_r} = g_i, \quad i \in \mathbb{I}. \tag{1.5}$$

The properties of the solution and regularization of this problem are discussed in Section III.1 in the case that $\{\varphi_i\}$ is a Bessel system, a Riesz-Fischer system or a Riesz basis.

Our next objective is to obtain norm estimates for elements of $\mathbb{P}_r$. These estimates are used in section V.1, where we derive stability results for interpolation in the space $\mathbb{P}_r$.
If f lies in $\mathbb{P}_r$, then by the Fourier inversion formula

$$f(t) = \frac{1}{\sqrt{2\pi}} \int_{-r}^{r} \hat{f}(\xi) e^{j\xi t} d\xi,$$

where $j^2 = -1$. By Jensen's inequality it follows that

$$|f(t)|^2 \le \frac{1}{2\pi} \int_{-r}^{r} |\hat{f}(\xi)|^2 d\xi = \frac{1}{2\pi} \int_{R} |f(t)|^2 dt.$$

Denoting $\|f\|_\infty := \sup_{t\in R}|f(t)|$, we obtain

$$\|f\|_\infty \le (1/\sqrt{2\pi})\ \|f\|_{P_r}, \quad f \in \mathbb{P}_r. \tag{1.6}$$

In the same manner we derive the Bernstein inequality.

$$\|(\partial/\partial t)f\|_{P_r}^2 = \int_{-r}^{r} |(j\xi)\hat{f}(\xi)|^2 d\xi \le r^2 \|f\|_{P_r}^2. \tag{1.7}$$

IV.2. Bessel Systems, Riesz-Fischer Systems and Riesz bases in P_r

Let $\{t_i\}_{i\in I}$ be a sequence of increasing real numbers. As above, we define for $i \in \mathbb{I}$

$$h_i := (\sqrt{r/\pi})\ \mathrm{sinc}_r(\cdot - i\pi/r) \quad \text{and} \quad \varphi_i := (\sqrt{r/\pi})\ \mathrm{sinc}_r(\cdot - t_i\pi/r). \tag{2.1}$$

In this section we give conditions on the time points t_i such that $\{\varphi_i\}$ is a Bessel system, Riesz-Fischer system or a Riesz basis in $\mathbb{P}_r$.
First we prove a useful lemma.

Lemma 2.1 . *Let $\{s_i\}_{i\in I}$ be a sequence of real numbers such that*

$$(\pi/r)\sum_{i\in I}|f(s_i\pi/r)|^2 \le B^2\|f\|^2_{\mathbb{P}_r}, \quad f\in \mathbb{P}_r,$$

where B is a positive constant. If $\{p_i\}_{i\in I}$ is a sequence of real numbers satisfying

$$|s_i - p_i| \le \gamma, \quad i\in \mathbb{I}$$

then for all $f\in \mathbb{P}_r$,

$$(\pi/r)\sum_{i\in I}|f(s_i\pi/r) - f(p_i\pi/r)|^2 \le B^2(e^{\pi\gamma}-1)^2\|f\|^2_{\mathbb{P}_r}.$$

Proof:

The space $\mathbb{P}_r$ is closed under differentiation. The Bernstein inequality (1.7) yields $\|(\partial/\partial t)f\| \le r\|f\|_{\mathbb{P}_r}$. Let $|s_i - p_i| \le \gamma$. Denote the kth derivative as $(\partial/\partial t)^k f(t)$. For any real number $\rho \neq 0$ we obtain by the Taylor series expansion and the Cauchy Schwarz inequality,

$$|f(s_i\pi/r) - f(p_i\pi/r)|^2 = |\sum_{k\in\mathbb{N}}\frac{(\partial/\partial t)^k f(s_i\pi/r)}{k!}((s_i-p_i)\pi/r)^k|^2 \le$$

$$\Big(\sum_{k\in\mathbb{N}}\frac{|(\partial/\partial t)^k f(s_i\pi/r)|^2}{k!\rho^{2k}}\Big)\Big(\sum_{k\in\mathbb{N}}\frac{|(s_i-p_i)\pi/r|^{2k}\rho^{2k}}{k!}\Big) \le$$

$$\Big(e^{(\pi^2\rho^2\gamma^2/r^2)}-1\Big)\Big(\sum_{k\in\mathbb{N}}\frac{|(\partial/\partial t)^k f(s_i\pi/r)|^2}{k!\rho^{2k}}\Big).$$

It follows by assumption and the Bernstein inequality that

$$\sum_{k\in\mathbb{N}}\sum_{i\in I}\frac{|(\partial/\partial t)^k f(s_i\pi/r)|^2}{k!\rho^{2k}} \le (B^2\|f\|^2_{\mathbb{P}_r})\Big(\sum_{\kappa\in\mathbb{N}}\frac{r^{2k}}{k!\rho^{2k}}\Big) = B^2\|f\|^2_{\mathbb{P}_r}(e^{(r^2/\rho^2)}-1).$$

Interchanging the order of summation, we obtain

$$(\pi/r)\sum_{i\in I}|f(s_i\pi/r) - f(p_i\pi/r)|^2 \le B^2\|f\|^2_{\mathbb{P}_r}\ (e^{(\pi^2\rho^2\gamma^2/r^2)}-1)(e^{(r^2/\rho^2)}-1).$$

The result follows with

$$\rho = \frac{r}{\sqrt{\gamma\pi}}.$$

□

In order to prove that $\{\varphi_i\}$ is a Bessel system, we have to find a bounded linear operator R on $\mathbb{P}_r$ (cf. Definition I.5.1 (i)) such that

$$Rh_i = \varphi_i, \quad i\in \mathbb{I}.$$

Theorem 2.2 . *If, for some positive constant γ,*

$$|t_i - i| \le \gamma, \quad i\in \mathbb{I},$$

then $\{\varphi_i\}$, given by formula (2.1), is a Bessel system in $\mathbb{P}_r$. In that case, the operator R which is given by

$$Rh_i = \varphi_i, \quad i\in \mathbb{I}$$

satisfies

$$\|R\| \le e^{\pi\gamma}.$$

Proof:

Since $\{h_i\}$ is an orthonormal basis for $\mathbb{P}_r$ we have by (1.2) and Theorem I.4.4

$$(\pi/r)\sum|f(i\pi/r)|^2 = \sum_{i\in I}|\langle f, h_i\rangle|^2 = \|f\|^2.$$

We put $s_i = i$, $p_i = t_i$ and $B = 1$ in Lemma 2.1 and obtain by (1.2)

$$\sum_{i\in I}|\langle f, h_i - \varphi_i\rangle|^2 \leq (e^{\pi\gamma} - 1)^2\|f\|^2_{\mathbb{P}_r}.$$

Define the linear operator W on $\mathbb{P}_r$ by the following expression

$$Wf := \sum_{i\in I}\langle f, h_i - \varphi_i\rangle h_i,$$

for $f \in \mathbb{P}_r$. It follows from the above estimate that W is a bounded operator: $\|W\| \leq (e^{\pi\gamma} - 1)$. Its adjoint has the property that $W^*h_i = h_i - \varphi_i$ for $i \in \mathbb{I}$, since

$$\langle f, W^*h_i\rangle = \langle Wf, h_i\rangle = \langle f, h_i - \varphi_i\rangle,$$

for arbitrary $f \in \mathbb{P}_r$. The result follows from the fact that $\|W\| = \|W^*\|$ and by taking $R := I - W^*$. □

Let $\{h_i\}$ and $\{\varphi_i\}$ be given by formula (2.1). In order to prove that $\{\varphi_i\}$ is a Riesz-Fischer system, we first formulate a lemma, which is proved in Young [55] Theorem 5, p. 162.

Lemma 2.3 . *Let $\{t_i\}_{i\in I}$ be a sequence of increasing real numbers such that*

$$t_{i+1} - t_i \geq \gamma > 1, \quad i \in \mathbb{I}.$$

Then for all $n \in \mathbb{N}$ and for all sequences of complex numbers $\{c_i\}_{i=-n}^{n}$, we have

$$m\sum_{i=-n}^{n}|c_i|^2 \leq \int_{-\pi}^{\pi}|\sum_{i=-n}^{n}(\sqrt{1/(2\pi)}c_ie^{jt_ix}|^2dx,$$

where $j^2 = -1$ and

$$m = (\frac{2}{\pi})(1 - \frac{1}{\gamma^2}).$$

Theorem 2.4 . *If $\{t_i\}$ is a sequence of increasing real numbers such that*

$$t_{i+1} - t_i \geq \gamma > 1, \quad i \in \mathbb{I},$$

then $\{\varphi_i\}$ is a Riesz-Fischer system. Moreover, there exists a bounded linear operator T on $\mathbb{P}_r$ such that

$$T\varphi_i = h_i, \quad i \in \mathbb{I},$$

and

$$\|T\| \leq \sqrt{\pi/(2 - 2/\gamma^2)}.$$

Proof:

We have the following relation between sinc functions and the exponentials,

$$\Big(\sqrt{r/\pi}\ \mathrm{sinc}_r(\cdot - t_i\ \pi/r)\Big)\widehat{\ }(\xi) = (1/\sqrt{2r})\ \chi(\xi/r)\ e^{-j(\pi/r)\ t_i\xi}. \tag{2.2}$$

Here χ is the characteristic function of the unit interval $[-1,1]$. Choose $n \in I\!N$ and a sequence of complex numbers $\{c_i\}_{i=-n}^{n}$ arbitrarily. Then

$$\| \sum_{i=-n}^{n} c_i\ \sqrt{r/\pi}\ \mathrm{sinc}_r(t - (\pi/r)t_i)\|_{I\!P_r}^2 = \| \sum_{i=-n}^{n} c_i\ (1/\sqrt{2r})\ \chi(\xi/r)\ e^{-j(\pi/r)t_i\xi}\|_{I.2}^2.$$

After the change of variables $\zeta = -\xi\pi/r$, we have

$$\| \sum_{i=-n}^{n} c_i\ \sqrt{r/\pi}\ \mathrm{sinc}_r(t - (\pi/r)t_i)\|_{I\!P_r}^2 = \| \sum_{i=-n}^{n} c_i\ (1/\sqrt{2\pi})\ \chi(\zeta/\pi)\ e^{jt_i\zeta}\|_{I.2}^2.$$

By Lemma 2.3 it follows that

$$\sum_{i=-n}^{n} |c_i|^2 \le 1/m \| \sum_{i=-n}^{n} c_i\ \sqrt{r/\pi}\ \mathrm{sinc}_r(t - (\pi/r)t_i)\|_{I\!P_r}^2,$$

where

$$m = (\frac{2}{\pi})(1 - \frac{1}{\gamma^2}).$$

Then, by Theorem I.5.2 (ii) b it follows that $\{\varphi_i\}$ is a Riesz Fischer system for $I\!P_r$. Hence there exists a bounded linear operator U such that $U\varphi_i = h_i$ for $i \in I\!I$. By the above estimate it follows that for any $h \in \mathrm{span}\{\varphi_i\}$ we have that

$$\|Uh\| \le (\sqrt{1/m})\|h\|.$$

Now define $T := U$ on $\overline{\mathrm{span}}\{\varphi_i\}$ and $T := 0$ on $(\overline{\mathrm{span}}\{\varphi_i\})^{\perp}$. □

Let $\{h_i\}$ and $\{\varphi_i\}$ be given by formula (2.1). To provide a condition for $\{\varphi_i\}$ to be a Riesz basis, we formulate the following result (cf. Young [55] Theorem 14, p.42).

Theorem 2.5 *Kadec's 1/4 theorem* .
Let $\{t_i\}$ be a sequence of real numbers such that

$$|t_i - i| \le \alpha < 1/4, \quad i \in I\!I.$$

Then for all $n \in I\!N$ and for an arbitrary sequence $\{c_i\}_{i=-n}^{n}$ we have

$$(1/2\pi) \int_R |\sum_{i \in I} c_i(e^{jix} - e^{jt_ix})|^2 dx \le \lambda^2 (\sum_{i=-n}^{n} |c_i|^2).$$

Here $j^2 = -1$ and $\lambda = (1 - \cos\pi\alpha + \sin\pi\alpha) < 1$.

Theorem 2.6 . *If*

$$|t_i - i| \le \alpha < 1/4, \quad i \in I\!I,$$

then $\{\varphi_i\}_{i \in I}$ is a Riesz basis in $I\!P_r$. The bounded linear invertible operator T on $I\!P_r$, given by

$$T\varphi_i = h_i, \quad i \in I\!I,$$

satisfies

$$\|T\| \le \frac{1}{1-\lambda}, \quad \|T^{-1}\| \le 1 + \lambda.$$

Here $\lambda = (1 - \cos\pi\alpha + \sin\pi\alpha) < 1$.

Proof:

We prove that there is a $\lambda < 1$ such that for all $m \in \mathbb{N}$ and for complex numbers c_i, $i = -m, \ldots, m$, that satisfy $\sum_{i=-m}^{m} |c_i|^2 \leq 1$, the following estimate holds

$$\| \sum_{i=-m}^{m} c_i \left(\sqrt{r/\pi}\, \mathrm{sinc}_r(\cdot - (\pi/r)t_i) - \sqrt{r/\pi}\, \mathrm{sinc}_r(\cdot - (\pi/r)i) \right) \|_{P_r} \leq \lambda. \tag{2.3}$$

By identity (2.2) we have that the left hand side of (2.3) is equal to

$$\| \sum_{i=-m}^{m} c_i\, (1/\sqrt{2r})\, \chi(\xi/r) \left(e^{-j(\pi/r)t_i\xi} - e^{-i(\pi/r)i\xi} \right) \|_{L^2(-\pi,\pi)}.$$

After the change of variables $\zeta = -\xi\pi/r$, and by Theorem 2.5 this expansion reduces to

$$\| \sum_{i=-m}^{m} c_i\, (1/\sqrt{2\pi})\, \chi(\zeta/\pi) \left(e^{jt_i\zeta} - e^{ji\zeta} \right) \|_{L^2[-\pi,\pi]} \leq$$

$$\leq (1 - \cos\pi\alpha + \sin\pi\alpha) =: \lambda.$$

If $\alpha < 1/4$, then $\lambda < 1$. Then from Theorem I.5.3 it follows that $\{\varphi_i\}$ is a Riesz basis for P_r and there exists an operator T on P_r such that $T\varphi_i = h_i$, that satisfies

$$\|T\| \leq \frac{1}{1-\lambda}, \quad \|T^{-1}\| \leq 1 + \lambda.$$

□

The results of Theorem 2.5 and Lemma 2.3 are sharp in the sense that if

$$t_i := \begin{cases} i - 1/4, & \text{if } i > 0 \\ 0, & \text{if } i = 0 \\ i + 1/4, & \text{if } i < 0 \end{cases},$$

then $\{e^{jt_i(\cdot)}\}_{i \in I}$ is neither a Riesz basis nor a Riesz-Fischer system for $L^2([-\pi,\pi])$ (cf. Young [55] p. 44, p. 164).

IV.3. Spline functions of odd degree

In this section we consider interpolation by polynomial spline functions of odd degree and we show that the interpolation problem is a special type of moment problem in the space $\mathcal{K}^{2n-1}$. Accounts of spline theory are given in Ahlberg et al. [1], de Boor [9], Schoenberg [47], and Greville [21]. Here we follow mainly Greville [21].

Given an interval $[a,b]$ we define the mesh Δ as a division of this interval.

Definition 3.1 . The mesh Δ of $[a,b]$ is a sequence of increasing real numbers $\{t_1\pi/r, \ldots, t_I\pi/r\}$ such that $a = t_1\pi/r < t_2\pi/r < \ldots < t_I\pi/r = b$. The intervals $(t_i\pi/r, t_{i+1}\pi/r)$ are called (open) mesh intervals.

The space $\mathcal{K}^m$ is defined as follows (cf. de Boor [9]).

Definition 3.2 . $\mathcal{K}^m := \{f \in C^{m-1}[a,b] \mid f$ is a polynomial of degree m or less, on each mesh interval $\}$.

The set $\mathcal{K}^{2n-1}$ consists of the so called polynomial spline functions of odd degree. The linear space $\mathcal{K}^{2n-1}$ has the inner product (cf. de Boor [9])

$$\langle f,g\rangle_{\mathcal{K}^{2n-1}} := \sum_{k=0}^{n-1} f^k(a)\overline{g^k(a)} + \langle f^n, g^n\rangle_{I.^2[a,b]}.$$

Here f^k denotes the kth derivative of f and $\langle f,g\rangle_{I.^2[a,b]} := \int_{[a,b]} f(t)\overline{g(t)}dt$. The space $\mathcal{K}^{2n-1}$ is characterized by (cf. Greville [21])

$$f \in \mathcal{K}^{2n-1} \iff \text{there exists a polynomial } p_{2n-1} \text{ and complex numbers } c_i, (i \in I\!I)$$
$$\text{such that } \quad f = p_{2n-1} + \sum_{i\in I} c_i(\,\cdot - t_i\pi/r)_+^{2n-1}.$$

Here p_{2n-1} is a polynomial of degree $2n-1$ or less and for any $t \in I\!R$

$$(t)_+^k := \begin{cases} t^k, & t \geq 0 \\ 0, & t < 0 \end{cases}.$$

Since $\mathcal{K}^{2n-1}$ is a finite dimensional inner product space, it is complete, i.e. $\mathcal{K}^{2n-1}$ is a separable Hilbert space. Moreover $\mathcal{K}^{2n-1}$ is a Hilbert space with reproducing kernel (cf. section I.2):

$$\sigma(t,s) := (\sqrt{\pi/r})\sum_{k=0}^{n-1}\frac{(t-a)^k(s-a)^k}{(k!)^2} \quad +$$
$$(\sqrt{\pi/r})\sum_{k=0}^{n-1}(-1)^{n+k+1}\frac{(t-a)^{2n-k-1}(s-a)^k}{(2n-k-1)!k!} \quad +$$
$$\frac{(-1)^n(\sqrt{\pi/r})}{(2n-1)!}(t-s)_+^{2n-1}. \tag{3.1}$$

Define the system of independent vectors $\{\varphi_i\}_{i\in I}$ in $\mathcal{K}^{2n-1}$, corresponding to the mesh Δ as

$$\varphi_i := \sigma(\cdot, t_i\pi/r)$$

For any function $f \in \mathcal{K}^{2n-1}$ Taylor's formula holds,

$$f = \sum_{k=0}^{n-1}\frac{f^k(a)(\,\cdot - a)^k}{(k!)} + \frac{1}{(n-1)!}\int_{[a,(\cdot)\,]}(\,\cdot - t)^{n-1}f^n(t)dt.$$

Using this formula, the point evaluation can be written as the inner product (cf. Bertero [5])

$$\sqrt{\pi/r}f(t_i\pi/r) = \langle f,\varphi_i\rangle_{\mathcal{K}^{2n-1}}. \tag{3.2}$$

So the interpolation problem is a special type of moment problem for functions in the space $\mathcal{K}^{2n-1}$.

One can derive from Taylor's formula the estimate (cf. formula (1.6))

$$\|f\|_\infty \leq C\|f\|_{\mathcal{K}^{2n-1}}, \tag{3.3}$$

where

$$C = \sup\Big\{\Big(\sum_{k=0}^{n-1}\frac{(b-a)^{2k}}{k!^2}\Big)^{1/2}, \frac{(b-a)^{n-1/2}}{(n-1)!\,\sqrt{2n-1}}\Big\}. \tag{3.4}$$

IV.4. Interpolation and regularization

In this section we discuss examples of sinc- and spline-interpolation curves and illustrate the necessity of a regularization method.

Let $\{t_i\}_{i\in I}$ and $\{g_i\}_{i\in I}$ be sequences of real and complex numbers, respectively. The interpolation problem consists in finding a function f lying in $\mathcal{H}$ such that

$$(\sqrt{\pi/r})f(t_i\pi/r) = g_i, \quad i \in \mathbb{I}. \tag{4.1}$$

Here $\mathcal{H}$ can be the Hilbert space of bandlimited functions $\mathbb{P}_r$ or the space of odd degree splines $\mathcal{K}^{2n-1}$.

If $\mathcal{H} = \mathbb{P}_r$, then we define

$$\varphi_i := (\sqrt{r/\pi})\ \operatorname{sinc}_r(\cdot - t_i\pi/r)$$

and if $\mathcal{H} = \mathcal{K}^{2n-1}$, we put

$$\varphi_i := \sigma(\cdot, t_i\pi/r).$$

The function σ is given by formula (3.1). In either case, by (1.2) and (3.2) the interpolation problem is a moment problem. It consists in finding $f \in \mathcal{H}$ such that

$$\langle f, \varphi_i\rangle = g_i, \quad i \in \mathbb{I}. \tag{4.2}$$

By substitution in (4.2) and from Proposition III.1.2 it follows that the unique minimum norm solution of problem (4.2) is

$$f = \sum_{i\in I} g_i\psi_i,$$

where

$$\psi_i := \sum_{j\in I} \overline{(G^{-1})}_{ij}\ \varphi_j.$$

The Gram matrix G is given by

$$G_{ij} := \langle \varphi_j, \varphi_i\rangle, \quad i,j \in \mathbb{I}.$$

If $\mathcal{H} = \mathbb{P}_r$ the elements of the Gram matrix are (formula (1.3))

$$G_{ij} = \operatorname{sinc}_\pi(t_i - t_j), \quad i,j \in \mathbb{I}. \tag{4.3}$$

If $\mathcal{H} = \mathcal{K}^{2n-1}$, then from formula's (3.1) and (3.2)

$$G_{ij} = \sigma(t_j\pi, r, t_i\pi/r). \tag{4.4}$$

If the time points $\{t_i\}$ are positioned equidistantly, we call it uniform sampling, otherwise non-uniform sampling. In Figure 4.1 the function $h(t) = \cos(7\pi t)$ is plotted for $t \in [0,1]$. It is sampled at the uniform time markers $t_i = i/10$ for $i = 0, 1, ..., 10$. The interpolation curves in the case of sinc, degree 0, degree 1 and degree 3 spline functions are illustrated in Figures 4.2 - 4.5. If $h(t)$ is sampled at nonuniform time markers, the behaviour of the interpolating sinc functions in Figure 4.7 changes drastically. The main reason for this behaviour is that the interpolation problem can be ill-conditioned for nonuniform sampling, as we will see in Section V.1.

Figure 4.6 is a plot of the interpolating spline of degree 3 for nonuniform sampling. If the degree of the spline is high then the interpolating function tends to oscillate quickly.

One way to avoid this oscillating behaviour of the interpolating functions in the case of nonuniform sampling can be by applying Tychonov-Phillips regularization. By Theorem III.1.5 we know that this regularization $\{T^\gamma\}$ corresponding to the moment problem (4.2) is given by

$$T^\gamma g := \sum_{j\in I}\sum_{i\in I}((G+\gamma I)^{-1})_{ji}\; g_i\; \varphi_j. \tag{4.5}$$

In Figure 4.9 formula (4.5) is applied in the case of sinc interpolation in $I\!P_r$ with parameter value $\gamma = 10^{-4}$. The regularization for third degree spline interpolation is illustrated in Figure 4.8 with regularization parameter $\gamma = 10^{-5}$.

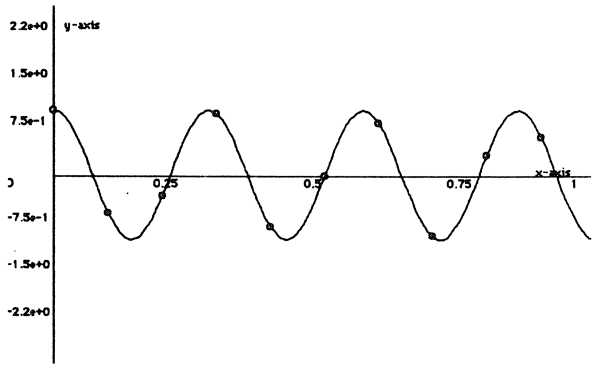

Figure 4.1. Original function: $cos(7\pi x)$ with uniform sampling points.

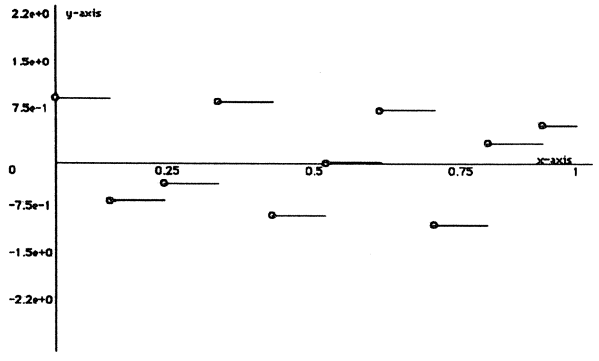

Figure 4.2. Uniform samples; interpolation by a spline of degree 0

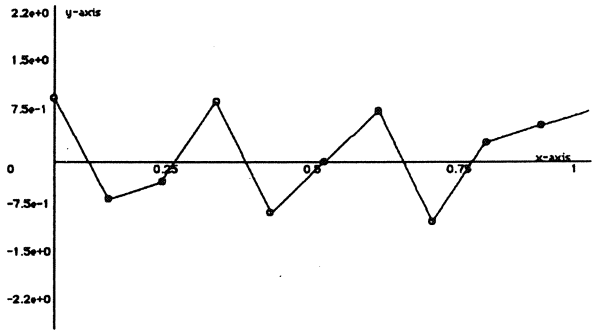

Figure 4.3. Uniform samples; interpolation by a spline of degree 1

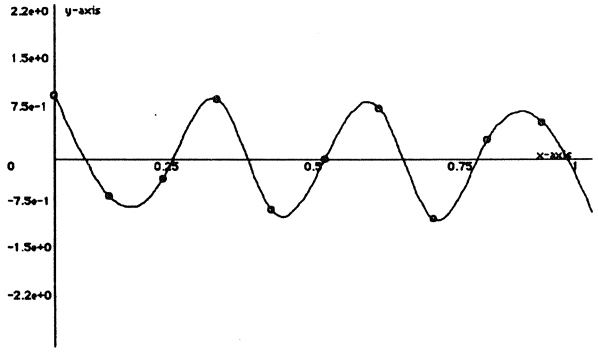

Figure 4.4. Uniform samples; interpolation by a spline of degree 3

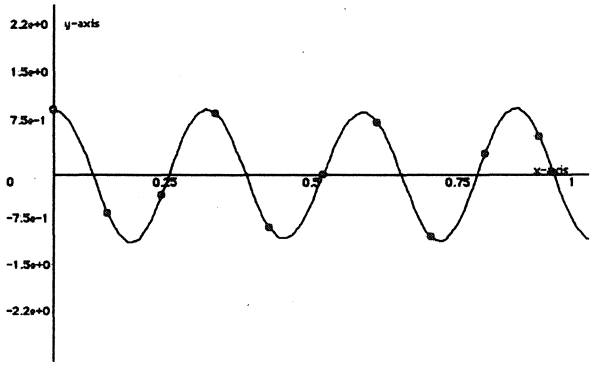

Figure 4.5. Uniform samples; interpolation by sinc functions

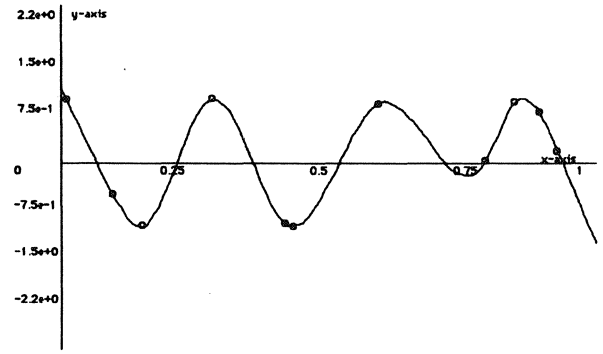

Figure 4.6. Non uniform samples; interpolation by splines of degree 3

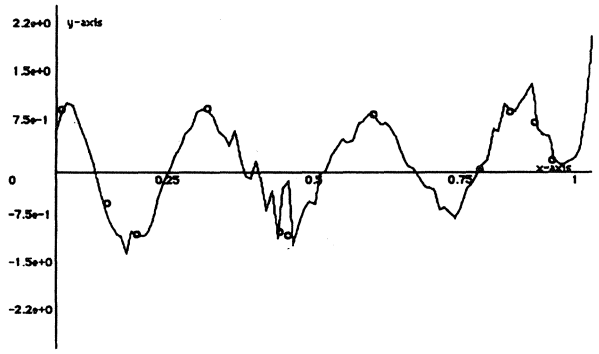

Figure 4.7. Non uniform samples; interpolation by sinc functions

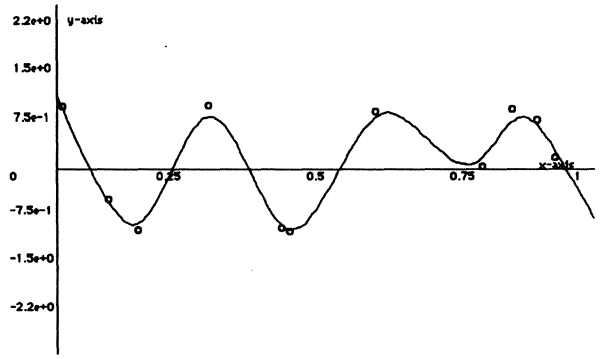

Figure 4.8. Non uniform samples; regularized interpolation by splines of degree 3

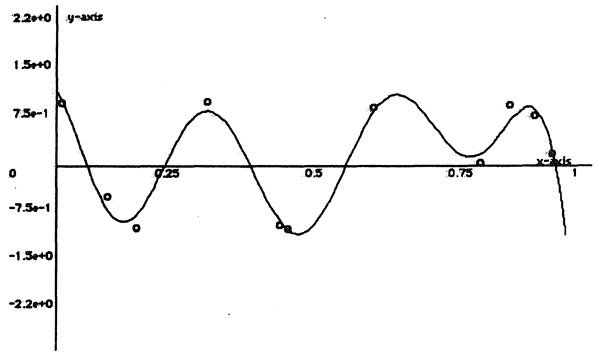

Figure 4.9. Non uniform samples; regularized interpolation by sinc functions

IV.5. Solution and regularization of the mixed Fourier interpolation problem

In this section we characterize the solution f of problem (0.1). We demand f to lie in the space $L^2(D,\mathcal{H})$. Since in practice the data set will always be finite, we assume only for this section that the index set $\mathbb{I}$ is also finite in the case of bandlimited functions, say $\mathbb{I} = \{1,...,I\}$. (Because the results which are presented here are automatically valid if $\mathbb{K}$ is finite, it is for theoretical purposes still assumed that the index set $\mathbb{K} = \mathbb{Z}$.)

In the case of the mixed problem, we have measured a sequence of complex values $\{g_{\kappa,i}\} \in \ell^2(\mathbb{K}\times\mathbb{I})$ at the time points $\{t_{\kappa,i}\pi/r\}_{\kappa\in K, i\in I}$. Assume that for each $\kappa \in \mathbb{K}$, the sequence $\{t_{\kappa,i}\}_{i\in I}$ consists of distinct time points. $f \in L^2(D,\mathcal{H})$ is called a solution of the mixed problem if it satisfies,

$$\sqrt{\pi/r}\,\widehat{f}(\kappa, t_{\kappa,i}\pi/r) = g_{\kappa,i}, \quad \kappa \in \mathbb{K}, i \in \mathbb{I}. \tag{5.1}$$

In the case that $\mathcal{H} = \mathbb{P}_r$, we define

$$\varphi_{\kappa,i} := (\sqrt{r/\pi})\ \mathrm{sinc}_r(\cdot - t_{\kappa,i}\pi/r). \tag{5.2}$$

If $\mathcal{H} = \mathcal{K}^{2n-1}$, then

$$\varphi_{\kappa,i} := \sigma(\cdot, t_{\kappa,i}\pi/r). \tag{5.3}$$

The function σ is given by formula (3.1). In either case, it follows from the results of Section 1 and Section 3, that the mixed problem (5.1) can be solved by finding a function $f \in L^2(D,\mathcal{H})$, which satisfies

$$\langle \widehat{f}(\kappa), \varphi_{\kappa,i}\rangle = g_{\kappa,i}, \quad \kappa \in \mathbb{K}, i \in \mathbb{I}.$$

In order to compute the solution we define

$$G_{ij}(\kappa) := \langle \varphi_{\kappa,j}, \varphi_{\kappa,i}\rangle_{\mathcal{H}}, \tag{5.4}$$

$$\psi_{\kappa,i} := \sum_{j\in I} \overline{(G(\kappa)^{-1})}_{ij}\varphi_{\kappa,j} \tag{5.5}$$

and

$$c_\kappa := \sum_{i\in I} g_{\kappa,i}\psi_{\kappa,i}. \tag{5.6}$$

Note that for each $\kappa \in \mathbb{K}$, the Gram matrix $G(\kappa)$ is invertible, since $\{t_{\kappa,i}\}_{i\in I}$ is a finite sequence consisting of distinct time points.

For fixed $\kappa \in \mathbb{K}$, c_κ is the minimum norm solution of the interpolation problem:

$$(\sqrt{\pi/r})c_\kappa(t_{\kappa,i}\pi/r) = g_{\kappa,i}, \quad i \in \mathbb{I}. \tag{5.7}$$

The following theorem guarantees existence of a solution f of the mixed problem.

Theorem 5.1 . *Let the sequence $\{c_\kappa\}_{\kappa\in K} \subset \mathcal{H}$ be given by (5.6), where $\mathcal{H}$ is a separable Hilbert space. If*

$$\sum_{\kappa\in K} \|c_\kappa\|^2_{\mathcal{H}} < \infty, \tag{5.8}$$

then

$$f = \sum_{\kappa\in K} c_\kappa e_\kappa \tag{5.9}$$

is the unique minimum norm solution of problem (0.1) in the space $L^2(D,\mathcal{H})$.

Proof:

For $\kappa \in \mathbb{K}$ fixed, c_κ is the minimum norm solution of the problem

$$\langle c_\kappa, \varphi_{\kappa,i}\rangle = g_{\kappa,i}, \quad i \in \mathbb{I}.$$

By Parseval 's relation from Theorem II.1.6, $|||f|||^2 = \sum_{\kappa\in K} \|\widehat{f}(\kappa)\|^2$, for $f \in L^2(D,\mathcal{H})$, and by putting $\widehat{f}(\kappa) := c_\kappa$ it follows that $f := \sum_{\kappa\in K} c_\kappa e_\kappa$ is unique minimum norm solution of the problem

$$\langle \widehat{f}(\kappa), \varphi_{\kappa,i}\rangle = g_{\kappa,i}, \quad \kappa \in \mathbb{K}, i \in \mathbb{I}.$$

□

From Theorem 5.1 it follows that the minimum norm solution of (0.1) is obtained by interpolation in time followed by Fourier inversion. It is not required to perform an interpolation in the Fourier domain. This result is of practical importance because for each $\kappa \in \mathbb{K}$ one can solve the partial problem (5.7) and then obtain a solution of the entire problem (0.1) by Fourier inversion. This implies that, when solving (0.1) on a computer, one only has to store (for certain $\kappa \in \mathbb{K}$) the partial data set $\{g_{\kappa,i}\}_{i\in I}$ and find the corresponding minimum norm solution c_κ. Repeating this procedure for each $\kappa \in \mathbb{K}$ independently we then find the minimum norm solution f of the mixed problem by Fourier inversion. We can also formulate this result in another manner: the information contained in the data $\{g_{\kappa,i}\}_{i\in I}$ is used only once for different values of $\kappa \in \mathbb{K}$.

If, however, the system $\{e_\kappa\}$ is not an orthonormal basis for $L^2(D,\mathbb{C})$, then we have to perform an interpolation in the Fourier domain as well.

The Tychonov-Phillips regularization $\{T^\gamma\}$ corresponding to the mixed Fourier interpolation problem is given by Theorem III.3.3, $T^\gamma := \{T^\gamma_\kappa\}$, where for $g \in \ell^2(\mathbb{I})$

$$T^\gamma_\kappa g := \sum_{j\in I}\sum_{i\in I}((G(\kappa)+\gamma I)^{-1})_{ij}\, g_i\, \varphi_{\kappa,j}.$$

From this result it follows that the Tychonov-Phillips regularization is obtained by regularizing for each $\kappa \in \mathbb{K}$ independently.

IV.6. Examples of solutions of the mixed Fourier interpolation problem

We now give examples of solutions of the mixed problem in the Hilbert space $L^2(D, \mathbb{P}_r)$. Let the sequence of time points $\{t_{\kappa,i}\}_{\kappa\in K, i\in I}$ and the sequence of complex numbers $\{g_{\kappa,i}\} \in \ell^2(K \times I)$ be given. The mixed Fourier interpolation problem in $L^2(D, \mathbb{P}_r)$ consists in finding an element f lying in $L^2(D, \mathbb{P}_r)$ such that

$$\sqrt{\pi/r}\hat{f}(\kappa, t_{\kappa,i}\pi/r) = g_{\kappa,i}, \quad \kappa \in K, i \in I.$$

In the following we give examples such that the conditions of Theorems III.3.2. and III.3.3 are satisfied.

Define $\{h_i\}$ by formula (2.1) and $\{\varphi_{\kappa,i}\}$ by formula (5.2). $\{h_i\}_{i\in I}$ is an orthonormal basis for $\mathbb{P}_r$ (cf. Section 1). From Section 5 we know that the mixed Fourier interpolation problem can be solved, by finding a solution of the mixed Fourier moment problem in $L^2(D, \mathbb{P}_r)$:

$$\langle \hat{f}(\kappa), \varphi_{\kappa,i}\rangle = g_{\kappa,i}, \quad \kappa \in K, i \in I.$$

To solve the mixed Fourier moment problem, we use the results of Section III.3.

Example 6.1 .

Assume that $\{t_{\kappa,i}\}$ satisfies

$$|t_{\kappa,i} - i| \leq \gamma, \quad \kappa \in K, i \in I.$$

Then by Theorem 2.2 the sequence $\{\varphi_{\kappa,i}\}_{i\in I}$ is a Bessel system in $\mathbb{P}_r$ for all $\kappa \in K$. Moreover for each $\kappa \in K$ there exists a bounded linear invertible operator R_κ such that

$$R_\kappa h_i = \varphi_{\kappa,i}, \quad i \in I.$$

The norm of R_κ satisfies the uniform estimate $\kappa \in K$,

$$\|R_\kappa\| \leq e^{\pi\gamma},$$

hence $\{R_\kappa\}_{\kappa\in K}$ is a uniformly bounded family of linear operators. By Theorem II.2.1 $\{e_\kappa\varphi_{\kappa,i}\}$ is a Bessel system in $L^2(D, \mathbb{P}_r)$ and there exists a bounded linear operator $\mathcal{R}$ on $L^2(D, \mathbb{P}_r)$ such that

$$\mathcal{R}(e_\kappa h_i) = e_\kappa\varphi_{\kappa,i}, \quad \kappa \in K, i \in I.$$

Moreover

$$\|\mathcal{R}\| \leq e^{\pi\gamma}.$$

Introduce the linear operator $\mathcal{A} : L^2(D, \mathbb{P}_r) \to \ell^2(K \times I)$, by

$$\mathcal{A}f := \{\langle\langle f, e_\kappa\varphi_{\kappa,i}\rangle\rangle\}_{\kappa\in K, i\in I}.$$

That $\mathcal{A}$ is a bounded linear operator can be seen as follows.

$$\|\mathcal{A}f\|^2_{\ell^2(K\times I)} = \sum_{\kappa\in K, i\in I} |\langle\langle f, e_\kappa\varphi_{\kappa,i}\rangle\rangle|^2 \leq \sum_{\kappa\in K, i\in I} |\langle\langle f, \mathcal{R}(e_\kappa h_i)\rangle\rangle|^2 \leq$$

$$\sum_{\kappa\in K, i\in I} |\langle\langle \mathcal{R}^* f, e_\kappa h_i\rangle\rangle|^2 = |||\mathcal{R}^* f|||^2 \leq \|\mathcal{R}\|^2 \; |||f|||^2.$$

The mixed Fourier interpolation problem can now be written as an equation:

$$\mathcal{A}f = g$$

By Theorem III.3.3 we have that the Tychonov-Phillips regularization $\{T^\gamma\}_{\gamma>0}$ of $\mathcal{A}^+$ has the decomposition

$$T^\gamma = \{T^\gamma_\kappa\}_{\kappa\in K},$$

where

$$T^\gamma_\kappa h = \sum_{j\in I}\sum_{i\in I}((G(\kappa) + \gamma I)^{-1})_{ij} h_i \varphi_{\kappa,j}, \quad h \in \ell^2(I).$$

In the case of a Riesz-Fischer system in $L^2(D, \mathbb{P}_r)$ we have the following situation.

Example 6.2 .

Assume that for each fixed $\kappa \in \mathbb{K}$ the sequence $\{t_{\kappa,i}\}_{i\in I}$ is increasing and satisfies

$$t_{\kappa,i+1} - t_{\kappa,i} \geq \gamma > 1, \quad i \in \mathbb{I}.$$

Then by Section 1 there exists for each $\kappa \in \mathbb{K}$ a bounded linear operator T_κ on $\mathbb{P}_r$ such that

$$T_\kappa \varphi_{\kappa,i} = h_i, \quad i \in \mathbb{I}.$$

Moreover by Theorem 2.4 the norm of T_κ can be estimated uniformly in $\kappa \in \mathbb{K}$,

$$\|T_\kappa\| \leq \sqrt{\frac{\pi}{2 - 2/\gamma^2}}.$$

Hence $\{T_\kappa\}$ is a uniformly bounded family of operators. By Theorem II.2.2 $\{e_\kappa \varphi_{\kappa,i}\}$ is a Riesz-Fischer system in $L^2(D, \mathbb{P}_r)$ and there existst a bounded linear operator T on $L^2(D, \mathbb{P}_r)$ such that

$$T(e_\kappa \varphi_{\kappa,i}) = e_\kappa h_i, \quad \kappa \in \mathbb{K}, i \in \mathbb{I}.$$

Moreover

$$\|T\| \leq \sqrt{\frac{\pi}{2 - 2/\gamma^2}}.$$

For a Riesz basis in $L^2(D, \mathbb{P}_r)$ we have the following example.

Example 6.3 .

Assume that for each fixed $\kappa \in \mathbb{K}$ the sequence $\{t_{\kappa,i}\}_{i\in I}$ satisfies

$$|t_{\kappa,i} - i| \leq \alpha < 1/4, \quad i \in \mathbb{I}.$$

Let $\kappa \in \mathbb{K}$ be fixed. By Theorem 2.6 there exists a bounded linear invertible operator T_κ on $\mathbb{P}_r$ such that

$$T_\kappa \varphi_{\kappa,i} = h_i, \quad i \in \mathbb{I}.$$

Moreover the norms of T_κ and T_κ^{-1} can be estimated uniformly in $\kappa \in \mathbb{K}$,

$$\|T_\kappa\| \leq \frac{1}{1-\lambda} \quad \text{and} \quad \|T_\kappa^{-1}\| \leq 1 + \lambda, \quad \lambda := 1 - \cos \pi\alpha + \sin \pi\alpha.$$

Hence $\{T_\kappa\}$ and $\{T_\kappa^{-1}\}$ are uniformly bounded families of operators. By Theorem II.2.3 $\{e_\kappa \varphi_{\kappa,i}\}$ is a Riesz basis in $L^2(D, \mathbb{P}_r)$ and there existst a bounded linear invertible operator T on $L^2(D, \mathbb{P}_r)$ such that

$$T(e_\kappa \varphi_{\kappa,i}) = e_\kappa h_i, \quad \kappa \in \mathbb{K}, i \in \mathbb{I}.$$

Moreover

$$\|T\| \leq \frac{1}{1-\lambda} \quad \text{and} \quad \|T^{-1}\| \leq 1 + \lambda.$$

The solution of the mixed Fourier interpolation problem is given by Theorem III.3.2.

IV.7. Historical remarks

In this section we give a brief sketch of the historical development behind the theory on the nonharmonic exponentials $\{e^{jt_i(\cdot)}\}$, where $\{t_i\}_{i\in I}$ is a sequence of real numbers and $I = \mathbb{Z}$.

The study of nonharmonic Fourier expansions was initiated by Paley and Wiener (1934), who discovered the possibility of representing a function $f \in L^2[-\pi,\pi]$ as a series of the form

$$f = \sum_{i\in I} c_i e^{jt_i(\cdot)}.$$

Here the c_i are complex numbers. In 1942, Duffin and Eachus showed that $\{e^{jt_i(\cdot)}\}$ is a Riesz basis for $L^2[-\pi,\pi]$ if

$$|t_i - i| \le \alpha < \frac{\log 2}{\pi}, \quad i \in I.$$

This result also holds for a sequence of complex numbers. Ultimately it was Kadec [28] who showed (cf. Theorem 2.5) that for real $\{t_i\}$ the bound on the differences $|t_i - i|$ could be improved to 1/4:

$$|t_i - i| \le \alpha < 1/4, \quad i \in I.$$

That 1/4 is in fact the "best possible" constant was already proved by Levinson [36] in 1940.

Since then the result of Kadec has been generalized, e.g. by Katznelson (1971 in [29]): If $\{t_i\}$ is a sequence of complex numbers, such that

$$\sup_{i\in I}|\mathrm{Re}\ t_i - i| < 1/4, \quad \text{and} \quad \sup_{i\in I}|\mathrm{Im}\ t_i| < \infty,$$

then $\{e^{jt_i(\cdot)}\}$ is a Riesz basis for $L^2[-\pi,\pi]$. (In fact, Katznelson proved a stronger result, which we do not state here.)

There remain many open problems in this area; we only mention one. Every Schauder basis for $L^2[-\pi,\pi]$ (Definition I.4.3) of the form $\{e^{jt_i(\cdot)}\}$ encountered so far was proved to be a Riesz basis. Open problem: Are there bases of complex exponentials that are *not* Riesz bases?

Chapter V

Stability of the Mixed Fourier Interpolation Problem

The mixed Fourier-interpolation problem consists in finding a function $f \in L^2(D,\mathcal{H})$ such that

$$(\sqrt{\pi/r})\widehat{f}(\kappa, t_{\kappa,i}\pi/r) = g_{\kappa,i}, \quad \kappa \in I\!K, i \in I\!I. \tag{0.1}$$

We refer to this problem as the unperturbed problem. Here the data $\{g_{\kappa,i}\} \in \ell^2(I\!K \times I\!I)$ and the time points $\{t_{\kappa,i}\}$ are given.

In this chapter we prove three types of error estimates. The first one is the aliasing error. Suppose the original function which is to be reconstructed is g. The data $\{g_{\kappa,i}\}$ are associated with this function g by the following relation

$$g_{\kappa,i} := (\sqrt{\pi/r})\widehat{g}(\kappa, t_{\kappa,i}\pi/r), \quad \kappa \in I\!K, i \in I\!I.$$

Suppose that g lies in the function space $L^2(D,\mathcal{G})$ and not in $L^2(D,\mathcal{H})$, where the Banach space $\mathcal{G}$ contains the subspace $\mathcal{H}$. (Note that then $L^2(D,\mathcal{G})$ contains $L^2(D,\mathcal{H})$). The solution f of problem (0.1), however, is required to be an element of $L^2(D,\mathcal{H})$. This causes an error,

$$\mathrm{E}_{\mathrm{al}}^{\mathcal{H}} := \Big(\int_D \|g(x,.) - f(x,.)\|_{\mathcal{G}}^2 d\mu(x)\Big)^{1/2},$$

which we call the *aliasing error*. (A precise definition is given in Section 2.)

The second error estimate is the amplitude error. Suppose the data $\{g_{\kappa,i}\}$ are perturbed to $\{g'_{\kappa,i}\}$. The solution which corresponds to the perturbed data is called f' and satisfies

$$(\sqrt{\pi/r})\ \widehat{f}'(\kappa, t_{\kappa,i}\pi/r) = g'_{\kappa,i} \quad \kappa \in I\!K, i \in I\!I. \tag{0.2}$$

The *amplitude error* is defined as the difference between f and f' in $L^2(D,\mathcal{H})$-norm:

$$\mathrm{E}_{\mathrm{amp}}^{\mathcal{H}} := \Big(\int_D \|f(x,.) - f'(x,.)\|_{\mathcal{H}}^2 d\mu(x)\Big)^{1/2}.$$

The third error estimate is called the *time jitter error*. Suppose the time points $\{t_{\kappa,i}\}$ are perturbed to $\{t'_{\kappa,i}\}$. The solution that corresponds to the perturbed problem is again denoted by f' and satisfies

$$(\sqrt{\pi/r})\ \widehat{f}'(\kappa, t'_{\kappa,i}\ \pi/r) = g_{\kappa,i} \quad i \in I\!I. \tag{0.3}$$

The time jitter error is the difference between f and f' in $L^2(D,\mathcal{H})$-norm and is denoted as $E_{tj}^{\mathcal{H}}$.

In section one we prove error estimates for sinc interpolation in the Paley-Wiener space $\mathbb{P}_r$. These error estimates will be used in section two to prove the stability of the mixed Fourier interpolation problem in the case of reconstruction by sinc functions. There we also prove error estimates for the mixed problem in the case of spline functions. Conclusions which can be drawn from the error analysis of section two are presented in the third section.

The notational convention in this chapter is as follows. $\mathbb{K}$ is a countable index set and $\mathbb{I}$ is the finite index set $\{1,...,I\}$ in the case of spline functions and $\mathbb{Z}$ in the case of bandlimited functions. Define $D := [-\pi,\pi]^n$ and let $\{e_\kappa\}_{\kappa\in K}$ be the canonical orthonormal basis for $L^2(D,\mathbb{C})$,

$$e_\kappa(x) := (1/\sqrt{2\pi})\, e^{i\kappa x},$$

where $x \in D$.

V.1. Stability of Sinc Interpolation

In this section we consider stability and error estimates for the following interpolation problem. Given are data $\{g_i\} \in \ell^2(\mathbb{I})$ and time markers $\{t_i\}_{i\in I}$. The problem is to find a function f in $\mathbb{P}_r$ such that

$$\sqrt{\pi/r}\ f(t_i\ \pi/r) = g_i \quad i \in \mathbb{I}. \tag{1.1}$$

The definitions of aliasing error, amplitude error and time jitter error for the time dependent problem (1.1) are given below. These errors are denoted as e_{al}, e_{amp} and e_{tj} to emphasize the distinction between the errors for the mixed problem (0.1).

The first error estimate is the aliasing error, which we define as follows. (A precise formulation is given in Section 1.1.) Suppose g is the original function which has to be reconstructed from the data $\{g_i\}$, where $g_i := g(t_i\pi/r)$, for $i \in \mathbb{I}$. Suppose g lies outside the Hilbert space $\mathbb{P}_r$. Since the solution of problem (1.1) is required to lie in $\mathbb{P}_r$, we make an error,

$$e_{al} := \|f - g\|_\infty$$

which is called the *aliasing error*. Here the supremum norm of a function $f : \mathbb{R} \to \mathbb{C}$ is defined as

$$\|f\|_\infty := \sup_{t\in R}|f(t)|.$$

The second error estimate we compute is the amplitude error, which is defined as follows. Suppose the data $\{g_i\}$ are perturbed to $\{g_i'\}$. The solution which corresponds to the perturbed data denoted as f' and satisfies

$$\sqrt{\pi/r}\ f'(t_i\ \pi/r) = g_i' \quad i \in \mathbb{I}. \tag{1.2}$$

The *amplitude error* is defined as the difference between f and f' in norm,

$$e_{amp} = \|f - f'\|_{P_r}.$$

A third error estimate, called the time jitter error, is defined as follows. Suppose the measurement times $\{t_i\}$ are perturbed to $\{t_i'\}$. The solution that corresponds to the perturbed problem is again denoted by f' and satisfies

$$\sqrt{\pi/r}\ f'(t_i'\ \pi/r) = g_i \quad i \in \mathbb{I}. \tag{1.3}$$

The *time jitter error* is the difference between f and f' in norm,

$$e_{tj} = \|f - f'\|_{P_r}.$$

In subsections 1.1, 1.2 and 1.3 estimates for the aliasing error, the amplitude error and the time jitter error, are given.

1.1. The aliasing error

Here we give an estimate for the aliasing error. We restrict ourselves to the case of uniform sampling, i.e. $t_i = i$ for $i \in \mathbb{I}$. First, define the operator $P : \mathcal{S} \to \mathbb{P}_r$ by

$$Ph := \sum_{i \in I} (\sqrt{\pi/r})\ h(i\pi/r)\ \mathrm{sinc}_r(\,. - i\pi/r), \tag{1.4}$$

for $h \in \mathcal{S}$. Here $\mathcal{S}$ is the linear space of rapidly decreasing functions, cf. Hörmander [26] Definition 7.1.2. p. 160, which is defined as the collection of all $C^\infty(\mathbb{R})$-functions f such that

$$\sup_{x \in R} |x^\alpha\ (d/dx)^\beta f(x)| < \infty,$$

for all positive integers α and β. $L^\infty(\mathbb{R})$ is the space of bounded measurable functions with norm $\|\ \|_\infty$. $L^\infty(\mathbb{R})$ is a Banach space. Note that $\mathcal{S}$ and $\mathbb{P}_r$ are subspaces of $L^\infty(\mathbb{R})$. So, we can define the aliasing error as

$$e_{\mathrm{al}} := \|h - Ph\|_\infty.$$

Note that this definition coincides with the previous one.
To prove an estimate for the aliasing error, we use the Poisson summation formula, which we state as a Lemma.

Lemma 1.1 . *For any function $h \in \mathcal{S}$ the Poisson summation formula holds, that is*

$$\sum_{k=-\infty}^{\infty} \widehat{h}(\xi - 2k/r) = (\sqrt{\pi/2})(1/r) \sum_{i=-\infty}^{\infty} h(i\pi/r) e^{-j\xi i\pi/r}.$$

Here $j^2 = -1$.

The next lemma provides a bound for the aliasing error.

Lemma 1.2 . *For $h \in \mathcal{S}$,*

$$e_{al} \le \sqrt{\frac{2}{\pi}} \int_{R \setminus [-r,r]} |\widehat{h}(\xi)| d\xi. \tag{1.5}$$

Proof:

For $h \in \mathcal{S}$ we have the relation

$$|h(t)| = |\frac{1}{\sqrt{2\pi}} \int_R \widehat{h}(\xi) e^{jt\xi} d\xi| \le \frac{1}{\sqrt{2\pi}} \int_R |\widehat{h}(\xi)| d\xi.$$

So,

$$\|h\|_\infty \le \frac{1}{\sqrt{2\pi}} \|\widehat{h}\|_{L^1(R)}.$$

We recall the relation between *sinc* functions and the complex exponentials (cf. Section IV.2),

$$\Big(\mathrm{sinc}_r(\cdot - i\pi/r) \Big)\widehat{\ }(\xi) = (\sqrt{\pi/2})(1/r)\ \chi(\xi/r) e^{-j\xi i\pi/r}.$$

Here χ is the indicator function of the interval $[-1, 1]$. Now it follows by Lemma 1.1 and the two relations above that

$$\|h - Ph\|_\infty \le \frac{1}{\sqrt{2\pi}} \|\widehat{h} - (Ph)\widehat{\ }\|_{L^1(R)} =$$

$$\frac{1}{\sqrt{2\pi}} \int_R |\widehat{h}(\xi) - \sum_{i=-\infty}^{\infty} (\sqrt{\pi/2})(1/r)\ h(i\pi/r)\chi(\xi/r) e^{-j\xi i\pi/r}| d\xi =$$

$$\frac{1}{\sqrt{2\pi}} \int_{[-r,r]} |(1 - \chi(\xi/r))\widehat{h}(\xi) - \sum_{k=-\infty, k\neq 0}^{\infty} \widehat{h}(\xi - 2k/r)| \le \sqrt{\frac{2}{\pi}} \int_{R \setminus [-r,r]} |\widehat{h}(\xi)| d\xi.$$

□

A proof of a similar statement can be found in Natterer [42] Theorem 1.3, pp. 57-59.

1.2. The amplitude error

Let $\{g_i\}_{i\in I}$, $\{g_i'\}_{i\in I} \in \ell^2(I\!I)$ be the data corresponding to problem (1.1), and the perturbed data corresponding to (1.2) respectively.
The following proposition holds in the case of a separable Hilbert spaces $\mathcal{H}$ with orthonormal basis $\{h_i\}_{i\in I}$.

Proposition 1.3 . *Let $\{\varphi_i\}_{i\in I}$ be a Riesz basis in a Hilbert space $\mathcal{H}$, with biorthogonal system $\{\psi_i\}_{i\in I}$, and suppose $\{g_i\}, \{g_i'\} \in \ell^2(I\!I)$. The following estimate holds,*

$$\|\sum_{i\in I}(g_i - g_i')\psi_i\|_{\mathcal{H}} \le \|G^{-1}\|^{1/2} \|g - g'\|_{\ell^2},$$

where G is the Gram matrix given by

$$G_{ij} := \langle\varphi_j, \varphi_i\rangle_{\mathcal{H}}, \quad i,j \in I\!I.$$

Proof:

By (I.5.3) and (I.5.2) we obtain

$$\|\sum_{i\in I}(g_i - g_i')\psi_i\|_{\mathcal{H}} =$$

$$\|\sum_{i\in I}(g_i - g_i')T^*h_i\|_{\mathcal{H}} \le \|T\| \, \|\sum_{i\in I}(g_i - g_i')h_i\|_{\mathcal{H}} =$$

$$\|T\| \, \|g - g'\|_{\ell^2} = \|G^{-1}\|^{1/2} \, \|g - g'\|_{\ell^2}.$$

This proves the proposition. □

Now take $\mathcal{H} = I\!P_\tau$ and let $\{h_i\}$ and $\{\varphi_i\}$ be given by formula (IV.2.1). The biorthogonal system $\{\psi_i\}$ of $\{\varphi_i\}$ is computed by (I.5.4). The solution of problem (1.1) is called f, the solution of the perturbed problem (1.2) is denoted by f', which are $\sum_{i\in I} g_i\psi_i$ and $\sum_{i\in I} g_i'\psi_i$ respectively (cf. Theorem III.1.4). By Proposition 1.3 we obtain,

$$e_{\text{amp}} \le \|G^{-1}\|^{1/2} \, \|g - g'\|_{\ell^2}, \tag{1.6}$$

where the Gram matrix G is

$$G_{ij} := \text{sinc}_\pi(t_i - t_j), \quad i,j \in I\!I.$$

From this estimate it follows that the solution is stable for perturbation of the data, since G^{-1} is a bounded operator on $\ell^2(I\!I)$ if $|t_i - i| < \alpha < 1/4$, for $i \in I\!I$. By Theorem IV.2.6 and (I.5.2) the norm of G^{-1} is estimated by $\|G^{-1}\|^{1/2} \le \frac{1}{1-\lambda}$, where $\lambda := 1 - \cos\pi\alpha + \sin\pi\alpha$. We see that the norm of G^{-1} in the case of uniform sampling is equal to 1. In the case of nonuniform sampling the norm of G^{-1} may become larger if α tends to 1/4. The problem (1.1) is called well-conditioned if $\|G^{-1}\|$ is close to 1, otherwise it is called ill-conditioned. In the case of uniform sampling ($\alpha = 0$) the problem is well-conditioned under perturbation of the data and the problem is ill conditioned if α is close to 1/4.

1.3. The time jitter error

Let $\{t_i\}_{i\in I}$ and $\{t'_i\}_{i\in I}$ be the sequences of exact, respectively perturbed time markers. The solution of the exact problem (1.1) is written as f and the solution of the perturbed problem (1.3) as f'. Recall formula (IV.2.1:

$$h_i := (\sqrt{r/\pi})\ \operatorname{sinc}_r(\cdot - i\pi/r) \quad \text{and} \quad \varphi_i := (\sqrt{r/\pi})\ \operatorname{sinc}_r(\cdot - t_i\pi/r).$$

The system corresponding to the perturbed time points is defined as

$$\varphi'_i := \sqrt{r/\pi}\ \operatorname{sinc}_r(\cdot - t'_i\pi/r).$$

Suppose

$$|t'_i - i| \le \alpha' < 1/4, \quad i \in \mathbb{I}.$$

Then, by Theorem IV.2.6, $\{\varphi'_i\}_{i\in I}$ is a Riesz basis for $\mathbb{P}_r$. So, there exists a bounded linear invertible operator T', satisfying

$$T'\varphi'_i = h_i, \quad i \in \mathbb{I}. \tag{1.7}$$

Moreover

$$\|T'\| \le \frac{1}{1-\lambda'}, \quad \|T'^{-1}\| \le 1 + \lambda', \tag{1.8}$$

where

$$\lambda' := 1 - \cos\pi\alpha' + \sin\pi\alpha'. \tag{1.9}$$

The biorthogonal system of $\{\varphi'_i\}$ is denoted by $\{\psi'_i\}$, which can be computed by

$$\psi'_i = \sum_{j\in I} \overline{(G'^{-1})}_{ij}\varphi'_j, \quad i \in \mathbb{I}. \tag{1.10}$$

Here G' is the Gram matrix of the system $\{\varphi'_i\}$,

$$G'_{ij} = \langle \varphi'_j, \varphi'_i \rangle = \operatorname{sinc}_\pi(t'_i - t'_j). \tag{1.11}$$

Again we have a relation between T' and G',

$$\|G'^{-1}\|^{1/2} = \|T'\|. \tag{1.12}$$

The solutions f of problem (1.1) and f' to problem (1.3) are $f = \sum_{i\in I} g_i\psi_i$, and $f' = \sum_{i\in I} g_i\psi'_i$. $\{\psi_i\}$ can be computed by (I.5.4):

$$\psi_i = \sum_{j\in I} \overline{(G^{-1})}_{ij}\varphi_j,$$

the Gram matrix G is given by (IV.1.3).

In order to find an estimate for the time jitter error, we choose the following approach. We look for a perturbation operator V, such that $V\varphi_i = \varphi'_i$, for all $i \in \mathbb{I}$. If such an operator and unique biorthogonal sequences exist, then we have the relation $\psi_i = V^*\psi'_i$. The following proposition expresses the difference between f and f' in terms of the norm of the operators T' and $I - V$. Note that this proposition holds for arbitrary separable Hilbert spaces $\mathcal{H}$.

Proposition 1.4 . *Let $\{\varphi_i\} \subset \mathcal{H}$, where $\mathcal{H}$ is a separable Hilbert space. Define $\varphi_i' := V\varphi_i$ for $i \in \mathbb{I}$, where V is a bounded linear operator. If $\{\varphi_i'\}_{i\in I}$ is a Riesz basis for $\mathcal{H}$, then*

$$\|\sum_{i\in I} g_i\psi_i - \sum_{i\in I} g_i\psi_i'\|_{\mathcal{H}} \leq \|I - V\| \, \|T'\| \, \|g\|_{\ell^2}.$$

Here $\{\psi_i'\}_{i\in I}$ is the unique biorthogonal system corresponding to $\{\varphi_i'\}$; $\{\psi_i\}$ is given by $\psi_i := V^*\psi_i'$ and $\{g_i\} \in \ell^2(\mathbb{I})$.

Proof:

$$\|\sum_{i\in I} g_i(\psi_i' - \psi_i)\|_{\mathcal{H}} = \|\sum_{i\in I} g_i(I - V^*)\psi_i'\|_{\mathcal{H}} \leq \|I - V\| \, \|\sum_{i\in I} g_i\psi_i'\|_{\mathcal{H}} =$$

$$\|I - V\| \, \|\sum_{i\in I} g_i T'^* h_i\|_{\mathcal{H}} \leq \|I - V\| \, \|T'\| \, \|\sum_{i\in I} g_i h_i\|_{\mathcal{H}} = \|I - V\| \, \|T'\| \, \|g\|_{\ell^2}.$$

which proves the estimate. □

In the following we give conditions under which such an operator V exists, and in addition, we obtain an estimate for the norm of $I - V$ in terms of the differences of t_i and t_i'. First we prove a lemma.

Lemma 1.5 . *Let $\{\varphi_i\}_{i\in I}$ be a Riesz basis for a separable Hilbert space $\mathcal{H}$. Suppose $\{\varphi_i'\}_{i\in I}$ satisfies*

$$\sum_{i\in I} |\langle f, \varphi_i - \varphi_i'\rangle_{\mathcal{H}}|^2 \leq C^2\|f\|_{\mathcal{H}}^2, \quad f \in \mathcal{H},$$

where C is a constant. Then there exists a bounded linear operator V on $\mathcal{H}$ such that

$$V\varphi_i = \varphi_i', \quad i \in \mathbb{I},$$

and $\|I - V\| \leq \|T\|C$.

Proof:

Let $\{\varphi_i\}$ be a Riesz basis for $\mathcal{H}$, then $T\varphi_i = h_i$ and $\psi_i := T^*h_i$ is its biorthogonal system. Define the bounded linear operator W on $\mathcal{H}$ by

$$Wf = \sum_{i\in I} \langle f, \varphi_i - \varphi_i'\rangle_{\mathcal{H}} \, \psi_i.$$

Then,

$$\|Wf\|^2 = \|\sum_{i\in I} \langle f, \varphi_i - \varphi_i'\rangle_{\mathcal{H}} \, \psi_i\|_{\mathcal{H}}^2 \leq$$

$$\|T\|^2 \, (\sum_{i\in I} |\langle f, \varphi_i - \varphi_i'\rangle_{\mathcal{H}}|^2) \leq \|T\|^2C^2\|f\|_{\mathcal{H}}^2.$$

So $\|W\| \leq C\|T\|$. The adjoint of W is

$$W^*f = \sum_{i\in I} \langle f, \psi_i\rangle_{\mathcal{H}} \, (\varphi_i - \varphi_i'),$$

and

$$(I - W^*)\varphi_i = \varphi_i'.$$

The result follows by taking $V = I - W^*$. □

Lemma 1.5 is a slight generalization of Schäfke's Theorem(cf. Young [55]) where the system $\{\varphi_i\}_{i\in I}$ is assumed to be an orthonormal basis.

An estimate for the time jitter error can now be derived, by means of a norm estimate for $I - V$. The Gram matrices G and G' are given by formula's (IV.1.3) and (1.11), respectively.

Theorem 1.6 . *Let $\{t_i\}_{i\in I}$ and $\{t'_i\}_{i\in I}$ be sequences of real numbers which satisfy,*

$$|t_i - i| \leq \alpha < 1/4, \quad i \in I\!I, \tag{1.13}$$

$$|t'_i - i| \leq \alpha' < 1/4, \quad i \in I\!I. \tag{1.14}$$

The time jitter error can be estimated by

$$e_{tj} \leq (\|G'^{-1}\| \, \|G^{-1}\| \, \|G\|)^{1/2} \, (e^{\pi\gamma} - 1) \, \|g\|_{I^2},$$

where

$$\gamma := \sup_{i\in I}|t_i - t'_i| \leq \alpha + \alpha'. \tag{1.15}$$

Proof:

If $\{t_i\}$ satisfies the estimate of Theorem 1.6, then $\{\varphi_i\}$ is a Riesz basis for $I\!P_r$. Let $f \in I\!P_r$, then

$$(\pi/r)\sum_{i\in I}|f(t_i\pi/r)|^2 = \|\sqrt{\pi/r}\ \sum f(t_i\pi/r)h_i\|^2_{I\!P_r} =$$

$$\|\sqrt{\pi/r}\ \sum_{i\in I} f(t_i\pi/r)T^{*^{-1}}\psi_i\|^2_{I\!P_r} \leq \|T^{-1}\|^2\|\sum_{i\in I}\langle f,\varphi_i\rangle\psi_i\|^2_{I\!P_r} = \|T^{-1}\|^2\|f\|^2_{I\!P_r}.$$

So, the conditions of Lemma IV.2.1 are satisfied with $B = \|T^{-1}\|$. After putting $s_i = t_i$ and $p_i = t'_i$ in Lemma IV.2.1, it follows that

$$\sum_{i\in I}|\langle f, \varphi_i - \varphi'_i\rangle_{I\!P_r}|^2 = \sum_{i\in I}(\pi/r)|f(t_i\pi/r) - f(t'_i\pi/r)|^2 \leq$$

$$\|T^{-1}\|^2(e^{\pi\gamma} - 1)^2\|f\|^2_{I\!P_r}.$$

Hence the sequences $\{\varphi_i\}$ and $\{\varphi'_i\}$ satisfy the conditions of Lemma 1.5, with $C = \|T^{-1}\|(e^{\pi\gamma} - 1)$. This implies the existence of a linear operator V on $I\!P_r$ such that $V\varphi_i = \varphi'_i$ and

$$\|I - V\| \leq \|T\| \, \|T^{-1}\| \, (e^{\pi\gamma} - 1).$$

Since the $\{t'_i\}_{i\in I}$ satisfy (1.14), the system $\{\varphi'_i\}_{i\in I}$ is by Theorem IV.2.6 a Riesz basis. By Proposition 1.4 we have that

$$\|f - f'\|_{I\!P_r} \leq (\|G'^{-1}\| \, \|G^{-1}\| \, \|G\|)^{1/2} \, (e^{\pi\gamma} - 1) \, \|g\|_{I^2}.$$

f and f' are solutions of (1.1) and (1.3) respectively. □

A few remarks are in order. From this estimate we see that problem (1.1) is stable for perturbation of the time markers. Theorem IV.2.6 and the norm estimates (I.5.2), (1.12) yield

$$\|G\|^{1/2} \leq 1 + \lambda,$$

$$\|G^{-1}\|^{1/2} \leq \frac{1}{1-\lambda}$$

and

$$\|G'^{-1}\|^{1/2} \leq \frac{1}{1-\lambda'}.$$

Here

$$\lambda := 1 - \cos \pi\alpha + \sin \pi\alpha$$

and

$$\lambda' := 1 - \cos \pi\alpha' + \sin \pi\alpha'.$$

In the case of uniform sampling (α is zero and α' is close to zero) the problem (1.1) is well-conditioned for perturbation of the time markers. If we sample nonuniformly, especially when α or α' is close to $1/4$, the problem may become ill-conditioned for perturbation of the time markers.

There is an alternative way to obtain an estimate for the time jitter error. Suppose we did measure the data $\{g_i\}_{i\in I}$ at the time markers $\{t_i\pi/r\}_{i\in I}$. But somehow, the sequence of measurement times is registered by our device as $\{t_i'\pi/r\}_{i\in I}$. The function we sampled is denoted by f, so $g_i = \sqrt{\pi/r}\, f(t_i\pi/r)$. The situation which is registered by our measuring device is false, since it says that the value of f at $t_i'\pi/r$ is equal to g_i. However, the true value of f at $t_i'\pi/r$ is $g_i' := (\sqrt{\pi/r})\, f(t_i'\pi/r)$. So we should consider $\{g_i'\}_{i\in I}$ as the exact data and $\{g_i\}_{i\in I}$ as the perturbed data at $\{t_i'\pi/r\}_{i\in I}$. With the above notation, we have

$$f = \sum_{i\in I} g_i\psi_i = \sum_{i\in I} g_i'\psi_i', \tag{1.16}$$

and we define $f' = \sum_{i\in I} g_i\psi_i'$. The time jitter error is given by

$$e_{tj} = \|f - f'\|_{P_r} = \|\sum_{i\in I} g_i\psi_i - \sum_{i\in I} g_i\psi_i'\|_{P_r} = \|\sum_{i\in I} g_i'\psi_i' - \sum_{i\in I} g_i\psi_i'\|_{P_r}.$$

The estimate in Theorem 1.6 can now be derived from estimate (1.6) of the amplitude error. Let $\{t_i\}$ and $\{t_i'\}$ satisfy the conditions of Theorem 1.6. By applying (1.6) with ψ_i' and G' in the role of ψ_i and G respectively, we find

$$e_{tj}^2 = \|f - f'\|_{P_r}^2 = \|\sum_{i\in I}(g_i - g_i')\psi_i'\|_{P_r}^2 \leq$$

$$\|G'^{-1}\| \sum_{i\in I} |g_i - g_i'|^2 = \|G'^{-1}\|\, (\pi/r) \sum_{i\in I} |f(t_i\pi/r) - f(t_i'\pi/r)|^2.$$

From the proof of Theorem 1.6, we know that the sequence $\{t_i\}_{i\in I}$ satisfies the condition of Lemma IV.2.1, with $B = \|T^{-1}\|$. Hence

$$e_{tj} \leq \|G'^{-1}\|^{1/2}\, \|T^{-1}\|\, (e^{\pi\gamma} - 1)\, \|f\|.$$

The desired estimate now follows from the formula's (1.16), (I.5.3) and (I.5.2). This shows that the estimate of Theorem 1.6 can be proved by using formula (1.6).

V.2. Error Estimates for the Mixed Problem

The previous estimates are used to derive conclusions for the stability of the solution of the mixed problem in practical situations. The different types of error estimates are derived throughout several subsections.

2.1. The aliasing error for the mixed problem in the case of sinc-interpolation

We give a bound for the aliasing error for the mixed problem in the case of sinc-interpolation for uniform sampling only. Let $\mathcal{H} = \mathbb{P}_r$ and $t_{\kappa,i} = i$, for all $\kappa \in \mathbb{K}$ and $i \in \mathbb{I}$.

The aliasing error is due to the fact that the solution of the mixed problem is not lying in the same function space as the sampled function.

Define the operator $\mathcal{U}$ from $L^2(D,\mathcal{S})$ into $L^2(D,\mathbb{P}_r)$, as

$$\mathcal{U}g(x,.) := \sum_{\kappa\in\mathbb{K}} P[\widehat{g}(\kappa,.)]e_\kappa(x),$$

where P is the operator defined in Section 1.1. Note that $L^2(D,\mathcal{S})$ and $L^2(D,\mathbb{P}_r)$ are subspaces of $L^2(D,L^\infty(\mathbb{R}))$. The definition of the aliasing error is

$$\mathrm{E}_{\mathrm{al}}^{\mathcal{H}} := \Big(\int_D \|g(x,.)-\mathcal{U}g(x,.)\|_\infty^2 d\mu(x)\Big)^{1/2}. \tag{2.1}$$

Definition (2.1) is motivated as follows. Let $g \in L^2(D,\mathcal{S})$ and suppose $\widehat{g}(\kappa,.) \in \mathcal{S}$ for arbitrary $\kappa \in \mathbb{K}$, then by definition $(\widehat{\mathcal{U}g})(\kappa,.) = P(\widehat{g}(\kappa,.))$. If it is evaluated at the time marker $t_{\kappa,i}\pi/r$, we obtain the equality,

$$(\sqrt{\pi/r})(\widehat{\mathcal{U}g})(\kappa,t_{\kappa,i}\pi/r) = (\sqrt{\pi/r})\ \widehat{g}(\kappa,t_{\kappa,i}\pi/r).$$

So the term $\mathcal{U}g$ is a solution to the mixed problem lying in $L^2(D,\mathcal{H})$, if $g \in L^2(D,\mathcal{S})$.

We now give a bound for the aliasing error. The Fourier transform of a function $g \in L^2(D,\mathcal{S})$ which is taken with respect to t, is denoted by $\widehat{g}(x,\xi)$.

Theorem 2.1 .

$$E_{\mathrm{al}}^{P_r} \le \sqrt{\frac{2}{\pi}}\Big(\int_D\Big(\int_{R\setminus[-r,r]}|\widehat{g}(x,\xi)|d\xi)^2 d\mu(x)\Big)^{1/2}. \tag{2.2}$$

Proof:

By definition of $\mathcal{U}$ and by Theorem II.1.6, we obtain $\mathcal{U}g(x,.) = P[g(x,\cdot)]$, μ almost everywhere. The estimate follows by Lemma 1.2.

□

2.2. The aliasing error for the mixed problem in the case of spline interpolation

The aliasing error for the mixed problem in the case of spline functions is as follows. Let $\mathcal{H} = \mathcal{K}^{2n-1}$, and assume that for each $\kappa \in \mathbb{K}$ the sequence $\{t_{\kappa,i}\}_{i\in I}$ consists of distinct real numbers. Define the operator P_κ by

$$P_\kappa h := \sum_{i\in I}(\sqrt{\pi/r})h(t_{\kappa,i}\pi/r)\ \psi_{\kappa,i}, \quad h \in \mathcal{S}.$$

Here $\psi_{\kappa,i}$ is given by (IV.5.5). Assume that for arbitrary $g \in L^2(D,\mathcal{S})$, the Fourier transform $\widehat{g}(\kappa,.)$ lies in $\mathcal{S}$, for $\kappa \in \mathbb{K}$ and suppose $\sum_{\kappa\in K}\|P_\kappa[\widehat{g}(\kappa,\cdot)]\|^2_{\mathcal{K}^{2n-1}} < \infty$, for all $g \in L^2(D,\mathcal{S})$. Define $\mathcal{U}$ by

$$\mathcal{U}g := \sum_{\kappa\in K} P_\kappa(\widehat{g}(\kappa,.))e_\kappa, \quad g \in L^2(D,\mathcal{S}).$$

$\mathcal{U}$ is an operator from $L^2(D,\mathcal{S})$ into $L^2(D,\mathcal{K}^{2n-1})$. The aliasing error for the case of odd degree splines is defined as

$$E_{\mathrm{al}}^{\mathcal{K}^{2n-1}} := \Big(\int_D \|g(x,.) - \mathcal{U}g(x,.)\|^2_{I.^2([a,b])}d\mu(x)\Big)^{1/2}.$$

Before estimating the aliasing error, we give a lemma.

Lemma 2.2 . *For any $h \in \mathcal{S}$ and for $\kappa \in \mathbb{K}$ fixed,*

$$\|h - P_\kappa h\|_{I.^2([a,b])} \le \|\Delta_\kappa\|^{1/2}\|d/dt\ h - d/dt\ (P_\kappa h)\|_{I.^2[a,b]}, \tag{2.3}$$

where $\|\Delta_\kappa\| = \sum_{i=0}^{l-1}(1/2)(t_{\kappa,i+1}\pi/r - t_{\kappa,i}\pi/r)^2$.

Proof:

By the Cauchy-Schwarz and Taylor's formula (Section IV.3) it follows that for $t \in (t_{\kappa,i}\pi/r, t_{\kappa,i+1}\pi/r)$

$$|h(t) - P_\kappa h(t)| \le \int_{[t_{\kappa,i}\pi/r,t]} |d/ds\ h(s) - d/ds\ (P_\kappa h)(s)|ds \le$$

$$(t - t_{\kappa,i}\pi/r)^{1/2}\|d/ds\ h - d/ds\ (P_\kappa h)\|_{I.^2[a,b]}.$$

So

$$\int_{[a,b]} |h(t) - P_\kappa(h(t))|^2 \le \Big(\sum_{i=0}^{l-1}\int_{t_{\kappa,i}\pi/r}^{t_{\kappa,i+1}\pi/r}(t - t_{\kappa,i}\pi/r)dt\Big)\|(d/ds)h - (d/ds)P_\kappa h\|^2_{I.^2[a,b]} =$$

$$(1/2)\sum_{i=0}^{l-1}((t_{\kappa,i+1} - t_{\kappa,i})\pi/r)^2\|(d/ds)h - (d/ds)P_\kappa h\|^2_{I.^2[a,b]}.$$

This proves the result. □

Theorem 2.3 .

$$E_{\mathrm{al}}^{\mathcal{K}^{2n-1}} \le (\sup_{\kappa\in K}\|\Delta_\kappa\|)^{1/2}\Big(\sum_{\kappa\in K}\Big\|\frac{\partial}{\partial t}\widehat{g}(\kappa,.) - \frac{\partial}{\partial t}(\widehat{\mathcal{U}\,g})(\kappa,.)\Big\|^2_{I.^2[a,b]}\Big)^{1/2}. \tag{2.4}$$

Proof:

It follows from Lemma 2.2 that

$$E_{\mathrm{al}}^{\mathcal{K}^{2n-1}} = \Big(\sum_{\kappa\in K}\|(I - P_\kappa)\widehat{g}(\kappa,.)\|^2_{I.^2([a,b])}\Big)^{1/2} \le$$

$$\le \Big(\sum_{\kappa\in K}\|\Delta_\kappa\|\ \|(\delta/\delta t)(I - P_\kappa)\widehat{g}(\kappa,.)\|^2_{I.^2[a,b]}\Big)^{1/2} \le$$

$$\le (\sup_{\kappa\in K}\|\Delta_\kappa\|)^{1/2}\Big(\sum_{\kappa\in K}\Big\|\frac{\partial}{\partial t}\Big\{(I - P_\kappa)\widehat{g}(\kappa,.)\Big\}\Big\|^2_{I.^2[a,b]}\Big)^{1/2}.$$

□

2.3. The amplitude error for the mixed problem in the case of sinc- and spline- interpolation

We consider the amplitude error for the mixed problem in the case of sinc- and spline-interpolation. Let $\mathcal{H} = \mathbb{P}_r$ or $\mathcal{H} = \mathcal{K}^{2n-1}$. In this subsection we take for $\mathbb{K}$ a finite index set and assume (for each $\kappa \in \mathbb{K}$) that the time points $\{t_{\kappa,i}\}_{i\in I}$ are increasing real numbers. Suppose the data $\{g_{\kappa,i}\}_{\kappa\in K, i\in I}$ are perturbed to $\{g'_{\kappa,i}\}_{\kappa\in K, i\in I}$. The solution of the unperturbed problem is given by (Example IV.6.3) $f = \sum_{\kappa\in K} c_\kappa e_\kappa$, where $c_\kappa = \sum_{i\in I} g_{\kappa,i}\psi_{\kappa,i}$. The solution of the perturbed problem (0.2) is given by $f' = \sum_{\kappa\in K} c'_\kappa e_\kappa$, where $c'_\kappa := \sum_{i\in I} g'_{\kappa,i}\psi_{\kappa,i}$.

Theorem 2.4 .

$$E^{\mathcal{H}}_{amp} \leq \sup_{\kappa\in K}\|G(\kappa)^{-1}\|^{1/2}\ \|g - g'\|_{\ell^2(K\times I)}. \tag{2.5}$$

Proof:

By Theorem II.1.6

$$(\mathrm{E}^{\mathcal{H}}_{\mathrm{amp}})^2 = \int \|f(x,.) - f'(x,.)\|^2_{\mathcal{H}} d\mu(x) = \sum_{\kappa\in K} \|\widehat{f}(\kappa) - \widehat{f}'(\kappa)\|^2_{\mathcal{H}}.$$

By Proposition 1.3, it follows that

$$\sum_{\kappa\in K} \|\widehat{f}(\kappa,:) - \widehat{f}'(\kappa,.)\|^2_{\mathcal{H}} \leq \sum_{\kappa\in K} \|G(\kappa)^{-1}\| \sum_{i\in I} |g_{\kappa,i} - g'_{\kappa,i}|^2 \leq$$

$$\leq \sup_{\kappa\in K}\|G(\kappa)^{-1}\|\ \|g - g'\|^2_{\ell^2(K\times I)}.$$

□

2.4. The time jitter error for the mixed problem in the case of sinc- and spline-interpolation

Let $\mathcal{H} = \mathbb{P}_r$ or $\mathcal{H} = \mathcal{K}^{2n-1}$. In this subsection we take for $\mathbb{K}$ a finite index set. Assume (for each $\kappa \in \mathbb{K}$) that the time points $\{t_{\kappa,i}\}_{i\in I}$ are sequence of increasing real numbers. Now suppose the time points $t_{\kappa,i}$ are perturbed to $t'_{\kappa,i}$, such that

$$|t_{\kappa,i} - t'_{\kappa,i}| \leq \gamma, \quad \kappa \in \mathbb{K}, i \in \mathbb{I}.$$

The solution of the unperturbed problem is (Example IV.6.3) $f = \sum_{\kappa\in K} c_\kappa e_\kappa$, where $c_\kappa = \sum_{i\in I} g_{\kappa,i}\psi_{\kappa,i}$. The solution of the perturbed problem (0.3) is $f' = \sum_{\kappa\in K} c'_\kappa e_\kappa$, where in this case

$$c'_\kappa := \sum_{i\in I} g_{\kappa,i}\psi'_{\kappa,i}.$$

Here

$$\psi'_{\kappa,i} := \sum_{j\in I}(G'(\kappa)^{-1})_{ij}\varphi'_{\kappa,j},$$

where for $\kappa \in \mathbb{K}$ fixed, the Gram matrix is

$$(G'(\kappa))_{ij} := \langle\varphi'_{\kappa,j}, \varphi'_{\kappa,i}\rangle_{\mathcal{H}},$$

and $\varphi'_{\kappa,j}$ is defined by (IV.5.2) and (IV.5.3) if $\mathcal{H} = \mathbb{P}_r$ and if $\mathcal{H} = \mathcal{K}^{2n-1}$, respectively.

Before giving an estimate for the time jitter error, we prove two lemma's. We denote the sequence $\{t_{\kappa,i}\}_{i\in I}$ by t_κ, for $\kappa \in \mathbb{K}$ and $\{g_{\kappa,i}\}_{i\in I}$ by g_κ. (For the perturbed time points and data analogous notation is used.)

Lemma 2.5 . *If $\mathcal{H} = I\!P_r$, then for fixed $\kappa \in I\!K$,*

$$\|c_\kappa - c'_\kappa)\|_{I\!P_r} \leq (\|G'(\kappa)^{-1}\| \, \|G(\kappa)^{-1}\| \, \|G(\kappa)\|)^{1/2} \, (e^{\pi\gamma} - 1) \, \|g_\kappa\|_{\ell^2(I)}.$$

This is an application of Theorem 1.6. The following lemma deals with the case that $\mathcal{H} = \mathcal{K}^{2n-1}$.

Lemma 2.6 . *If $\mathcal{H} = \mathcal{K}^{2n-1}$, then for fixed $\kappa \in I\!K$,*

$$\|c_\kappa - c'_\kappa)\|_{\mathcal{K}^{2n-1}} \leq$$

$$\Big(2\|G(\kappa)^{-1}\|^{1/2} + (\pi/r)^{3/2}\|G'(\kappa)^{-1}\|^{1/2} \, \|t_\kappa - t'_\kappa\|_{\ell^2(I)}\Big) \, \Big(\|d/dt \; c_\kappa\|_\infty \; + \|g_\kappa\|_{\ell^2(I)}\Big).$$

Proof:

The inequality will be proved using (1.5), as follows. Define, for $\kappa \in I\!K$ fixed, $h_\kappa := \sum_{i\in I} g_{\kappa,i}\psi_{\kappa,i}$ and $h'_\kappa := \sum_{i\in I} g_{\kappa,i}\psi'_{\kappa,i}$. (Note that $h_\kappa = c_\kappa$ and $h'_\kappa = c'_\kappa$.) Let $g'_{\kappa,i} := (\sqrt{\pi/r})h_\kappa(t'_{\kappa,i}\pi/r)$. Define $f_\kappa = \sum_{i\in I} g'_{\kappa,i}\psi'_{\kappa,i}$. Then f_κ satisfies $(\sqrt{\pi/r}) \; f_\kappa(t'_{\kappa,i}\pi/r) = g'_{\kappa,i} = \sqrt{\pi/r}h_\kappa(t'_{\kappa,i}\pi/r)$. By the minimum norm property we have $\|f_\kappa\|_{\mathcal{K}^{2n-1}} \leq \|h_\kappa\|_{\mathcal{K}^{2n-1}}$. So,

$$\|\sum_{i\in I} g_{\kappa,i}(\psi_{\kappa,i} - \psi'_{\kappa,i})\|_{\mathcal{K}^{2n-1}} = \|h_\kappa - h'_\kappa\|_{\mathcal{K}^{2n-1}} \leq \|h_\kappa - f_\kappa\|_{\mathcal{K}^{2n-1}} + \|f_\kappa - h'_\kappa\|_{\mathcal{K}^{2n-1}} \leq$$

$$\|f_\kappa - h'_\kappa\|_{\mathcal{K}^{2n-1}} + \|f_\kappa\| + \|h_\kappa\|_{\mathcal{K}^{2n-1}} \leq \|f_\kappa - h'_\kappa\|_{\mathcal{K}^{2n-1}} + 2\|h_\kappa\|_{\mathcal{K}^{2n-1}} =$$

$$\|\sum_{i\in I}(g'_{\kappa,i} - g_{\kappa,i})\psi'_{\kappa,i}\|_{\mathcal{K}^{2n-1}} + 2\|h_\kappa\|_{\mathcal{K}^{2n-1}}.$$

We have $g_{\kappa,i} = (\sqrt{\pi/r}) \; h_\kappa(t_{\kappa,i}\pi/r)$ and $g'_{\kappa,i} = (\sqrt{\pi/r}) \; h_\kappa(t'_{\kappa,i}\pi/r)$. Using (1.5), with ψ_i and G replaced by $\psi'_{\kappa,i}$ and $G'(\kappa)$ and applying the mean value theorem to h_κ, we get

$$\|h_\kappa - h'_\kappa\|_{\mathcal{K}^{2n-1}} \leq \|G'(\kappa)^{-1}\|^{1/2} \, \|g_\kappa - g'_\kappa\|_{\ell^2(I)} =$$

$$\|G'(\kappa)^{-1}\|^{1/2} \, (\sqrt{\pi/r})\|h_\kappa(t_\kappa\pi/r) - h_\kappa(t'_\kappa\pi/r)\|_{\ell^2(I)} \leq$$

$$(\pi/r)^{3/2}\|G'(\kappa)^{-1}\|^{1/2} \, \|d/dt \; h_\kappa\|_\infty \, \|t_\kappa - t'_\kappa\|_{\ell^2(I)}.$$

Again by using formula (1.5) with ψ_i replaced by $\psi_{\kappa,i}$, G by $G(\kappa)$, g_i by $g_{\kappa,i}$ and with $g'_i = 0$ for all $i \in I\!I$, we obtain the estimate

$$\|h_\kappa\|_{\mathcal{K}^{2n-1}} = \|\sum_{i\in I} g_{\kappa,i}\psi_{\kappa,i}\|_{\mathcal{K}^{2n-1}} \leq \|G(\kappa)^{-1}\|^{1/2}\|g_\kappa\|_{\ell^2(I)}.$$

□

Theorem 2.7 .

$$E_{tj}^{I\!P_r} \leq \sup_{\kappa\in I\!K}(\|G'(\kappa)^{-1}\| \, \|G(\kappa)^{-1}\| \, \|G(\kappa)\|)^{1/2} \, (e^{\pi\gamma} - 1) \, \|g\|_{\ell^2(I\!K\times I)}. \tag{2.6}$$

$$E_{tj}^{\mathcal{K}^{2n-1}} \leq \sup_{\kappa\in I\!K}\Big(2\|G(\kappa)^{-1}\|^{1/2} + (\pi/r)^{3/2} \, \|G'(\kappa)^{-1}\|^{1/2} \, \|t_\kappa - t'_\kappa\|_{\ell^2(I)}\Big)$$

$$\Big(\sum_{\kappa\in I\!K} \|\frac{\partial}{\partial t}\widehat{f}(\kappa,\cdot)\|_\infty^2 + \|g_\kappa\|_{\ell^2(I)}^2\Big)^{1/2}. \tag{2.7}$$

Proof:

Using Theorem II.1.6 we obtain

$$(\mathrm{E}_{\mathrm{tj}}^{\mathcal{H}})^2 = \int_D \|f(x,.) - f'(x,.)\|_{\mathcal{H}}^2 = \sum_{\kappa \in K} \|\widehat{f}(\kappa,.) - \widehat{f}'(\kappa,.)\|_{\mathcal{H}}^2.$$

Note that (for $\kappa \in \mathbb{K}$ fixed) $\widehat{f}(\kappa,.) = \sum_{i \in I} g_{\kappa,i} \psi_{\kappa,i}$ and $\widehat{f}'(\kappa,.) = \sum_{i \in I} g_{\kappa,i} \psi'_{\kappa,i}$. The result follows by applying Lemma 2.5 and Lemma 2.6 in the case that $\mathcal{H} = \mathbb{P}_r$ and $\mathcal{H} = \mathcal{K}^{2n-1}$, respectively. □

V.3. Conclusions and Remarks

In this section we make some additional remarks and state conclusions about the error estimates for the mixed problem.

A problem is called stable, if small perturbations of the data yield small errors in the solution. From the estimates (2.5), (2.6) and (2.7) we conclude that problem (0.1) is stable for perturbation of the data and time points. The bounds for the amplitude error and aliasing error, depend on the norms of $(G'(\kappa))^{-1}$, $G(\kappa)$, or $G(\kappa)^{-1}$. Problem (0.1) is called well-conditioned if the norms of the matrices are close to one (cf. Stoer and Bulirsch [52], p. 13). Otherwise it is called ill-conditioned.

The aliasing error for sinc-interpolation, formula (2.2), depends on the energy outside the band $[-r, r]$. If the measured function g is essentially bandlimited, i.e. for all $x \in D$,

$$\int_{R \setminus [-r,r]} |\widehat{g}(x,\xi)| d\xi \, d\mu(x) \leq \epsilon,$$

then $\mathrm{E}_{\mathrm{al}} \leq \sqrt{\frac{2\mu(D)}{\pi}}\, \epsilon$. It follows that if g is bandlimited (i.e. $\epsilon = 0$), then the aliasing error is zero.

The aliasing error for spline-interpolation, formula (2.4), depends on the temporal derivative. If the spline has a high degree, then it tends to oscillate quickly. So, if the measured function oscillates quickly in time, the degree of the interpolating splines should be high.

The amplitude error for sinc- and spline-interpolation, formula (2.5), depends on the norm of the Gram matrix $G(\kappa)^{-1}$. If for a certain $\kappa \in \mathbb{K}$ the norm of this matrix is large, the problem is ill-conditioned for perturbation of the data.

In the case of sinc functions, we can say more: If the time points $\{t_{\kappa,i}\}_{i \in I}$ (for all $\kappa \in \mathbb{K}$) are spaced uniformly, then $\|G(\kappa)^{-1}\| = 1$, hence the problem is well-conditioned for perturbation of the data.

The time jitter error for sinc-interpolation, formula (2.6), depends on the norms of $(G'(\kappa))^{-1}$, $G(\kappa)$, and $G(\kappa)^{-1}$. If (for all $\kappa \in \mathbb{K}$) the elements of the sequences $\{t_{\kappa,i}\}_{i \in I}$ and $\{t'_{\kappa,i}\}_{i \in I}$ are spaced uniformly, then these norms are equal to one, hence the problem is well-conditioned for perturbation of the time points. If, however, for one $\kappa \in \mathbb{K}$ this is not the case, the problem may become ill-conditioned.

The time-jitter error for spline-interpolation, formula (2.7) depends on the inverses of Gram matrices $(G'(\kappa))^{-1}$ and $G(\kappa)^{-1}$ and on the temporal derivative of the reconstructed function. So, the problem becomes ill-conditioned for perturbation of the time points if (for a certain $\kappa \in \mathbb{K}$) the degree of the spline is too high or if the norms of the matrices are large.

The conclusion is that the reconstruction algorithms for sinc-interpolation are well-conditioned, if (for each $\kappa \in \mathbb{K}$) the time points $\{t_{\kappa,i}\}_{i \in I}$ are sampled uniformly. The

reconstruction by spline interpolation is well-conditioned if the norms of the inverses of the Gram matrices are small and if the degree of the interpolating spline is not too high. On the other hand, if the degree of the spline is too low, then the aliasing error may become large, which will also cause serious errors in the reconstruction.

If the problem is ill-conditioned a regularization technique can be employed to compute the solution. In this chapter the Tychonov-Phillips regularization corresponding to the mixed Fourier interpolation problem is used (see section IV.5).

Part Two

Dynamic MRI Reconstruction

This part consists of two chapters and deals with measuring and reconstruction techniques of magnetic resonance imaging (MRI) and with stability of the reconstruction methods. This part is self-contained and can be read independently of Part One. The emphasis lies on the practical aspects of MR-imaging and not on the underlying mathematical theory. For convenience, the results of Part One will be discussed briefly and consequences for the reconstruction problem are stated and illustrated by means of pictures.

In chapter six we explain the measurement and reconstruction technique for magnetic resonance imaging in the case of the beating human heart. The measuring technique discussed here is called 'retrospective gating' (also called retrospective triggering), see Bohning [8], Glover and Pelc [17] and Lenz et al. [35].
Good introductions to the physics of MR-imaging can be found in Hinshaw and Lent [25], Locher [37], King and Moran [30] and Mansfield and Morris [39]. Some references from by now classical literature about MR-imaging are Lauterbur [33] [34] and Kumar, Welti and Ernst [31]. References about imaging the beating human heart (with techniques different from retrospective gating) are McKinnon and Bates [40] in the case of computerized tomography (CT), and Van Dijk [16] for MRI.

Chapter seven presents a discussion of the stability of the algorithms, which will be illustrated by reconstructions of test images from perturbed data. Here we use the results obtained in Chapter five. We also discuss the practical error sources, which are not taken into account in the reconstruction problem considered in Chapter six.

Chapter VI

Problem Formulation and Solution Method for Dynamic MRI Reconstruction

In this chapter we formulate and solve a reconstruction problem concerning Magnetic Resonance Imaging (MRI), which is a diagnostic technique to measure and display cross sections of human organs. In particular the problem how to reconstruct a cross section of the beating heart is considered. The general problem in dynamic MRI is that, due to physical limitations, the standard measurement technique is not suited to acquire all the necessary data for a single time frame, in a time period which is short enough to neglect the motion of the heart. The word 'dynamic' in dynamic MRI refers here to the motion which is involved, to make a distinction between MRI which only involves a spatial parameter.

In the case of the beating heart one can make use of the (approximate) periodicity of the heart motion. That is, data corresponding to the same relative heart phase may be recorded at different heartbeats. This presupposes, of course, some degree of reproducibility of the heart motion in successive cycles. There have been various ways to deal with this problem. McKinnon and Bates [40], who considered cardiac imaging in the context of computerized tomography (CT), assumed the number of cycles to be sufficiently small such that the heart motion during these cycles can be assumed to be 'quasi-stationary'. This led them to consider no more than 12 cycles, leading to a reconstruction problem with a considerable amount of missing data.

Another alternative, which will be pursued in the following two chapters, is to assume that there is a simple rule to map heart intervals of different duration to a standard heart interval of unit length. Different rules can be imagined, the simplest one being to rescale linearly with time on each heart interval. In v1.3 to perform this synchronization of the data, the electrocardiogram (ECG) is simultaneously recorded and used as a reference signal.

In Section 1 we first review the data acquisition process of MRI in general. Then we discuss the retrospective gating technique for cardiac imaging and explain how reconstructions at different heart phases can be obtained in principle. In Section 2 we describe the solution method which was obtained in Part one of this thesis. Section 3 contains reconstructions of test images and Section 4 contains reconstructions of MR-data. In Section 5 we state our conclusions.

VI.1. Problem Definition of dynamic MRI

In this section we give an introduction to cardiac imaging by MRI techniques. In particular we explain the data acquisition based upon the concept of 'retrospective gating', as compared to the more conventional technique of ECG-triggered cardiac imaging. To make this part self-contained we start with a brief discussion of the principles of MRI.

1.1. The physics of magnetic resonance imaging.

As we will show in this section, the Fourier coefficients of the *spin density* of tissue in a cross section can be measured. Here a spin density is represented by a function $f : D \rightarrow \mathbb{C}$, where D is a bounded set representing the cross section of the human body. For simplicity we assume that $D = [0, 2\pi]^2 := [0, 2\pi] \times [0, 2\pi]$. The amplitude $|f(\mathbf{r})|$ is the proton density at position $\mathbf{r}$, i.e. it is a measure for the 'number' of protons per unit area. For muscle and fat tissue $|f(\mathbf{r})|$ has a larger value than for bone or lung tissue. This is because the density of hydrogen atoms, which are built up from elementary particles like protons, is higher for muscle or fat tissue than for lung or bone tissue.

The principle underlying MRI is to reconstruct this spin density from the measured Fourier coefficients and to display its amplitude $|f|$ on a computer screen. In this section we explain the physics and the data collection strategy of MRI.

The measurements are performed with the aid of magnetic fields by which the spins of hydrogen atoms in the human body are forced to emit radiation with a unique frequency at each point.
This radiation is measured by the MR-device, in which (approximately) a signal given by

$$S(t) \simeq \int_D f(\mathbf{r})\, e^{-j\gamma\, t(\mathbf{G}.\mathbf{r})} d\mathbf{r} \tag{1.1}$$

is induced. Here $j^2 = -1$, $f : D \rightarrow \mathbb{C}$ is the spin density of the measured cross section, t is time, $\mathbf{r} := (x, y)$ is position, γ is the gyromagnetic ratio and $\mathbf{G} = (G_x, G_y)$ is the xy-component of the magnetic gradient vector, as explained in Hinshaw and Lent [25]. The notational convention used in this chapter is to denote vectors and matrices in bold face. From formula (1.1) it is seen that $S(t)$ is the Fourier transform of the spin density $f : D \rightarrow \mathbb{C}$, for fixed t. In the following we explain how formula (1.1) can be obtained.

We distinguish the following four types of magnetic fields. The fields described in 1,3 and 4 are parallel to the z-axis, and the radio frequency pulse, a rotating magnetic field in the xy-plane, is described in 2.

1. A strong *homogeneous field* to align the spins in one direction, called the z-direction; this direction is the equilibrium direction of the spins.
2. A radio frequency pulse (*rf-pulse*), that is, a rotating electromagnetic field in the xy-plane, which is applied for a very short time to push the spins out of equilibrium.
3. The z-component G_z of the gradient vector, by which the cross section is selected, see for example Hinshaw and Lent [25]. We will not take this component into consideration, but we always assume that the spin density of a particular two dimensional object will be measured.
4. The magnetic *gradient field*, $(0, 0, \mathbf{G}.\mathbf{r})^t$, which forces the protons at position $\mathbf{r} = (x, y)$ to resonate with a unique frequency. Here $\mathbf{G} = (G_x, G_y)$ is the xy-component of the gradient vector (G_x, G_y, G_z).

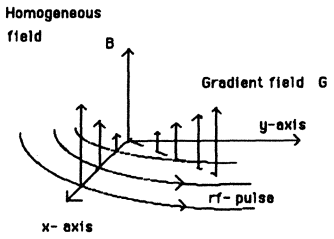

Figure VI.1 . A sketch of the homogeneous field, the magnetic gradient field and the rf-pulse.

A complete sequence of rf and magnetic gradient pulses is sketched in Figure VI.2.

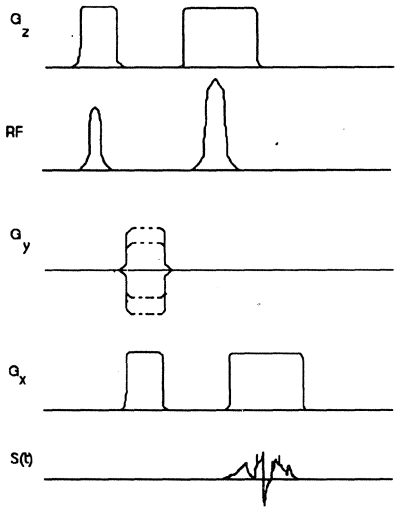

Figure VI.2 . Sequences of gradient field, rf- pulse and echo $S(t)$

In order to study the effect of magnetic fields on the protons in the selected cross section of a human organ, we consider the magnetization $\mathbf{M}(\mathbf{r},t)$, which is the spin density at position $\mathbf{r}$ and at time t.
The three magnetic fields described in 1, 2 and 4, are here denoted, for computational convenience, as one magnetic field which is position and time dependent,

$$\mathbf{B}(\mathbf{r},t) = \mathbf{B_0} + \mathbf{\Delta B}(\mathbf{r}) + \mathbf{B}_1(t). \tag{1.2}$$

Here $\mathbf{B_0}$ is the homogeneous field parallel to the z-axis, $\mathbf{B_1}(t)$ is the rf-pulse which depends on the Larmor frequency $\omega_I = \gamma B_0$ and $\mathbf{\Delta B}$ is the magnetic gradient field, that is

$$\mathbf{B_0} = \begin{pmatrix} 0 \\ 0 \\ B_0 \end{pmatrix},$$

$$\mathbf{\Delta B(r)} = \begin{pmatrix} 0 \\ 0 \\ \mathbf{G.r} \end{pmatrix}, \quad \mathbf{B_1}(t) = \begin{pmatrix} B_1 \cos\omega_I t \\ -B_1 \sin\omega_I t \\ 0 \end{pmatrix}.$$

The magnetization $\mathbf{M}(\mathbf{r},t)$ satisfies the so called *Bloch equation*,

$$\frac{\partial \mathbf{M}(\mathbf{r},t)}{\partial t} = \gamma \mathbf{M}(\mathbf{r},t) \times \mathbf{B}(\mathbf{r},t) + \begin{pmatrix} -M_x(\mathbf{r},t)/T_2(\mathbf{r}) \\ -M_y(\mathbf{r},t)/T_2(\mathbf{r}) \\ (M_0 - M_z(\mathbf{r},t))/T_1(\mathbf{r},t) \end{pmatrix}, \tag{1.3}$$

where $T_1(\mathbf{r})$ and $T_2(\mathbf{r})$ are relaxation times and $\mathbf{M_0}$ is the equilibrium magnetization,

$$\mathbf{M_0} = \begin{pmatrix} 0 \\ 0 \\ M_0 \end{pmatrix}.$$

The relaxation times T_1 and T_2 represent the effect of the relaxation processes. T_1 is the *longitudinal* or *spin-lattice relaxation time* which governs the evolution of M_z towards its equilibrium value M_0; T_2 is the *transverse* or *spin-spin relaxation time* which governs the evolution of the magnitude of the transverse magnetization (M_x, M_y) towards its equilibrium value zero; in general T_1 is much larger than T_2.

Dropping the variables $\mathbf{r}$ and t, we rewrite the equation (1.3) as (cf. Mansfield and Morris [39])

$$\frac{\partial \mathbf{M}}{\partial t} = \mathbf{Q}\mathbf{M} + \mathbf{M_0}/T_1, \tag{1.4}$$

where

$$\mathbf{Q} = \begin{pmatrix} -1/T_2 & \omega & \gamma B_1 \sin\omega_I t \\ -\omega & -1/T_2 & \gamma B_1 \cos\omega_I t \\ -\gamma B_1 \sin\omega_I t & -\gamma B_1 \cos\omega_I t & -1/T_1 \end{pmatrix}.$$

Here $\omega = \gamma(B_0 + \mathbf{G.r})$.

Now consider (1.4) in a coordinate frame that rotates with the Larmor frequency ω_I around the z-axis. We introduce the variable $\tilde{\mathbf{M}} = \mathbf{R}\mathbf{M}$, where the rotation matrix $\mathbf{R}$ is given by

$$\mathbf{R} = \begin{pmatrix} \cos\omega_I t & -\sin\omega_I t & 0 \\ \sin\omega_I t & \cos\omega_I t & 0 \\ 0 & 0 & 1 \end{pmatrix}.$$

The tilde indicates that a variable is transformed to the rotating coordinate frame. Then the Bloch equation (1.4) reduces to

$$\frac{\partial \tilde{\mathbf{M}}}{\partial t} = \Lambda \tilde{\mathbf{M}} + \mathbf{M_0}/T_1. \tag{1.5}$$

Here

$$\mathbf{\Lambda} = \begin{pmatrix} -1/T_2 & \Delta\omega & 0 \\ -\Delta\omega & -1/T_2 & \omega_1 \\ 0 & -\omega_1 & -1/T_1 \end{pmatrix},$$

and $\omega_1 = \gamma B_1, \Delta\omega = \mathbf{G}.\mathbf{r}$.

The unique solution of (1.5) with initial value $\tilde{\mathbf{M}}(0)$ is

$$\tilde{\mathbf{M}}(t) = e^{\mathbf{\Lambda} t}\, \tilde{\mathbf{M}}(0) + \mathbf{\Lambda}^{-1}[e^{\mathbf{\Lambda} t} - \mathbf{Id}]\mathbf{M_0}/T_1, \tag{1.6}$$

where **Id** is the identity matrix. The inverse of $\mathbf{\Lambda}$ is

$$\mathbf{\Lambda}^{-1} = \frac{1}{\det(\mathbf{\Lambda})} \begin{pmatrix} \frac{1}{T_1 T_2} + {\omega_1}^2 & \frac{\Delta\omega}{T_1} & (\Delta\omega)\omega_1 \\ -\frac{\Delta\omega}{T_1} & \frac{1}{T_1 T_2} & \frac{\omega_1}{T_2} \\ (\Delta\omega)\omega_1 & -\frac{\omega_1}{T_2} & \frac{1}{{T_2}^2} + (\Delta\omega)^2 \end{pmatrix},$$

with $\det(\mathbf{\Lambda}) = -(\frac{1}{T_1 {T_2}^2} + \frac{\omega_1^2}{T_2} + \frac{(\Delta\omega)^2}{T_1})$.

It is convenient to decompose $\mathbf{\Lambda}$ as the sum of its symmetric part and its anti-symmetric part, **T** and **F** respectively.

$$\mathbf{T} = \begin{pmatrix} -1/T_2 & & \\ & -1/T_2 & \\ & & -1/T_1 \end{pmatrix}, \quad \mathbf{F} = \begin{pmatrix} 0 & \Delta\omega & 0 \\ -\Delta\omega & 0 & \omega_1 \\ 0 & -\omega_1 & 0 \end{pmatrix}.$$

We now consider the effect of the three magnetic fields on the magnetization **M**. The homogeneous magnetic field is a constant magnetic field in time. The other fields, which are switched on and off now and then, are being used to influence the state of the magnetization.

1. Due to the homogeneous field $\mathbf{B_0}$ we have that $\omega = \omega_L \neq 0$, $\omega_1 = 0$ and $\Delta\omega = 0$; hence $\mathbf{\Lambda} = \mathbf{T}$ and (1.6) reduces to

$$\tilde{\mathbf{M}}(t) = e^{\mathbf{T}t}\tilde{\mathbf{M}}(0) + (1 - e^{-t/T_1})\mathbf{M}_0. \tag{1.7}$$

   If t is large, then $\tilde{\mathbf{M}}(t) \simeq \mathbf{M}_0$, parallel to the z-axis, i.e. $\tilde{\mathbf{M}}$ is approximately in the equilibrium state if t is large.

2. The rf-pulse is a strong field which is applied for a very short time, while the magnetic gradient field is zero, so

$$\mathbf{F} = \begin{pmatrix} 0 & & \\ & 0 & \omega_1 \\ & -\omega_1 & 0 \end{pmatrix}$$

   and

$$\mathbf{\Lambda}^{-1}[e^{\mathbf{\Lambda} t} - Id]\mathbf{M_0}/T_1 \simeq 0$$

   and $\mathbf{\Lambda} \simeq \mathbf{F}$. Suppose $\tilde{\mathbf{M}}(0) = \mathbf{M_0}$, then (1.6) becomes

$$\tilde{\mathbf{M}}(t) \simeq e^{-\mathbf{F}t}\mathbf{M_0}, \tag{1.8}$$

   which is a rotation around the $\tilde{x}$-axis with frequenty $\omega_1 = \gamma B_1$. Applying the rf-pulse for a time period of $t_{\omega_1} = \frac{1}{2}\pi/\omega_1$, we obtain the so called 90° pulse, which results in the following state for the magnetization,

$$\tilde{\mathbf{M}}(t_{\omega_1}) = \begin{pmatrix} 0 \\ M_0 \\ 0 \end{pmatrix}.$$

3. The magnetic gradient field ($\Delta\mathbf{B}$) is considered, which is applied after the rf-pulse. The matrix element $\Delta\omega \neq 0$, but $\omega_1 = 0$ (because the rf-pulse is off). Then equation (1.6) becomes

$$\tilde{\mathbf{M}}(t + t_{\omega_1}) = e^{\mathbf{F}t + \mathbf{T}t}\tilde{\mathbf{M}}(t_{\omega_1}) + (1 - e^{-t/T_1})\mathbf{M}_0. \tag{1.9}$$

After some time the magnetization has returned to equilibrium:

$$\tilde{\mathbf{M}}(t) \simeq \begin{pmatrix} 0 \\ 0 \\ M_0 \end{pmatrix}.$$

Note that the magnetization at position $\mathbf{r}$ depends on the frequency $\omega_L + \Delta\omega$ ($\Delta\omega = \gamma\mathbf{G}.\mathbf{r}$).

The receiver coil of the MR-machine measures the magnetization $\mathbf{M}(t + t_{\omega_1})$, (that can be obtained by transforming formula (1.9) to the nonrotating coordinate frame) before it has returned to equilibrium and an output signal $S(t)$ is generated. In Hinshaw and Lent [25] it is explained how in practice the magnetization $\mathbf{M}(t + t_{\omega_1})$ induces the signal $S(t)$ in the receiver coils of the MR-machine,

$$S(t) = const \int_D e^{-t/T_2} M_\perp(\mathbf{r}) e^{-j\Delta\omega t} d\mathbf{r}.$$

Here $M_\perp$ is the *transverse magnetization* defined as $M_\perp := M_x + jM_y$ where $j^2 = -1$. Now let $f(\mathbf{r}) = M_\perp(\mathbf{r})$. With $\Delta\omega = \gamma\mathbf{G}.\mathbf{r}$, we have

$$S(t) = const \int_D e^{-t/T_2} f(\mathbf{r}) e^{-j\gamma\mathbf{G}.\mathbf{r}t} d\mathbf{r}. \tag{1.10}$$

This does not take into account that the relaxation time T_2 depends on the position $\mathbf{r}$. Because the time period during which the measurements are made is much smaller than T_2, we have $e^{-t/T_2} \simeq 1$ so (1.10) simplifies to formula (1.1):

$$S(t) \simeq const \int f(x, y) e^{-j\gamma t(G_x x + G_y y)} dx dy.$$

In the current practice of MRI one uses time dependent magnetic gradient fields: $\mathbf{G}(t)$. In that case formula (1.1) generalizes to

$$S(t) \simeq const \int f(x, y) e^{-j\gamma(\int_0^t G_x(t')x + G_y(t')y dt')} dx dy.$$

Writing $k_x := \int_0^t \gamma G_x(t')dt'$, $k_y := \int_0^t \gamma G_y(t')dt'$, we recognize $S(t)$ as the Fourier coefficient of f at the frequency (k_x, k_y), denoted by $\widehat{f}(k_x, k_y)$.

In the practice of MRI it is only possible to measure a finite number of Fourier coefficients, say $k_x = -N_x, ..., N_x - 1$ and $k_y = -N_y, ..., N_y - 1$. In practice one often takes the values for N_x and N_y to be 64 or 128. The magnetic gradient fields are chosen such that $\widehat{f}$ is sampled at a rectangular grid. The sampling strategy in practice is to scan on horizontal lines from left to right. That is, for k_y running from $-N_y$ to $N_y - 1$ the corresponding *profile*: $\widehat{f}(-N_x, k_y), ..., \widehat{f}(N_x - 1, k_y)$ is measured. (In practice it may take from 2 to

10 *msec* to measure a profile.) For physical reasons there has to be a small time period between two consecutive profiles, which lasts in practice from 10 up to 100 *msec*. So, to obtain the desired Fourier coefficients for making an image, one needs at least $2N_y \times 10$ *msec*. The scanning geometry is given in the figure below, where the horizontal lines denote the profiles and a tick mark denotes a sample within a profile.

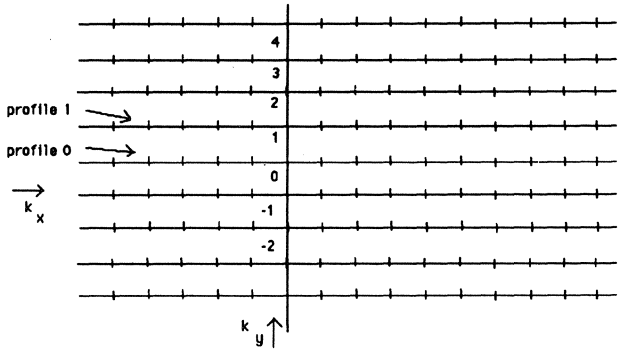

Figure VI.3 . Profiles in the Fourier plane

For this reason G_x is called the *readout* or *detection* gradient and G_y the *phase encoding* or *preparation* gradient.
An approximation of the spin density f is then obtained by Fourier inversion:

$$f(x,y) \approx \frac{1}{2\pi} \sum_{k_x=-N_x}^{N_x-1} \sum_{k_y=-N_y}^{N_y-1} \widehat{f}(k_x,k_y) e^{j(k_x x + k_y y)}.$$

1.2. Dynamic MRI

For diagnostic purposes a sequence of images of the heart at consecutive phases, presented in a movie loop, will give useful information (e.g. cardiac output, heartwall motion, leaking heart valves) which cannot easily be obtained from static pictures. In the previous section it turned out that the minimum time period needed for obtaining the desired information is $2N_y \times 10$ *msec*. If $N_y = 64$, then it takes 1.28 seconds to measure the needed profiles. One heartbeat lasts approximately 1 second. So, the data collection strategy explained in the previous section is not suited for reconstruction of the beating human heart. In this subsection we explain two data collection and reconstruction strategies, which are used in practice, to obtain images of the heart at the desired phases: *ECG triggering* and *retrospective gating*. Both methods use information from the electrocardiogram (ECG). For easy reference we repeat the terminology already given in Section 4 of the Introduction.

R-pulse: the pulse in the ECG-signal which marks the beginning of a heartbeat.
RR-interval: the duration in seconds between two consecutive R-pulses.
Unit RR-interval: an RR-interval of unit length which will be used as reference interval. We denote this interval by $J := [0,1]$.
Heart phase: a phase in the approximately periodic motion of the heart.

In the conventional ECG-triggered technique [16], the same slice is excited with a *fixed* number of RF pulses following the R-pulse of the ECG. Subsequently, the phase encoding gradient is increased if the next R-pulse occurs, see Figure VI.4. In the following figure short tick marks represent the time instants where profiles are measured; long tick marks represent R-pulses.

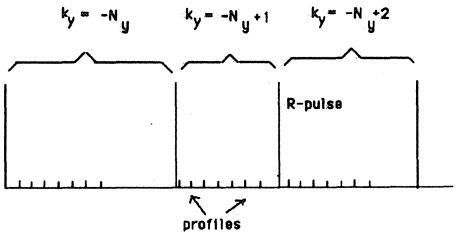

Figure VI.4 . ECG-triggered acquisition method: no measurements are available at the last part of the heartbeat.

This means that no data are measured in the last portion of relatively long heartbeats. This is the main disadvantage of ECG-triggered data collection. Another undesirable effect is the lightening artefact. From formula (1.9) it can be seen that the magnetization has not fully returned to its equilibrium state at the time the next profile is measured. This results in a loss of signal intensity. So the last profile in a sequence of measurements does not have the same signal intensity as the first. In the last part of the heartbeat however, there are no profiles obtained. Thus the magnetization vector returns to its equilibrium state. The first profile in a new sequence of data then has higher signal intensity. This yields a higher intensity in the image at the first heartphase compared to the images at the other phases. This is the lightening artefact.

The *retrospective gating* technique has been proposed [17],[8],[35] to overcome these difficulties. In this technique the data acquisition occurs continuously, independently of the position of the R-pulse. The ECG is simply recorded to enable a posteriori synchronization of the data to the correct heart phase. The main advantage is that now also measurements from the last part of the heartbeat are available, moreover the lightening artefact does not occur.

Acquisition method of retrospective gating

In the retrospective gating technique, one records an uninterrupted sequence of profiles which are measured at equidistant time intervals at distance ΔT, called *repetition time*. Recall that a profile is a sequence of measurements with k_y fixed and k_x increasing from $-N_x$ to $N_x - 1$. Simultaneously, but independently of the profile measurements, the ECG is recorded (see Figure VI.5). In Figure VI.5, the short tick marks represent the profiles and long tick marks R-pulses; the value of k_y is increased after 15 measurements.

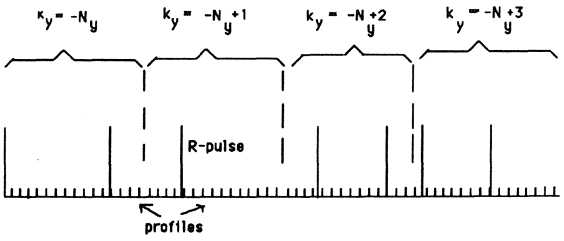

Figure VI.5 . Acquisition method of retrospective gating: k_y is incresed after $N_{pr} = 15$ profiles have been measured

This enables one to assign the data a posteriori to corresponding phases on the unit RR-interval. In principle, the value k_y of the phase-encoding gradient ought to be increased immediately after each heartbeat. However, during the measuring process the information about the duration of the heartbeats is not available to influence the data acquisition. Therefore the value of the phase-encoding gradient G_y is increased after a *fixed* number N_{pr} of profiles has been measured. To circumvent the problem that occurs in the case of ECG-triggering one chooses N_{pr} such that at least one entire heartbeat occurs during one phase-encoding step. Assume for example that the RR-intervals of a patient scanned in the MR-machine are approximately one second. If one chooses N_{pr} such that $N_{pr} \times \Delta T \geq 1.5$ seconds, then profiles both at the beginning as well as at the end of the heartbeat can be obtained within each phase encoding step.

The total amount of data to be measured is $2N_x \times 2N_y \times N_{pr}$. For practical reasons the spatial resolution $2N_x \times 2N_y$ is required to be high, in practice $N_x = N_y = 64$ or 128. It is important that the data collection time, which is proportional to the value $2N_x \times 2N_y \times N_{pr}$, is small. This means that the value of N_{pr} cannot be too high, in practice $N_{pr} = 25$, or $N_{pr} = 50$.
To sum up, the data acquisition process contains the following steps:

(i) Initialize the phase encoding gradient: $k_y = -N_y$.
(ii) Measure profiles with a repetition time ΔT until N_{pr} profiles have been recorded. Each profile consists of $2N_x$ measurements ($k_x = -N_x, ..., N_x - 1$) of the Fourier transform of the cross-section, with k_y fixed.
(iii) Increase the phase-encoding gradient: $k_y \rightarrow k_y + 1$; if $k_y = N_y$ then stop, otherwise go to (ii).
(iv) Meanwhile measure the time markers $\{R_k\}$ of occurrence of the R-pulses in the ECG signal.

1.3. Model building: a mathematical problem definition

After data acquisition has been completed we want to reconstruct images of the heart at various phases during the unit heart interval. As we explain in this section, all one can do is to reconstruct a sort of average heartbeat. It is not possible to obtain a 'movie' of the actual situation. At the end of this section we present a mathematical inversion problem for dynamic MRI reconstruction.

The measurement times $\{\tau_i\}$ of the Fourier coefficients obtained by the acquisition method, which is described above, are in our model computed as follows. We remark that in practice the computation of these time markers is more complicated.

Recall that the profiles are sampled equidistantly with consecutive distance ΔT. Within each profile the measurements are also spaced uniformly in time, say with distance δt. Denote the measurement time for the k_xth sample within the ith profile in the k_yth phase encoding step by $\tau_i(k_x, k_y)$. These measurement times $\tau_i(k_x, k_y)$ are called *time markers*. Since the data within a profile are sampled equidistantly at distance δt, we have

$$\tau_i(k_x, k_y) = \tau_i(0, k_y) + k_x \delta t. \tag{1.11}$$

The number of profiles within each k_yth encoding step is N_{pr}, so the first element of the ith profile is measured at

$$\tau_i(0, k_y) = (k_y N_{pr} + i)\Delta T. \tag{1.12}$$

In the case of dynamic MRI the spin density of a cross section of the heart at position $\mathbf{r}$ and time τ is denoted by $F(\mathbf{r}, \tau), \tau \in \mathbb{R}$. The Fourier coefficients of F with respect to the spatial parameter $\mathbf{r}$ can be obtained by means of the previously described data acquisition method, at time markers $\{\tau_i(k_x, k_y)\}$, denoted as

$$\{\widehat{F}(k_x, k_y, \tau_i(k_x, k_y))\}.$$

These Fourier coefficints are obtained during various RR-intervals. In order to make a reconstruction based on these data, we will make two *model assumptions* .

The first assumption is the existence of a conversion rule $\tau \rightarrow t(\tau)$, which maps a time marker $\tau_i(k_x, k_y)$ on an RR-interval to a corresponding phase $t_i(k_x, k_y)$ on the unit RR-interval,

$$t_i(k_x, k_y) := t(\tau_i(k_x, k_y)). \tag{1.13}$$

This conversion is called *rescaling*; the $t_i(k_x, k_y)$'s are called *rescaled time markers*. For clarity, we will refer to a time point on an RR-interval as 'time' τ and to a time point on the unit RR-interval as 'phase' t.

The simplest rule to rescale measurement times is *linear stretching*, where the total duration of a heartbeat is used. However, it is known that the variation in the duration af a heartbeat is mainly due to the variation in the second part of the heartbeat. The time interval corresponding to the first part of the *kth* heartbeat is denoted as $[R_k, t_T]$ and the time interval corresponding to the second part as $[t_T, R_{k+1})$. The point t_T can be computed by the empirically established formula

$$t_T := 0.36\sqrt{R_{k+1} - R_k}. \tag{1.14}$$

The rescaling rule which takes this effect into account, called *piecewise linear stretching*, will also be considered.

The second assumption is the existence of a *model heartbeat* g, depending on the position $\mathbf{r}$ and phase t, denoted by $(\mathbf{r}, t) \rightarrow g(\mathbf{r}, t)$, such that its Fourier coefficients at the rescaled time markers are equal to the data,

$$\widehat{g}(k_x, k_y, t_i(k_x, k_y)) = \widehat{F}(k_x, k_y, \tau_i(k_x, k_y)), \quad k_x, k_y, i.$$

Here the Fourier transform is taken with respect to the spatial parameter $\mathbf{r}$. We emphasize that the model heartbeat is only an artificial construction and not a physical reality.

However, the model heartbeat can be considered as a realistic approximation of the spin density of the human heart F, when rescaled to an RR-interval,

$$g(\mathbf{r}, t(\tau)) \approx F(\mathbf{r}, \tau), \tag{1.15}$$

for τ lying in an RR-interval $\tau \in [R_k, R_{k+1})$.

We now pay attention to two rescaling algorithms: linear stretching and piecewise linear stretching.
In the case of linear stretching on each RR-interval, the relation between τ and t is

$$t(\tau) = \frac{\tau - R_k}{R_{k+1} - R_k}, \quad \tau \in [R_k, R_{k+1}), \tag{1.16}$$

where R_k is the time at which the kth R-pulse in the ECG-signal occurs ($k = 1, 2, ...$).
Piecewise linear stretching on each RR-interval corresponds to the empirically established conversion rule

$$t(\tau) = \begin{cases} \frac{\tau}{t_T} \times 0.36, & \tau - R_k < t_T \\ \frac{\tau - t_T}{R_{k+1} - R_k - t_T} \times 0.64 + 0.36, & \tau - R_k \geq t_T \end{cases} \tag{1.17}$$

for $\tau \in [R_k, R_{k+1})$, where t_T is given by (1.14). The two different scale transformations are sketched in Figure VI.6.

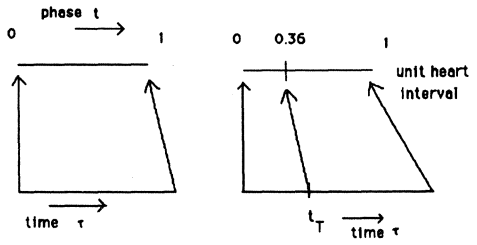

Figure VI.6 . Time-to-phase conversion. (a) linear stretching; (b) piecewise linear stretching.

Note that as a result of the time-to-phase conversion, the data must be rearranged: when a new R-pulse occurs while the value of k_y is still unchanged, the next profile is mapped to the beginning of the unit heart interval J, whereas the previous profile corresponds to the end of J (see Figure VI.7). Another problem is that the positions of the profiles on the unit heart interval J do not match with the desired phases, which ususally consist of a number of equally spaced positions. Furthermore, for each value of k_y the pattern of rearranged phases is different. We use interpolation techniques to deal with this problem. The details will be given in the next section.

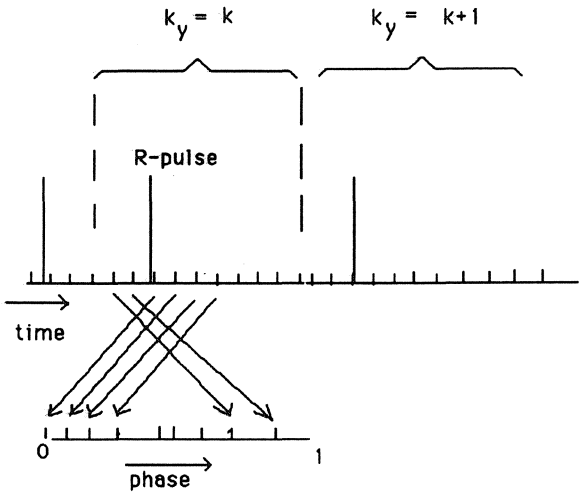

Figure VI.7 . Rearrangement of the profiles on the unit heart interval.

Having obtained the time markers $\tau_i(k_x, k_y)$ and the corresponding Fourier coefficients of the spin density $\widehat{F}(k_x, k_y, \tau_i(k_x, k_y))$ the time-to phase-conversion is performed. That is, the rescaled time markers are computed by formula (1.16) and we get, by assumption,

$$\widehat{g}(k_x, k_y, t_i(k_x, k_y)) := \widehat{F}(k_x, k_y, \tau_i(k_x, k_y)).$$

Here the rescaling strategy is still arbitrary. In our examples we most of the time consider linear stretching on each RR-interval.

For easy reference we explicitly state the *model assumptions*:

- The algorithm to obtain rescaled time markers on the unit RR-interval from time markers on an RR-interval is linear stretching.
- There exists a model heartbeat such that its Fourier coefficients at the rescaled time markers are equal to the measurements from the spin density of a beating human heart.

This leads to the following problem formulation. Let the sequence $\{g_i(k_x, k_y)\}$ be defined as

$$g_i(k_x, k_y) := \widehat{g}(k_x, k_y, t_i(k_x, k_y)), \tag{1.18}$$

for $k_x = -N_x, ..., N_x - 1; k_y = -N_y, ..., N_y - 1$ and $i = 0, ..., N_{pr} - 1$. Note that $g_i(k_x, k_y)$ denotes the value of $\widehat{g}(k_x, k_y, t_i(k_x, k_y))$. Here the spatial Fourier transform of the function g is defined by

$$\widehat{g}(k_x, k_y, t) := \frac{1}{2\pi} \int_D g(x, y, t) e^{-j(k_x x + k_y y)} dx dy. \tag{1.19}$$

We will refer to the sequences $\{g_i(k_x, k_y)\}$ and $\{t_i(k_x, k_y)\}$ as the *data* and the *rescaled time markers* respectively. D is the rectangle $[0, 2\pi]^2$ and $J = [0, 1]$ is the unit RR-interval. The problem then is: find the model heartbeat $g : D \times J \to \mathbb{C}$ such that

$$\hat{g}(k_x, k_y, t_i(k_x, k_y)) = g_i(k_x, k_y), \tag{1.20}$$

for $k_x = -N_x, ..., N_x - 1; k_y = -N_y, ..., N_y - 1$ and $i = 0, ..., N_{pr} - 1$.

It is the aim in dynamic MRI to obtain the model heartbeat g. However, in general the model heartbeat is not uniquely determined by the data $\{g_{\mathbf{k},i}\}$. That is, any function f satisfying (1.20) will be an approximation of g and will not be identical to g. The topic of the next section is the construction of a solution of problem (1.20).

Since the solution of problem (1.20) involves Fourier inversion in the spatial domain and interpolation in the time domain, we will refer to (1.20) as the *mixed Fourier-interpolation problem*, or simply, the *mixed problem*.

VI.2. Solution to the Reconstruction Problem of dynamic MRI

For notational convenience we write the pair (k_x, k_y) as $\mathbf{k}$. Denote $g_{\mathbf{k},i} := g_i(k_x, k_y)$, $t_{\mathbf{k},i} := t_i(k_x, k_y)$. Define the set $\mathbb{K}$ by

$$\mathbb{K} := \{(k_x, k_y) \mid k_x = -N_x, ..., N_x - 1; k_y = -N_y, ..., N_y - 1\}$$

and $\mathbb{I} := \{i \mid i = 0, ..., N_{pr} - 1\}$. Note that these index sets are finite. In this section we will apply Theorems IV.5.1 and III.3.3 of Part One for the case of finite index sets.

We now give a formal statement of the problem associated with dynamic MRI.

Mixed Fourier Interpolation Problem

Given a sequence of rescaled time markers $\{t_{\mathbf{k},i}\}$ and the data $\{g_{\mathbf{k},i}\}$, find the model heartbeat $g : D \times \mathbb{R} \to \mathbb{C}$ such that

$$\hat{g}(\mathbf{k}, t_{\mathbf{k},i}) = g_{\mathbf{k},i}, \quad \mathbf{k} \in \mathbb{K}, i \in \mathbb{I}. \tag{2.1}$$

As we explained in the previous section this model heartbeat is in general not uniquely determined by the data $\{g_{\mathbf{k},i}\}$. Any function f satisfying (2.1) is an approximation of the model heartbeat. We will call f a *reconstruction* of the model heartbeat.

Suppose we have found such a (complex valued) function f. In practice a sequence of images at the time phases ϕ_m $(m = 0, ..., M - 1)$ of the amplitude of this function f is displayed on a computer screen. A computer screen, represented here as the square $[0, 2\pi]^2$, is divided up into pixels (picture elements). Assume that there are $2N_x \times 2N_y$ pixels. Digital images are realized by assigning grey values to pixels. An image of the function $|f|$ at phase ϕ_m is then obtained by assigning the grey value $|f(i/\pi, j/\pi, \phi_m)|$ to the i, jth pixel, $i = 0, ..., 2N_x - 1$ and $j = 0, ..., 2N_y - 1$. By displaying images of $|f|$ at consecutive phases ϕ_m $(m = 0, 1, ..., M - 1)$ one can simulate the motion of the heart. The larger M the better the dynamic character of the movie. (After the image of the Mth phase is shown, the image of phase ϕ_0 is displayed again.)

An idea to solve problem (2.1) is as follows. Interpolate the data $\{g_{\mathbf{k},i}\}_{i \in I}$ at the phases ϕ_m for each frequency vector $\mathbf{k} \in \mathbb{K}$. Using interpolated data for each of the phases, the reconstruction is then obtained by the Fourier inversion formula. Different interpolation

techniques are briefly considered here: *spline interpolation* and *sinc interpolation*. For more details we refer to Section IV.1 and IV.3 of Part One.

Now we discuss our mathematical framework. We want to find a solution f of problem (2.1) such that the mapping $t \to f(\mathbf{r},t)$ is an element of the Hilbert space $\mathcal{H}$ for all $\mathbf{r} \in D$. This can be formalized in the following manner.

Definition 2.1 . Let $\mathcal{H}$ be a Hilbert space of functions $f : \mathbb{R} \to \mathbb{C}$, with inner product $\langle\ ,\ \rangle_{\mathcal{H}}$ and norm $\|\ \|_{\mathcal{H}}$. $L^2_{\mathcal{H}}(D \times \mathbb{R})$ is the space of functions $f : D \times \mathbb{R} \to \mathbb{C}$ such that for each $\mathbf{r} \in D$, the function $t \to f(\mathbf{r},t)$ is an element of $\mathcal{H}$, and

$$\int_D \|f(\mathbf{r},\cdot)\|^2_{\mathcal{H}} d\mathbf{r} < \infty.$$

Here the '$\cdot$' in the fomula above means that the norm is computed with respect to the time parameter t.

In the course of this section two cases are distinguished:
- — *Case 1* $\mathcal{H}$ is the space of bandlimited functions;
- — *Case 2* $\mathcal{H}$ is the space of polynomial spline functions of odd degree.

Our approach is to give a solution of problem (2.1) for both cases at once in terms of the space $L^2_{\mathcal{H}}(D \times \mathbb{R})$. Then, we will pay attention to case 1 and 2 separately.

We assume that $\mathcal{H}$ possesses a system of *point evaluation functionals* $\{\varphi_{\mathbf{k},i}\}$ (cf. Section I.1) such that

$$f(t_{\mathbf{k},i}) = \langle f, \varphi_{\mathbf{k},i}\rangle_{\mathcal{H}}, \quad f \in \mathcal{H}. \tag{2.2}$$

The *Gram matrix* corresponding to the sequence $\{\varphi_{\mathbf{k},i}\}_{i\in I}$ is defined as

$$(G(\mathbf{k}))_{ij} := \langle \varphi_{\mathbf{k},j}, \varphi_{\mathbf{k},i}\rangle_{\mathcal{H}}, \quad i,j \in \mathbb{I}, \mathbf{k} \in \mathbb{K}.$$

From property (2.2) it follows that

$$(G(\mathbf{k}))_{ij} = \varphi_{\mathbf{k},j}(t_{\mathbf{k},i}) \quad i,j \in \mathbb{I}, \mathbf{k} \in \mathbb{K}. \tag{2.3}$$

Define the system $\{\psi_{\mathbf{k},i}\}$ lying in $\mathcal{H}$ as

$$\psi_{\mathbf{k},i}(t) := \sum_{j\in I} \overline{(G^{-1}(\mathbf{k}))}_{ij} \varphi_{\mathbf{k},j}(t), \tag{2.4}$$

where the bar denotes the complex conjugate. A solution of problem (2.1) can be obtained in terms of the $\psi_{\mathbf{k},i}$'s. In Part One, Theorem IV.5.1 it is proved the solution thus obtained has smallest norm among all solutions:

Solution of the Mixed Fourier Interpolation Problem
If, for each $\mathbf{k} \in \mathbb{K}$, the sequence of rescaled time markers $\{t_{\mathbf{k},i}\}_{i\in I}$ consists of distinct values, then the mixed problem (2.1) has the unique minimum norm solution

$$f(\mathbf{r},t) = \frac{1}{2\pi} \sum_{\mathbf{k}\in\mathbb{K}} c_{\mathbf{k}}(t) e^{j\mathbf{k}.\mathbf{r}}. \tag{2.5}$$

Here $c_{\mathbf{k}}$ is defined by

$$c_{\mathbf{k}}(t) := \sum_{i\in I} g_{\mathbf{k},i} \psi_{\mathbf{k},i}(t), \quad \mathbf{k} \in \mathbb{K}. \tag{2.6}$$

Note that this solution f is obtained in two steps, which has the practical advantage that for each $\mathbf{k} \in \mathbb{K}$ one only has to read and store the partial data vector $\{g_{\mathbf{k},i}\}_{i\in I}$, to compute the interpolating function $c_{\mathbf{k}}$ for this value of $\mathbf{k}$. Then, after we have computed the $c_{\mathbf{k}}$'s for all values of $\mathbf{k} \in \mathbb{K}$, we compute the minimum norm solution by the Fast Fourier Transform. The reason why such a decomposition exists is that the system of exponentials $\{e^{j\mathbf{k}.\mathbf{r}}\}_{\mathbf{k}\in K}$ is orthogonal in $L^2(D)$.

In the remainder of this section we consider the case that $\mathcal{H}$ is the space of bandlimited functions and the case that $\mathcal{H}$ is the space of odd degree polynomial splines.

Case 1: interpolation by bandlimited functions.

Introduce the Hilbert space of bandlimited functions $\mathbb{P}_r$ by

Definition 2.2 .

$$\mathbb{P}_r := \{f \in L^2(\mathbb{R}) \mid \hat{f}(\xi) = 0 \text{ for } \xi \text{ outside the interval } [-r, r]\ \}.$$

$\mathbb{P}_r$ becomes a Hilbert space with the inner product:

$$\langle f, g\rangle_r := \int f(t)\overline{g(t)}dt,$$

and norm

$$\|f\|_r^2 := \langle f, f\rangle_r, \quad f \in \mathbb{P}_r.$$

Let $\{t_{\mathbf{k},i}\}_{\mathbf{k}\in K, i\in I}$ be a sequence of real numbers. The set of point evaluation functionals is defined as

$$\varphi_{\mathbf{k},i}(t) := (r/\pi)\ \mathrm{sinc}_r(t - t_{\mathbf{k},i}), \quad \mathbf{k} \in \mathbb{K}, i \in \mathbb{I}, \tag{2.8}$$

where the *sinc*-function is defined by (cf. Papoulis [44])

$$\mathrm{sinc}_r(t) := \begin{cases} \dfrac{\sin(rt)}{rt}, & t \neq 0 \\ 1, & t = 0. \end{cases}$$

In Part One it is shown (formula (IV.1.2)) that then condition (2.2) is satisfied.

Case 2: interpolation by spline functions.

Accounts of spline theory are given in Ahlberg et al. [1], de Boor [9], Schoenberg [47], and Greville [21]. Here we mainly follow Greville [21].

Definition 2.3 . A mesh Δ of an interval $[a, b]$ is a sequence of distinct real numbers $\{t_1, ..., t_N\}$ such that $a = t_1 < t_2 < ... < t_N = b$. The intervals (t_i, t_{i+1}) are called (open) mesh intervals.

The space $\mathcal{K}^m$ of polynomial spline functions of degree m is defined as follows (cf. de Boor [9]).

Definition 2.4 . $\mathcal{K}^m := \{f \in C^{m-1}[a, b] \mid$ on each mesh interval f is a polynomial of degree at most m $\}$.

We are particularly interested in spline functions of odd degree. Any spline function f of degree $2n-1$ is of the form

$$f(t) = p_{2n-1}(t) + \sum_{i\in I} c_i(t - t_i\pi/r)_+^{2n-1}.$$

Here p_{2n-1} is a polynomial of degree $2n-1$ or less, the c_i's are complex numbers and $(.)_+^k$ is defined as

$$(t)_+^k := \begin{cases} t^k, & t \geq 0 \\ 0, & t < 0. \end{cases}$$

$\mathcal{K}^{2n-1}$ is a Hilbert space with inner product

$$\langle f, g\rangle_{\mathcal{K}} := \sum_{k=0}^{n-1} f^{(k)}(a)\overline{g^{(k)}(a)} + \int_{[a,b]} f^{(n)}(t)\overline{g^{(n)}(t)}dt.$$

Here $f^{(k)}$ denotes the kth derivative of f. The norm of a spline function f is denoted by $\|f\|_{\mathcal{K}}$.

Introduce the function σ by

$$\sigma(t,s) := \sum_{k=0}^{n-1} \frac{(t-a)^k(s-a)^k}{(k!)^2} \quad +$$

$$\sum_{k=0}^{n-1}(-1)^{n+k+1}\,\frac{(t-a)^{2n-k-1}(s-a)^k}{(2n-k-1)!k!} \quad + \frac{(-1)^n}{(2n-1)!}(t-s)_+^{2n-1}, \quad t,s \in \mathbb{R}. \tag{2.9}$$

The system of point evaluation functionals $\{\varphi_{\mathbf{k},i}\}_{i\in I}$ is defined by

$$\varphi_{\mathbf{k},i}(t) := \sigma(t, t_{\mathbf{k},i}) \tag{2.10}$$

for $t \in \mathbb{R}$. Note that this system is linearly independent. In Part One is is shown (formula (IV.3.2)) that condition (2.2) is satisfied in this case.

We now show how to transform our solution method into a concrete algorithm.

Algorithm
Given are the MR-data $\{g_{\mathbf{k},i}\}_{\mathbf{k}\in K, i\in I}$, and the rescaled time markers $\{t_{\mathbf{k},i}\}_{\mathbf{k}\in K, i\in I}$. Then the reconstruction, at the phases ϕ_m $(m = 0, ..., M-1)$ is obtained in the following way:

begin
for $\mathbf{k} \in \mathbb{K}$ **do**
Fill the Gram matrix $G(\mathbf{k})$ according to

$$(G(\mathbf{k}))_{ij} := \varphi_{\mathbf{k},j}(t_{\mathbf{k},i}), \quad i,j \in \mathbb{I}, \mathbf{k} \in \mathbb{K}.$$

Invert the Gram matrix.
for $i \in \mathbb{I}$ **do**
Compute $\psi_{\mathbf{k},i}$ by

$$\psi_{\mathbf{k},i} = \sum_{j\in I} \overline{(G(\mathbf{k})^{-1})}_{ij}\varphi_{\mathbf{k},j}.$$

done
Evaluate $c_{\mathbf{k}}$ at ϕ_m: $c_{\mathbf{k}}(\phi_m) = \sum_{i\in I} g_{\mathbf{k},i}\psi_{\mathbf{k},i}(\phi_m)$.
done
Compute f at ϕ_m: $f(\mathbf{r},\phi_m) = \sum_{\mathbf{k}\in K} c_{\mathbf{k}}(\phi_m)e^{j\mathbf{k}.\mathbf{r}}$.
end

Note that this algorithm can be used for reconstruction by means of splines as well as by means of bandlimited functions. In this manner the algorithm above provides several reconstruction methods which we call sinc, degree 1 and degree 3 reconstruction. These different kinds of methods are obtained by assigning a value to r in formula (2.8) for bandlimited functions and by assigning a value to 'n' in the case of formula (2.9) for spline functions of odd degree. The reconstruction method proposed by Bohning [8] (see Section 4 of the Introduction) does not fit into this setting of spline functions of odd degree, but it is considered for practical purposes. In this reconstruction algorithm the approximation of the Fourier coefficients at the phase ϕ_m is not done by means of bandlimited, or spline functions, but it is obtained by averaging the measured Fourier coefficients in the interval $[\phi_m, \phi_{m+1})$. If there are no data lying in this interval, then the Fourier coefficients at phase ϕ_m are set to the value zero. This reconstruction technique is referred to as degree 0 reconstruction.

A prerequisite for the existence of a minimum norm solution is that the time points $\{t_{\mathbf{k},i}\}_{i\in I}$ are distinct for each $\mathbf{k} \in I\!K$. In the case of cardiac MRI this condition may be violated, since the rescaled time points $\{t_{\mathbf{k},i}\}$ are obtained by means of the rescaling formulas (1.16), or (1.17). In other words, if for fixed $\mathbf{k} \in I\!K$ the time markers $\tau_{\mathbf{k},i}$ and $\tau_{\mathbf{k},j}$ are measured in distinct heart intervals, it can happen that after time-to-phase conversion the corresponding rescaled time markers $t_{\mathbf{k},i}$ and $t_{\mathbf{k},j}$ coincide. In such cases regularization techniques prove very useful.
Define the operator $\mathcal{T} : L^2_{\mathcal{H}}(D \times I\!R) \to \ell^2(I\!K \times I\!I)$ by

$$\mathcal{T}f := \{\widehat{f}(\mathbf{k}, t_{\mathbf{k},i})\}_{\mathbf{k}\in K, i\in I}.$$

Here $\mathcal{H}$ is $\mathcal{K}^{2n-1}$ or $I\!P_r$. The mixed problem (2.1) can now be reformulated:
find $f \in L^2_{\mathcal{H}}(D \times I\!R)$ such that

$$\mathcal{T}f = g, \tag{2.11}$$

where the data vector g is defined by $g := \{g_{\mathbf{k},i}\}_{\mathbf{k}\in K, i\in I}$. If the time points $\{t_{\mathbf{k},i}\}_{i\in I}$ are distinct for $\mathbf{k} \in I\!K$, then the inverse of $\mathcal{T}$, denoted by $\mathcal{T}^{-1}$ is (cf. formulas (2.5) and (2.6))

$$(\mathcal{T}^{-1}g)(\mathbf{r},t) = \sum_{\mathbf{k}\in K}\sum_{i\in I} g_{\mathbf{k},i}\psi_{\mathbf{k},i}(t)e^{j\mathbf{k}.\mathbf{r}}.$$

If the time markers do not satisfy this condition, then there exists no inverse of $\mathcal{T}$. In such cases we try to approximate a substitute for an inverse of $\mathcal{T}$ by a sequence of bounded linear operators $\{\mathcal{T}^\gamma\}_{\gamma>0}$ acting from $\ell^2(I\!K \times I\!I)$ into $L^2_{\mathcal{H}}(D \times I\!R)$.

Tychonov-Phillips regularization of the mixed problem

Let $\{t_{\mathbf{k},i}\}_{\mathbf{k}\in K, i\in I}$ be rescaled time markers and let $g \in \ell^2(I\!K \times I\!I)$ be the data. The Tychonov-Phillips regularization $\{T^\gamma\}$ is defined as

$$(\mathcal{T}^\gamma g)(\mathbf{r},t) = \sum_{\mathbf{k}\in K} (T^\gamma_{\mathbf{k}} g_{\mathbf{k}})(t)\ e^{j\mathbf{k}\mathbf{r}}.$$

Here $g_{\mathbf{k}}$ denotes the sequence $\{g_{\mathbf{k},i}\}_{i\in I}$ and

$$(T^\gamma_{\mathbf{k}} g_{\mathbf{k}})(t) := \sum_{j\in I}\sum_{i\in I}((G(\mathbf{k}) + \gamma I)^{-1})_{ji}\ g_{\mathbf{k},i}\ \varphi_{\mathbf{k},i}(t),$$

where $\varphi_{\mathbf{k},i}$ is given by formula (2.8) in the case of bandlimited and by (2.10) in the case of spline functions. The Gram matrix $G(\mathbf{k})$ is given by formula (2.3).

(The behaviour of $T^\gamma g$ when $\gamma \to 0$ is discussed in Section I.2.) Note that the regularization can also be obtained in two steps. First, for fixed $\mathbf{k} \in I\!K$, we compute the term $T_{\mathbf{k}}^\gamma g_{\mathbf{k}}$ from the partial data vector $g_{\mathbf{k}} := \{g_{\mathbf{k},i}\}_{i \in I}$. Next obtain the regularization by Fourier inversion: $T^\gamma g = \sum_{\mathbf{k} \in K} T_{\mathbf{k}}^\gamma g_{\mathbf{k}} e^{j\mathbf{k}.\mathbf{r}}$. So, the regularization has a decomposition similar to the minimum norm solution. Again this is useful for practical purposes. In Section VI.3 we give an example of regularization of the reconstruction by means of bandlimited functions.

VI.3. Reconstruction of the chest phantom

In this section we compare degree 0, degree 1, degree 3 and sinc reconstruction discussed in the previous section. In the following we simulate the chest and beating heart by means of a continuous sequence of images which are built up from ellipses (see Section 3.1). Such a sequence of images is called *chest phantom.*

The MRI-data collection strategy (retrospective gating) is simulated for this chest phantom (Section 3.1). Then, from these data, the several reconstructions are computed and displayed on a computer screen. These images are illustrated in Section 3.2. The performance of the methods is considered by comparing the differences of the reconstructions and the original chest phantom. The simulations are carried out on a Sun 4 Sparc workstation. We emphasize that it is not our aim to improve the speed of the reconstruction algorithms.

In the case of MR-imaging of the beating human heart it is difficult to find objective criteria for the quality of the reconstructions. The performance of the reconstruction algorithms then depends on the correctness of the model assumptions and the noise on the data.

The reason for performing simulations by means of a chest phantom is that we can focus on a comparison of the quality of the reconstruction algorithms, since we do not have to bother about the validity of the model assumptions.

3.1. Definition of the chest phantom

In this section we explain how the chest phantom is defined and how it is used to compare the several reconstruction techniques.

The chest phantom we use (see Fig. VI.8) is built up from a number of solid ellipses with different shapes, sizes or orientations. The phantom is taken as in [40]. It should be regarded as a 'model' for a cross section of the human chest, including the heart. For this reason the shape and size of three specific ellipses within the phantom are varying in time (Ellipses E_2, E_6 and E_7 in Fig. VI.8). The ellipses E_2, E_6 and E_7 should be regarded as a simple representation of a cross section of the heart. The ellipses E_6 and E_7 imitate two heart chambers. The heart muscle is simulated by the second ellipse E_2 which contracts and expands in time. E_6 and E_7 do not only contract and expand, but they also change position.

A solid ellipse is parametrized by five time dependent parameters. The centre is $(\alpha(t), \beta(t))$, the lengths of the major and minor half axes are $\rho(t)$ and $\sigma(t)$ and the angle of the ellipse with respect to the horizontal axis is $\theta(t)$.

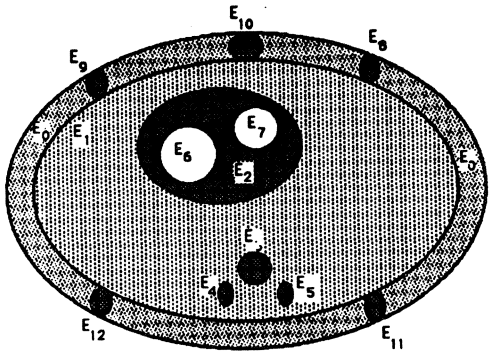

Figure VI.8 . The ellipses defining the chest phantom.

The kth ellipse E_k is parametrized by

$$E_k(\alpha_k(t), \beta_k(t), \rho_k(t), \sigma_k(t), \theta_k(t)).$$

To every ellipse is assigned a 'colour' or 'grey-value'. The values of the parameters and grey-values of the ellipses are given in the following table. The parameters α, β, ρ and σ are given in pixel units, where we use a square of 256 x 256 pixels; θ is given in radians and grey-values range from 0 (black) to 255 (white).

	α	β	ρ	σ	$\theta(\pi/16rad)$	$grey-value$
E_0	128	128	120	80	0	200
E_1	128	128	110	70	0	128
E_2	112	105	$\rho_2(t)$	$\sigma_2(t)$	5	64
E_3	128	175	10	16	0	64
E_4	104	175	5	10	−5	64
E_5	152	175	5	10	5	64
E_6	$\alpha_6(t)$	$\beta_6(t)$	$\rho_6(t)$	$\sigma_6(t)$	0	255
E_7	$\alpha_7(t)$	$\beta_7(t)$	$\rho_7(t)$	$\sigma_7(t)$	−5	255
E_8	220	82	8	4	−4	255
E_9	36	82	8	4	4	255
E_{10}	128	52	8	4	0	255
E_{11}	220	174	8	4	4	255
E_{12}	36	174	8	4	−4	255

Table VI.1 Parameters of the ellipses defining the chest phantom.

Here

$$\rho_2(t) = \sigma_2(t) = 35(1 + 0.3\sin(2\pi t + \pi/4))$$
$$\alpha_6(t) = \rho_2(t) + (104 - \rho_2(t))(1 + 0.3\sin(2\pi t + \pi/4) + 0.2\sin(4\pi t))$$
$$\beta_6(t) = \sigma_2(t) + (116 - \sigma_2(t))(1 + 0.3\sin(2\pi t + \pi/4) + 0.2\sin(4\pi t))$$
$$\rho_6(t) = \sigma_6(t) = 12(1 + 0.3\sin(2\pi t + \pi/4) + 0.2\sin(4\pi t))$$
$$\alpha_7(t) = \rho_2(t) + (120 - \rho_2(t))(1 + 0.2\sin(2\pi t) + 0.1\sin(4\pi t + \pi/2) + 0.1\sin(6\pi t))$$
$$\beta_7(t) = \sigma_2(t) + (90 - \sigma_2(t))(1 + 0.2\sin(2\pi t) + 0.1\sin(4\pi t + \pi/2) + 0.1\sin(6\pi t))$$
$$\rho_7(t) = 2\sigma_7(t)10(1 + 0.2\sin(2\pi t) + 0.1\sin(4\pi t + \pi/2) + 0.1\sin(6\pi t)).$$

3.2. Generation of test-data

In this section we explain how the MRI data collection strategy is simulated in the case of the chest phantom.

In the case of MRI of the beating human heart the R-pulses from the ECG signal are recorded, which indicate the beginning of a heartbeat. Furthermore, the time markers $\{\tau_{\mathbf{k},i}\}$ are computed and the Fourier coefficients $\{g_{\mathbf{k},i}\}$ of spin density are measured. In the case of the chest phantom these sequences $\{R_k\}$, $\{\tau_{\mathbf{k},i}\}$ and $\{g_{\mathbf{k},i}\}$ are obtained in the following manner.

Generation of time markers

The generation of the time markers is done by formulas (1.11) and (1.12):

$$\tau_{\mathbf{k},i} := (k_y N_{pr} + i)\Delta T + k_x \delta t, \tag{3.1}$$

where $\mathbf{k} \in I\!K$ is the vector (k_x, k_y). (Note that these time markers can be negative, since k_x and k_y run from $-N_x$ and $-N_y$ up to $N_x - 1$ and $N_y - 1$ respectively.) The index $i \in I\!I := \{0, 1, ..., N_{pr} - 1\}$ and N_{pr} is the number of profiles which are measured within one phase encoding step. ΔT is the time between two consecutive profiles and δt is the period of time between two samples within a profile.

Generation of heart-interval times

We assume that on the average a heartbeat lasts one second. The times $\{R_k\}$ $(k = 0, ..., L)$ of R-pulses are such that $\{R_{k+1} - R_k\}$ are uniformly distributed random numbers lying in the interval $[1 - \epsilon, 1 + \epsilon]$, where he first R-pulse is given by (cf. Forumula (3.1)) $R_0 = -N_y N_{pr} \Delta T - N_x \delta t$. The case $\epsilon = 0$ corresponds to a perfectly regular heartbeat.

Generation of Fourier coefficients

We denote the function describing the chest phantom above by $g(\mathbf{r}, t)$. This function governs a single heartbeat with period one. We extend this function to a larger time interval $[R_0, R_{I_*}) \subset I\!R$ by means of the linear stretching time-to-phase conversion described in Section 1. That is, given the sequence of times $\{R_k\}$ of R-pulses, $R_0 < R_1 < R_2 < ... < R_{I_*}$, we define the extension $F : D \times I\!R \to \mathbb{C}$ of g to the larger time interval $[R_0, R_{I_*})$ by (cf. formula 1.15)

$$F(\mathbf{r}, \tau) := g(\mathbf{r}, t(\tau)), \quad \text{for } \tau \in [R_j, R_{j+1}), \tag{3.2}$$

where the linear stretching time to-phase-conversion is given by formula (1.16):

$$t(\tau) = \frac{\tau - R_j}{R_{j+1} - R_j}.$$

This function F simulates the beating human heart with varying RR-intervals.
Our simulation requires Fourier coefficients of this function F with respect to the spatial parameter $\mathbf{r}$, that is

$$\widehat{F}(\mathbf{k},\tau) := \frac{1}{2\pi}\int_D F(\mathbf{r},\tau)e^{j(\mathbf{k}\cdot\mathbf{r})}d\mathbf{r},$$

for $\mathbf{k} \in I\!K := \{-N_x,..,N_x-1\} \times \{-N_y,..,N_y-1\}$. Combining the formulas (3.1) and (3.2) we obtain

$$\widehat{F}(\mathbf{k},\tau_{\mathbf{k},i}) = \widehat{g}(\mathbf{k},t_{\mathbf{k},i}). \tag{3.3}$$

Therefore, the corresponding Fourier coefficients of the phantom can be computed after the rescaled times $t(\tau_{\mathbf{k},i})$ have been determined. The data

$$g_{\mathbf{k},i} := \widehat{g}(\mathbf{k},t_{\mathbf{k},i}) \quad \mathbf{k} \in I\!K, i \in I\!I$$

obtained in this way will be called *test-data* from now on.

3.3. Reconstruction from test-data

In the following we apply the reconstruction algorithms to the test data using sinc, degree 1 and degree 3 interpolation. We also implemented the reconstruction method proposed by Bohning [8], referred to as degree 0 reconstruction (cf. Section 2).

The object to be reconstructed is the phantom g. However, the reconstruction obtained will only be an approximation of the function g. The reconstructed images will be compared with the images of the phantom g at the phases ϕ_0, ϕ_2, ϕ_4 and ϕ_6. The maximum number of phases is taken here as $M = 8$. We will give some intuitive criteria for the quality of the reconstructions, and we also use the L^2-norm as a measure for the performance of the algorithms.

In the next section we reconstruct the model heartbeat from MR-data instead of test-data. The motivation for the use of the chest phantom, besides the possibility to compare performance, is that the model assumptions are valid which do not, perhaps, hold true in practice. The advantage of the test situation over the practical situation is that we can focus on the performance of the reconstruction algorithms, without bothering about the validity of the model assumptions. In the practice of dynamic MRI reconstruction both assumptions will generally not be valid. This will be discussed in Sections VI.4 and VII.5.

The quality of the reconstructions depends on the amount of data which are measured, that is $2N_x \times 2N_y \times N_{pr}$. A mathematically interesting question is whether the reconstruction f will converge to the original function g if N_x, N_y and N_{pr} tend to infinity. Theorem III.2.2 gives an affirmative answer to this question in the case of bandlimited functions, under certain conditions. In practice however, the values of N_x, N_y and N_{pr} cannot be taken arbitrarily large, due to physical limitations. The spatial resolution $2N_x \times 2N_y$ is chosen as high as possible in practical situations $N_x = N_y = 64$ or 128. This is because one wants to distinguish small details in the image for diagnostic purposes. For the use of MRI in practice it is important that a patient occupies the MR-scanner for as short a time as possible. So, the data collection time, which is proportional to $N_x \times N_y \times N_{pr}$ is required to be short. This implies that the value of N_{pr} has to be chosen small; in practice one often takes $N_{pr} = 25$ or $N_{pr} = 50$. Accordingly, the performance between the reconstruction algorithms is compared with fixed values for the parameters N_x, N_y and N_{pr}.

The time period δt between two consecutive samples within a profile is neglected in the reconstruction algorithms for the purpose of computer implementation and the speed of

the algorithms. (We want to emphasize that the parameter δt is taken into account in the generation of test-data.)

The time markers $\{\tau_{\mathbf{k},i}\}$ are rescaled by the linear stretching time-to-phase conversion expressed by formula (1.16). It may occur that after rescaling time markers (numerically) coincide, though the corresponding profiles are distinct. In this case an interpolation curve cannot be computed. To remove this deficiency, the profiles with mutual distance smaller than 2γ are averaged along with the associated rescaled time markers. This procedure is an ad hoc regularization technique, which is different from the Tychonov-Phillips regularization. In our algorithms the parameter-value γ is taken as 0.005 for spline interpolation of degree 3 and 0.04 for sinc interpolation. Tychonov-Phillips regularization is implemented in the case of sinc-interpolation, which is called $tp - sinc$ interpolation. In this case $\gamma = 0.01$.

The parameter values used in the generation of the test-data are:

$$N_x = N_y = 64, \quad \delta t = \frac{0.01}{2N_x} \quad \text{and} \quad \epsilon = 0.25.$$

This implies that the images are displayed on a grid of 128 x 128 pixels. The time period to measure one profile is 0.01 seconds. The maximum number M of phases is 8.

In Figure VI.9 the original chest phantom is shown. Then, in Figures VI.10, VI.11, VI.12 and VI.13 we show spline and sinc reconstruction in the case $N_{pr} = 5$. In Figure VI.10 we show degree 0 degree 1 degree 3 and sinc reconstruction at the phase ϕ_0. In Figure VI.11 we show these reconstructions at the phase ϕ_2, etc. Then in Figure VI.14, VI.15, VI.16 and VI.17 we apply the reconstructions in the case of $N_{pr} = 15$.

Before showing the reconstructions we briefly discuss the effects that can be expected in advance. Criteria for the reconstruction quality will be more extensively discussed in the next Section. Here we only point out that the main criterion for the quality of the reconstructions is that the time-varying ellipses in the reconstructed images have sharp contours.

The quality of the reconstructions at phase $\phi_0 = 0$ with degree 0, and sinc reconstruction will be worse than the reconstructions at the other phases. The reason for this is as follows. The rescaled time markers $\{t_{\mathbf{k},i}\}$ lie inside the interval $J = [0, 1]$. The curve which interpolates the profiles at these rescaled time markers is then evaluated at phase $\phi_0 = 0$. Since there are no data at or before phase ϕ_0, we performed an extrapolation. This causes an error which is larger than that for interpolation of the data. The spline reconstructions are expected to behave better, because the implemented spline function was made periodic, see de Boor [9].
The quality of the reconstructions for $N_{pr} = 5$ can be expected to be worse than the reconstructions for $N_{pr} = 15$. This is because the approximation of an interpolating function based on a small data set will be worse than in the case of a larger data set. This effect will occur predominantly for lower degree splines.

For degree 0 reconstruction the following effect will occur in the case of small data sets. Recall that degree 0 reconstruction (see Section 1.2) approximates the Fourier coefficient at phase ϕ_m by averaging the data in the interval $[\phi_m, \phi_{m+1})$. If no data occur in this interval the value of the Fourier coefficient at phase ϕ_m is set to zero. It is likely that degree 0 reconstruction in the case of $N_{pr} = 5$ causes a ringing artefact, due to the Fourier coefficients which are set to zero.

At phases where the motion of the time varying ellipses is fast, the algorithms will not be able to reconstruct this motion exactly. For, if there are high frequencies in the motion of the function to be reconstructed, the approximation of this function by a bandlimited,

or spline function need not contain these high frequency components. This will result in a blurring of the time-varying ellipses within the reconstructed images. This effect can be seen at phase ϕ_4.

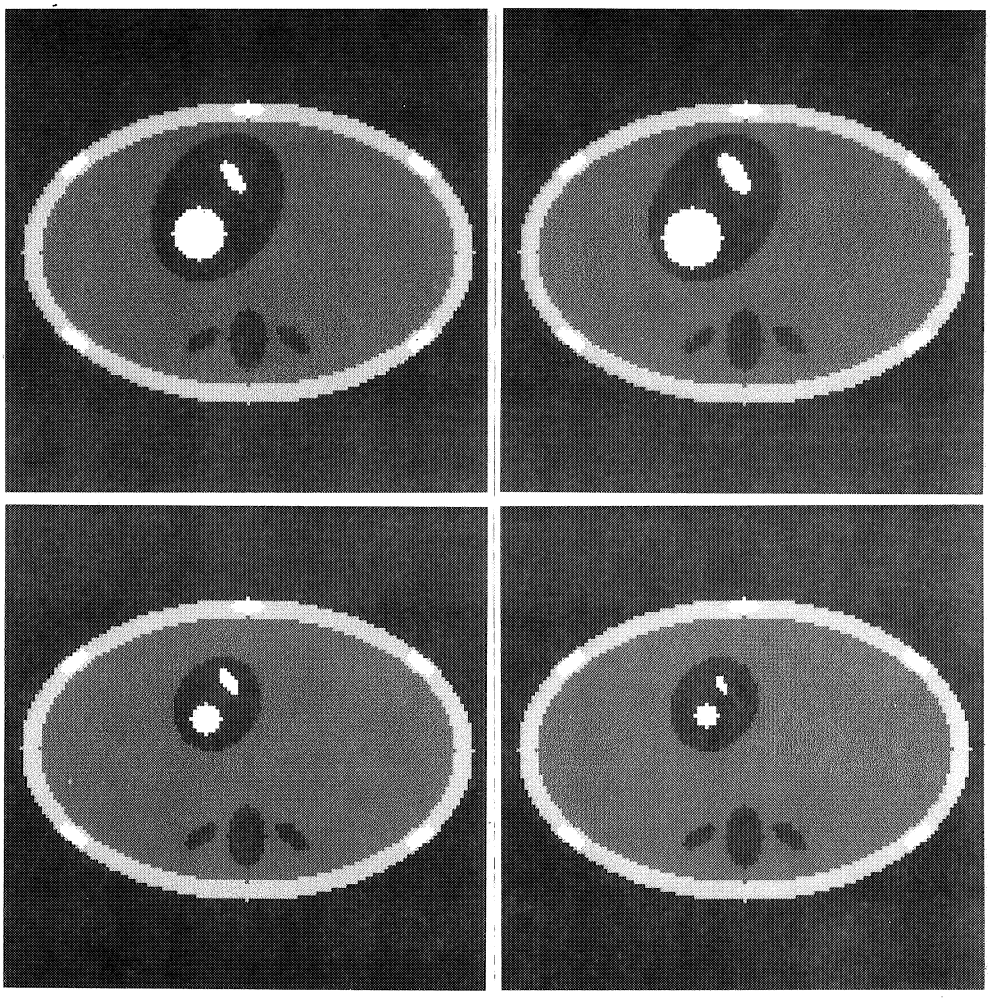

Figure VI.9 . Original chest phantom.
Top left: phase ϕ_0, Top right: phase ϕ_2, Bottom left: phase ϕ_4, Bottom right: phase ϕ_6.

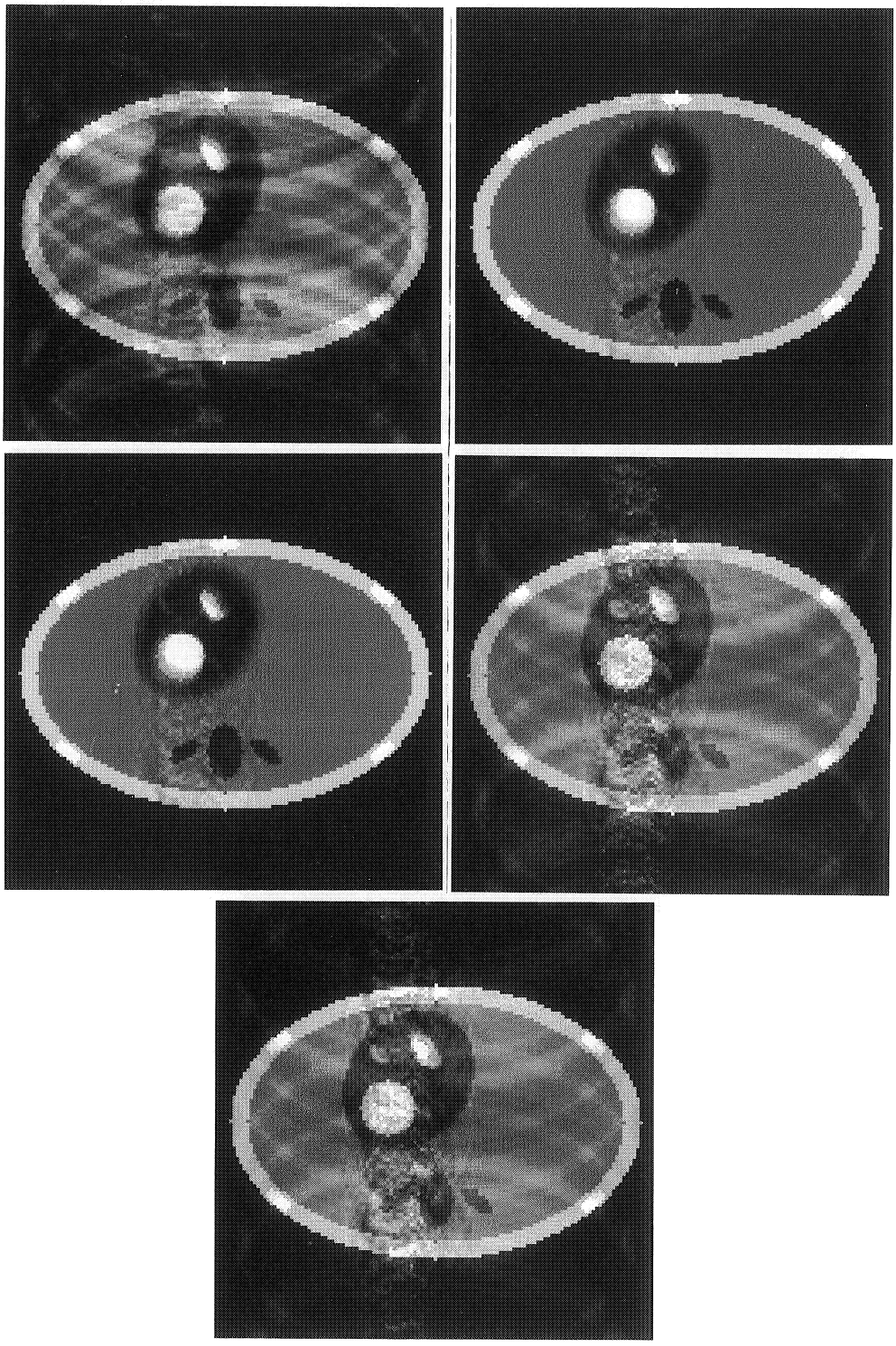

Figure VI.10 . Reconstructions at phase ϕ_0 for $N_{pr} = 5$.
Top left: degree 0, Top right: degree 1, Middle left: degree 3, Middle right: sinc, Bottom: tp-sinc reconstruction

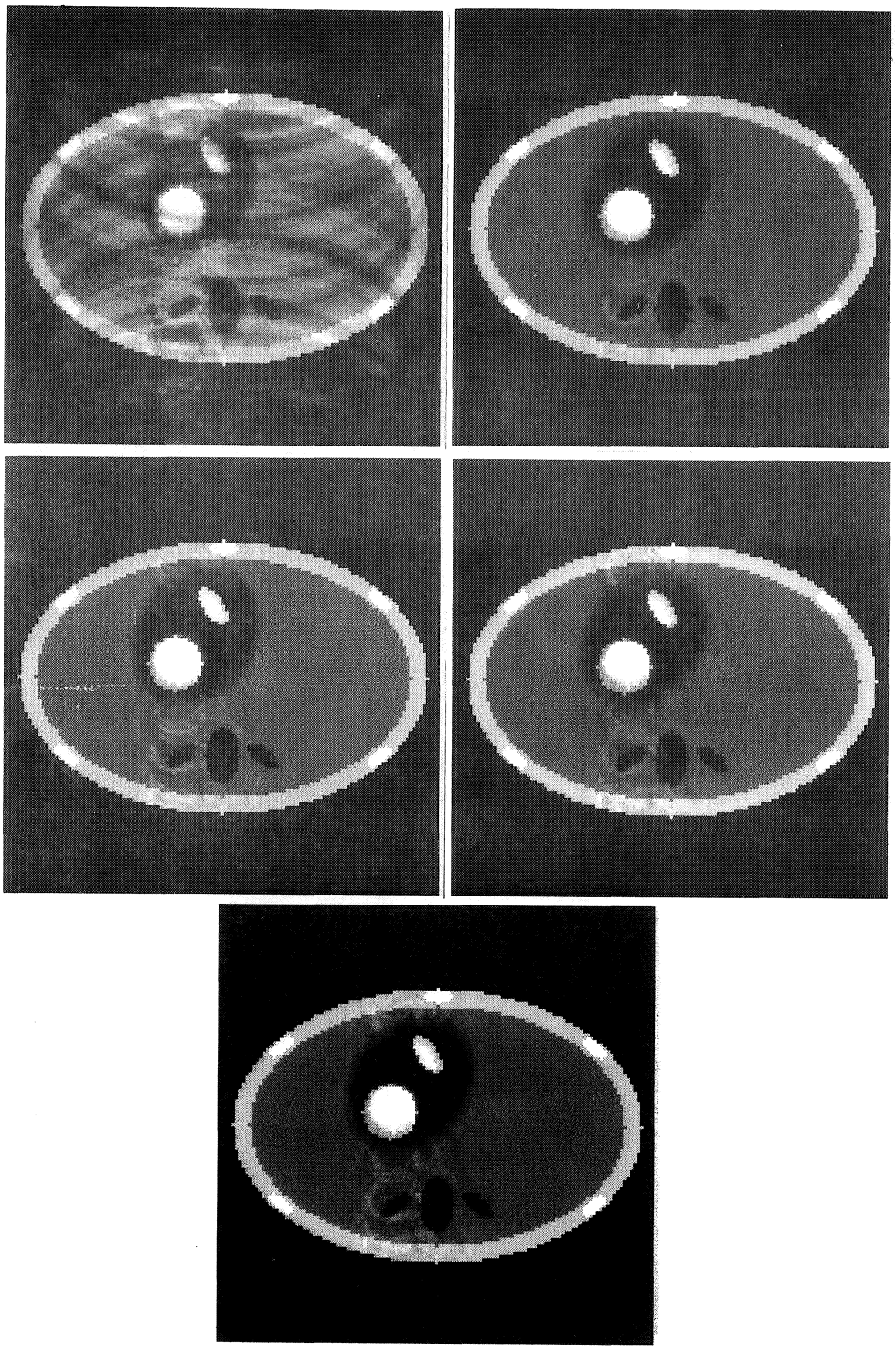

Figure VI.11. Reconstructions at phase ϕ_2 for $N_{pr} = 5$.
Top left: degree 0, Top right: degree 1, Middle left: degree 3, Middle right: sinc, Bottom: tp-sinc

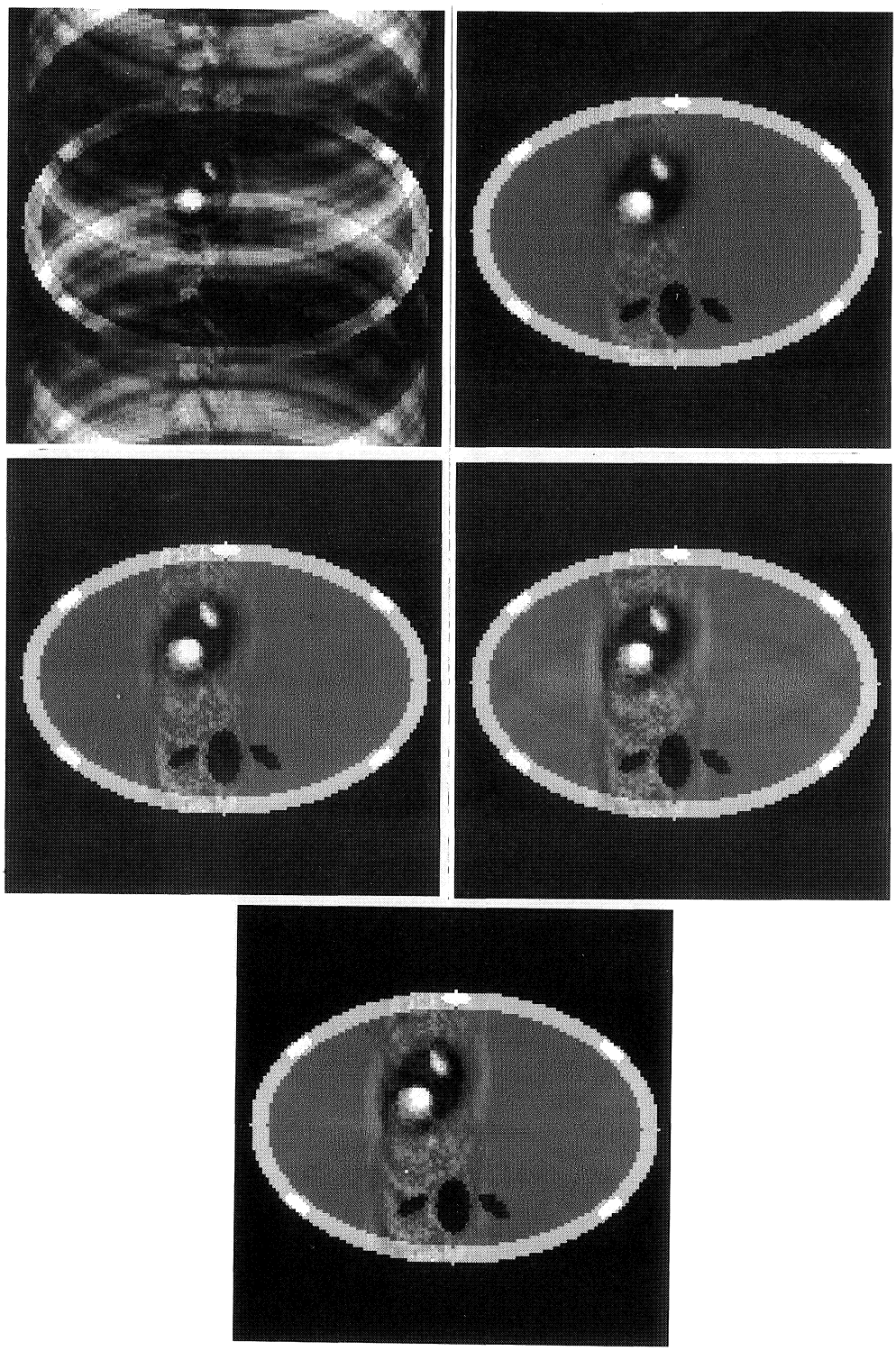

Figure VI.12 . *Reconstructions at phase ϕ_4 for $N_{pr} = 5$.*
Top left: degree 0, Top right: degree 1, Middle left: degree 3, Middle right: sinc, Bottom: tp-sinc.

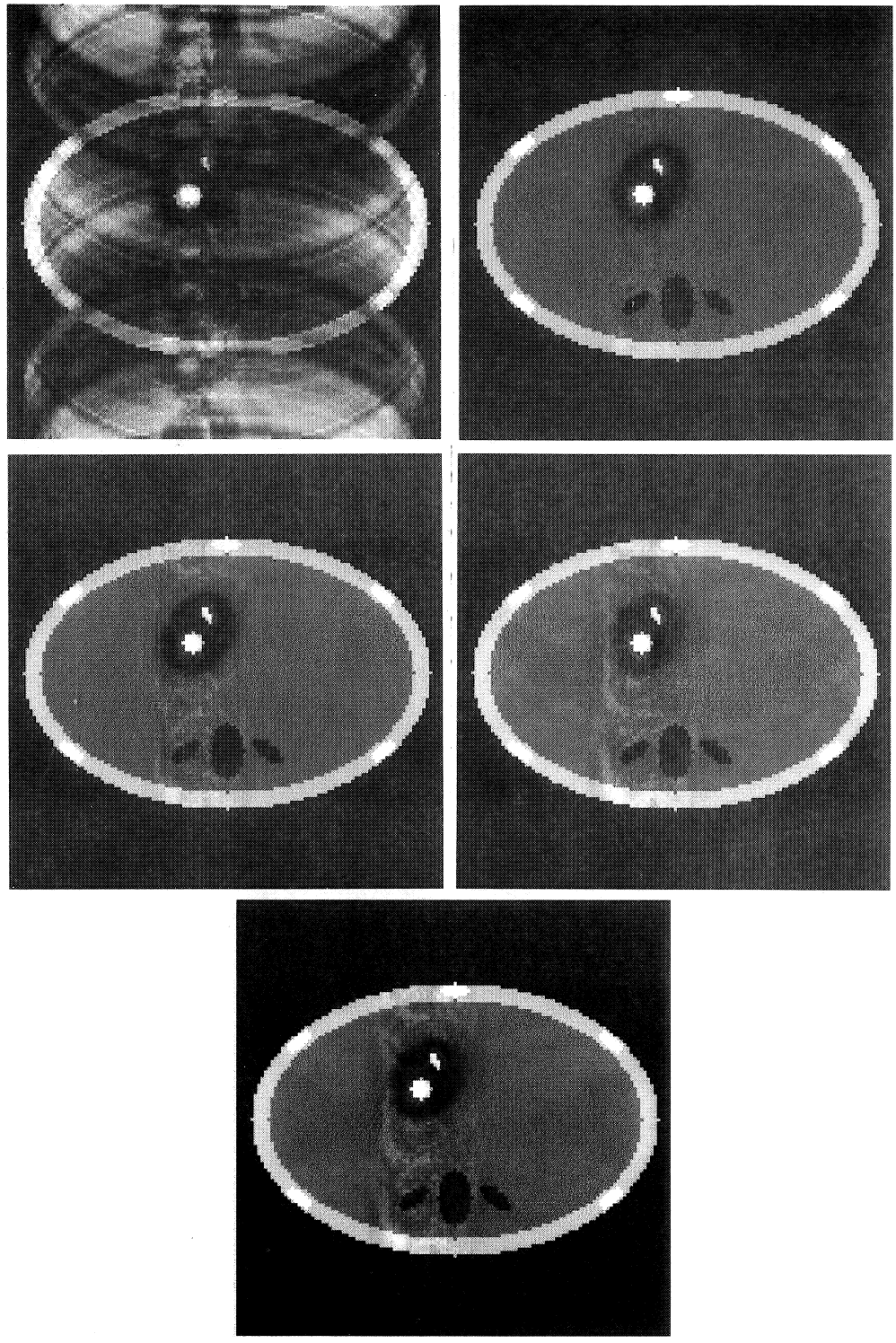

Figure VI.13 . Reconstructions at phase ϕ_6 for $N_{pr} = 5$.
Top left: degree 0, Top right: degree 1, Middle left: degree 3, Middle right: sinc, Bottom: tp-sinc.

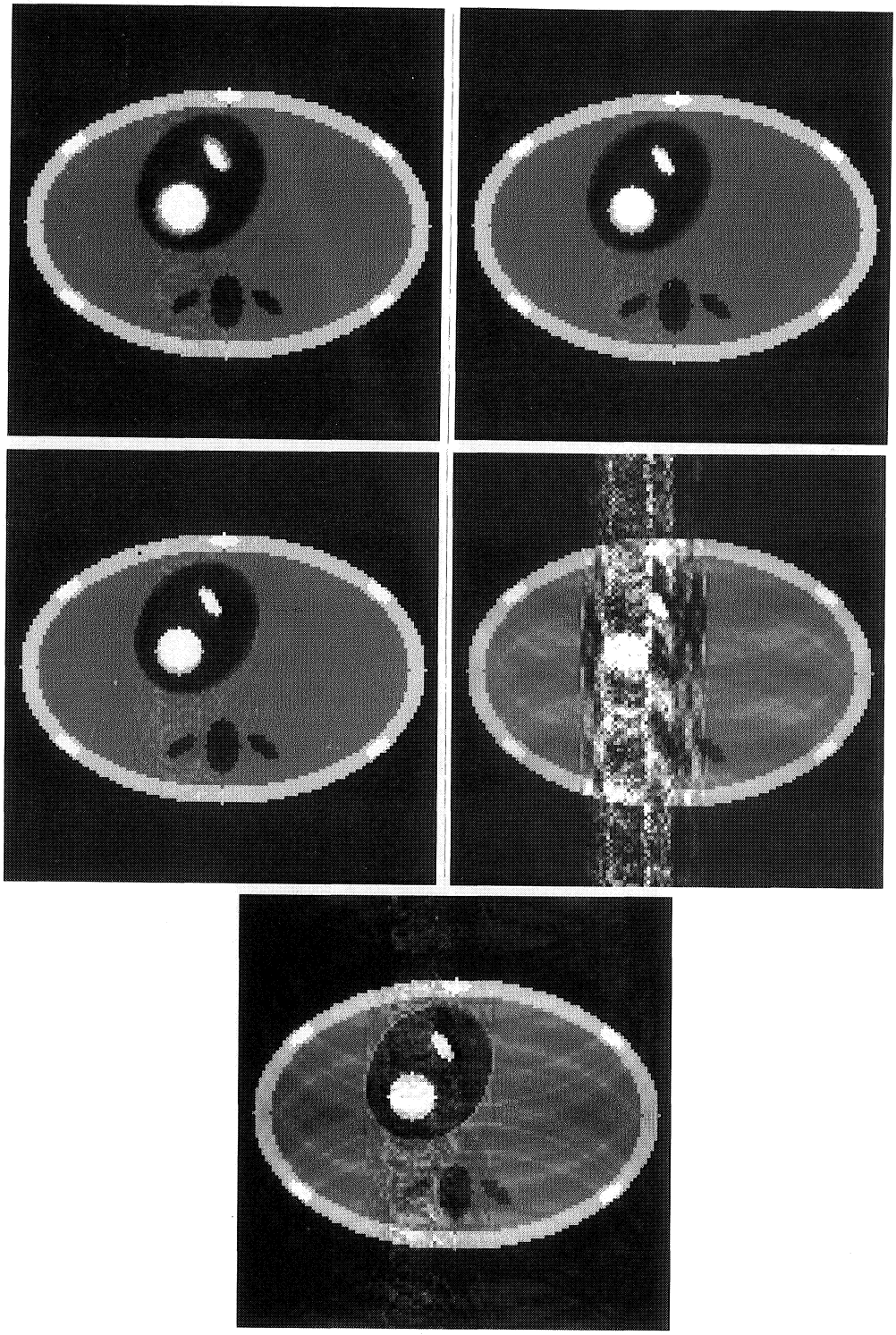

Figure VI.14 . Reconstructions at phase ϕ_0 for $N_{pr} = 15$.
Top left: degree 0, Top right: degree 1, Middle left: degree 3, Middle right: sinc, Bottom: tp-sinc.

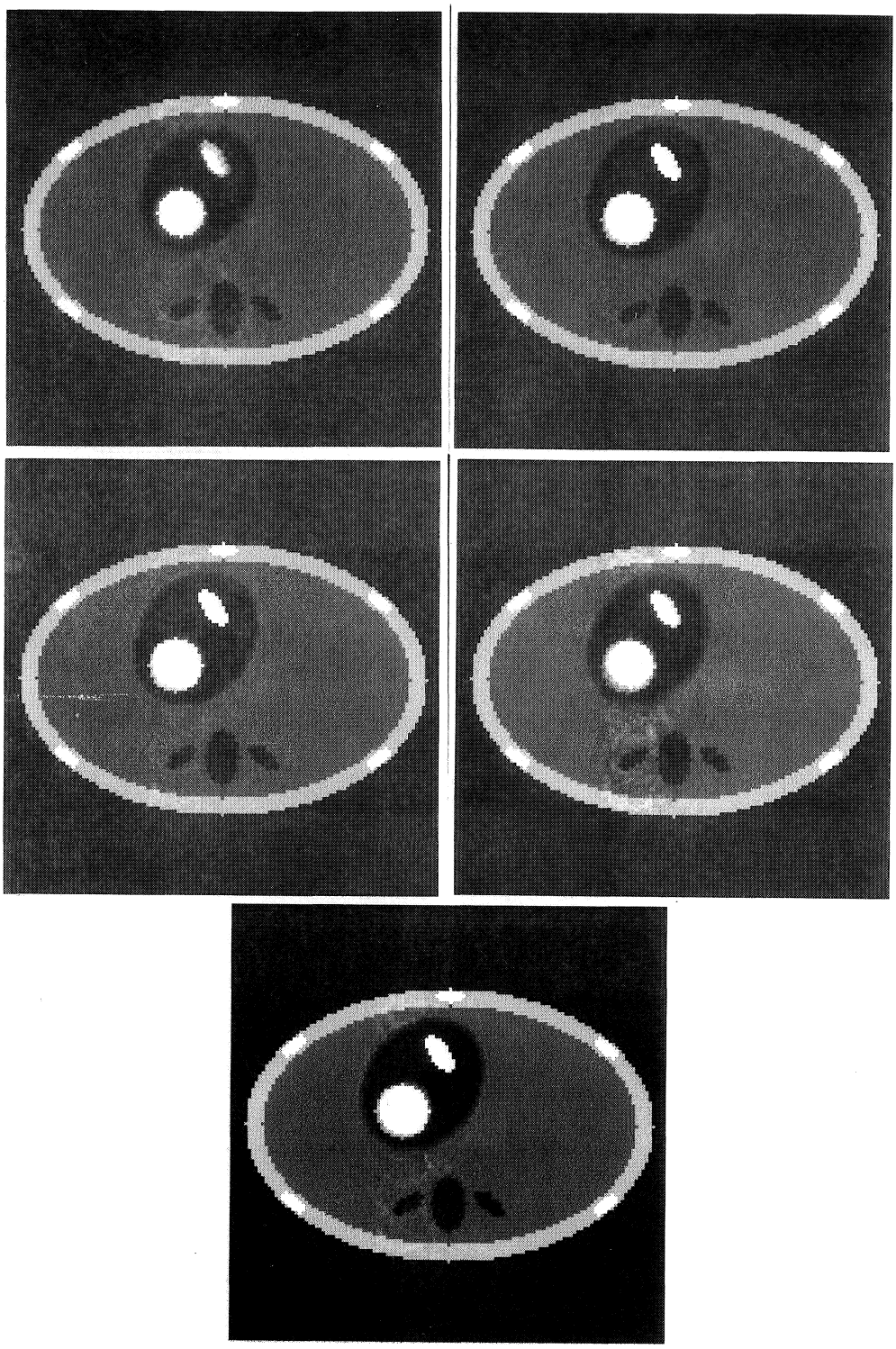

Figure VI.15 . Reconstructions at phase ϕ_2 for $N_{pr} = 15$.
Top left: degree 0, Top right: degree 1, Middle left: degree 3 Middle right: sinc Bottom: tp-sinc.

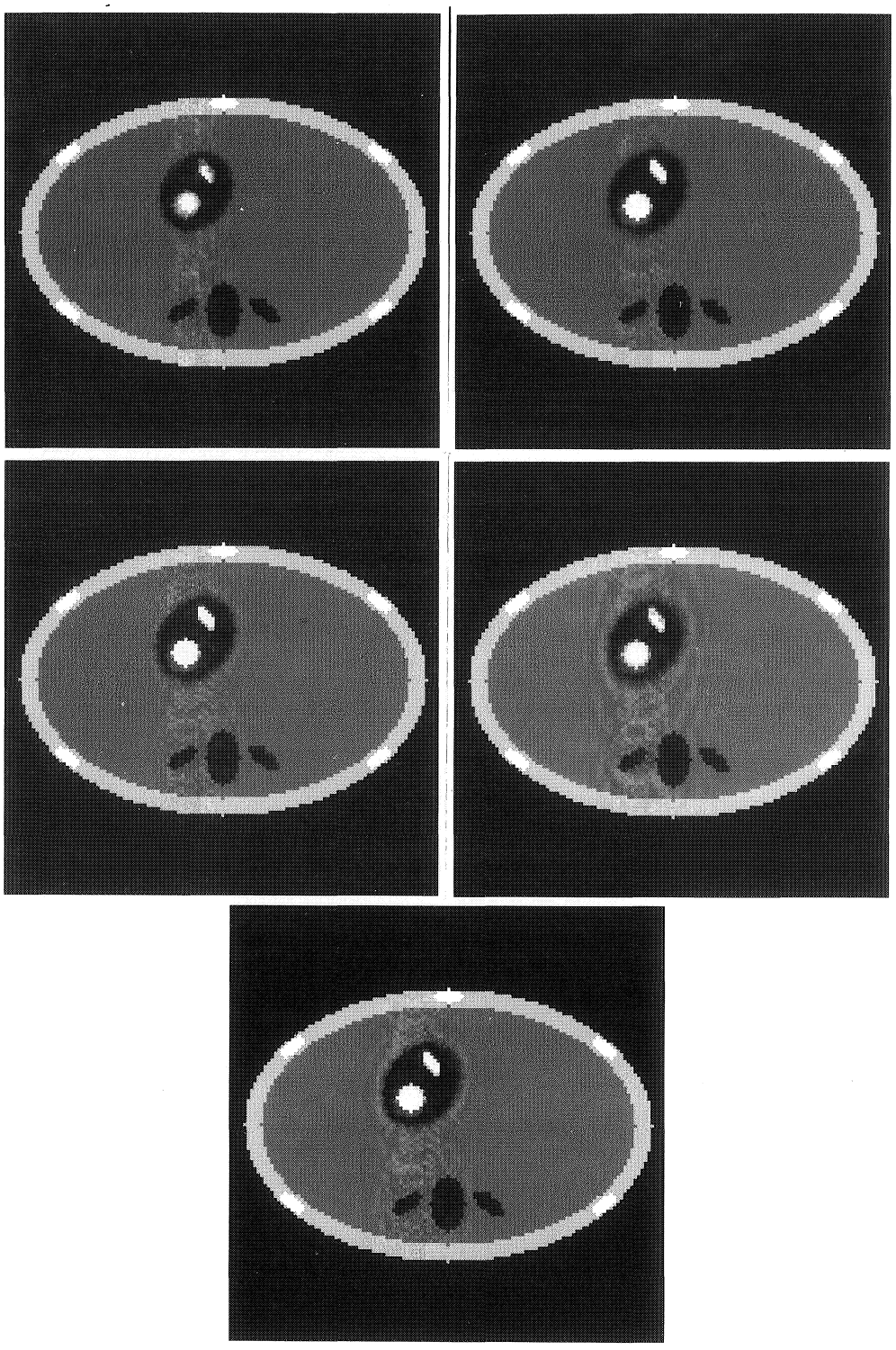

Figure VI.16 . *Reconstructions at phase ϕ_4 for $N_{pr} = 15$.*
Top left: degree 0, Top right: degree 1, Middle left: degree 3, Middle right: sinc, Bottom: tp-sinc.

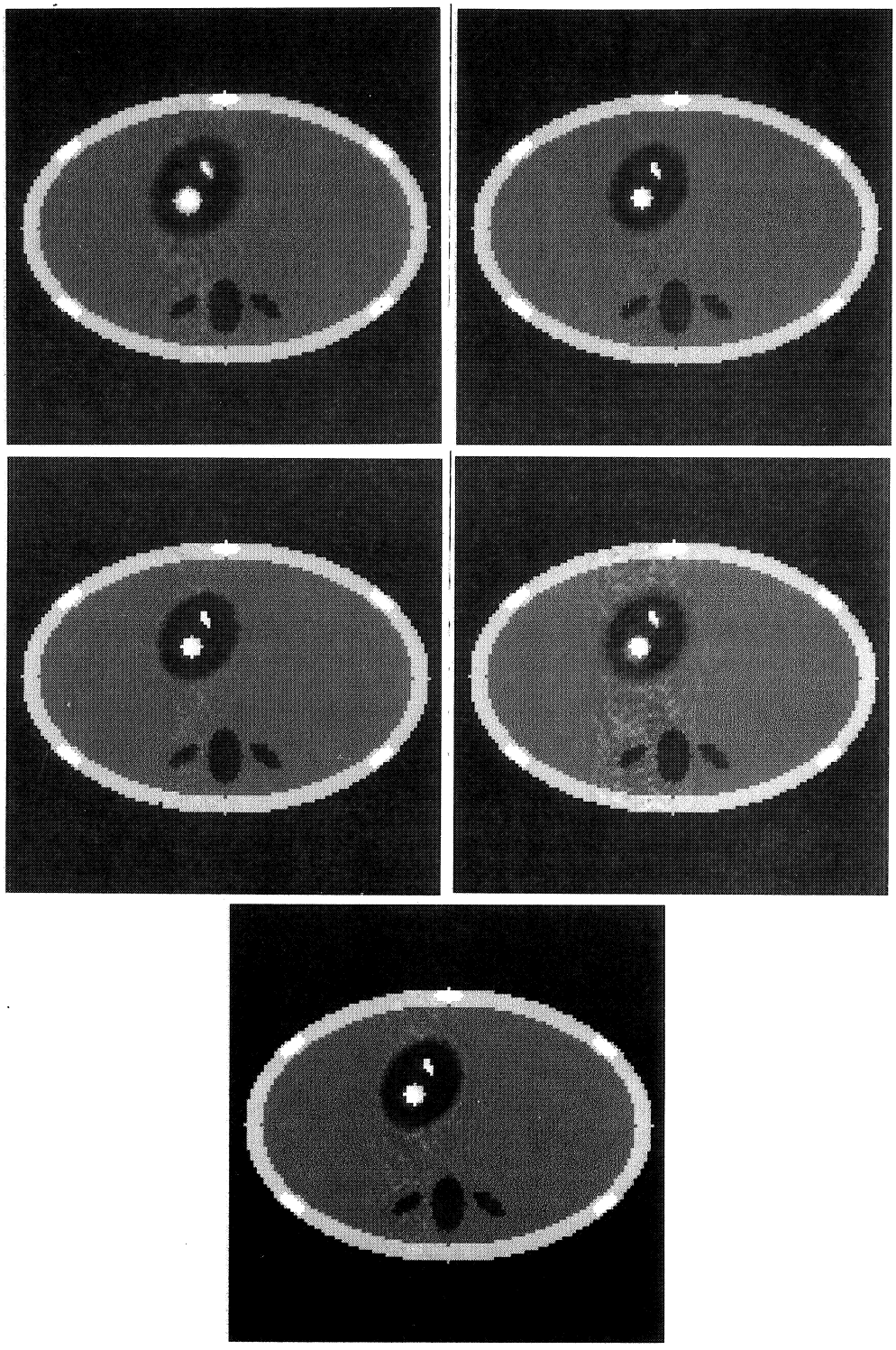

Figure VI.17 . Reconstructions at phase ϕ_6 for $N_{pr} = 15$.
Top left: degree 0, Top right: degree 1, Middle left: degree 3, Middle right: sinc Bottom: tp-sinc.

In the reconstructions of Figures VI.9 up to VI.16 we see a vertical band of noise in the images localized at the position of the moving ellipses. This *noise band*, which also occurs in MR-images, is caused by the motion of the ellipses. Recall that the data collection strategy consists in measuring profiles which are horizontal lines in the Fourier domain (see Figure VI.1). The time period needed to measure such a profile can be neglected in practice. This implies that one horizontal line within the original image at that time point can be found by Fourier inversion of the profile. So, in the horizontal direction, the perturbation of the reconstruction due to the motion is negligible. But for the vertical direction this argument is not valid. After collecting all the data, the time markers of the profiles are rescaled by a time-to-phase conversion. Then, because the rescaled times do not coincide with the phases at which we want to make the reconstructions, we apply interpolation techniques. That is, for each k_y we estimate a profile at the desired phase by interpolation and rescaling. So, at every phase the motion causes errors in the reconstructed image in the vertical direction.

We first make an intuitive comparison of the quality of the reconstructions. Later, we present the L^2-differences of the reconstruction and the original chest phantom at the corresponding phases.

The main criterion for the reconstruction quality is the vertical noise band. Other criteria stem from diagnostic practice and are discussed in Section 4. Here we only point out that it is important from a diagnostic point of view to reconstruct sharp contours of the time varying ellipses. We first compare the several reconstructions in the case of $N_{pr} = 5$. Degree 0 reconstruction performs worst. The ringing artefact in this image is caused by setting Fourier coefficients at phase ϕ_m to the value zero, if there are no data lying in the interval $[\phi_m, \phi_{m+1})$. If N_{pr} is taken larger than 5, say $N_{pr} = 15$, then it is less likely that this effect occurs. Intuitively, degree 1 and degree 3 perform best. The structures of the moving ellipses are reconstructed sufficiently sharp. The reconstructions by sinc and tp-sinc interpolation perform better than degree 0, but worse than degree 1 and degree 3. For all methods the reconstructions get worse for phases where the motion of the ellipses in the phantom is fast. Degree 0 reconstruction turns out to be a quite useless method in the case of small data sets.

First and third degree reconstructions appear to perform equally well for $N_{pr} = 15$ and their performance is better than degree 0, sinc and tp-sinc reconstruction. The first phase in the sinc reconstruction is of low quality, which may be due to the intrinsic non-periodicity of the interpolating function. If we use Tychonov-Phillips regularization, the quality of this first phase improves. The reconstructions are much better in the case of $N_{pr} = 15$ than for $N_{pr} = 5$.

To provide an objective quality measure, we also compared the differences of the original and the reconstructions (for $N_{pr} = 5$ and $N_{pr} = 15$ respectively) in L^2-norm, i.e. we computed

$$error := \sum_{x=0}^{2N_x-1} \sum_{y=0}^{2N_y-1} |g(x,y,\phi_l) - f(x,y,\phi_l)|^2, \tag{3.4}$$

where g and f denote the original and the reconstructed image, respectively. Note that it is hard to interpret the L^2-norm differences in terms of our intuitive criteria for quality of the images.

	phase0	phase2	phase4	phase6
degree0	43.37	44.62	74.86	71.83
degree1	9.20	7.84	8.37	5.65
degree3	9.89	8.36	9.25	5.83
sinc	42.9	10.97	10.44	8.10
tp-sinc	39.77	9.92	10.15	7.64

Table VI.2 The reconstruction error at four phases for various interpolation algorithms, with $N_{pr} = 5$. Phase i corresponds to time i/M, with $M = 8$.

	phase0	phase2	phase4	phase6
degree0	9.67	11.50	7.13	8.35
degree1	5.33	4.57	4.69	2.78
degree3	5.65	5.05	4.80	3.02
sinc	41.96	9.72	6.84	7.26
tp-sinc	36.84	6.45	5.04	3.85

Table VI.3 The reconstruction error at four phases for various interpolation algorithms, with $N_{pr} = 15$. Phase i corresponds to time i/M, with $M = 8$.

First, these tables illustrate that the performance of the reconstruction methods is improved when the value of N_{pr} is increased from 5 to 15. If N_{pr} is increased from 15 to 25 the gain is much smaller.

These results confirm our intuitive conclusions. We see that in the case of small data sets ($N_{pr} = 5$) degree 0 is not suitable, while degree 1, degree 3 and sinc reconstruction perform relatively well.

If the data set is larger ($N_{pr} = 15$), the quality of the reconstuction algorithms improve. For still larger values of N_{pr} the quality of the reconstructions does not increase much more.

VI.4. Reconstruction of MR-Images

In this section we reconstruct images from data which were obtained by the Philips Gyroscan S-15 (an MR-scanner of Philips Medical Systems). We call this data *MR-data* to distinguish it from test-data. Just as in the case of test-data, the sequences $\{R_k\}$ of R-pulses, $\{\tau_{\mathbf{k},i}\}$ of time markers, and $\{g_{\mathbf{k},i}\}$ of MR-data form the input for the reconstruction algorithms. The rescaled time markers $\{t_{\mathbf{k},i}\}$ are obtained from $\{\tau_{\mathbf{k},i}\}$ by means of linear stretching, see formula (1.16). For further details about the reconstruction techniques we refer to the previous section.

The reconstructions from MR-data are displayed on a computer screen. The parameters N_x, N_y, M and γ are the same as in the case of test-data. The parameter N_{pr} has a different value, namely $N_{pr} = 50$. Here we discuss the criteria that are important for diagnostic purposes and draw conclusions about the performance of the reconstructions.

The interesting feature from a medical point of view is the contraction of the heart muscle. Sometimes, as a result of a myocardial infarct (a so-called heart attack), part of the muscle does not contract. In the case of a mild infarct a darker region can be spotted on the muscle-tissue in the MR image. Another disease that can be traced by MR imaging is the ventricular septal defect which is a small hole in the tissue that separates the right and left ventricle (these are the 'big heart chambers'). A darker region, now and then appearing in the image sequence in the vincinity of the heart tissue indicates this deficiency. Thus, from a diagnostic point of view the quality of the reconstruction depends largely upon

how well the heart muscle is depicted, in particular on the sharpness of its contours. For this purpose, the vertical noise band is undesirable.

In Figure VI.18 we indicate the cross section of the chest, the heart muscle, and the ventricles.

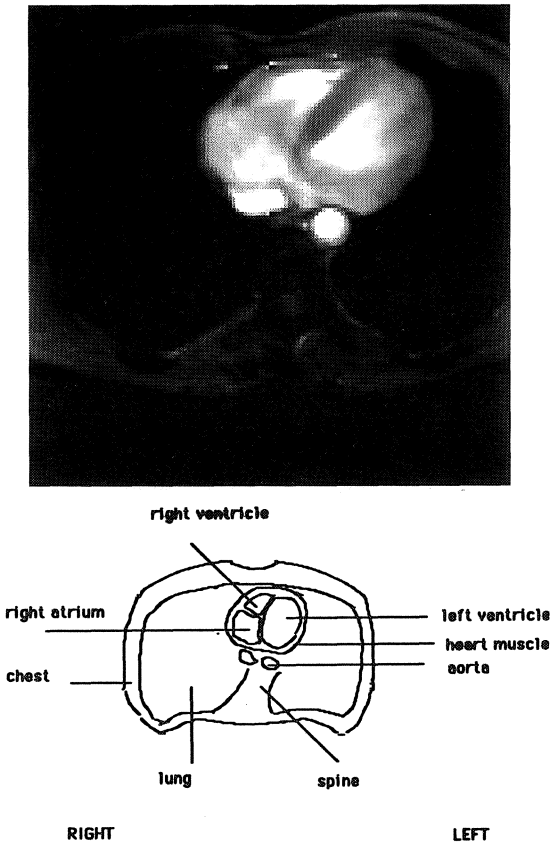

Figure VI.18 . a) Reconstruction of a cross section of the chest; b) Some anatomic details in the cross section.

The images presented here are cross sections of the human chest. The big oval (which appears rather dark in the image), is the bone-structure of the chest. The heart is located at the front side of the chest (in the picture it is located at the top on the right). The grey part of the heart-image is the muscle tissue. The light-coloured parts of the heart-image are the heart-chambers (left and right ventricles and the left and right atria).
In Figures VI.19, VI.20, VI.21 and VI.22, we present reconstructions by means of the linear stretching time-to-phase conversion.

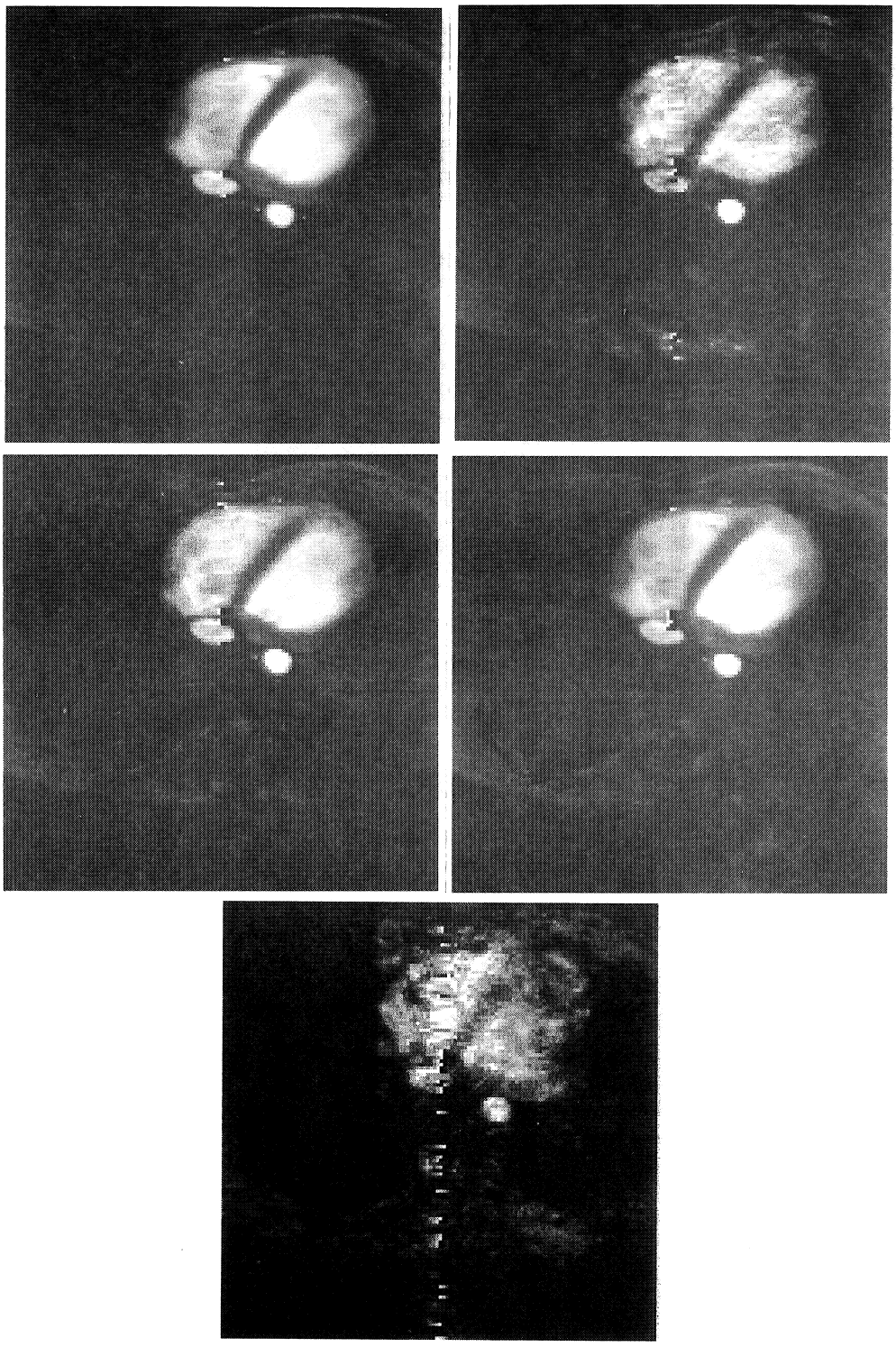

Figure VI.19 . Reconstructions of MR images with linear stretching at phase ϕ_0. Top left: degree 0 Top right: degree 1, Middle left: degree 3, Middle right: sinc Bottom: tp-sinc.

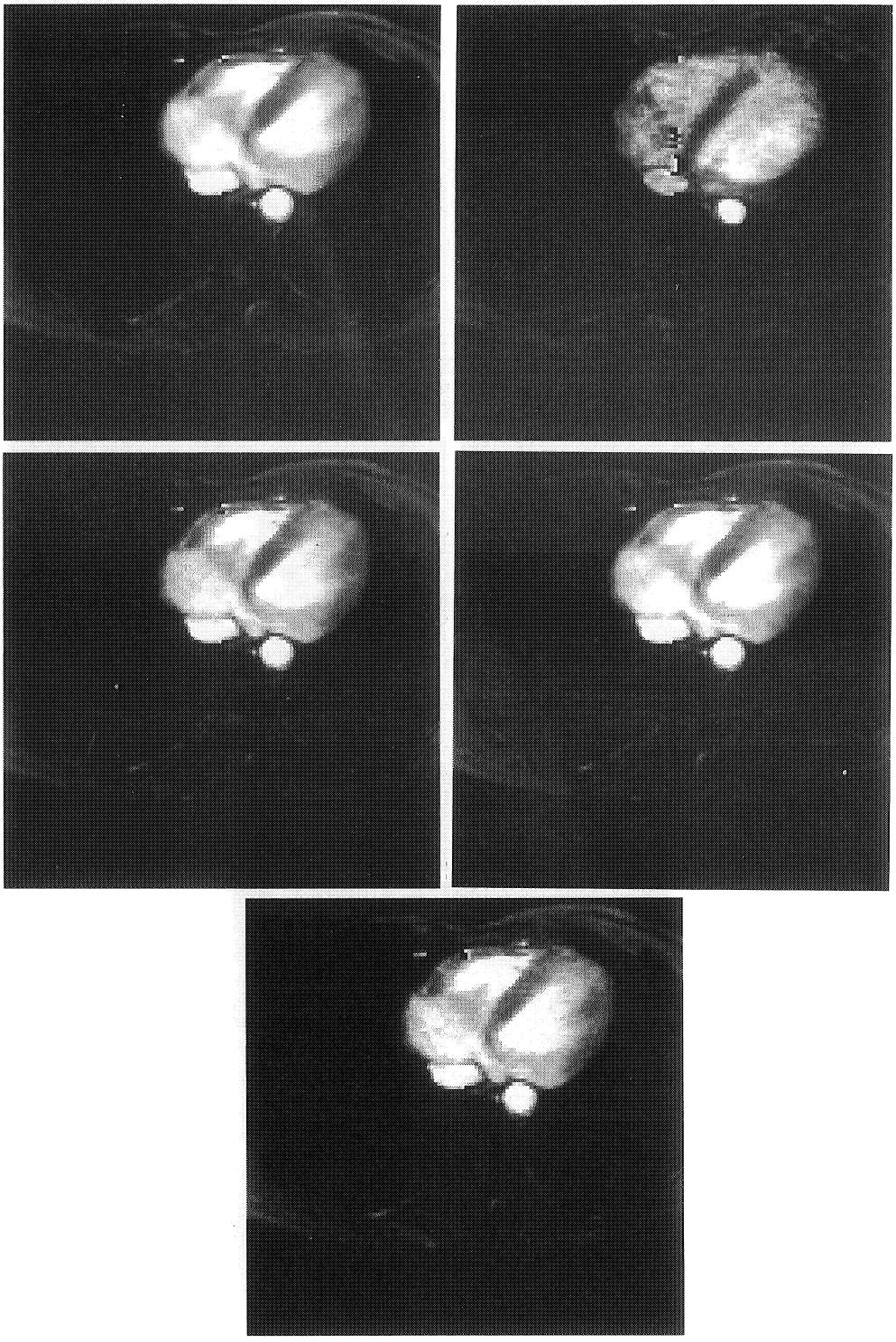

Figure VI.20 . *Reconstructions of MR images with linear stretching at phase ϕ_2. Top left: degree 0, Top right: degree 1, Middle left: degree 3, Middle right: sinc, Bottom: tp-sinc.*

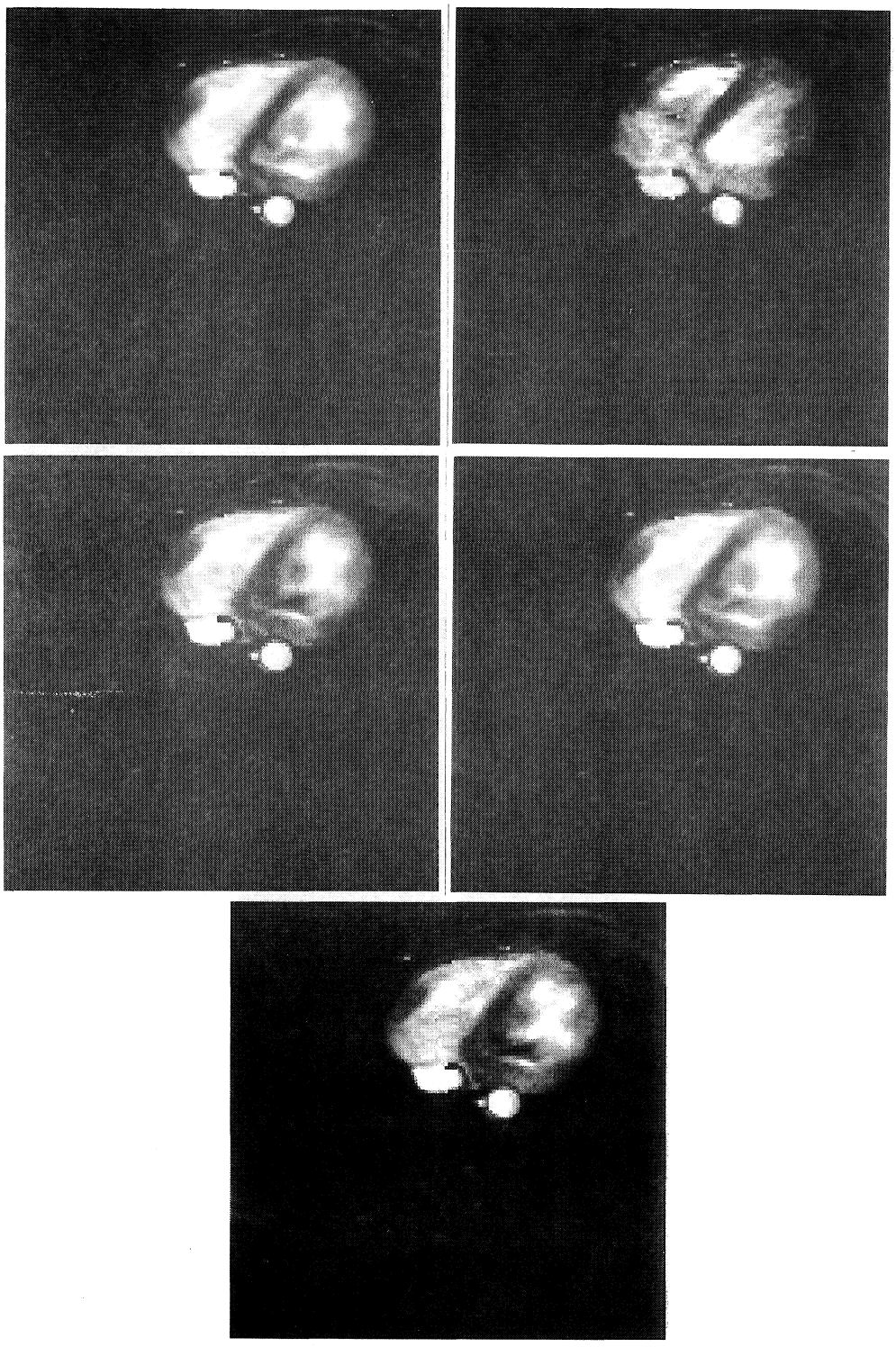

Figure VI.21 . Reconstructions of MR images with linear stretching at phase ϕ_4. Top left: degree 0, Top right: degree 1, Middle left: degree 3, Middle right: sinc, Bottom: tp-sinc.

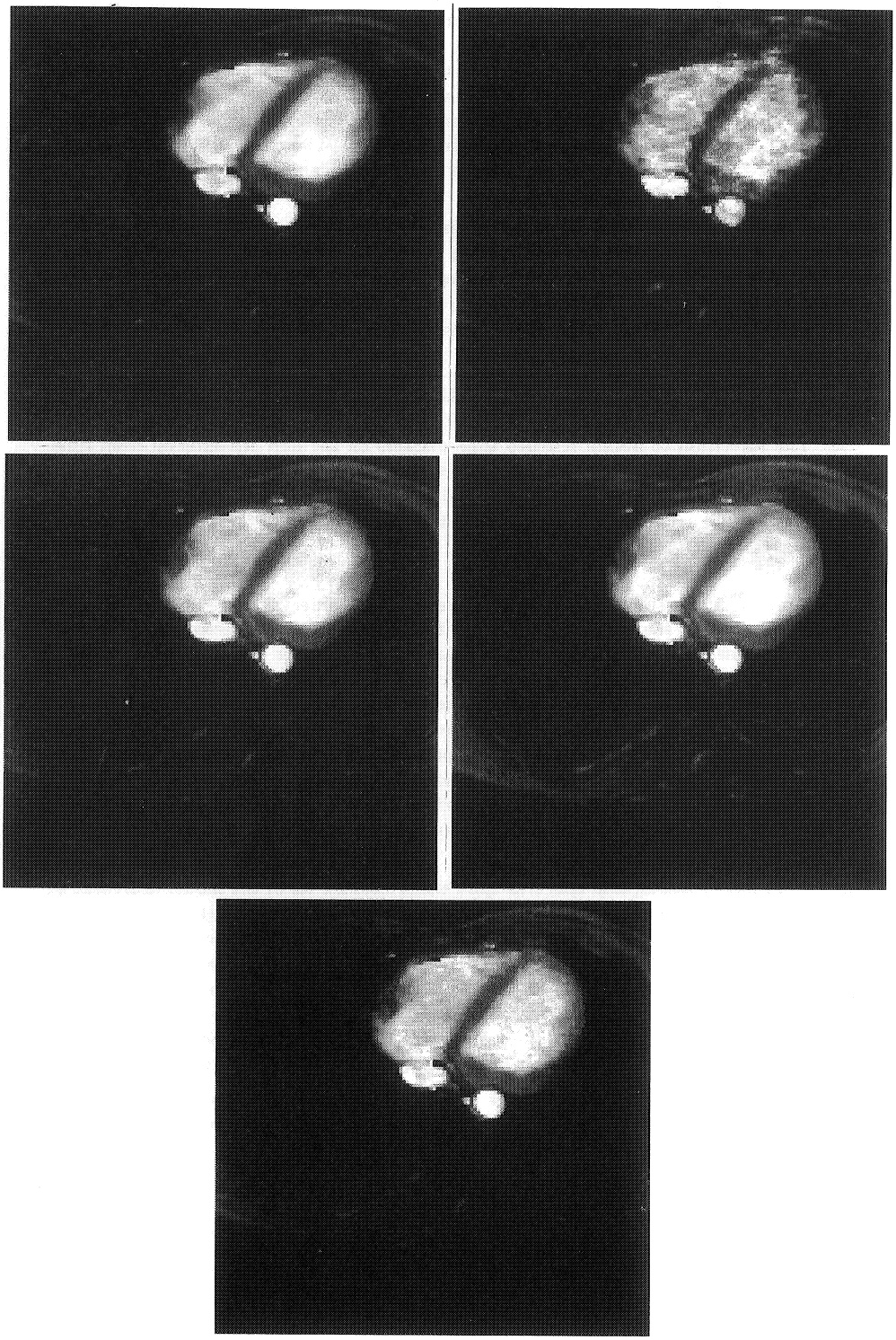

Figure VI.22 . *Reconstructions of MR images with linear stretching at phase ϕ_6. Top left: degree 0, Top right: degree 1, Middle left: degree 3, Middle right: sinc, Bottom: tp-sinc.*

Comparing these reconstructions with the criteria stated above, we conclude that the degree 1 reconstruction performs worst of all, since the noise band is rather intense. The difference between the other reconstruction methods is rather small, but we point out some distinctions. Degree 0 and sinc reconstruction provide images where the contours of the heart muscle are rather smooth. In the images of degree 3 and tp-sinc reconstruction the contours of the heart muscle are somewhat sharper. The conclusion is that degree 1 reconstruction perfoms worst of all and the other methods perform equally well in the case of MRI of the beating human heart.

We also obtained rescaled time markers times $\{t_{\mathbf{k},i}\}$ by means of piecewise linear stretching, see formula 1.17. We found the reconstructed images at all phases visually indistinguishable from their counterparts obtained by means of linear stretching. So, we think that in practice linear and piecewise linear stretching perform the same. But, since the choice of time-to-phase conversion is an important factor in the reconstructions, it seems worth to go on looking for realistic rescaling formulas.

Finally, we want to discuss the validity of the model assumptions (see Section VI.1.3), which we recall for convenience:

- The algorithm to obtain rescaled time markers on the unit RR-interval from time markers on an RR-interval is linear stretching.
- There exists a model heartbeat such that its Fourier coefficients at the rescaled time markers are equal to the measurements from the spin density of the beating human heart.

Concerning the first assumption, any rule to rescale an RR-interval to the unit RR-interval is a simplification of the real situation, since the behaviour of the beating heart can be different to some degree in RR-intervals of equal length. In other words, given a rescaling algorithm, the model heartbeat g which is stretched to an RR-interval will be at best an approximation of the spin density F, where the rescaling rule plays a role in the accuracy of the approximation. (Note that this accuracy is not only determined by the rescaling rule, but also by e.g. the number of sampling points N_x, N_y and N_{pr}, the noise level in the signal, etc.) Now, assume the existence of a model heartbeat g with an accurate rescaling algorithm. If linear stretching is used in our model for reconstructing g, then the positions of the rescaled time markers will in this sense most likely be incorrect, causing a *time-jitter error* in the reconstructed images.

The second model assumption concerns the Fourier coefficients of the model heartbeat g. It is assumed that Fourier coefficients of g over a two dimensional set D (the cross section) are equal to the data at the rescaled time markers. In practice, however, the heart not only contracts, but it also rotates, meaning that the part of the cross section of the heart which is measured at a given time, does not remain in one plane. Moreover the respiratory motion of the patient will also cause displacement of the heart outside the plane, sometimes causing a 'breathing artefact'. So, the assumption that Fourier coefficients of the model heartbeat over a two dimensional set are equal to the measurements is violated.

The violation of the model assumptions will be considered in more detail in the next chapter which deals with error estimates. The next chapter also gives possible future directions for improving the reconstruction quality.

VI.5. Conclusions and additional remarks

The performance of the reconstruction methods in the case of test-data and MR-data has been compared for fixed parameters N_x, N_y and N_{pr}.

The conclusions are that in the case of the chest phantom, for $N_{pr} = 5$ and $N_{pr} = 15$, that first and third degree reconstruction perform equally well and that they perform better than zeroth degree and sinc reconstruction. The first two phases in the sinc-reconstruction are of low quality. This may be due to the intrinsic nonperiodicity of the interpolating sinc-function. If we use the regularized version of the sinc-reconstruction, denoted as tp-sinc, the quality of the image at phase ϕ_0 improves considerably. The conclusion is that degree 1 and degree 3 reconstruction are the best reconstruction techniques in the case of test-data.

The reconstructed images obtained from MRI-data by using linear stretching and by using piecewise linear stretching are of the same quality in practice.
In this case of MRI-data, the reconstruction algorithms based on linear stretching perform equally well, except for degree 1. In this case the performance of degree 1 reconstruction is unsatisfactory. On the other hand, degree 1 and degree 3 reconstruction behave better that the other algorithms for test-data. That the performance of degree 1 and degree 3 reconstruction is not as expected in the case of MRI-data, is probably due to the violation of the model assumptions in practice (cf. Section 4).

Chapter VII

Stability Analysis of MRI Reconstruction

In this Chapter we analyze the stability of the reconstruction methods under perturbation of the data or time markers. Stability means that small errors in the data or time markers yield small errors in the reconstruction. The aim of our analysis is to determine for which type of perturbation a reconstruction algorithm is sensitive. We will discuss and illustrate three types of errors: aliasing error, amplitude error and time jitter error, by applying the different reconstruction algorithms to the test data corresponding to the chest phantom.

The first section defines three different kinds of errors and describes how stability of the reconstructions is tested. In the second section we explain the occurrence of these errors in practice and give bounds for the errors in the case of sinc and spline reconstruction. The effects of perturbations of the test-data and the rescaled time markers is illustrated in Section 3. In Section 4 we formulate our conclusions and make some additional remarks. Section 5 finally, presents some suggestions for future directions to improve the quality of the reconstructed images.

VII.1. Introduction

In this section the aliasing error, amplitude error and the time jitter error are defined formally. The effect of these errors are illustrated in the next section using test-data and a chest phantom. There we also comment on the occurrence of these errors in practice.

We refer to the notational conventions introduced in Chapter VI. Let $g : D \times J \to \mathbb{C}$ be a function depending on the spatial parameter $\mathbf{r}$ and the time parameter t. We can extend g to the larger domain $D \times \mathbb{R}$ by putting g equal to zero outside $D \times J$. We assume that $g \in L^2(D \times \mathbb{R})$ (g is square integrable with respect to the variables $\mathbf{r}$ and t) and such that for each $\mathbf{r} \in D$, the function $t \to g(\mathbf{r}, t)$ is a bounded function on $\mathbb{R}$. Denoting the rescaled time markers by $\{t_{\mathbf{k},i}\}$ the data are obtained by

$$g_{\mathbf{k},i} := \widehat{g}(\mathbf{k}, t_{\mathbf{k},i}), \quad \mathbf{k} \in \mathbb{K}, i \in \mathbb{I}.$$

Here the Fourier transform is taken with respect to the spatial parameter $\mathbf{r}$.
The inversion problem of MRI consists in finding a function $f \in L^2_{\mathcal{H}}(D \times \mathbb{R})$ such that:

$$\widehat{f}(\mathbf{k}, t_{\mathbf{k},i}) = g_{\mathbf{k},i}, \quad \mathbf{k} \in \mathbb{K}, i \in \mathbb{I}. \tag{1.1}$$

Because the function g is in general not uniquely determined by the data and rescaled time markers, a solution f of problem (1.1) is in general not equal to the original function g from which the data have been derived.
The difference in norm between f and g is called *aliasing error.*

A second error measure is the *amplitude error.* (For a discussion on the occurrence of the amplitude error in practice, we refer to Section 2 of the Introduction and to Section VI.4.) Suppose the data $\{g_{\mathbf{k},i}\}$ are perturbed by a sequence of random numbers $\{\eta_{\mathbf{k},i}\}$:

$$g'_{\mathbf{k},i} := g_{\mathbf{k},i} + \eta_{\mathbf{k},i}, \quad \mathbf{k} \in \mathbb{K}, i \in \mathbb{I}. \tag{1.2}$$

The sequence $\{g'_{\mathbf{k},i}\}$ is called the *perturbed data.* The solution of the mixed Fourier interpolation problem from the perturbed data is denoted by f' and satisfies

$$\widehat{f}'(\mathbf{k}, t_{\mathbf{k},i}) = g'_{\mathbf{k},i}, \quad \mathbf{k} \in \mathbb{K}, i \in \mathbb{I}.$$

The difference in norm between f and f' is called *amplitude error* :

$$\mathrm{E_{amp}} := \left(\int_D \int_R |f(\mathbf{r}, t) - f'(\mathbf{r}, t)|^2 dt d\mathbf{r} \right)^{1/2}.$$

The third error measure is called the *time jitter error.* (For an explanation of the occurrence of the time jitter error in practice, we refer to Section VI.4, where the validity of the first model assumption is discussed.) Suppose the time markers $\{t_{\mathbf{k},i}\}$ are perturbed by a sequence of random numbers which we denote by $\{\theta_{\mathbf{k},i}\}$:

$$t'_{\mathbf{k},i} := t_{\mathbf{k},i} + \theta_{\mathbf{k},i}, \quad \mathbf{k} \in \mathbb{K}, i \in \mathbb{I}. \tag{1.3}$$

The solution that corresponds to the perturbed problem

$$\widehat{f}'(\mathbf{k}, t'_{\mathbf{k},i}) = g_{\mathbf{k},i} \quad \forall i \in \mathbb{I} \tag{1.4}$$

is again denoted by f'. The time jitter error $\mathrm{E_{tj}}$ is the difference in norm between f and f':

$$\mathrm{E_{tj}} := \left(\int_D \int_R |f(\mathbf{r}, t) - f'(\mathbf{r}, t)|^2 dt d\mathbf{r} \right)^{1/2}.$$

A problem is called stable, if small perturbations yield small errors in the reconstruction. In the next section we derive the following bound for the amplitude error

$$E_{\text{amp}} \leq C\|g - g'\|_{\ell^2(K\times I)}.$$

Here

$$\|g\|^2_{\ell^2(K\times I)} := \sum_{\mathbf{k}\in K, i\in I} |g_{\mathbf{k},i}|^2.$$

This proves the stability of problem (1.1) under perturbation of the data. The value of C is of numerical interest. Intuitively, if C is small, say close to one, then the error in the reconstruction is of the same magnitude as the error in the data. In that case the problem is called *well-conditioned* under perturbation of the data. However, if C is large, the error in the reconstructions may be much larger than the error in the data. Then the problem is called *ill-conditioned*. Well- or ill-conditionedness in the case of perturbation of the time markers is defined analogously.
In section two we study the stability of the mixed Fourier interpolation problem in the case of reconstruction by sinc and spline functions and we present conclusions which can be drawn from the error analysis.

VII.2. Error Estimates

In this section we derive bounds for the aliasing error, amplitude error and time jitter error.

First, we consider the aliasing error. The classical analogy of this error is very illustrative. In the Western movies of the early days, stage-coaches were always hurrying forward on wheels rotating in a direction opposite to the direction corresponding to the motion. The explanation of this phenomenon is that the time resolution of the camera was too low for imaging the motion of the wheels realistically. A mathematical formulation of this aliasing error can be given in terms of bandlimited functions. Suppose a function g is an element of the space $L^2(\mathbb{R})$. Assume that this function is sampled at rate π/r. It is known from sampling theory (see e.g. Jerri [27]) that one can find a reconstruction of this function from its samples in the space $\mathbb{P}_r$. So, the frequencies higher than r are lost in the reconstruction process. (In the case of the Western movies, the high frequency components in the motion of the wheels could not be imaged by the camera, due to undersampling.) In other words, the aliasing error is due to the fact that the original function is an element of $L^2(\mathbb{R})$ whereas the reconstruction is within the smaller space $\mathbb{P}_r$. The last formulation is the motivation for our definition of aliasing error: in dynamic MRI we obtain data in terms of the model heartbeat g, which lies in $L^2(D \times \mathbb{R})$; on the other hand the reconstruction f must belong to $L^2_{\mathcal{H}}(D \times \mathbb{R})$. In general f will not be the same as g and the aliasing error is the difference between f and g. In view of the above discussion it can be expected that the aliasing error in the case of $L^2_r(D \times \mathbb{R})$ depends on the frequency band r. The following bounds for the aliasing error are proved in Theorems V.2.1 and V.2.3 of Part One for bandlimited and spline functions respectively. The estimates are not given in the general case that $g \in L^2(D \times \mathbb{R})$, but only for g lying in a subspace of $L^2(D \times \mathbb{R})$. For the details, we refer to Part One. The notation $\widehat{g}(\mathbf{r}, \xi)$ denotes the Fourier transform of g taken with respect to the temporal parameter.

The aliasing error
For sinc-interpolation:

$$E_{al} := \Big(\int_D \sup_{t\in R}|f(\mathbf{r},t)-g(\mathbf{r},t)|^2 d\mathbf{r}\Big)^{1/2} \leq$$

$$\sqrt{\frac{2}{\pi}}\Big(\int_D\Big(\int_{R\setminus[-r,r]}|\widehat{g}(\mathbf{r},\xi)|d\xi\Big)^2 d\mathbf{r}\Big)^{1/2}. \tag{2.1}$$

For spline interpolation:

$$E_{al} := \Big(\int_D\int_a^b |f(\mathbf{r},t)-g(\mathbf{r},t)|^2 dt d\mathbf{r}\Big)^{1/2} \leq$$

$$(\sup_{\mathbf{k}\in K}\|\Delta_{\mathbf{k}}\|)\Big(\sum_{\mathbf{k}\in K}\int_{[a,b]}\Big|\frac{\partial}{\partial t}\widehat{g}(\mathbf{k},t)-\frac{\partial}{\partial t}\widehat{f}(\mathbf{k},t)\Big|^2 dt\Big)^{1/2}. \tag{2.2}$$

Here $\|\Delta_{\mathbf{k}}\|$ *is*

$$\|\Delta_{\mathbf{k}}\|^2 := \sum_{i=0}^{N_{pr}-1}(1/2)(t_{\mathbf{k},i+1}-t_{\mathbf{k},i})^2, \quad \mathbf{k}\in I\!K.$$

The aliasing error for sinc-interpolation, formula (2.1), depends on the frequencies outside the band $[-r,r]$; if for each $\mathbf{r}\in D$, the function $t\to g(\mathbf{r},t)$, is r-bandlimited, then the aliasing error is zero.

The aliasing error for spline-interpolation, formula (2.2), depends on the temporal derivative. So, if the motion of the chest phantom contains high frequencies, we should take care that the interpolating spline can oscillate quickly. This can be done by choosing the number N_{pr} large.

The amplitude error occurs in the case of data $\{g_{\mathbf{k},i}\}$ perturbed by external noise. In the practice of MRI-reconstruction the measurements contain thermal noise, mainly caused by the human body lying within the MR-scanner. From Section VI.1 we know that the amplitude of the Fourier coefficients of any L^2-function decreases if the frequency increases. If a noise term which is independent from the frequency, is added to these coefficients, the relative error in the coefficients increases with the frequency. Since the thermal noise in the practice of MRI may be assumed to be of constant amplitude (see Section 2 of the introduction), it follows by reasoning analogously that the relative error in the coefficients $g_{\mathbf{k},i}$ of the model heartbeat increases if $|\mathbf{k}|$ increases. There are many other error sources in practice, which we will not discuss here. For example, eddy currents in the magnet coils and errors caused by the bloodflow through the heart chambers.

The following error bound is proved in Theorem VI.5.2 of Part One.

The amplitude error

For sinc- and spline reconstruction:

$$E_{amp} \leq \sup_{\mathbf{k}\in K}\|G^{-1}(\mathbf{k})\|^{1/2}\ \|g-g'\|_{\ell^2(K\times I)}. \tag{2.3}$$

Here the Gram matrix $G(\mathbf{k})$, for fixed $\mathbf{k}\in I\!K$, is given by

$$(G(\mathbf{k}))_{ij} = (r/\pi)\ \operatorname{sinc}_r(t_{\mathbf{k},i}-t_{\mathbf{k},j}), \quad i,j\in I\!I,$$

in the case of sinc functions and by

$$(G(\mathbf{k}))_{ij} := \sigma(t_{\mathbf{k},j}, t_{\mathbf{k},i})$$

in the case of spline functions, where σ is given by formula (VI.2.4). In particular this formula shows how the amplitude error depends on the norm of $G(\mathbf{k})^{-1}$. This means that the problem is ill-conditioned if this norm is large and well-conditioned if this norm is close to one. In the case of sinc functions we can say more. If the time markers $\{t_{\mathbf{k},i}\}_{i\in I}$ are spaced equidistantly for all $\mathbf{k} \in I\!K$, then $\|G(\mathbf{k})^{-1}\| = 1$ and the problem is well-conditioned for perturbation of the data. If for a certain $\mathbf{k} \in I\!K$ the distribution of the time markers is irregular, then $\|G(\mathbf{k})^{-1}\|$ may get large and the problem becomes ill-conditioned.

Our third estimate concerns the time jitter error which occurs in the case of perturbation of the rescaled time markers $\{t_{\mathbf{k},i}\}$, which were computed by the linear stretching time-to-phase conversion formula (VI.1.16). In the case of reconstruction from test-data, this time-to-phase conversion yields the correct positions for the rescaling of the time markers. However, in the case of MRI-data, this conversion formula is at best an approximation of the real situation, and yields incorrect positions of the rescaled time markers. (See Section VI.4 for a detailed discussion.) This causes a *time jitter error* in the reconstructed images.

In the following example the sequence $\{t_{\mathbf{k},i}\}$ plays the role of exact time markers and the $\{t'_{\mathbf{k},i}\}$ are the perturbed time markers.

Denote the sequence $\{t_{\mathbf{k},i}\}_{i\in I}$ by $t_{\mathbf{k}}$, for $\mathbf{k} \in I\!K$. The notation $t'_{\mathbf{k}}$ is used analogously for the perturbed time markers. The Gram matrices corresponding to the perturbed time markers are defined by

$$(G'(\mathbf{k}))_{ij} = (r/\pi)\ \operatorname{sinc}_r(t'_{\mathbf{k},i} - t'_{\mathbf{k},j}), \quad i,j \in I\!I,$$

in the case of bandlimited functions and by

$$(G'(\mathbf{k}))_{ij} := \sigma(t'_{\mathbf{k},j}, t'_{\mathbf{k},i}), \quad i,j \in I\!I,$$

in the case of spline functions. The bound for the time jitter error is proved in Theorem V.2.7 of Part One. There we derived the estimate for the time jitter from the bound for the amplitude error.

The time-jitter error

For sinc-reconstruction,

$$\mathrm{E_{tj}} \le \sup_{\mathbf{k}\in K}(\|G'(\mathbf{k})^{-1}\|\ \|G(\mathbf{k})^{-1}\|\ \|G(\mathbf{k})\|)^{1/2}\ (e^{\pi\gamma} - 1)\ \|g\|_{\ell^2(K\times I)}. \tag{2.4}$$

Here

$$\gamma := \sup_{\mathbf{k}\in K, i\in I} |t_{\mathbf{k},i} - t'_{\mathbf{k},i}|.$$

For spline reconstruction,

$$\mathrm{E_{tj}} \le \sup_{\mathbf{k}\in K}\Big(2\|G(\mathbf{k})^{-1}\|^{1/2} + C\|G'(\mathbf{k})^{-1}\|^{1/2}\ \|t_{\mathbf{k}} - t'_{\mathbf{k}}\|_{\ell^2(I)}\Big)$$

$$\Big(\sum_{\mathbf{k}\in K} \sup_{t\in R}\Big|\frac{\partial}{\partial t}\widehat{f}(\mathbf{k},t)\Big|^2 + \|g_{\mathbf{k}}\|^2_{\ell^2(I)}\Big)^{1/2}. \tag{2.5}$$

Here the constant C depends on r only.

The time jitter error for sinc-interpolation, formula (2.4), depends on the norms of $(G'(\mathbf{k}))^{-1}$ $G(\mathbf{k})$, and $G(\mathbf{k})^{-1}$. If for all $\mathbf{k} \in I\!K$ the elements of the sequences $\{t_{\mathbf{k},i}\}_{i\in I}$ or $\{t'_{\mathbf{k},i}\}_{i\in I}$ lie close to the uniform grid then the norms of $G(\mathbf{k})^{-1}, G'(\mathbf{k})^{-1}$ and $G(\mathbf{k})$ are close to one and the problem is well-conditioned under perturbation of the time markers. Otherwise, if for one or more $\mathbf{k} \in I\!K$ the distribution of the time markers is very irregular, then the norm of one of the Gram matrices may get large and the problem becomes ill-conditioned. The time-jitter error for spline-interpolation, given by formula (2.5) depends on $(G'(\mathbf{k}))^{-1}$, $\|t_{\mathbf{k}} - t'_{\mathbf{k}}\|$ and on the time derivative of the function f, corresponding to the unperturbed problem. So, the problem becomes well-conditioned under perturbation of the time points if (for all $\mathbf{k} \in I\!K$) $\|G(\mathbf{k})^{-1}\|$ and the time derivative in supremum norm is small. If the degree of the spline is chosen smaller, then the norm of this time derivative gets smaller. The conclusion is that in the case of sinc interpolation the reconstruction algorithm is well-conditioned, if (for each $\mathbf{k} \in I\!K$) the time points $\{t_{\mathbf{k},i}\}_{i\in I}$ are sampled uniformly. The reconstruction by spline interpolation is well-conditioned if the degree of the interpolating spline is not too high.

If the problem is ill-conditioned, it may be useful to approximate the solution by means of a regularization technique e.g. the Tychonov-Phillips regularization (see Section VI.2).

VII.3. Perturbations of Reconstructions of the chest phantom

In this section we apply the reconstruction algorithms in the case of perturbations of test-data $\{g'_{\mathbf{k},i}\}$ and of rescaled time markers $\{t'_{\mathbf{k},i}\}$. Afterwards we shall briefly discuss the results obtained here. The parameters of the reconstruction algorithms are the same as those used in Section VI.3.3.

The aliasing error will not be explicitly visualized in this chapter by means of a sequence of reconstructed images. The reason for this is that the aliasing error is already visible in the reconstructions of the chest phantom in the previous chapter (cf. Section VI.3). The aliasing error in the case of test-data is the difference between the reconstructions and the chest phantom. It is predominantly illustrated by Figure VI.10: degree 0 reconstruction in the case of $N_{pr} = 5$. The performance of degree 0 reconstruction has improved when $N_{pr} = 15$, which also holds for the other reconstruction methods. This illustrates formula (2.3) which shows how the aliasing error for splines depends on N_{pr}. Also, when $N_{pr} = 15$ the aliasing error occurs in the reconstructions. Comparing the reconstructions of Figures VI.10, VI.11, VI.12 and VI.13 between the chest phantom Figure VI.9 we see that a feature of the the aliasing error is the occurrence of the vertical noise band over the image (Section VI.3.3) and the smearing out of the moving ellipses. In the reconstructions from the MRI-data, Figures VI.19, VI.20, VI.21 and VI.22, we see this phenomenon too: the noise band and vague boundaries in the image of the heart muscle. The position of the noise band is fixed by the position of the moving ellipses in the phantom or by the heart in MR-images, as explained in Section VI.3.

To illustrate the amplitude error, we apply the algorithms to perturbed test-data $\{g'_{\mathbf{k},i}\}$ which are obtained by formula (1.2). The complex numbers $\{\eta_{\mathbf{k},i}\}$ are chosen randomly such that Re $\eta_{\mathbf{k},i}$ and Im $\eta_{\mathbf{k},i}$ lie in the interval $[-4000, 4000]$. To get an impression of the relative magnitude of the error we give the value of the test-data $\{g_{\mathbf{k},i}\}$ for certain $i \in I\!I$,

$$g_{0,1,i} = 16624, \quad g_{64,1,i} = -3089, \quad g_{127,1,i} = 494.$$

The amplitude of the data $\{g_{\mathbf{k},i}\}$ decreases, if $|\mathbf{k}|$ increases. The maximum of the noise magnitude $\{\eta_{\mathbf{k},i}\}$ is 4000, independent of the frequency vector $\mathbf{k}$. This means that the signal to noise ratio is decreasing when $|\mathbf{k}|$ is increasing. In the following Figures we show

degree 0, degree 1, degree 3, sinc and tp-sinc reconstruction applied to perturbed test-data. In this case the maximum number of phases is $\Phi = 8$ and $N_{pr} = 15$.

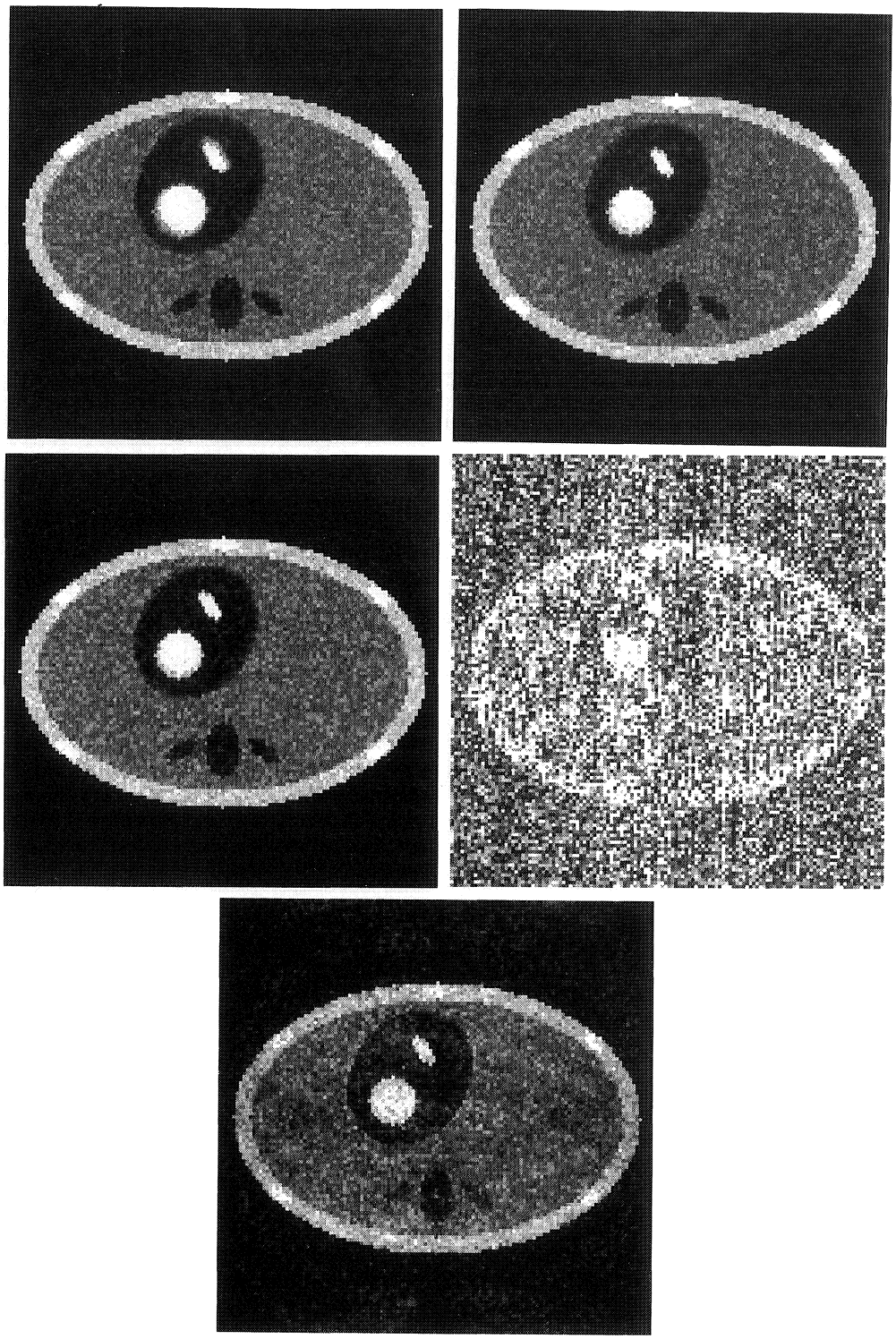

Figure VII.1 . *Reconstructions from perturbed data at phase ϕ_0.*
Top left: degree 0, Top right: degree 1, Middle left: degree 3, Middle right: sinc, Bottom: tp-sinc.

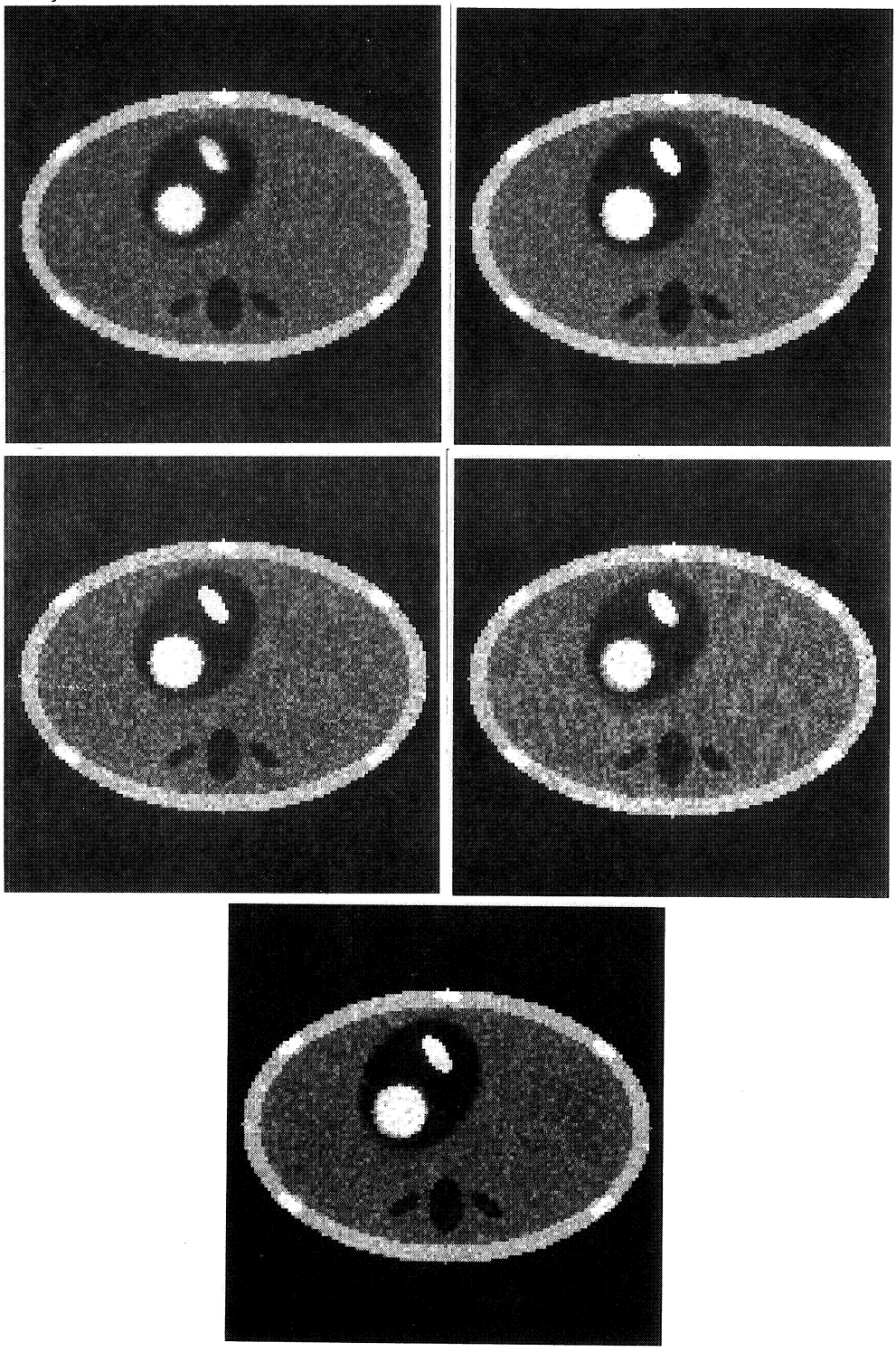

Figure VII.2 . Reconstructions from perturbed data at phase ϕ_2
Top left: degree 0, Top right: degree 1, Middle left: degree 3, Middle right: sinc, Bottom: tp-sinc.

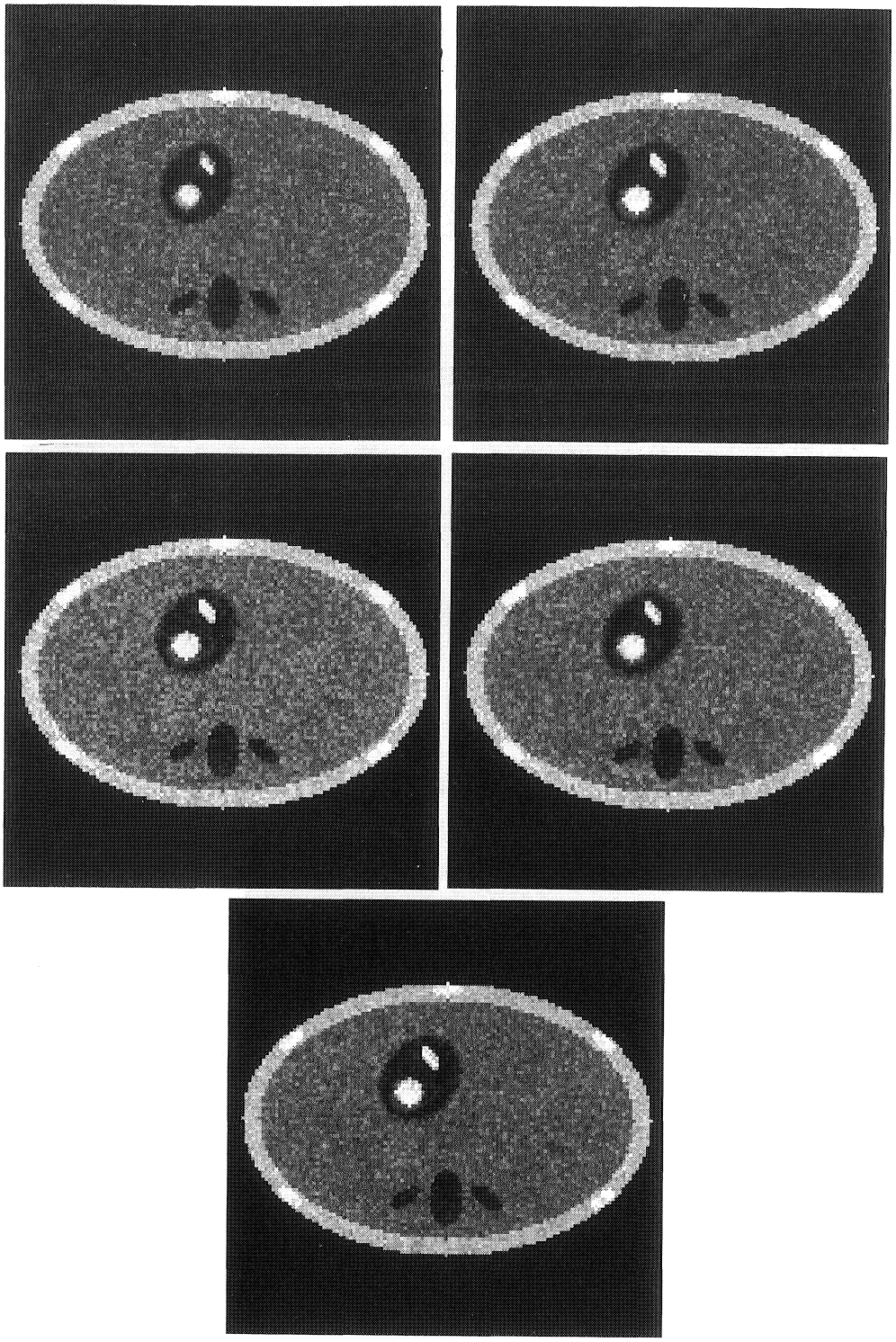

Figure VII.3 . Reconstructions from perturbed data at phase ϕ_4
Top left: degree 0, Top right: degree 1, Middle left: degree 3, Middle right: sinc, Bottom: tp-sinc.

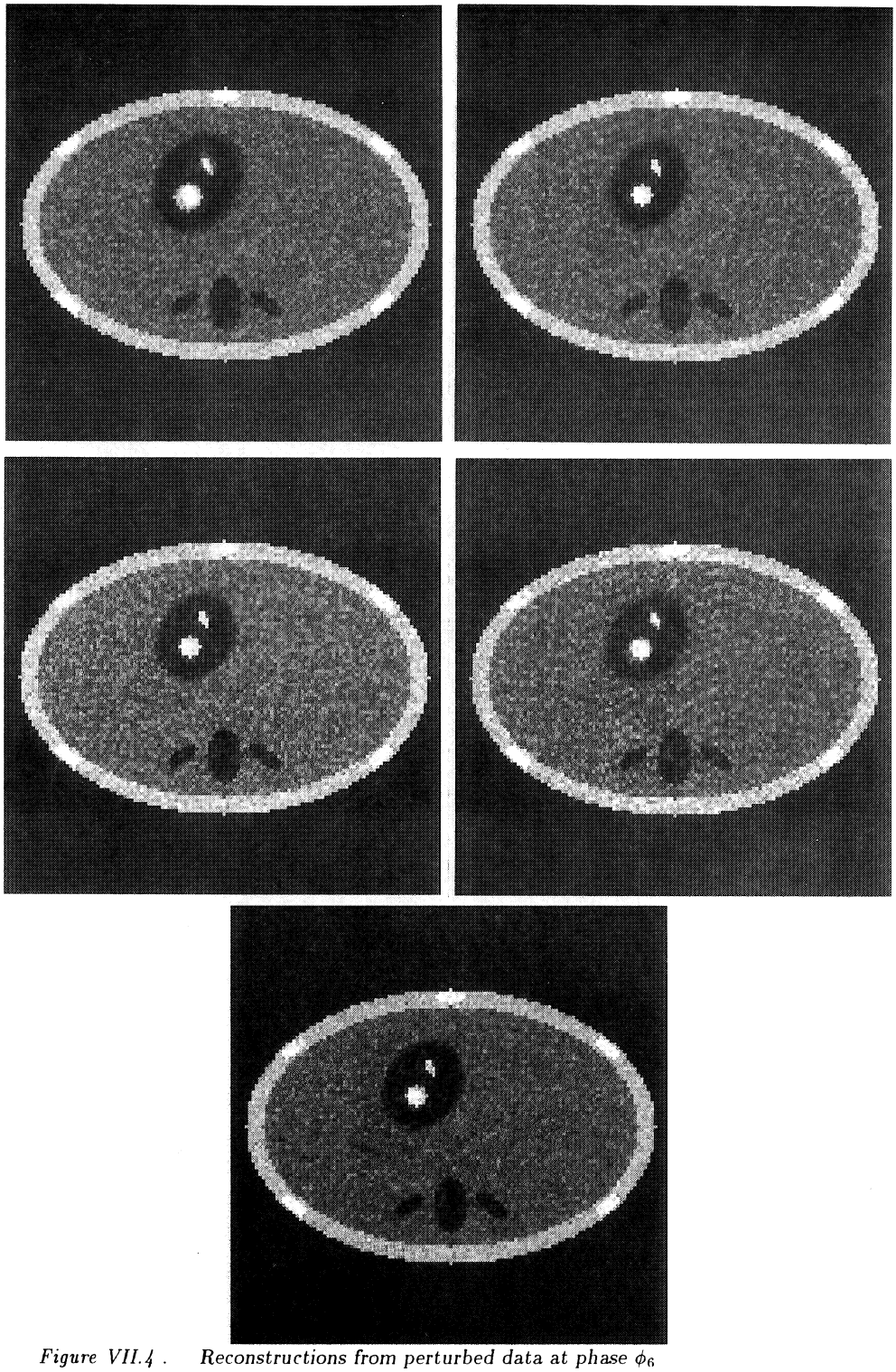

Figure VII.4 . Reconstructions from perturbed data at phase ϕ_6 at phase ϕ_6.
Top left: degree 0, Top right: degree 1, Middle left: degree 3, Middle right: sinc, Bottom: tp-sinc.

The differences in L^2-norm between the reconstructions (from perturbed test data) and the chest phantom are given in the following table.

	phase0	phase2	phase4	phase6
degree0	20.05	21.20	19.39	71.83
degree1	19.22	18.56	18.95	18.49
degree3	22.68	23.14	22.57	22.35
sinc	133.91	27.67	20.46	25.20
tp-sinc	38.13	8.49	7.46	6.79

Table VII.1 Reconstruction error at four phases from perturbed test data.

When intuitively comparing the reconstructions from the perturbed data we see that no drastic changes occur due to this perturbation. Comparing sinc and tp-sinc reconstruction we clearly see the effect of the Tychonov-Phillips regularization.

Finally we discuss the effect due to perturbation of the rescaled time markers by formula 1.3. The random numbers $\{\theta_{\mathbf{k},i}\}$ are chosen uniformly and independently from the interval $[-0.08, 0.08]$. The spacing of the profiles on an RR-interval is approximately 0.067. This yields a relative perturbation of the time markers of about 100%. Note that this relatively big perturbation can have drastic effects on the reconstructions. The different reconstruction algorithms for the perturbed rescaled time markers are illustrated in Figures VII.5, VII.6, VII.7 and VII.8.

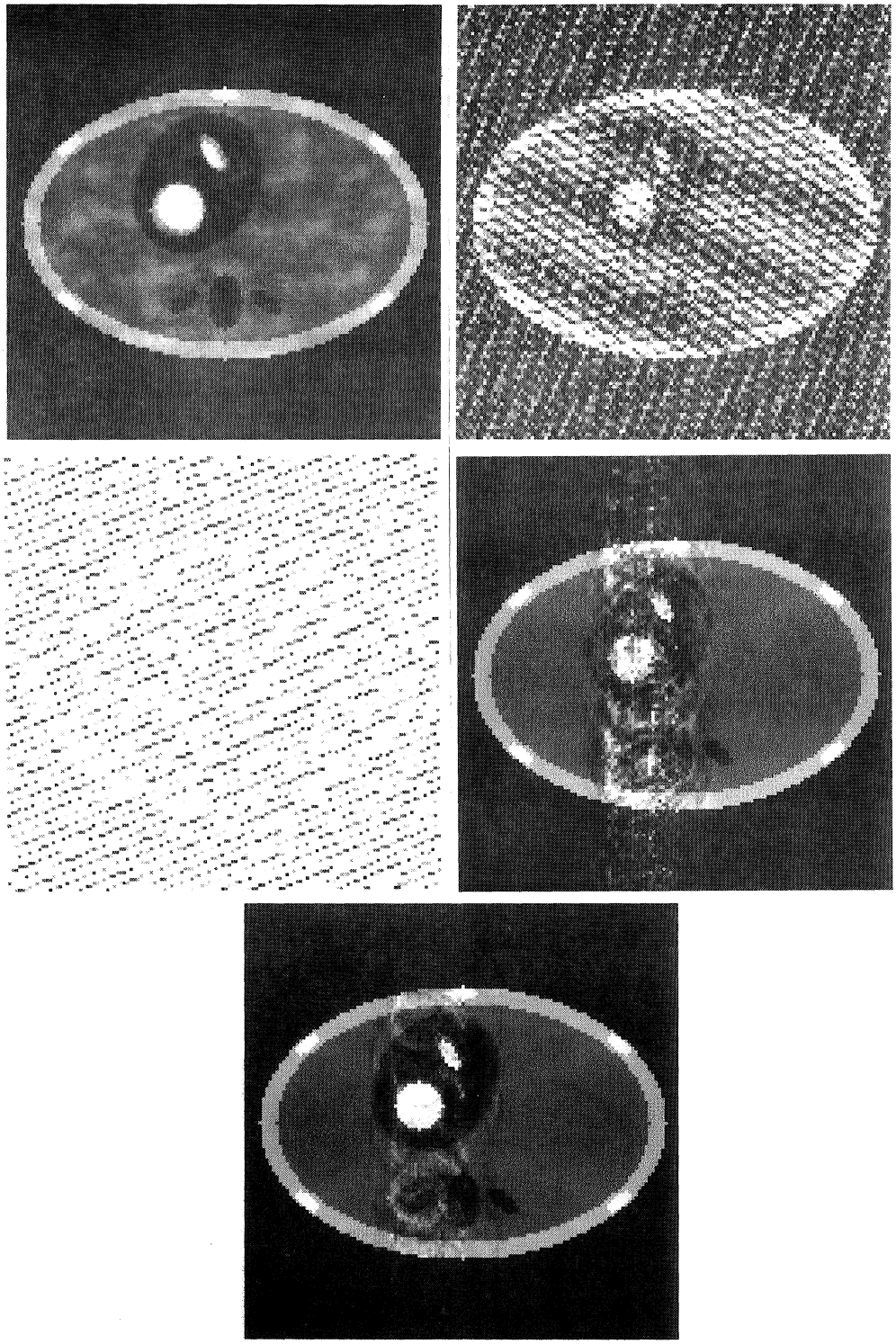

Figure VII.5 . Reconstructions from perturbed time markers at phase ϕ_0. Top left: degree 0, Top right: degree 1, Middle left: degree 3, Middle right: sinc, Bottom: tp-sinc.

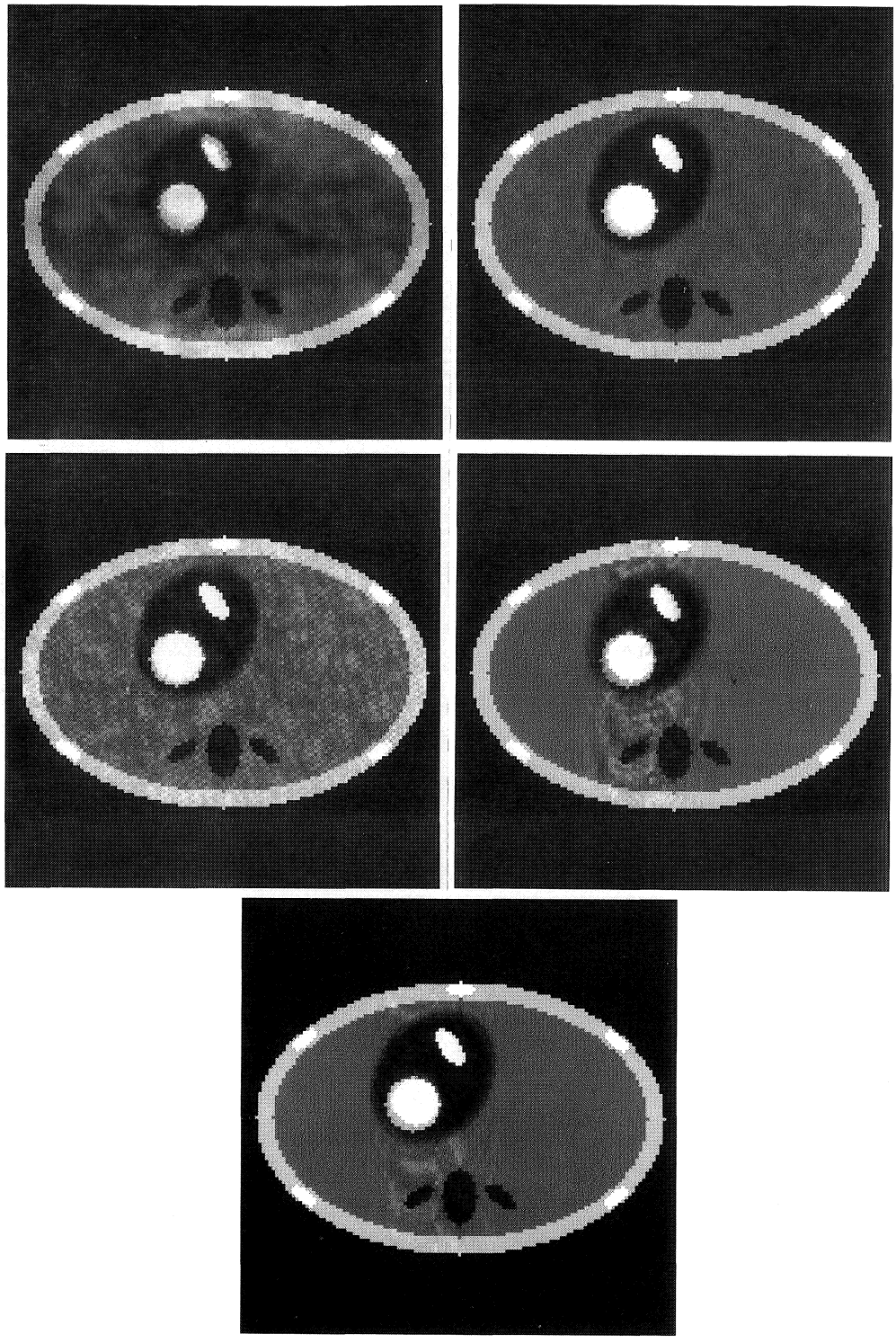

Figure VII.6 . Reconstructions from perturbed time markers at phase ϕ_2. Top left: degree 0, Top right: degree 1, Middle left: degree 3, Middle right: sinc, Bottom: tp-sinc.

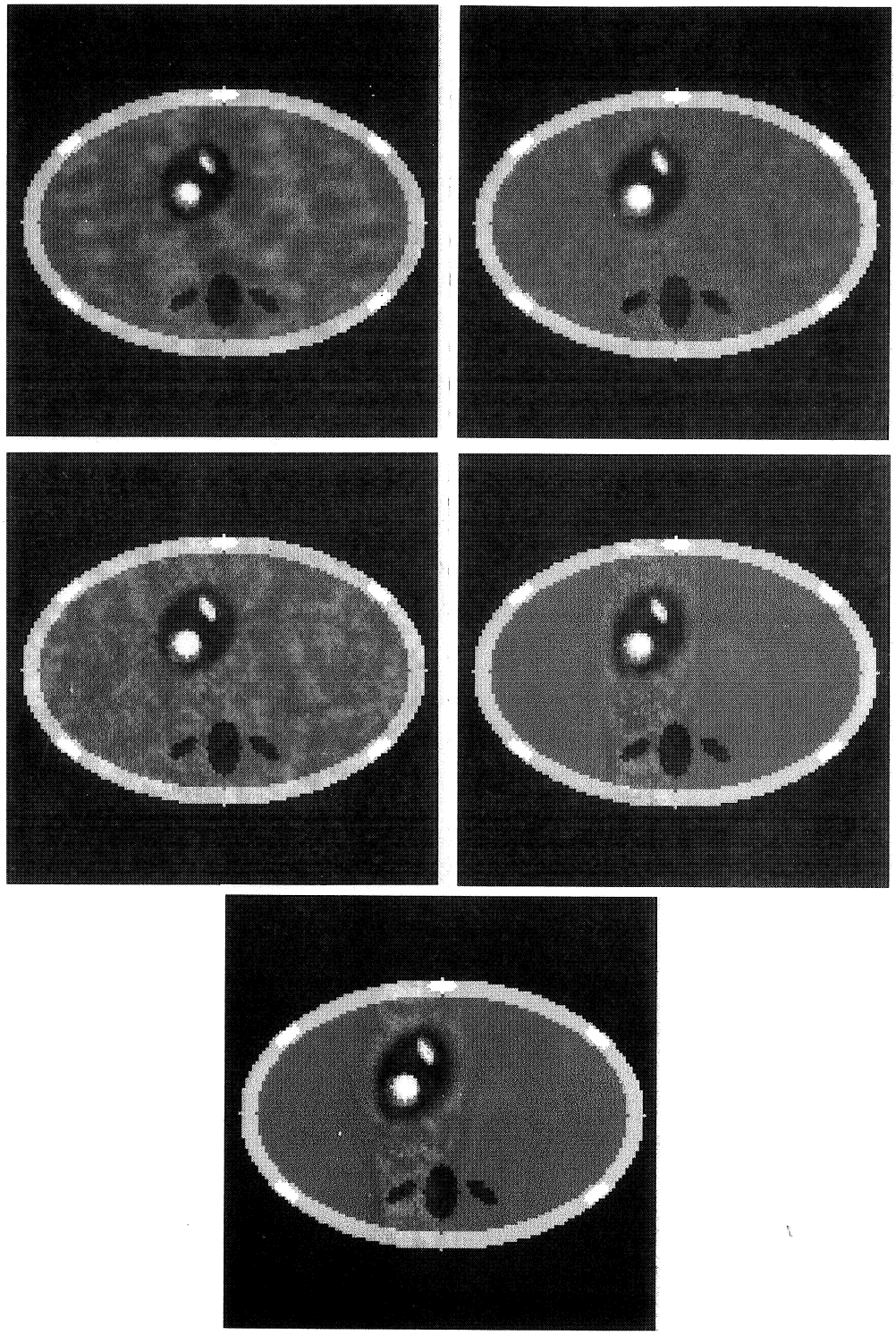

Figure VII.7 . Reconstructions from perturbed time markers at phase ϕ_4. *Top left: degree 0, Top right: degree 1, Middle left: degree 3, Middle right: sinc, Bottom: tp-sinc.*

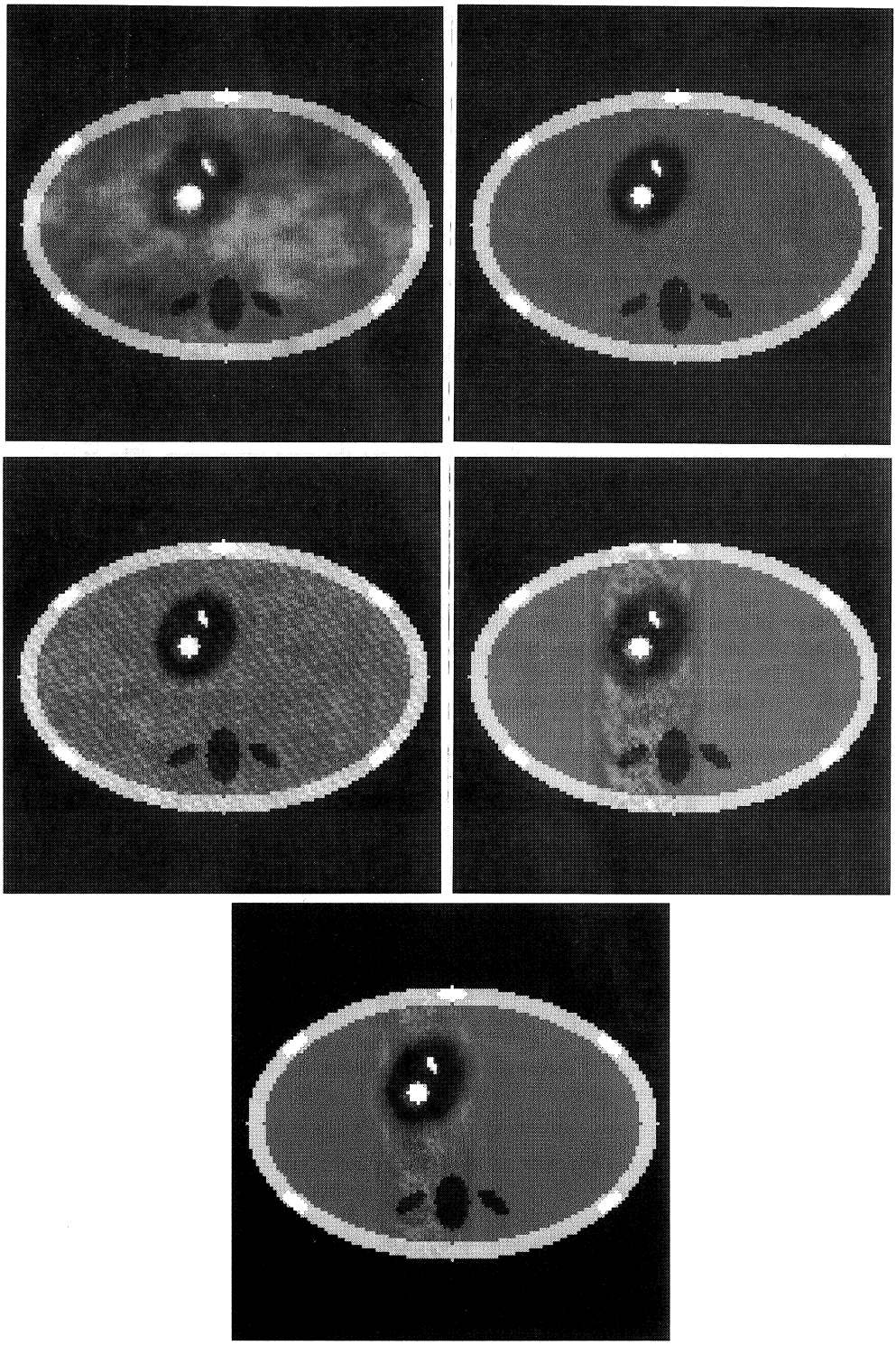

Figure VII.8 . *Reconstructions from perturbed time markers at phase ϕ_6. Top left: degree 0, Top right: degree 1, Middle left: degree 3, Middle right: sinc, Bottom: tp-sinc.*

The differences in L^2-norm of the reconstructions from perturbed time markers between the chest phantom are given in the following table.

	phase0	phase2	phase4	phase6
degree0	16.65	3.65	12.52	18.18
degree1	108.63	6.79	7.22	4.66
degree3	417.45	13.78	10.89	13.43
sinc	33.56	9.64	6.95	9.41
tp-sinc	25.99	6.79	7.07	5.01

Table VII.1 Reconstruction error at four phases from perturbed time markers.

What we see is that degree three reconstruction does not behave well for the time jitter error. This illustrates formula (2.5). From this formula, we see that the bound on the time jitter error depends on the time derivative of the interpolating function. If one chooses the degree of the spline high (degree three appears to be high enough) then the supremum norm of the derivative of the spline is higher, compared to the norm of the derivative of lower degree splines. So, the bound on the time jitter error is probably higher for higher degree splines. This illustrates the conclusion at the end of Section 2 that higher degree spline reconstruction may be ill-conditioned for the time jitter error. The other reconstruction algorithms behave better. However, the quality at phase ϕ_0 of degree one reconstruction is also poor. Regularized sinc reconstruction behaves well in the case of perturbed measurement times.

Finally we present our conclusions about the time jitter error. We see in Figures VII.5, VII.6, VII.7 and VII.8 that for degree 1 and degree 3 reconstruction the images of the first phases are of poor quality, while the images of the latter phases are better. It turns out that degree 3 reconstruction is sensitive for perturbation of the time markers.

VII.4. Conclusions and Remarks

In this section we briefly review some of our results and conclusions of this dissertation.

A model for dynamic MRI-reconstruction is presented in this thesis and an associated inversion problem is formulated. The model assumptions are that Fourier coefficients of the spin density of the heart observed at different time points and linear stretching as a time-to-phase conversion formula, can be used to reconstruct a model heartbeat.

The inversion problem was solved in Part One in the setting of L^2-spaces of vector valued functions, $L^2(D,\mathcal{H})$, using Riesz-Fischer systems, Riesz bases and Bessel systems. We showed that the minimum norm solution has a natural decomposition. In the case that no solution exists, the use of a regularization technique was proposed, e.g Tychonov-Phillips regularization. These results were applied in the case that $\mathcal{H}$ is either $I\!P_r$, the Hilbert space of bandlimited functions, or $\mathcal{K}^{2n-1}$ which is the space of odd degree polynomial spline functions. We proved estimates for the aliasing error, the amplitude error and the time jitter error. It turned out that the solution is stable under perturbation of the data and time markers.

In Part Two some of the mathematical results were reformulated within the practical context of MRI reconstruction. The reconstruction algorithms we considered are degree 0, degree 1, degree 3, sinc and tp-sinc reconstruction. These algorithms were applied to test-data. The reconstructed images were compared with the original chest phantom at corresponding phases. The conclusion is that degree 1 and degree 3 reconstruction perform better than the other methods in this test situation. We also showed that the quality of

the reconstructed images improves significantly when increasing the number of profiles N_{pr} from 5 to 15. The image quality will not improve much when increasing N_{pr} further.

The stability of the algorithms is illustrated by applying the algorithms to perturbed test-data and perturbed time markers. We saw that the reconstruction methods are stable under perturbation of the data. It turned out that degree 3 reconstruction is ill-conditioned under perturbation of the time markers.

The reconstruction algorithms were also applied to MR-data, using either linear or piecewise linear time-to-phase conversion. We conclude that reconstruction by using linear stretching and piecewise linear stretching give the same results.

Degree 1 and degree 3 reconstruction prevail over the other methods for test-data. On the other hand, in the case of MRI-data there is no essential difference between the reconstruction methods, except for degree 1, which gives low quality images. That the reconstruction methods do not behave as expected for MRI-data is probably due to the violation of the model assumptions. We refer to section VI.4 for a discussion on the validity of these assumptions.

Another point is the use of the L^2-norm as an error criterion. This may not be the most natural choice from a perceptual point of view. In particular, even if the difference between the reconstruction and the original phantom is small, the result may still be degraded by undesired effects, such as the vertical noise bands, discussed above.

The overal conclusion is that the performance of the reconstructions in practice will not get better by improving the interpolation techniques. (Note that the quality of the reconstructions is considered for fixed values of the spatial and temporal resolution. This resolution cannot be increased arbitrarily, as explained in Section 2 of the Introduction.) In other words, to improve the performance of the reconstruction algorithms we have to adapt our model assumptions. This is the subject of the following section.

VII.5. Future directions

This section gives suggestions for future directions to improve the quality of the reconstructed images.

> **Conclusion:** *The main quality improvement of dynamic MRI-reconstruction will be realized by refining the model.*

For convenience we recall the model assumptions:

- The algorithm to obtain rescaled time markers on the unit RR-interval from time markers on an RR-interval is linear stretching;
- There exists a model heartbeat such that its Fourier coefficients at the rescaled time markers are equal to the measurements from the spin density of the beating human heart.

These assumptions are an approximation of the real situation. This modelling can be improved by taking into account more parameters concerning the motion of the heart.

In practice, the exact motion of the heart in the plane of the measured cross section is unknown. One of the effects which can perhaps be taken into account is the respiratory motion. If the patient, lying in the MR-scanner, is breathing the chest is slightly moving in vertical direction, which causes a phase shift in the measured Fourier coefficients. This vertical displacement can be measured in practice, and could then be incorporated in the

model. A crucial question which would have to be answered first then, is whether this is a realistic approximation of the effect of the respiration on the heart motion. Another idea, is to take into account both the respiratory cycle and the heart cycle for rescaling the time markers. The first model assumption has to be adapted then, resulting in a model with two temporal parameters, one for the respiratory phase and one for the heartphase. The reconstruction algorithms as described in Section VI.2 can then be used after adapting them to handle a two dimensional temporal parameter.

This idea of taking into account the respiratory cycle was suggested by e.g. Bohning [8]. We propose to use the phantom of the model heartbeat to test whether these adaptions concerning the respiration will lead to a quality improvement of the reconstructions.

The heart does not only contract, but it also rotates meaning that the part of the cross section of the heart which is measured at a given time does not remain in one plane, which violates the second model assumption. For diagnostic purposes it is interesting to image this motion. Then one has to obtain Fourier coefficients in three instead of two dimensions. The second model assumption can then be adapted for the case of a three dimensional spatial parameter. The reconstruction algorithms as described in Section VI.2 can also be used in this case. We suggest the use of the phantom and test-data to check whether this adaption will improve the reconstruction quality.

The overal conclusion is that more parameters concerning the motion of the heart should be taken into account in order to improve the reconstruction algorithms. For example, using information from the respiratory cycle and using three dimensional Fourier coefficients could be considered.

REFERENCES

[1] J.H. Ahlberg, E.N. Nilson, J.L. Walsh.
The Theory of Splines and their Applications.
Academic Press, New York, 1967.

[2] N.I. Akhiezer.
The Classical Moment Problem.
Oliver & Boyd, Edinburg, 1965.

[3] A.V. Balakrishnan.
Applied Functional Analysis.
Springer-Verlag, Berlin, 1976.

[4] M. Bertero.
Regularization Methods for Linear Inverse Problems.
In: *Inverse Problems*
Lecture Notes in Mathematics no.1225, pp.52 - 113.
Eds. A. Dold, B. Eckman.
Springer-Verlag, Berlin, 1986.

[5] M. Bertero, C. de Mol, E.R. Pike.
Linear Inverse Problems with Discrete Data I:
General Formulation and Singular System Analysis.
Inv. Problems 1, pp. 301-330, 1985.

[6] M. Bertero, C. de Mol, E.R. Pike.
Linear Inverse Problems with Discrete Data II:
Stability and Regularization
Inv. Problems 4, pp. 573-594, 1988.

[7] F.J. Beutler, W.L. Root.
The Operator Pseudoinverse in Control and Systems Identification.
In: *Generalized Inverses and Applications.*
Academic Press, New York, 1976.

[8] D.E. Bohning.
Cardiac Gating Strategies.
New Concepts in Cardiac Imaging, Ch. 11.
Year Book Medical Publishers, 1988.

[9] C. de Boor.
A Practical Guide to Splines.
Springer-Verlag, Berlin, 1978.

[10] C. de Boor.
Bounding the Error in Spline Interpolation.
Siam Review, vol. 16, no.4, pp. 531-544, oct. 1974.

[11] P.L. Butzer.
A Survey of the Whittaker-Shannon Sampling Theorem and some of its extensions.
J. Math. Res. Exp., vol. 3, No.1, pp. 185-212, jan. 1983.

[12] P.L. Butzer, W. Engels.
On the Implementation of the Shannon Sampling Series for Band-Limited Signals.
IEEE Trans. Inform. Theory, vol IT-29, pp. 314-318, march 1983.

[13] P.L. Butzer, W. Splettstösser.
On Quantization, Truncation and Jitter Errors in the Sampling Theorem and its Generalizations.
Signal Proc. 2, pp. 101-112, 1980.

[14] P.L. Butzer, W. Splettstösser, R.L. Stens.
The Sampling Theory and Linear Prediction in Signal Analysis.
Jahres. Deutsch. Math.-Verein., vol. 90, no. 1, pp. 1-70, jan 1988.

[15] J. B. Conway
A Course in Functional Analysis.
Springer-Verlag, New York, 1985.

[16] P. van Dijk.
ECG-Triggered NMR Imaging of the heart.
Diagn. Imag. Clin. Med. 53, pp. 29 - 37, 1984.

[17] G.H. Glover, N.J. Pelc.
A rapid-gated Cine MRI Technique.
Magnetic Resonance Annual, pp.299-333.
Raven Press, New York, 1988.

[18] I.C. Gohberg, S. Goldberg.
Basic Operator Theory.
Birkhäuser, Boston, 1980.

[19] I.C. Gohberg, M.G. Krein.
Introduction to the Theory of Linear Nonselfadjoint Operators.
Translations of Mathematical Monographs, Volume 18.
AMS, Providence, Rhode Island, 1969.

[20] S. Goldberg.
Unbounded Linear Operators.
Dover Publications Inc, New York, 1966.

[21] T.N.E. Greville.
Theory and Applications of Spline Functions.
Academic Press, New York, 1969.

[22] C.W. Groetsch.
The Theory of Tikhonov Regularization for Fredholm Equations of the First Kind.
Pitman Publishing Ltd., London, 1984.

[23] J.R. Higgins.
Completeness and Basis Properties of Sets of Special Functions.
Cambridge University Press, Cambridge, 1977.

[24] E. Hille , R.S. Phillips.
Functional Analysis and Semigroups.
Colloquium Publications, Vol XXXI.
AMS, Providence, Rhode Island, 1957.

[25] W.S Hinshaw, A.H. Lent.
An Introduction to NMR Imaging: from the Bloch Equation to the Imaging Equation.
Proc. IEEE 71, pp. 338-350, 1983.

[26] L. Hörmander.
The Analysis of Linear Partial Differential Operators I.
Springer-Verlag, Berlin.

[27] A.J. Jerri.
The Shannon Sampling Theorem - Its Various Extensions and Applications.
Proc. IEEE, Vol. 6, pp. 1565-1596, july, 1966.

[28] M.I. Kadec.
The Exact Value of the Paley-Wiener Constant.
Sov. Math. Dokl. 5, pp. 559 - 561, 1964.

[29] V.E. Katznelson.
Exponential Bases in L^2.
Funct. Anal. Appl. 5 pp.31 - 38, 1971.

[30] K.F. King, P.R Moran.
A Unified Description of NMR Imaging, Data-Collection Strategies and Reconstruction.
Med. Phys. 11, pp. 1-14, 1984.

[31] A. Kumar, D. Welti, R. Ernst.
NMR Fourier Zeugmatography.
J. Magn. Res. 18, pp. 69 - 83, 1975.

[32] H.J. Landau (ed.).
Moments in Mathematics.
Proceedings of Symposia in Applied Mathematics, Volume 37.
AMS, Providence, Rhode Island, 1987.

[33] P.C. Lauterbur.
Medical Imaging by Nuclear Magnetic Resonance Zeugmatography.
IEEE Trans. Nucl. Sc. vol. NS-26, no 2, pp. 2808 - 2811, april 1979.

[34] P.C. Lauterbur.
Image Formation by Induced Local Interactions: Examples Employing Nuclear Magentic Resonance.
Nature, vol. 242, pp.190 - 191, march , 1973.

[35] G.W. Lenz, E.M. Haacke, R.D. White.
Retrospective Cardiac Gating: a Review of Technical Aspects and Future Directions.
Magnetic Resonance Imaging 7. pp. 445-554, 1989.

[36] N. Levinson.
Gap and Density Theorems.
AMS Colloquium Publications Vol. XXVI, 1940.

[37] P.R. Locher.
Tomografie met behulp van Protonspinresonantie.
Philips Technisch Tijdschrift jaarg. 41, no 3, pp.73 - 89, 1983.

[38] A.K. Louis.
Inverse und Schlecht Gestellte Probleme.
Teubner Studienbücher, 1989.

[39] P. Mansfield, P.G. Morris.
NMR Imaging in Biomedicine.
Academic Press, New York, 1982.

[40] G.C. McKinnon, R.H.T. Bates.
Towards Imaging the Beating Human Heart usefully with a Conventional CT Scanner.
IEEE Trans. Biomed. Engineering, BME-28 pp. 123-127, 1981.

[41] V.A. Morozov.
Methods for Solving Incorrectly Posed Problems.
Springer Verlag, New York, 1974.

[42] F. Natterer.
The Mathematics of Computerized Tomography.
John Wiley and Sons, Chichester, 1986.

[43] F. Natterer.
Regularization of Ill-Posed Problems by Projection Methods.
Num. Math. 28, pp. 329-341, 1977.

[44] A. Papoulis.
Signal Analysis.
McGraw Hill, New York, 1977.

[45] W. Rudin.
Real and Complex Analysis.
Mc Graw Hill, New Delhi, second edition, 1974.

[46] W. Rudin.
Functional Analysis.
McGraw Hill, New Delhi, 1974.

[47] I.J. Schoenberg.
Cardinal Spline Interpolation.
Regional Conference Series in Applied Mathematics.
SIAM,1973.

[48] H.S. Shapiro.
Topics in Approximation Theory.
Lecture Notes in Mathematics, vol. 187.
Springer-Verlag, Berlin.

[49] I. Singer.
Bases in Banach Spaces.
Springer-Verlag, Berlin, 1970.

[50] W. Splettstösser.
Unregelmässige Abtastung Determinierter und Zufälliger Signale.
DFG-Schwertpunktprogramm, Digitale Signalverarbeitung, pp. 1-4 march 1981.

[51] W. Splettstösser.
Error Estimates for Sampling Approximation of Non-Bandlimited Functions.
Math. Meth. Appl. Sci. 1, pp.127-137, 1979.

[52] J. Stoer, R. Bulirsch.
Introduction to Numerical Analysis.
Springer Verlag, Heidelberg, 1983.

[53] B. Sz-Nagy, C. Foias.
Harmonic Analysis of Operators on Hilbert Spaces.
North Holland Publ. Comp. Amsterdam, 1970.

[54] D.B. Twieg.
The k-Trajectory Formulation of the NMR Imaging Process with applications in Analysis and Synthesis of Imaging Methods.
Med. Phys. 10, pp. 610-621, 1983.

[55] R.M. Young.
An Introduction to Nonharmonic Fourier Series.
Academic Press, New York, 1980.

[56] M. Zwaan.
A Radon Transform on Circles through the Origin in $\mathbb{R}^2$.
CWI Quarterly, vol.2, No. 1, Amsterdam, March 1989.

[57] M. Zwaan.
Dynamic MRI Reconstruction as a Moment Problem.
Part I. The Beating Heart: a Problem Formulation.
Math. Meth. Appl. Sci., cf. CWI Report AM-R8905, March 1989.

[58] M. Zwaan.
Dynamic MRI Reconstruction as a Moment Problem.
Part II. Riesz Bases in L^2-spaces of Vector Valued Functions.
Math. Meth. Appl. Sci., cf. CWI Report AM-R8907, April 1989.

[59] M. Zwaan.
Dynamic MRI Reconstruction as a Moment Problem.
Part III. An Error Analysis of Reconstruction by Sinc and Spline Interpolation.
CWI Report AM-R9002, january 1990.

[60] M. Zwaan.
Error estimates for Nonuniform sampling.
Num. Funct. Anal. Opt., vol. 11, no. 5 & 6, pp. 589-599, 1990.
(cf. CWI Report AM-R8914, October, 1989.)

Index

For each entry in the list we give page numbers where the notion is first used, in the Introduction, Part One and Part Two respectively.

List of Symbols

For each entry in the list we give an explanation as well as the page numbers where the symbol is first used, in the introduction, Part One and Part Two respectively.

		page
$\mathbb{K}, \mathbb{I}$	finite or countable index sets	15, 30, 79
$\mathbb{C}$	the set of complex numbers	4
$\mathcal{G}, \mathcal{H}$	Hilbert spaces	4
$L^2(D, \mathcal{H})$	the Hilbert space of vector valued functions	19
$\mathbb{P}_\tau$	the space of bandlimited functions	34, 81
$\mathcal{K}^{2n-1}$	the space of odd order polynomial splines	39, 81
$\| \ \|_\infty$	the supremum norm	35
$T, R, \mathcal{T}, \mathcal{R}$	linear operators	4, 15, 21, 23
T^{-1}	the inverse operator of T	4
T^*	the adjoint operator of T	4
T^+	Moore-Penrose inverse of T	6
T^γ	Tychonov-Phillips regularization	7
G	Gram matrix	16, 41, 80
sinc	the sinc-function	34, 81
$\varphi_{\mathbf{k},i}$	system of point evaluation functionals	46, 81, 82
$\psi_{\mathbf{k},i}$	system of biorthogonal vectors	46, 80, 82
J	unit heart interval	*vi*, 73
τ	actual time during acquisition ($-\infty < \tau < \infty$)	*vii*, 76
t	rescaled time ($t \in J$)	*vii*, 76
$F(\mathbf{r}, \tau)$	proton density at position $\mathbf{r}$ at time τ	*vii*, 76
$\widehat{F}(\mathbf{k}, \tau)$	spatial Fourier coefficient of the proton density F at time τ	*vii*, 76
g	model heartbeat	*vii*, 76
$\widehat{f}(\mathbf{r}, \xi)$	temporal Fourier coefficient of f	111
$\mathrm{E}_{\mathrm{al}}, \mathrm{e}_{\mathrm{al}}$	the aliasing error	54, 60, 111
$\mathrm{E}_{\mathrm{amp}}, \mathrm{e}_{\mathrm{amp}}$	the amplitude error	51, 53, 109
$\mathrm{E}_{\mathrm{tj}}, \mathrm{e}_{\mathrm{tj}}$	the time-jitter error	51, 53, 109
$\mathbf{M}$	the magnetization	*ii*, 69
$m_\perp$	transverse magnetization	70
$\mathbf{B}_0$	homogeneous magnetic field	*ii*, 68
$\mathbf{G} := (G_x, G_y, G_z)$	the magnetic gradient field	*ii*, 68
G_x	readout/detection gradient	73
G_y	phase-encoding gradient	73
γ	gyromagnetic ratio	*ii*, 68
ω_L	Larmor frequency	70
δt	time between two samples in a profile	76
ΔT	time period between two consecutive profiles	74
$\mathbf{r}$	position vector (x, y)	*ii*, 68
k_x	integer counting the number of horizontal samples in the spatial Fourier plane	72

k_y	integer counting the number of vertical samples in the spatial Fourier plane	72
N_x	maximum value of k_x	72
N_y	maximum value of k_y	72
$\mathbf{k}$	wave vector (k_x, k_y)	*iii*, 79
i	integer counting the number of profiles for a fixed value of k_y	76
r_k, R_k	time of the kth R-pulse	*vii*, 75
N_{pr}	total number of profiles for a fixed value of k_y	75

MATHEMATICAL CENTRE TRACTS

1 T. van der Walt. *Fixed and almost fixed points.* 1963.

2 A.R. Bloemena. *Sampling from a graph.* 1964.

3 G. de Leve. *Generalized Markovian decision processes, part I: model and method.* 1964.

4 G. de Leve. *Generalized Markovian decision processes, part II: probabilistic background.* 1964.

5 G. de Leve, H.C. Tijms, P.J. Weeda. *Generalized Markovian decision processes, applications.* 1970.

6 M.A. Maurice. *Compact ordered spaces.* 1964.

7 W.R. van Zwet. *Convex transformations of random variables.* 1964.

8 J.A. Zonneveld. *Automatic numerical integration.* 1964.

9 P.C. Baayen. *Universal morphisms.* 1964.

10 E.M. de Jager. *Applications of distributions in mathematical physics.* 1964.

11 A.B. Paalman-de Miranda. *Topological semigroups.* 1964.

12 J.A.Th.M. van Berckel, H. Brandt Corstius, R.J. Mokken, A. van Wijngaarden. *Formal properties of newspaper Dutch.* 1965.

13 H.A. Lauwerier. *Asymptotic expansions.* 1966, out of print; replaced by MCT 54.

14 H.A. Lauwerier. *Calculus of variations in mathematical physics.* 1966.

15 R. Doornbos. *Slippage tests.* 1966.

16 J.W. de Bakker. *Formal definition of programming languages with an application to the definition of ALGOL 60.* 1967.

17 R.P. van de Riet. *Formula manipulation in ALGOL 60, part 1.* 1968.

18 R.P. van de Riet. *Formula manipulation in ALGOL 60, part 2.* 1968.

19 J. van der Slot. *Some properties related to compactness.* 1968.

20 P.J. van der Houwen. *Finite difference methods for solving partial differential equations.* 1968.

21 E. Wattel. *The compactness operator in set theory and topology.* 1968.

22 T.J. Dekker. *ALGOL 60 procedures in numerical algebra, part 1.* 1968.

23 T.J. Dekker, W. Hoffmann. *ALGOL 60 procedures in numerical algebra, part 2.* 1968.

24 J.W. de Bakker. *Recursive procedures.* 1971.

25 E.R. Paërl. *Representations of the Lorentz group and projective geometry.* 1969.

26 European Meeting 1968. *Selected statistical papers, part I.* 1968.

27 European Meeting 1968. *Selected statistical papers, part II.* 1968.

28 J. Oosterhoff. *Combination of one-sided statistical tests.* 1969.

29 J. Verhoeff. *Error detecting decimal codes.* 1969.

30 H. Brandt Corstius. *Exercises in computational linguistics.* 1970.

31 W. Molenaar. *Approximations to the Poisson, binomial and hypergeometric distribution functions.* 1970.

32 L. de Haan. *On regular variation and its application to the weak convergence of sample extremes.* 1970.

33 F.W. Steutel. *Preservation of infinite divisibility under mixing and related topics.* 1970.

34 I. Juhász, A. Verbeek, N.S. Kroonenberg. *Cardinal functions in topology.* 1971.

35 M.H. van Emden. *An analysis of complexity.* 1971.

36 J. Grasman. *On the birth of boundary layers.* 1971.

37 J.W. de Bakker, G.A. Blaauw, A.J.W. Duijvestijn, E.W. Dijkstra, P.J. van der Houwen, G.A.M. Kamsteeg-Kemper, F.E.J. Kruseman Aretz, W.L. van der Poel, J.P. Schaap-Kruseman, M.V. Wilkes, G. Zoutendijk. *MC-25 Informatica Symposium.* 1971.

38 W.A. Verloren van Themaat. *Automatic analysis of Dutch compound words.* 1972.

39 H. Bavinck. *Jacobi series and approximation.* 1972.

40 H.C. Tijms. *Analysis of (s,S) inventory models.* 1972.

41 A. Verbeek. *Superextensions of topological spaces.* 1972.

42 W. Vervaat. *Success epochs in Bernoulli trials (with applications in number theory).* 1972.

43 F.H. Ruymgaart. *Asymptotic theory of rank tests for independence.* 1973.

44 H. Bart. *Meromorphic operator valued functions.* 1973.

45 A.A. Balkema. *Monotone transformations and limit laws.* 1973.

46 R.P. van de Riet. *ABC ALGOL, a portable language for formula manipulation systems, part 1: the language.* 1973.

47 R.P. van de Riet. *ABC ALGOL, a portable language for formula manipulation systems, part 2: the compiler.* 1973.

48 F.E.J. Kruseman Aretz, P.J.W. ten Hagen, H.L. Oudshoorn. *An ALGOL 60 compiler in ALGOL 60, text of the MC-compiler for the EL-X8.* 1973.

49 H. Kok. *Connected orderable spaces.* 1974.

50 A. van Wijngaarden, B.J. Mailloux, J.E.L. Peck, C.H.A. Koster, M. Sintzoff, C.H. Lindsey, L.G.L.T. Meertens, R.G. Fisker (eds.). *Revised report on the algorithmic language ALGOL 68.* 1976.

51 A. Hordijk. *Dynamic programming and Markov potential theory.* 1974.

52 P.C. Baayen (ed.). *Topological structures.* 1974.

53 M.J. Faber. *Metrizability in generalized ordered spaces.* 1974.

54 H.A. Lauwerier. *Asymptotic analysis, part 1.* 1974.

55 M. Hall, Jr., J.H. van Lint (eds.). *Combinatorics, part 1: theory of designs, finite geometry and coding theory.* 1974.

56 M. Hall, Jr., J.H. van Lint (eds.). *Combinatorics, part 2: graph theory, foundations, partitions and combinatorial geometry.* 1974.

57 M. Hall, Jr., J.H. van Lint (eds.). *Combinatorics, part 3: combinatorial group theory.* 1974.

58 W. Albers. *Asymptotic expansions and the deficiency concept in statistics.* 1975.

59 J.L. Mijnheer. *Sample path properties of stable processes.* 1975.

60 F. Göbel. *Queueing models involving buffers.* 1975.

63 J.W. de Bakker (ed.). *Foundations of computer science.* 1975.

64 W.J. de Schipper. *Symmetric closed categories.* 1975.

65 J. de Vries. *Topological transformation groups, 1: a categorical approach.* 1975.

66 H.G.J. Pijls. *Logically convex algebras in spectral theory and eigenfunction expansions.* 1976.

68 P.P.N. de Groen. *Singularly perturbed differential operators of second order.* 1976.

69 J.K. Lenstra. *Sequencing by enumerative methods.* 1977.

70 W.P. de Roever, Jr. *Recursive program schemes: semantics and proof theory.* 1976.

71 J.A.E.E. van Nunen. *Contracting Markov decision processes.* 1976.

72 J.K.M. Jansen. *Simple periodic and non-periodic Lamé functions and their applications in the theory of conical waveguides.* 1977.

73 D.M.R. Leivant. *Absoluteness of intuitionistic logic.* 1979.

74 H.J.J. te Riele. *A theoretical and computational study of generalized aliquot sequences.* 1976.

75 A.E. Brouwer. *Treelike spaces and related connected topological spaces.* 1977.

76 M. Rem. *Associons and the closure statement.* 1976.

77 W.C.M. Kallenberg. *Asymptotic optimality of likelihood ratio tests in exponential families.* 1978.

78 E. de Jonge, A.C.M. van Rooij. *Introduction to Riesz spaces.* 1977.

79 M.C.A. van Zuijlen. *Emperical distributions and rank statistics.* 1977.

80 P.W. Hemker. *A numerical study of stiff two-point boundary problems.* 1977.

81 K.R. Apt, J.W. de Bakker (eds.). *Foundations of computer science II, part 1.* 1976.

82 K.R. Apt, J.W. de Bakker (eds.). *Foundations of computer science II, part 2.* 1976.

83 L.S. van Benthem Jutting. *Checking Landau's "Grundlagen" in the AUTOMATH system.* 1979.

84 H.L.L. Busard. *The translation of the elements of Euclid from the Arabic into Latin by Hermann of Carinthia (?), books vii-xii.* 1977.

85 J. van Mill. *Supercompactness and Wallman spaces.* 1977.

86 S.G. van der Meulen, M. Veldhorst. *Torrix I, a programming system for operations on vectors and matrices over arbitrary fields and of variable size.* 1978.

88 A. Schrijver. *Matroids and linking systems.* 1977.

89 J.W. de Roever. *Complex Fourier transformation and analytic functionals with unbounded carriers.* 1978.

90 L.P.J. Groenewegen. *Characterization of optimal strategies in dynamic games.* 1981.

91 J.M. Geysel. *Transcendence in fields of positive characteristic.* 1979.

92 P.J. Weeda. *Finite generalized Markov programming.* 1979.

93 H.C. Tijms, J. Wessels (eds.). *Markov decision theory.* 1977.

94 A. Bijlsma. *Simultaneous approximations in transcendental number theory.* 1978.

95 K.M. van Hee. *Bayesian control of Markov chains.* 1978.

96 P.M.B. Vitányi. *Lindenmayer systems: structure, languages, and growth functions.* 1980.

97 A. Federgruen. *Markovian control problems; functional equations and algorithms.* 1984.

98 R. Geel. *Singular perturbations of hyperbolic type.* 1978.

99 J.K. Lenstra, A.H.G. Rinnooy Kan, P. van Emde Boas (eds.). *Interfaces between computer science and operations research.* 1978.

100 P.C. Baayen, D. van Dulst, J. Oosterhoff (eds.). *Proceedings bicentennial congress of the Wiskundig Genootschap, part 1.* 1979.

101 P.C. Baayen, D. van Dulst, J. Oosterhoff (eds.). *Proceedings bicentennial congress of the Wiskundig Genootschap, part 2.* 1979.

102 D. van Dulst. *Reflexive and superreflexive Banach spaces.* 1978.

103 K. van Harn. *Classifying infinitely divisible distributions by functional equations.* 1978.

104 J.M. van Wouwe. *Go-spaces and generalizations of metrizability.* 1979.

105 R. Helmers. *Edgeworth expansions for linear combinations of order statistics.* 1982.

106 A. Schrijver (ed.). *Packing and covering in combinatorics.* 1979.

107 C. den Heijer. *The numerical solution of nonlinear operator equations by imbedding methods.* 1979.

108 J.W. de Bakker, J. van Leeuwen (eds.). *Foundations of computer science III, part 1.* 1979.

109 J.W. de Bakker, J. van Leeuwen (eds.). *Foundations of computer science III, part 2.* 1979.

110 J.C. van Vliet. *ALGOL 68 transput, part I: historical review and discussion of the implementation model.* 1979.

111 J.C. van Vliet. *ALGOL 68 transput, part II: an implementation model.* 1979.

112 H.C.P. Berbee. *Random walks with stationary increments and renewal theory.* 1979.

113 T.A.B. Snijders. *Asymptotic optimality theory for testing problems with restricted alternatives.* 1979.

114 A.J.E.M. Janssen. *Application of the Wigner distribution to harmonic analysis of generalized stochastic processes.* 1979.

115 P.C. Baayen, J. van Mill (eds.). *Topological structures II, part 1.* 1979.

116 P.C. Baayen, J. van Mill (eds.). *Topological structures II, part 2.* 1979.

117 P.J.M. Kallenberg. *Branching processes with continuous state space.* 1979.

118 P. Groeneboom. *Large deviations and asymptotic efficiencies.* 1980.

119 F.J. Peters. *Sparse matrices and substructures, with a novel implementation of finite element algorithms.* 1980.

120 W.P.M. de Ruyter. *On the asymptotic analysis of large-scale ocean circulation.* 1980.

121 W.H. Haemers. *Eigenvalue techniques in design and graph theory.* 1980.

122 J.C.P. Bus. *Numerical solution of systems of nonlinear equations.* 1980.

123 I. Yuhász. *Cardinal functions in topology - ten years later.* 1980.

124 R.D. Gill. *Censoring and stochastic integrals.* 1980.

125 R. Eising. *2-D systems, an algebraic approach.* 1980.

126 G. van der Hoek. *Reduction methods in nonlinear programming.* 1980.

127 J.W. Klop. *Combinatory reduction systems.* 1980.

128 A.J.J. Talman. *Variable dimension fixed point algorithms and triangulations.* 1980.

129 G. van der Laan. *Simplicial fixed point algorithms.* 1980.

130 P.J.W. ten Hagen, T. Hagen, P. Klint, H. Noot, H.J. Sint, A.H. Veen. *ILP: intermediate language for pictures.* 1980.

131 R.J.R. Back. *Correctness preserving program refinements: proof theory and applications.* 1980.

132 H.M. Mulder. *The interval function of a graph.* 1980.

133 C.A.J. Klaassen. *Statistical performance of location estimators.* 1981.

134 J.C. van Vliet, H. Wupper (eds.). *Proceedings international conference on ALGOL 68.* 1981.

135 J.A.G. Groenendijk, T.M.V. Janssen, M.J.B. Stokhof (eds.). *Formal methods in the study of language, part I.* 1981.

136 J.A.G. Groenendijk, T.M.V. Janssen, M.J.B. Stokhof (eds.). *Formal methods in the study of language, part II.* 1981.

137 J. Telgen. *Redundancy and linear programs.* 1981.

138 H.A. Lauwerier. *Mathematical models of epidemics.* 1981.

139 J. van der Wal. *Stochastic dynamic programming, successive approximations and nearly optimal strategies for Markov decision processes and Markov games.* 1981.

140 J.H. van Geldrop. *A mathematical theory of pure exchange economies without the no-critical-point hypothesis.* 1981.

141 G.E. Welters. *Abel-Jacobi isogenies for certain types of Fano threefolds.* 1981.

142 H.R. Bennett, D.J. Lutzer (eds.). *Topology and order structures, part 1.* 1981.

143 J.M. Schumacher. *Dynamic feedback in finite- and infinite-dimensional linear systems.* 1981.

144 P. Eijgenraam. *The solution of initial value problems using interval arithmetic; formulation and analysis of an algorithm.* 1981.

145 A.J. Brentjes. *Multi-dimensional continued fraction algorithms.* 1981.

146 C.V.M. van der Mee. *Semigroup and factorization methods in transport theory.* 1981.

147 H.H. Tigelaar. *Identification and informative sample size.* 1982.

148 L.C.M. Kallenberg. *Linear programming and finite Markovian control problems.* 1983.

149 C.B. Huijsmans, M.A. Kaashoek, W.A.J. Luxemburg, W.K. Vietsch (eds.). *From A to Z, proceedings of a symposium in honour of A.C. Zaanen.* 1982.

150 M. Veldhorst. *An analysis of sparse matrix storage schemes.* 1982.

151 R.J.M.M. Does. *Higher order asymptotics for simple linear rank statistics.* 1982.

152 G.F. van der Hoeven. *Projections of lawless sequences.* 1982.

153 J.P.C. Blanc. *Application of the theory of boundary value problems in the analysis of a queueing model with paired services.* 1982.

154 H.W. Lenstra, Jr., R. Tijdeman (eds.). *Computational methods in number theory, part I.* 1982.

155 H.W. Lenstra, Jr., R. Tijdeman (eds.). *Computational methods in number theory, part II.* 1982.

156 P.M.G. Apers. *Query processing and data allocation in distributed database systems.* 1983.

157 H.A.W.M. Kneppers. *The covariant classification of two-dimensional smooth commutative formal groups over an algebraically closed field of positive characteristic.* 1983.

158 J.W. de Bakker, J. van Leeuwen (eds.). *Foundations of computer science IV, distributed systems, part 1.* 1983.

159 J.W. de Bakker, J. van Leeuwen (eds.). *Foundations of computer science IV, distributed systems, part 2.* 1983.

160 A. Rezus. *Abstract AUTOMATH.* 1983.

161 G.F. Helminck. *Eisenstein series on the metaplectic group, an algebraic approach.* 1983.

162 J.J. Dik. *Tests for preference.* 1983.

163 H. Schippers. *Multiple grid methods for equations of the second kind with applications in fluid mechanics.* 1983.

164 F.A. van der Duyn Schouten. *Markov decision processes with continuous time parameter.* 1983.

165 P.C.T. van der Hoeven. *On point processes.* 1983.

166 H.B.M. Jonkers. *Abstraction, specification and implementation techniques, with an application to garbage collection.* 1983.

167 W.H.M. Zijm. *Nonnegative matrices in dynamic programming.* 1983.

168 J.H. Evertse. *Upper bounds for the numbers of solutions of diophantine equations.* 1983.

169 H.R. Bennett, D.J. Lutzer (eds.). *Topology and order structures, part 2.* 1983.

CWI TRACTS

1 D.H.J. Epema. *Surfaces with canonical hyperplane sections.* 1984.

2 J.J. Dijkstra. *Fake topological Hilbert spaces and characterizations of dimension in terms of negligibility.* 1984.

3 A.J. van der Schaft. *System theoretic descriptions of physical systems.* 1984.

4 J. Koene. *Minimal cost flow in processing networks, a primal approach.* 1984.

5 B. Hoogenboom. *Intertwining functions on compact Lie groups.* 1984.

6 A.P.W. Böhm. *Dataflow computation.* 1984.

7 A. Blokhuis. *Few-distance sets.* 1984.

8 M.H. van Hoorn. *Algorithms and approximations for queueing systems.* 1984.

9 C.P.J. Koymans. *Models of the lambda calculus.* 1984.

10 C.G. van der Laan, N.M. Temme. *Calculation of special functions: the gamma function, the exponential integrals and error-like functions.* 1984.

11 N.M. van Dijk. *Controlled Markov processes; time-discretization.* 1984.

12 W.H. Hundsdorfer. *The numerical solution of nonlinear stiff initial value problems: an analysis of one step methods.* 1985.

13 D. Grune. *On the design of ALEPH.* 1985.

14 J.G.F. Thiemann. *Analytic spaces and dynamic programming: a measure theoretic approach.* 1985.

15 F.J. van der Linden. *Euclidean rings with two infinite primes.* 1985.

16 R.J.P. Groothuizen. *Mixed elliptic-hyperbolic partial differential operators: a case-study in Fourier integral operators.* 1985.

17 H.M.M. ten Eikelder. *Symmetries for dynamical and Hamiltonian systems.* 1985.

18 A.D.M. Kester. *Some large deviation results in statistics.* 1985.

19 T.M.V. Janssen. *Foundations and applications of Montague grammar, part 1: Philosophy, framework, computer science.* 1986.

20 B.F. Schriever. *Order dependence.* 1986.

21 D.P. van der Vecht. *Inequalities for stopped Brownian motion.* 1986.

22 J.C.S.P. van der Woude. *Topological dynamix.* 1986.

23 A.F. Monna. *Methods, concepts and ideas in mathematics: aspects of an evolution.* 1986.

24 J.C.M. Baeten. *Filters and ultrafilters over definable subsets of admissible ordinals.* 1986.

25 A.W.J. Kolen. *Tree network and planar rectilinear location theory.* 1986.

26 A.H. Veen. *The misconstrued semicolon: Reconciling imperative languages and dataflow machines.* 1986.

27 A.J.M. van Engelen. *Homogeneous zero-dimensional absolute Borel sets.* 1986.

28 T.M.V. Janssen. *Foundations and applications of Montague grammar, part 2: Applications to natural language.* 1986.

29 H.L. Trentelman. *Almost invariant subspaces and high gain feedback.* 1986.

30 A.G. de Kok. *Production-inventory control models: approximations and algorithms.* 1987.

31 E.E.M. van Berkum. *Optimal paired comparison designs for factorial experiments.* 1987.

32 J.H.J. Einmahl. *Multivariate empirical processes.* 1987.

33 O.J. Vrieze. *Stochastic games with finite state and action spaces.* 1987.

34 P.H.M. Kersten. *Infinitesimal symmetries: a computational approach.* 1987.

35 M.L. Eaton. *Lectures on topics in probability inequalities.* 1987.

36 A.H.P. van der Burgh, R.M.M. Mattheij (eds.). *Proceedings of the first international conference on industrial and applied mathematics (ICIAM 87).* 1987.

37 L. Stougie. *Design and analysis of algorithms for stochastic integer programming.* 1987.

38 J.B.G. Frenk. *On Banach algebras, renewal measures and regenerative processes.* 1987.

39 H.J.M. Peters, O.J. Vrieze (eds.). *Surveys in game theory and related topics.* 1987.

40 J.L. Geluk, L. de Haan. *Regular variation, extensions and Tauberian theorems.* 1987.

41 Sape J. Mullender (ed.). *The Amoeba distributed operating system: Selected papers 1984-1987.* 1987.

42 P.R.J. Asveld, A. Nijholt (eds.). *Essays on concepts, formalisms, and tools.* 1987.

43 H.L. Bodlaender. *Distributed computing: structure and complexity.* 1987.

44 A.W. van der Vaart. *Statistical estimation in large parameter spaces.* 1988.

45 S.A. van de Geer. *Regression analysis and empirical processes.* 1988.

46 S.P. Spekreijse. *Multigrid solution of the steady Euler equations.* 1988.

47 J.B. Dijkstra. *Analysis of means in some non-standard situations.* 1988.

48 F.C. Drost. *Asymptotics for generalized chi-square goodness-of-fit tests.* 1988.

49 F.W. Wubs. *Numerical solution of the shallow-water equations.* 1988.

50 F. de Kerf. *Asymptotic analysis of a class of perturbed Korteweg-de Vries initial value problems.* 1988.

51 P.J.M. van Laarhoven. *Theoretical and computational aspects of simulated annealing.* 1988.

52 P.M. van Loon. *Continuous decoupling transformations for linear boundary value problems.* 1988.

53 K.C.P. Machielsen. *Numerical solution of optimal control problems with state constraints by sequential quadratic programming in function space.* 1988.

54 L.C.R.J. Willenborg. *Computational aspects of survey data processing.* 1988.

55 G.J. van der Steen. *A program generator for recognition, parsing and transduction with syntactic patterns.* 1988.

56 J.C. Ebergen. *Translating programs into delay-insensitive circuits.* 1989.

57 S.M. Verduyn Lunel. *Exponential type calculus for linear delay equations.* 1989.

58 M.C.M. de Gunst. *A random model for plant cell population growth.* 1989.

59 D. van Dulst. *Characterizations of Banach spaces not containing l^1.* 1989.

60 H.E. de Swart. *Vacillation and predictability properties of low-order atmospheric spectral models.* 1989.

61 P. de Jong. *Central limit theorems for generalized multilinear forms.* 1989.

62 V.J. de Jong. *A specification system for statistical software.* 1989.

63 B. Hanzon. *Identifiability, recursive identification and spaces of linear dynamical systems, part I.* 1989.

64 B. Hanzon. *Identifiability, recursive identification and spaces of linear dynamical systems, part II.* 1989.

65 B.M.M. de Weger. *Algorithms for diophantine equations.* 1989.

66 A. Jung. *Cartesian closed categories of domains.* 1989.

67 J.W. Polderman. *Adaptive control & identification: Conflict or conflux?.* 1989.

68 H.J. Woerdeman. *Matrix and operator extensions.* 1989.

69 B.G. Hansen. *Monotonicity properties of infinitely divisible distributions.* 1989.

70 J.K. Lenstra, H.C. Tijms, A. Volgenant (eds.). *Twenty-five years of operations research in the Netherlands: Papers dedicated to Gijs de Leve.* 1990.

71 P.J.C. Spreij. *Counting process systems. Identification and stochastic realization.* 1990.

72 J.F. Kaashoek. *Modeling one dimensional pattern formation by anti-diffusion.* 1990.

73 A.M.H. Gerards. *Graphs and polyhedra. Binary spaces and cutting planes.* 1990.

74 B. Koren. *Multigrid and defect correction for the steady Navier-Stokes equations. Application to aerodynamics.* 1991.

75 M.W.P. Savelsbergh. *Computer aided routing.* 1992.

76 O.E. Flippo. *Stability, duality and decomposition in general mathematical programming.* 1991.

77 A.J. van Es. *Aspects of nonparametric density estimation.* 1991.

78 G.A.P. Kindervater. *Exercises in parallel combinatorial computing.* 1992.

79 J.J. Lodder. *Towards a symmetrical theory of generalized functions.* 1991.

80 S.A. Smulders. *Control of freeway traffic flow.* 1993.

81 P.H.M. America, J.J.M.M. Rutten. *A parallel object-oriented language: design and semantic foundations.* 1992.

82 F. Thuijsman. *Optimality and equilibria in stochastic games.* 1992.

83 R.J. Kooman. *Convergence properties of recurrence sequences.* 1992.

84 A.M. Cohen (ed.). *Computational aspects of Lie group representations and related topics. Proceedings of the 1990 Computational Algebra Seminar at CWI, Amsterdam.* 1991.

85 V. de Valk. *One-dependent processes.* 1993.

86 J.A. Baars, J.A.M. de Groot. *On topological and linear equivalence of certain function spaces.* 1992.

87 A.F. Monna. *The way of mathematics and mathematicians.* 1992.

88 E.D. de Goede. *Numerical methods for the three-dimensional shallow water equations.* 1993.

89 M. Zwaan. *Moment problems in Hilbert space with applications to magnetic resonance imaging.* 1993.

90 C. Vuik. *The solution of a one-dimensional Stefan problem.* 1993.

91. E.R. Verheul. *Multimedians in metric and normed spaces.* 1993.